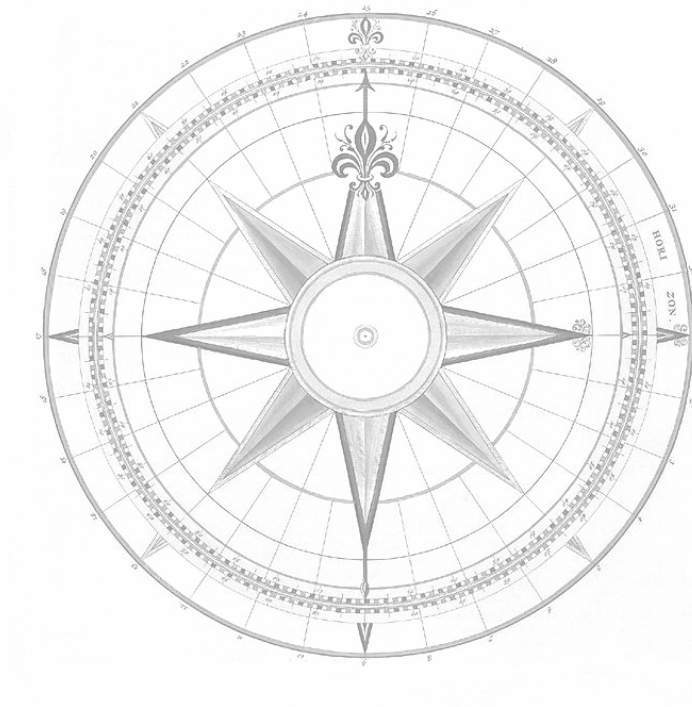


Mechanosensitivity of Fibroblasts

interaction between altered gravity conditions
and surface topography



Colofon

Thesis Radboud University Nijmegen Medical Center, Nijmegen, The Netherlands, with summary in Dutch.

Mechanosensitivity of fibroblasts; interaction between altered gravity conditions and surface topography.

Walter Anthonius Loesberg, Nijmegen 2008.

All rights reserved.

© by W.A. Loesberg, 2008

ISBN 978-909022706-1

Cover design & lay-out Walter Loesberg

Printing Print Partners Ipskamp BV, Enschede, The Netherlands

Mechanosensitivity of Fibroblasts

interaction between altered gravity conditions
and surface topography

Een wetenschappelijke proeve op het gebied van de medische wetenschappen

Proefschrift

ter verkrijging van de graad van doctor

aan de Radboud Universiteit Nijmegen

op gezag van de rector magnificus, prof. mr. S.C.J.J. Kortmann,

volgens besluit van het College van Decanen

in het openbaar te verdedigen op woensdag 20 februari 2008,

om 15.30 uur precies

door

Walter Anthonius Loesberg

geboren op 22 maart 1976

te Hilversum

Promotor

Prof. dr. J.A. Jansen

Copromotores

Dr. X.F. Walboomers

Dr. ing. J.J.W.A. van Loon, Vrije Universiteit Amsterdam

Manuscriptcommissie

Prof. dr. W.B. van den Berg (voorzitter)

Prof. dr. E.W. Roubos

Prof. dr. H. Weinans, Erasmus Universiteit Rotterdam

Paranimfen

Nathalie de Jonge-Loesberg

Dennis Link

Mechanosensitivity of Fibroblasts

interaction between altered gravity conditions
and surface topography

An academic essay in the field of medical sciences

Doctoral thesis

to obtain the degree of doctor

from Radboud University Nijmegen

by the authority of the Rector Magnificus, prof. dr. S.C.J.J. Kortmann,

according to the decision of the Council of Deans

to be defended in public on Wednesday 20th of February 2008,

at precisely 15.30 hours

by

Walter Anthonius Loesberg

born in Hilversum, The Netherlands

on March 22, 1976

Supervisor

Prof. dr. J.A. Jansen

Co-supervisors

Dr. X.F. Walboomers

Dr. ing. J.J.W.A. van Loon, VU University Amsterdam

Manuscript committee

Prof. dr. W.B. van den Berg (chairman)

Prof. dr. E.W. Roubos

Prof. dr. H. Weinans, Erasmus University Rotterdam

Ushers

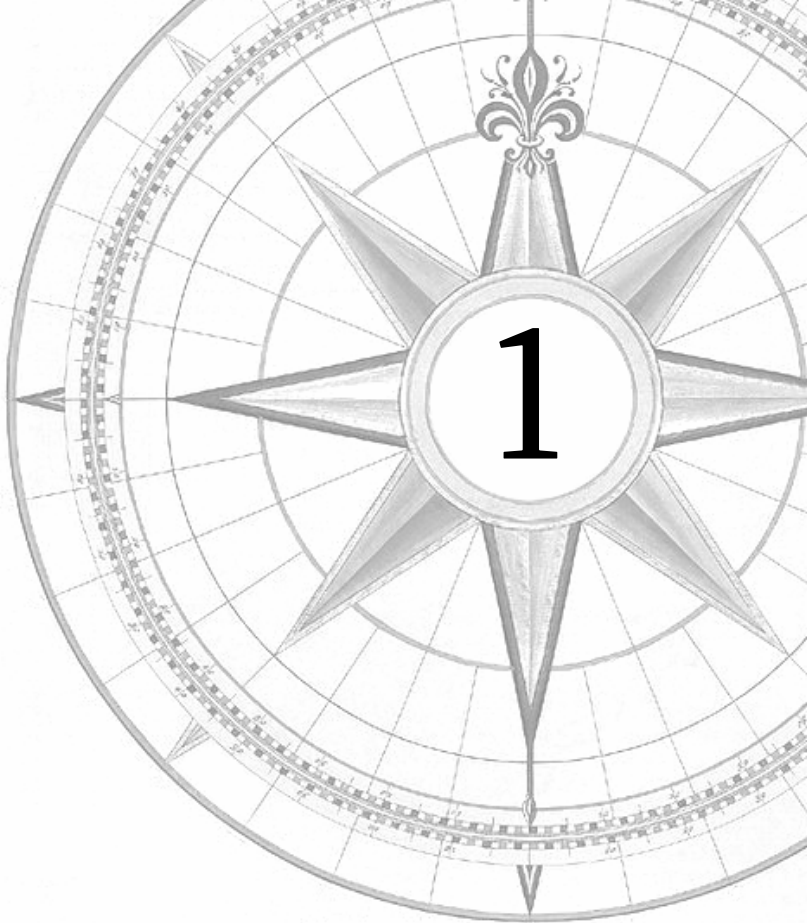
Nathalie de Jonge-Loesberg

Dennis Link

CONTENTS

CHAPTER 1	General Introduction	9
CHAPTER 2	The effect of combined cyclic mechanical stretching and microgrooved surface topography on the behaviour of fibroblasts	47
CHAPTER 3	The effect of combined hypergravity and microgrooved surface topography on the behaviour of fibroblasts	61
CHAPTER 4	The effect of combined simulated microgravity and microgrooved surface topography on fibroblasts	75
CHAPTER 5	Simulated microgravity activates MAPK pathways in fibroblasts cultured on microgrooved surface topography	89
CHAPTER 6	Mechanosensitivity of fibroblasts towards inertial shear force and microgrooved surface topography	107
CHAPTER 7	The threshold at which substrate nanogroove dimensions may influence fibroblast alignment and adhesion	125
CHAPTER 8	Summary and future perspectives	137
CHAPTER 9	Samenvatting en toekomst visie	143
CHAPTER 10	Dankwoord	149
CHAPTER 11	Curriculum Vitae	153
CHAPTER 12	List of publications	157
	Colour pictures of CLSM micrographs	161

General introduction



INTRODUCTION

The biological challenge for the next decennium will be to obtain more knowledge of systems that allow the culturing of different cell types in three-dimensional structures. This is essential for the controlled regeneration of complex organs, like liver and kidney, which can be used for transplantation purposes. In view of this, we know that the outside environment determines the shape and function of cells. For example, cells cultures on micro-textured culturing materials spread in a very orderly fashion. This condition resembles the situation in living organs, where tissues are characterised by a high degree of organisation. Numerous investigations indicate that there is a direct relationship between the shape and organisation of cells and their differentiated state. The basis of the controlled cell-spreading phenomenon, also known as “contact guidance”, is explained by the ability of the cell to sense a specific environment. Apparently, the micro- and nano-morphology of the substrate surface affects the mechanical state of the cell.

In addition to the cellular responses to surface topography, cells also react towards dynamic stresses, such as fluid flow, stretch force, or compression. These forces too affect the mechanical state of the cell. This interaction of static (surface) and dynamic (stress) forces results in the total response of cell towards their (changing) environment. One of such forces is gravity, and is the focus of this thesis. It has become clear from previous studies that cells behave differently under conditions of hypergravity and microgravity (near weightlessness) compared to their appropriate 1g controls. Some more theoretical studies have argued against cells sensing gravity or microgravity altogether. Nevertheless, until now no studies have been performed to examine cell shape changes in situ under various gravity conditions. A change in cell shape in situ under varying g levels contributes to the idea of direct effects of gravity onto cells. Since gravity acts on mass, it might well be expected that initially small changes in cells due to (micro-)gravity result in intracellular mass displacement and/or changes in general cell shape. These small changes might be integrated or amplified thus generating the various changes as seen under micro- or hypergravity conditions. Processes as mass displacement and cell shape involve the cytoskeleton system and the intracellular signalling system. Using various microtextured surfaces, combined with settings of hypergravity and simulated microgravity, might well elucidate to what extent cell shape and function are determined by the cell surrounding structures, and in what way they are able to sense (micro-)gravity.

In this introduction we will first discuss the structure of cells and cytoskeleton, and the important role played by the cytoskeleton in cell attachment and locomotion across substrates. We then continue with the design and production of microgrooved substrates, and give a description of how the different cells and tissues respond to these microgrooved surfaces. An introduction in gravity and the physical implications on cell cultures will be discussed, together with a summary of ground-based machines for simulating hyper- and microgravity, as well as the cell response to changes in gravity (gravisensing) in literature. We will end with the research objectives in which a formulation of a study hypothesis and several research questions are posted.

CELL STRUCTURE

Eukaryotic cells have the ability to organise the many components in their interior, to adopt a variety of shapes, to carry out coordinated movements, and provide a communication pathway between cellular protein complexes and organelles. This ability depends on the cytoskeleton – an intricate network of protein filaments that extends throughout the cytoplasm. The cytoskeleton is a highly dynamic structure that is continuously broken down and assembled in order for a cell to change shape, divide, and respond to its environment. The cytoskeleton is not only the “bones” (pre-stressed structures) of a cell but also its “muscles” (tensional forces), and it is directly responsible for large-scale movements such as the crawling of a cell along a surface. The

cytoskeleton of eukaryotic cells consists of three types of protein filaments: intermediate filaments, microtubules, and actin filaments (**Figure 1**). Each type of filament is formed from a different protein subunit. In each case, thousands of subunits assemble into a continuous thread of proteins that sometimes extends across the entire cell [1].

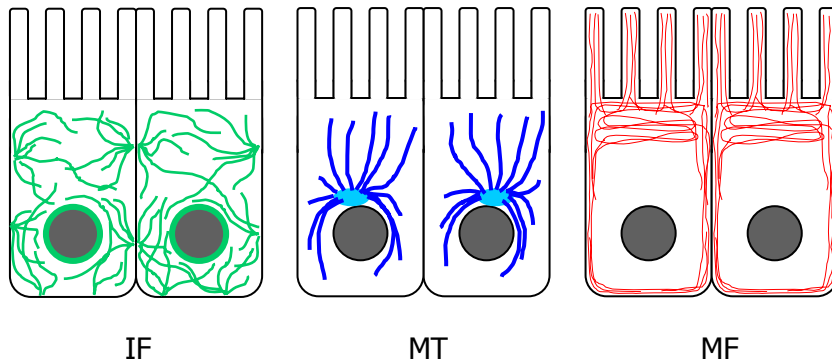


Figure 1. Schematic illustration of the three types of filaments in an epithelial cell lining the gut: intermediate filaments (IF), microtubules (MT), and microfilaments (MF).

Microfilaments

Microfilaments are found in all eukaryotic cells and are essential for many of their movements, especially those involving the cell surface. The microfilaments are a group of proteins consisting of actin, myosin, and several associated proteins. Depending on their association with different proteins, actin filaments can form stiff and relatively permanent structures such as the micro-villi, on the brush-border cells lining the intestine, or small bundles in the cytoplasm that can contract and act like the “muscles” of a cell. Actin filaments can also form temporary structures such as the protrusions formed at the leading edge of a crawling fibroblast, or the contractile ring that pinches the cytoplasm in two when an animal cell divides.

Each actin filament is a twisted chain of identical globular actin molecules, all of which “point” in the same direction along the axis of the chain. Like a microtubule, an actin filament has a structural polarity, with a plus end and a minus end. There is a crucial difference between actin filaments and microtubules; in case of the actin filaments, the organising cluster of proteins is situated at the plus end of the filament.

Actin filaments appear as threads about 7 nm in diameter, this filamentous form is called F-actin. Each filament may be thought of as a two-stranded helix with a twist repeating every 37 nm (**Figure 2**).

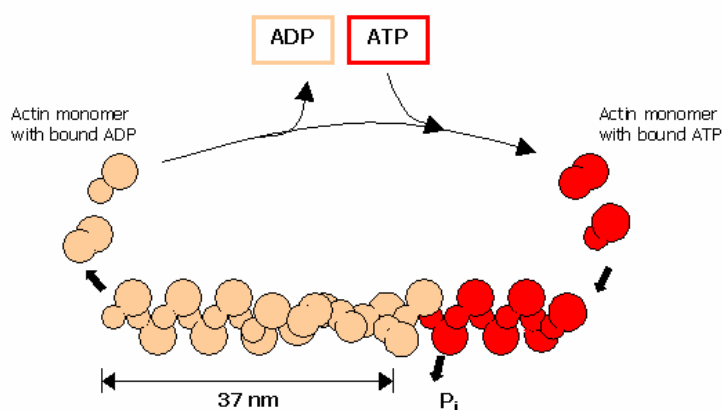


Figure 2. Actin polymerisation requires ATP hydrolysis. The actin monomers carry ATP, which is hydrolysed to ADP after assembly into a growing filament. The ADP stays bound with the actin monomer until the actin monomer dissociates from the filament. Each filament looks like a two-stranded helix with a twist every 37 nm.

In a fibroblast about half of the actin is filamentous, while the other half is free as actin-monomers, that is to say they are bound to actin-binding proteins profilin and thymosin. The binding proteins sequester free actin monomers in the cytoplasm, thereby keeping actin monomers in reserve until they are required. Although actin is found throughout the cytoplasm of a eukaryotic cell, in most cells actin is concentrated in a layer just beneath the plasma membrane.

In this region, called the cell cortex, actin filaments are linked by actin-binding proteins into a meshwork that supports the outer surface of the cell and gives it mechanical strength; the cell cortex also prevents the organelles from touching the inner cellular membrane.

During cell crawling, the cell makes use of internal contractions, to exert a pulling force. These contractions too depend on actin, through the interaction of actin filaments with the motor protein family known as myosin-II. Myosin-II binds and hydrolyzes ATP, which provides the energy for their movement along actin filaments from the minus end of the filament toward the plus end. The myosin filament has a polarity like that of a double-headed arrow, with two sets of heads pointing in opposite directions away from the centre. One set of heads binds to actin filaments in one orientation and moves them one way; the other set binds to other actin filaments in the opposite orientation and moves them in opposite direction. The overall effect is to slide sets of oppositely orientated actin filaments past one another. Therefore, when actin filaments and myosin filaments are organised into a bundle, they can generate a contractile force.

Other actin-associated proteins have various functions. Gelsolin fragments actin filaments into shorter lengths and thus converts an actin gel to a more fluid state. Spectrin forms a meshwork with actin filaments so that it connects to the membrane through intracellular attachment proteins, so called cap-proteins. Myosin-I is a motor protein that moves cell components and vesicles along actin filaments. Tropomyosin binds in the groove of the actin helix, overlapping seven actin monomers and prevents the myosin-II heads from associating with the actin filament. Together with troponin, tropomyosin controls the skeletal muscle contraction [2; 3].

Intermediate filaments

Intermediate filaments have great tensile strength, and their main function is to enable cells to withstand the mechanical stress that occurs when cells are stretched. They are called intermediate because their diameter (8-10 nm) is between that of the thinner actin filaments and the thicker myosin filaments. Intermediate filaments are the toughest and most durable of the three types of cytoskeleton filaments. They typically form a network throughout the cytoplasm, surrounding the nucleus and extending out to the cell periphery. Often they are anchored to the plasma membrane at cell-cell junctions.

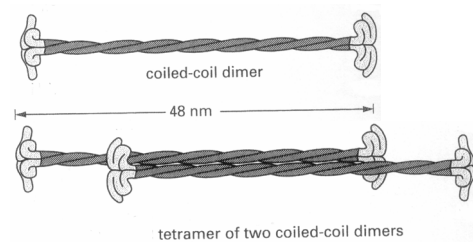
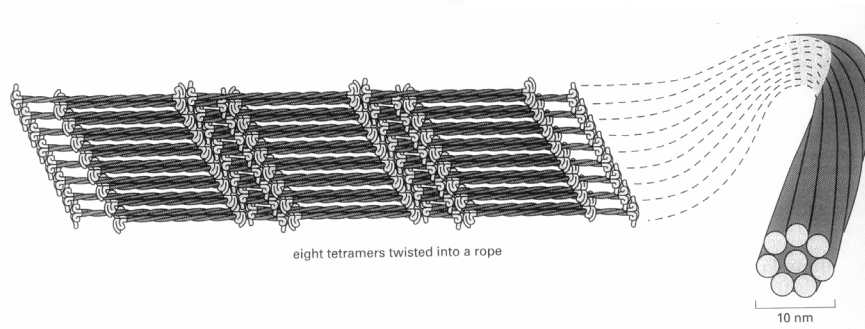


Figure 3. Build up of an intermediate filament. Pairs of monomers form dimers, and two dimers line up to form tetramers. Tetramers pack together and assemble into a helical array that produces the final rope like intermediate filament (adapted from Alberts et al).



Intermediate filaments are like ropes, the strands of this rope – the subunits of intermediate filaments – are dimer-forming filamentous proteins (48 nm in length). These dimers associate to form a tetramer, and the tetramers bind to one another to generate the final rope like intermediate filament (**Figure 3**). A family of fibrous proteins form the intermediate filaments and are grouped into four classes: (1) keratin filaments in epithelial cells; (2) vimentin and vimentin-related filaments in connective-tissue cells, muscle cells (desmin) and glial cells (glial fibrillary acidic protein); (3) neurofilaments in nerve cells; (4) nuclear lamina, present around the cell nucleus. This latter class disassembles and re-forms at each cell-division [2; 3].

Microtubules

Microtubules have a critical organizing role in all eukaryotic cells. They are long and relatively stiff hollow tubes of protein that can rapidly disassemble in one location and reassemble in another. In a typical animal cell, microtubules grow out from a small structure near the centre of the cell, called the centrosome. Extending out toward the cell periphery, they create a system of tracks within the cell, along which vesicles, organelles, and other cell components can be moved. Microtubules can also form permanent structures, called cilia and flagella.

Microtubules are built from molecules of tubulin; each one is itself a dimer of two very similar globular proteins called α -tubulin and β -tubulin. The tubulin subunits stack together to form the wall of the hollow cylindrical microtubule. This appears as a cylinder made of 13 parallel protofilaments, each a linear chain of tubulin subunits with α - and β -tubulin alternating along its length (**Figure 4**). Each protofilament has a structural polarity, and this polarity – the directional arrow embodied in the structure – is the same for all the protofilaments, giving a structural polarity to the microtubule as a whole. The α -tubulin end (at the centrosome) is called the minus end, and the other, the β -tubulin end (at the periphery) it's plus end.

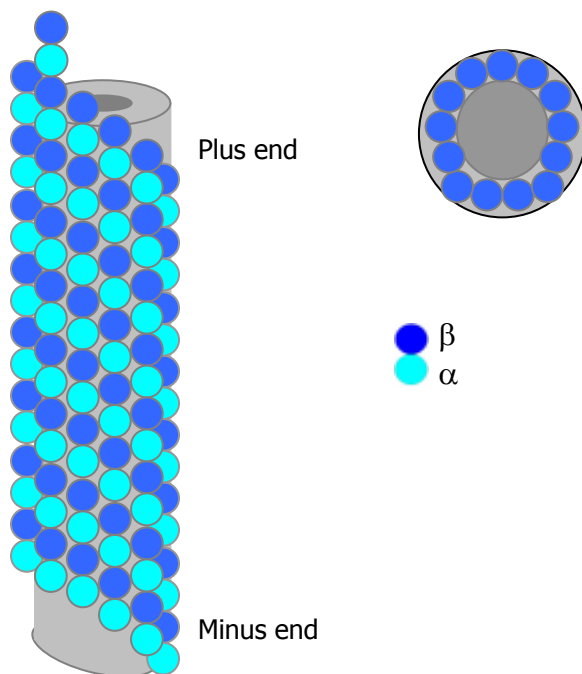


Figure 4. Microtubule structure consists of $\alpha\beta$ tubulin dimers which are arranged in protofilaments (one column). The cross section shows 13 subunits, each of which corresponds to a separate tubulin dimer. The orientation of both the tubulin molecules in the protofilaments, and the protofilaments themselves give the microtubule its structural polarity.

Both microtubules and actin filaments are involved in intracellular movements in eukaryotic cells. In both cases the movements are generated by motor proteins, which bind to actin filaments or microtubules and use the energy derived from repeated cycles of adenosine tri-phosphate (ATP) hydrolysis to travel steadily along the microtubule or the actin filament in a single direction. These motor proteins also attach other cell components, and thus transport this cargo along

filaments. The motor protein kinesin moves to the plus end and the protein dynein to the minus end (**Figure 5**) [2 ;3].

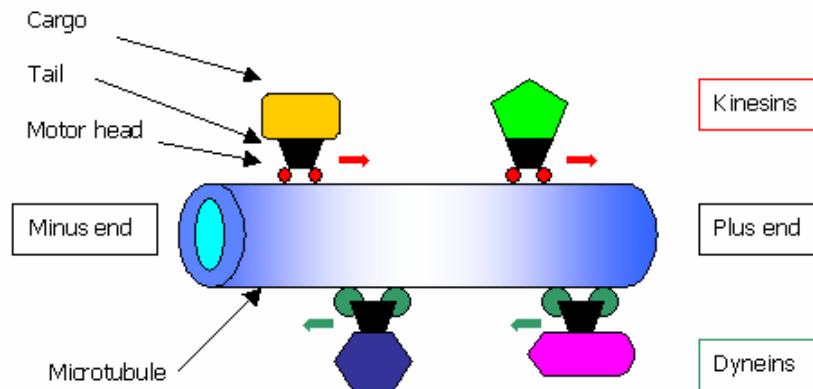


Figure 5. Transport is carried out by motor proteins along microtubules. Kinesins moves cargo toward the plus end and dyneins moves cargo towards the minus end. There are many forms of both types of motor proteins, each of which probably transports a different cargo. The difference in cargo is determined by the tail.

Fibroblast attachment to substrates

If cells are to crawl over a substrate, they must be able to attach to it. Cultured cells adhere to their substratum, as well as to each other. Morphological criteria, to be precise: the gap distances between the cell membrane and the substratum and the presence of submembranous densities, are often used to distinguish between the several types of cell-substratum adhesions. These types are: extracellular matrix (ECM) contacts; close contacts; and focal adhesions. ECM contacts are characterised by large separations (≥ 100 nm) between the cell and the substratum. ECM sites intracellular appear to be of two kinds, either both α -actinin and vinculin or α -actinin alone. Close contacts have a separation of 30-50 nm. Close contacts are comparable with one half of an adherens cell-cell junction; intracellular they appear to be α -actinin and extracellular fibronectin. Focal adhesions show a 10-20 nm gap between membrane and substratum. They can be compared to one half of a tight cell-cell junction. Intracellular both α -actinin and vinculin are present [1].

The cytoskeleton is bound to ECM proteins at focal adhesions. The formation of a focal adhesion complex (FAC) plays a central role. The FAC is a macromolecular scaffold that mechanically couples the cytoplasmatic portion of integrins to the internal actin cytoskeleton. It contains actin-associated molecules such as vinculin, talin, and α -actinin, as well as many signalling molecules that mediate stimulus-response coupling. The latter include tyrosine and serine protein kinases, inositol lipid kinases, ion channels and even a subset of growth factor receptors [2-8].

The aforementioned integrins form a transmembrane molecular bridge between ECM and the cytoskeleton that distributes mechanical stresses and helps bring forces into balance (**Figure 6**).

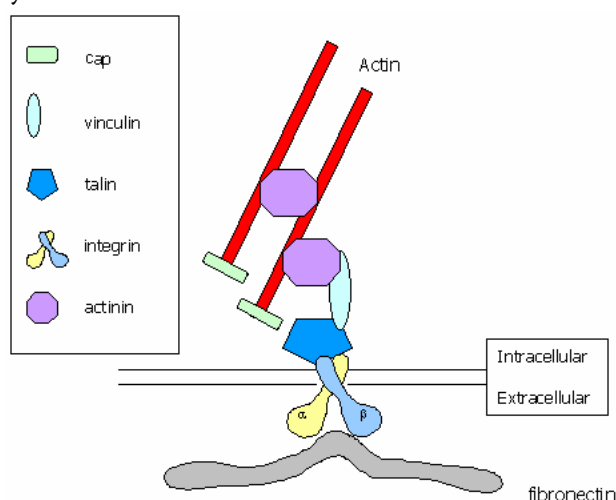


Figure 6. The transmembrane molecular bridge between ECM and the CSK. A number of proteins are involved in focal adhesion.

Integrins bind to ECM components, like fibronectin, vitronectin, or laminin. Integrins are a large family of heterodimeric transmembrane glycoproteins that consist of noncovalently linked alpha (120-170 kDa) and beta (90-100 kDa) subunits. Integrins contain binding sites for divalent cations Mg^{2+} and Ca^{2+} , which are necessary for their adhesive function. The specificity of a given integrin for binding various ligands appears to depend primarily on the extracellular portion of the alpha subunit. However, both subunits are required for an integrin to function properly. The beta subunits have several distinctive features, including tandem repeats of four cysteine-rich regions that are thought to be essential for maintaining the molecular shape. Until now 18 alpha and 8 beta subunits have been identified. From these subunits only some 23 integrins are formed in nature, which implicates that not all possible combinations exist. Matrix proteins often contain a RGD (sequence of the aminoacids arginine, glycine and aspartic acid). This sequence is the part of the matrix protein that is bound by the integrin [3; 4].

The beta subunit of the integrin is important in the connections between actin filaments and integrin (and thereby the outside world). Beta subunit can bind to the major structural proteins in focal adhesions: talin, vinculin, tensin, α -actinin and paxillin. Both tensin and talin strengthen the binding of vinculin and actinin. Vinculin can, besides bind indirectly to integrins via talin and actinin, bind actin and tensin. Paxillin appears important in the organisation and turnover of focal adhesion complexes. The attachment sites are well positioned to act as signal transducing centres to report on changes in the cell's immediate environment. Signalling pathways are mediated through autophosphorylation of the tyrosine kinase Focal Adhesion Kinase (FAK). Besides FAK, which takes up a central position in the signal transduction, other proteins are SrcFK, CAS, Crk and Csk (Figure 7) [6; 9-16].

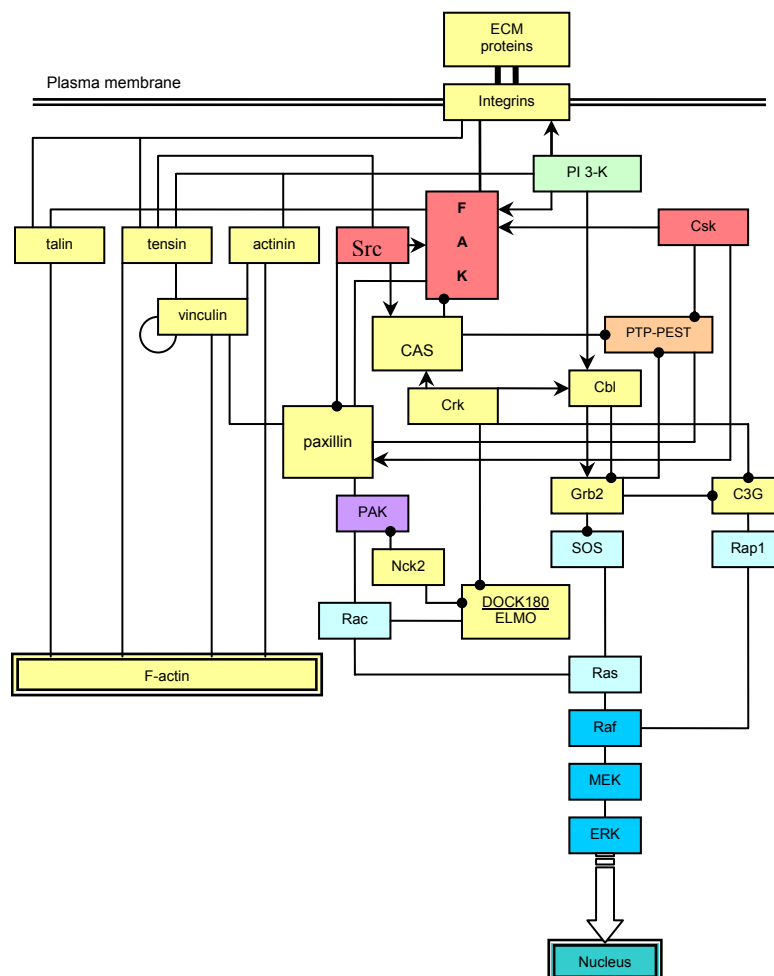


Figure 7. Interaction schematic among the proteins involved in integrin signalling. The integrin-mediated mechanotransduction includes multiple kinases (FAK, SrcFK, and Csk), adaptor molecules (CAS, Crk, Grb2, and paxillin), guanine nucleotide exchange factors (GEFs) (C3G, SOS), and small GTPases (Rap1, Ras) in activating Mitogen-Activating Protein Kinases (MAPKs) (MEK, ERK). Signals through FAK to Rac and PAK play a role in modulating cell adhesion and migration, actin polymerisation and MAP kinase signalling. SH2 interactions are marked by arrows, pointing to phosphotyrosine containing target, SH3 interactions are marked by dots pointing to proline rich target. Black lines indicate either cell-matrix or cell-cell adhesions (adapted from: Zamir et al).

Cell locomotion and the formation of focal adhesions

Cell locomotion is undoubtedly complex, requiring coordinated activity of cytoskeletal, membrane, and adhesion systems. Locomotion involves protrusion and adhesion at the cell front, and contraction and detachment at the rear. In migrating cells, membrane protrusion is driven by actin polymerisation and does not require microtubules; however directional cell movement requires dynamically growing microtubules [17].

A conventional breakdown of crawling along spatial/mechanical lines is shown in **Figure 8**, for a single cell moving over a two-dimensional substrate. Four interrelated processes are essential: (1) forward motility of the membrane at the “front” or leading edge (protrusion); (2) adherence of these protrusions to the surface of the substrate (adhesion); (3) dragging forward of the cell using the anchorage points (traction); the last process (4) is comprised of two mechanistically distinct steps: de-adhesion and retraction of the trailing edge of the cell. Whether this step is actively motile depends on the cell type: strongly adhesive cells such as cultured fibroblasts tend to have a strongly adherent, extended tail and leave behind a trail of cytoplasmic fragments as they move [18].

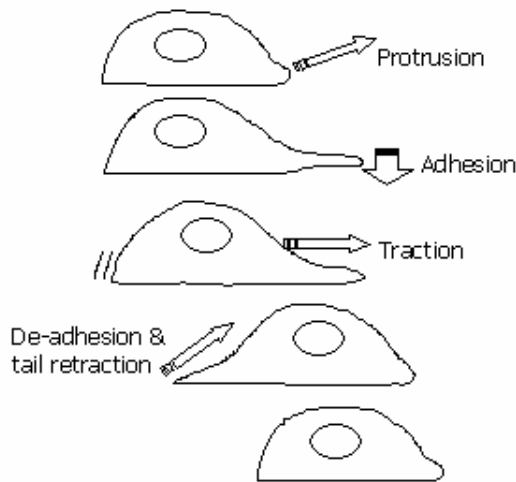


Figure 8. Cell locomotion in cartoon form. Actin polymerisation at the leading edge of the cell pushes the plasma membrane forward. New anchorage points are made between the actin cortex and the substratum surface. Cortical tension then draws the body of the cell forward. The rear of the cell detaches from the substratum and retracts, actin filaments in the retracting tail depolymerise, and the released actin molecules move forward through the cytosol to sites of new polymerisation. This cycle is repeated time and time again, moving the cell forward (adapted from: Mitchison et al 1996).

This dynamic organisation of the actin cytoskeleton, which provides the force for cell motility, is regulated by the members of the Rho family of small GTPases (Guanine Tri-Phosphate). Each of these GTPases act as a molecular switch, cycling between active GTP-bound and inactive GDP-bound state. Guanine-nucleotide-exchange factors (GEFs) facilitate the exchange of GDP for GTP. GTPases-activating proteins (GAPs) increase the rate of GTP hydrolysis of Rho GTPases (**Figure 9**) [3].

The members RhoA, Rac1 and Cdc42 are required for respectively stress fibre formation, lamellipodia and filopodia. Lamellipodia and its accompanying membrane ruffles at the advancing cell front are made up of a laminar meshwork of actin filaments. Lamellipodia are often punctuated by the rib-like filopodia, they can extend as finger-like projections beyond the lamellipodium tip. The adhesion sites in lamellipodia and filopodia are called focal complexes. Focal complexes may be of a transient event and turn over with in a few minutes, or they can differentiate into larger and long-lived focal adhesions. Focal complexes can be induced by Rac1 and Cdc42, and the transition to focal adhesions is put in motion by the upregulation of Rho (**Figure 10**) [19-24]. Rho upregulation comes forth from the activities of Rho effectors formin mDia and Rho kinase (ROCK) [25]. They are responsible for polymerisation of actin bundles and myosin contractility respectively, which in turn is necessary for focal adhesion formation and

maintenance. Both focal complexes and early focal adhesions remain stationary relative to the substrate and serve as traction points for forward translocation [20].

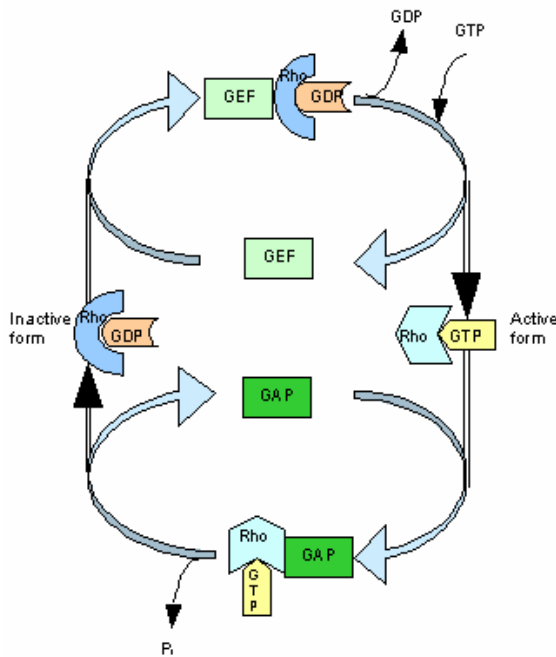


Figure 9. Cycling of Rho protein between its inactive form and active form. Guanine nucleotide-exchange factor (GEF) facilitates dissociation of GDP from Rho. GTP binds spontaneously, and GEF dissociates resulting in the active Rho-GTP form. Hydrolysis of bound GTP to regenerate the inactive Rho-GDP form is accelerated a hundredfold by GTP-activating protein (GAP).

New adhesions sites are formed at the front as the cell moves forward, while the preceding sites are disassembled. At the trailing edge of the cell there are also focal adhesions to be found, they are the remainder of previous protrusion and focal complex assemblies. These focal adhesions can “slide” relative to the substrate and fuse together to form large adhesions.

Microtubule polymerisation dynamics is directly linked to substrate adhesion dynamics. Depolymerisation of microtubules leads to depolarisation of cell shape, increased cytoskeleton contractility and amplified focal adhesion size, changes which are equal to RhoA activation. Activation of Rac1 is associated with repolymerisation of microtubules. Via the Rho GTPases there is extensive cross-talk between microtubule polymerisation with the actin cytoskeleton organisation and substrate adhesion dynamics [19; 20].

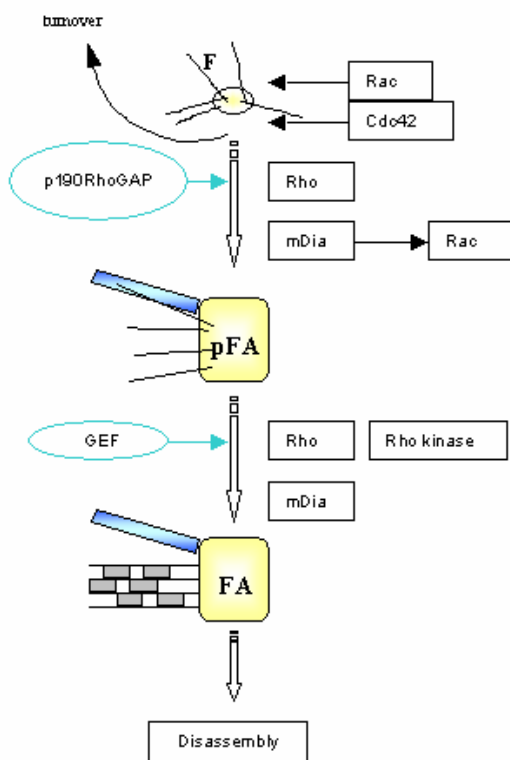


Figure 10. Primary contacts are focal complexes (FC) associated with lamellipodia and filopodia which are formed through Rac and Cdc42 signalling. Lamellipodia and filopodia support protrusion and can either turnover within minutes or differentiate into focal adhesions via Rho upregulation. Inhibitor of this differentiation is probably p190RhoGAP, in order to promote turnover and protrusion. There is reason to believe there is a precursor focal adhesion (pFA) by the finding that Rac can be activated by Rho via mDia, which also stimulates actin polymerisation. The differentiation to focal adhesion requires the recruitment of myosin (grey chequered bars) and the activation of contractility via Rho/Rho kinase, by exchange factors such as GEF. Focal adhesions behind the advancing front stay there and are turned over by disassembly. Microtubules (blue bars) target focal adhesions and could clean up GEF and thereby reduce Rho kinase activity, in this way microtubule-linked signals could decrease the growth of focal complexes or promote disassembly of focal adhesions (adapted from: Small et al 2003).

Microtubules exert their influence on cell polarisation by modulating adhesion site turnover through the point delivery of Rho-family GTPases signals that antagonise myosin contractility at adhesion foci. To allow for molecular crosstalk on the local level, microtubules need to get close to adhesion sites. This targeting of adhesion sites by microtubules is in the range of nanometres. Targeting consists of microtubule growth to the adhesion site and a brief contact between members of the microtubule tip complex and adhesion complex. How this signalling comes about and what microtubule-associated proteins are involved is still under investigation. In order to guide microtubule polymerisation towards adhesion sites; microtubule tip complex proteins interact via an adapter (proposed is an unconventional myosin) with the tensioned actin filaments. This adapter docks onto and moves along actin filaments, thereby steering the microtubule polymerisation into the adhesion site. Obviously, the actin filaments must be linked to the adhesion complex, to allow directed movement of this myosin motor protein (**Figure 11**) [20].

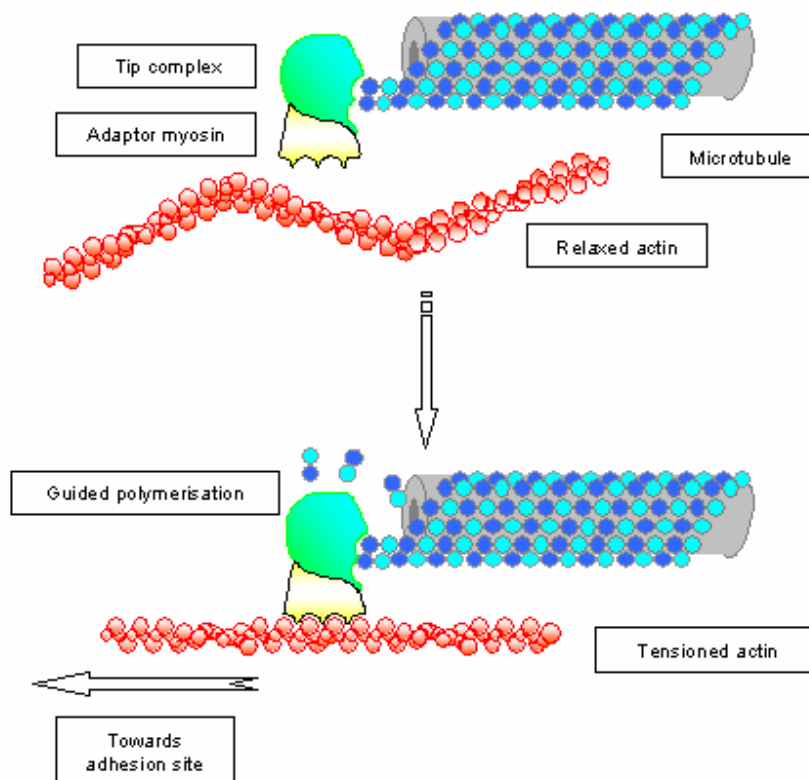


Figure 11. A proposed guidance mechanism of microtubule polymerisation towards adhesion sites. Microtubule polymerisation is stimulated by mechanical stress in the actin filament. Tensioned actin filaments, linked to adhesion foci with their plus end, could be recognised by adaptors associated with the Tip complex proteins which arise in growing microtubules. This adaptor, a possible unconventional type of myosin, attaches to and moves along the tensioned actin, taking the microtubule with it and guiding the microtubule polymerisation in the direction of the adhesion site (adapted from: Small et al 2003).

Cytoskeleton inhibitors

The role of microtubules and microfilaments are also part of continuous investigation, often a specific inhibitor is added and the changes in the cell of interest induced by this substance are observed. Substances like colcemid and nocodazole, which are specific MT inhibitors, or the blocking of kinesin-1 and dynein activity and thereby blocking of the MT motor activity. Also, the use of specific inhibitors for microfilaments like cytochalasin B. Inhibition of both MF and MT by chloropropham and 12-o-tetradecanoyl-phorbol-13-acetate (TPA) have elucidated the importance of the cytoskeleton in growth and cell distribution and of course cell locomotion and shape. Polarisation and locomotion of fibroblasts requires intact MT cytoskeleton. Kaverina *et al.* used contractility inhibitor ML-7 and conclude that regional contractility is modulated by the interfacing of microtubule-linked events with focal adhesions and that microtubules determine cell polarity via this route [26]. Their findings showed that microtubules are dispensable for fibroblast protrusion, but are required for the turnover of substrate adhesions that normally occurs during cell locomotion. Earlier Yokoyama *et al.* applying inhibitors concluded that, although MTs are not essential for elongation of filamentous cell tips, MF are essential for this process [27]. The

interaction of the actin cortex and the MT system has been also been investigated by Dugina *et al.* who induced a cytoskeleton reorganisation with TPA resulting in an actin-rich and MT rich division in the cell. TPA effects were reversible and suppressed by cytochalasin B and colcemid. By targeting MT motor activity through inhibition of kinesin-1 increases the size, but also reduces the number of substrate adhesions thereby mimicking nocodazole effects [28]. The balance of MT minus end capture and release from the centrosome, vital in cell migration, has been uncovered by blocking the dynein activity. Choquet *et al.* used phenylarsine oxide and observed an inhibition of strengthening of CSK linkages, indicating a role for dephosphorylation. They conclude that the strength of integrin-CSK linkages is dependent on matrix rigidity and on its biochemical composition. Matrix rigidity may therefore serve as a guidance cue in a process of mechanotaxis [7]. Another example of a study concerning the connection between cytoskeleton and the outside world through integrins was performed by Uitto *et al.* where the attachment of periodontal ligament epithelial cells to fibronectin, laminin, collagen type I and vitronectin was reduced by arg-gly-asp-ser peptide. The cells treated with this peptide demonstrated prevention of spreading and migration [29]. *et al.*

CELL ADHESION TO MICROGROOVED BIOMATERIALS SURFACES

Tissue Engineering

Tissue engineering, a multidisciplinary scientific field, unravels the fundamentals of structure-function interactions in both normal and diseased tissues. Tissue engineering aims to develop artificial biological substitutes as well as methods to repair damaged or diseased tissues, and ultimately the creation of entire tissue replacements. Driven by the dramatically increasing need for medical implants to replace malfunctioning or lost tissues and organs, tissue engineering has become a billion euro market. The basic principle of tissue engineering is to culture cells and combine them with artificial matrices (scaffolds). These scaffolds are implanted into defects in order to repair damaged tissue or to regenerate new and functional tissue. In the wake of this basic principle is the production of cells, tissues, and matrices. Matrices should be a dynamic microenvironment, not only to manipulate the healing environment, so it can control the structure of regenerated tissue, but also to control the cellular responses of the cells seeded upon the matrices. They should give appropriate signals to the cells, hence mediating their biological activity and function. One way to exert control over cell shape, orientation, metabolic rate, and migration is the use of microgrooved biomaterials [30-40].

Microgrooved surfaces

Cell behaviour can be affected by substrata surface topography. Topography of a substrate can be explained as the morphology of the substrate surface. Surface topography can be divided into roughness and texture [41]. Roughness is characterised by random size and distribution of patterns. Roughness is sometimes applied with a purpose, but it can be the additive result of the material's structure or the fabrication process. Texture is characterised by a deliberate and controlled pattern. Textures are the result of regular surface topography with defined dimensions and surface distribution. A vast array of configurations can be used like: grooves/ridges (v-section, rectangular section, round, multiple grooves, branching, spiral grooves), hills, dots, pits, mesh, and pores [42; 43]. The influence of the topographical morphology of the surface on cell behaviour was first discovered in 1914 by Ross Harrison who used spider webs for cells to migrate along. In 1945, Weiss conducted a range of experiments and described the changes in cell behaviour as "contact guidance". Both Rovensky and Maroudas rediscovered this behaviour in the early 1970s. Ever since, investigators have studied the behaviour of various cell types on a variety of microtextured substrate material [44; 45].

Production of microgrooves

The microtextured pattern can be applied by machining, sintering, or etching the surface. To achieve micron (or even nano) textured dimensions, mostly computer controlled photolithographic techniques are used. These techniques, which come forth from the ever expanding electronics microfabrication technology, are relatively cheap and fast, the textured surfaces are of reasonable size, and a wide range of patterns can be applied on a wide range of biocompatible materials [46].

A microtexturing process can be briefly described as follows: a silicon wafer, after cleaning and being dried with filtered air, is coated with a primer and photo-resist. The samples are patterned by exposing to light through a mask that has the desired pattern. The exposed photo-resist is rinsed of. The next step concerns the etching itself, this can be done by either chemicals (wet conditions), UV light for details of down to 1 μm , or electron beams for details of 100 nm or less (dry conditions). An advantage of physical etching over wet technique is that it allows for a higher resolution, and could also be applicable in amorphous materials. Finally, after the etching process the remaining resist is removed (**Figure 12**) [47]. In case of microgrooved substrates the texture dimensions are described as: pitch (or spacing), ridge width, depth and groove width (**Figure 13**) [47]. The microtextured material can be used as a template for the production of polymeric substrates. For this usually solvent casting procedures are used. Here a polymer (e.g. polystyrene) is dissolved in an organic solvent like chloroform. After casting this solution on the silicon template, the chloroform evaporates. This procedure allows the production of vast numbers of identical replicas, and thus is to be preferred over directly using the silicon materials for experimentation.

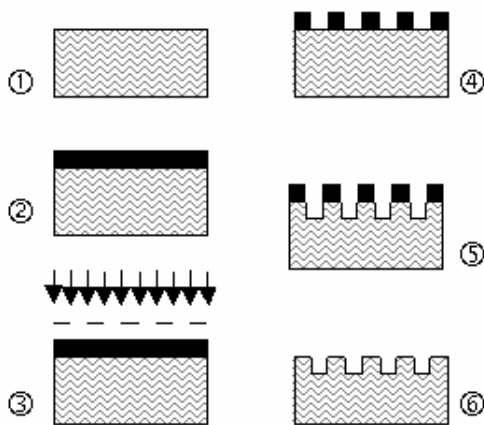


Figure 12. The process of photolithographic etching. The silica material (1) is covered with photo resist (2). The photo resist layer is illuminated through a desired patterned mask (3). The developed resist is washed off (4) and the material is etched by chemicals, UV light or ion beam (5). The remaining resist is removed (adapted from: Walboomers 2000).

Cell response to microgrooved surfaces

Over the years several materials have been used to construct substrates: Polystyrene [46-61], Poly-Lactic Acid [46; 62-69], Poly(glycolic-co-lactic)acid [70-75], Gold [76; 77], Titanium [46; 57; 78-95], Ceramic [72; 83; 96-99], Silicone rubber [46; 67; 68; 100-117], Polyethylene Terephthalate [71; 78; 101; 118-123], Perspex [44; 45], nylon [124; 125], glass [126-132], silica [133-136], and gelatine [137-139]. The surfaces of these materials were microtextured or left smooth (control). These substrates were untreated or treated by ultraviolet irradiation, or received a radio frequency glow discharge treatment (RFGD) or both [67; 86; 101; 104; 140-142]. Sometimes the surfaces were coated with ECM proteins like collagen or fibronectin, the aim of those protein coatings is to increase the surface bioactivity [57; 67; 129; 143-145]. Transforming growth factor (TGF) has been applied to microtextured implants to reduce scar-tissue formation *in vivo* [52; 64; 96; 98; 146-151].

Numerous cells, seeded upon those materials, have been studied: fibroblasts from different tissues [5; 45-50; 60; 84; 85; 89; 94; 100; 116; 129; 145; 152-162], osteoblast-like cells [51; 62; 63; 71; 80; 81; 83; 87; 91; 93; 163-169], keratinocytes [138; 141; 144; 170; 171], hepatocytes [61; 172], bone marrow cells [62; 63; 71; 99; 173; 174], epithelial cells [44; 52; 82; 175-178], endothelial cells [9; 56; 114; 123; 179-185], various nerve cells [186; 187], smooth muscle cells [74; 75; 107; 110; 147; 188; 189], several tumour cell lines [14; 70; 190-193], polymorphonuclear cells, and macrophages [130; 133; 194-196].

Methods used in these experiments range from proliferation studies, immunocytochemistry, green fluorescent protein techniques to several forms of microscopy: Scanning electron microscopy (SEM), Transmission electron microscopy (TEM), Confocal laser scanning microscopy (CLSM), Interference reflection microscopy (IRM), Dual wavelength time-lapse fluorescent speckle microscopy (FSM), Atomic force microscopy (AFM) and Optical emission spectroscopy (OES); the last two forms are used in microtexture profiling analysis.

Effects of topographical control on cells which have been studied are: cell-orientation, -shape, -migration, -proliferation, -growth, mRNA transcription expressions of integrin, vinculin, fibronectin, and collagen, tyrosine phosphorylation, adhesion strength, and (de)polymerisation of micro-filaments and microtubules.

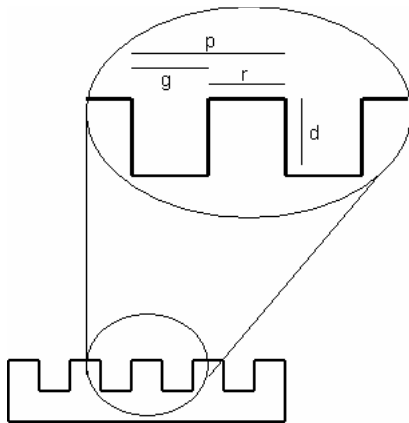


Figure 13. Dimensions of a surface groove pattern as seen in a cross section:

p = pitch, r = ridge- width, g = groove-width, d = groove-depth (adapted from: Walboomers 2000).

What is clear from most studies is that cells elongate and align to the surface grooves. Cells may bridge from one ridge to another ridge, without touching the groove bottom, on patterns up to 2 μm wide. This bridging is independent on the groove depth. Groove/ridge width, ranging from 10 μm to 70 nm, and groove depth, 1 μm to 150 nm, have shown the importance of the ridge in the establishment of topographical control. Microfilaments and vinculin (marker for focal adhesions) appear to be orientated parallel to the surface grooves, this aggregation is most obvious on grooved substrates of 4 μm or less, although, depending on the material used, this alignment has also been observed on larger (> 5 μm) grooved substrates. Vinculin was observed mainly on the ridge of the surface patterns. Depositions of endogenous fibronectin and vitronectin have been studied, and found to be orientated along the surface grooves. As far as migration is concerned; cell protrusions are found extending into the grooves. In case of wider grooves, these cell protrusions extend all the way to the bottom of the grooves. The behaviour of osteoblast-like cells on microtextured surfaces is characterised, besides alignment of cells and cellular extensions, by deposition of collagen fibrils and the formation of calcified nodules. Neither the presence of grooves, nor the dimensions of the grooves have an effect on cell proliferation. Wettability (contact angle between a cell and the substrate surface) and surface free energy (energy required to create a surface of one unit area) influence the cell growth, but play no measurable role in the shape and orientation of cells on microtextured substrates.

Although many studies have shown the cellular alignment along the microgrooved substrates, this field of study continuously pushes the border forward. The grooves now a day are of nanometre scale [56; 133; 134; 196-199]. Once it was thought that cellular effects disappear at about 1 μm level, but Clark proved with 130 nm wide grooves that epithelial cells still responded by alignment of isolated cells and of the cytoskeleton to the grooves [178]. This is interesting in the area of whether the cells react to local patterns of chemical difference or to features such as topography. The shallow grooves loose out to chemical tracks, but when the grooves are deeper than 500 nm topographic effects overwhelm the chemical effects. Besides grooves, pits and pillars, “island” topography on nanometre scale has also found its way in the *in vitro* study of cells [54]. Here, 95 nm high, flat topped discs of different diameters (300 nm to 2.5 μm) have shown to evoke fibroblast cytoskeleton changes and temporal cell morphology. Endothelial cells have also been seeded upon these islands, which resulted in good spreading of the cells, which in turn is claimed to be a good morphology for monolayer cells. The nano-topography provides cues similar to those given by collagen, resulting in a more natural phenotype.

The effects of multigrooved surfaces are also a new area of investigation. Yoshinari *et al.* used a gold alloy as master material and with a trapezoid-shaped diamond cutting tool cut macrogrooved (25 μm high, 150 μm wide) mounds. Subsequently, using a V-shaped tip cut 1 μm deep, 2 μm high microgrooves into the macrogrooves. The multigrooves were able to control the orientation of extra cellular matrix produced by the fibroblasts, and thus production, much better than microgrooves alone or flat surfaces [50].

A recent addition to the different substrates is seeding fibroblasts on a combination of collagen gels and microgrooved or smooth titanium or polystyrene substrates [57]. The gels were first added either to the confluent fibroblast culture on the surface or to the fibroblasts were suspended within the collagen gel and then placed onto the surface. Their results suggest that the order in which fibroblasts encounter substratum and extracellular matrix can influence the eventual matrix-cell interactions, and that substratum topography can influence matrix and cell orientation in zones not immediately in contact with the surface.

A new addition in the use of metal oxide based surfaces was presented by Winkelmann *et al.* which combined titanium, aluminium, vanadium, and niobium in producing patterns (dots and stripes) with one metal as the background and the second metal superimposed on the background metal. The seeded osteoblasts exhibited a pronounced reaction on bimetallic surfaces that contained aluminium. Cells tended to stay away from aluminium. Fibronectin and albumin absorption were significantly greater on non-aluminium regions. The investigators believe that the positive surface charge of aluminium account for the controlling factor in the observed cell behaviour [81].

An area where research is just beginning to focus on is the gene-level responses topography. Dalby *et al.* used microarray to probe for consistent gene changes in response to lithographically produced topography with time. They observed that genes involved in cell signalling, DNA transcription, RNA-protein translation, and ECM formation and remodelling are important in the cell response to the grooves [155].

Tissue response to microgrooved surfaces both in vitro and in vivo

The response of tissues on the use of microgrooved surfaces is described extensively. While some research groups simply observe the effects of soft tissues on the implanted substrates [105], others add cells and growth factors to their elaborate implants and focus “just” on the wound healing for 3 weeks [148]. The migration of an epithelial tissue sheet was found to be enhanced by polystyrene microgrooves, while migration across the microgrooves was inhibited. This pattern found by Dalton *et al.* is similar to that of intact epithelial tissue [176]. By adding Transforming

growth factor- β 1, 2, or 3 (TGF- β) on the substrates the outgrowth of epithelial tissue was inhibited on both smooth and microgrooved surfaces [52]. The relevance of TGF- β in wound healing has been investigated by several researchers [64; 65; 143; 147]. Pandit *et al.* [148] incorporated TGF- β into collagen scaffolds and observed an enhanced healing process in terms of faster epithelialisation and contraction rate. In an extension to these findings Gehrke *et al.* [200] added TGF- β 3 to their microgrooved silicone implants to see whether TGF- β influences the fibrous capsule formation. Although they did not find a significant difference it is still believed that surface topography is important in establishing tissue organisation adjacent to implants, with smooth surfaces generally being associated with fibrous tissue encapsulation. Grooved topographies appear to have promise in reducing encapsulation in the short term, but additional studies employing three-dimensional reconstruction and diverse topographies are needed to understand better the process of connective-tissue organisation adjacent to implants [82; 85; 106]. The formation of fibrous capsule in vivo are quite complicated as mentioned in the studies by Johnson *et al.* [119], Butler *et al.* [118], Shannon *et al.* [201], and Parker *et al.* [67]; implant location, surface charge, collagen types, and coating are just some of the factors involved. Huang *et al.* [146] investigated if a polycaprolactone (PCL) scaffold and TGF-beta1-loaded fibrin glue could be used for tissue engineering applications and found that the scaffold loaded with TGF-beta1 and implanted subperiosteally was found to be richly populated with chondrocytes. Mature bone formation was also identified. They conclude that scaffolds loaded with TGF-beta1 can successfully recruit mesenchymal cells and that chondrogenesis occurred when this construct was implanted subperiosteally.

Research groups [82;175] have observed that grooved implants can obstruct epithelial downgrowth on percutaneous devices and improve performance and longevity of percutaneous devices by promoting tissue integration. As well as, that grooved topographies show reduction of encapsulation and increases in mineralized bone tissue process of connective tissue organisation adjacent to the microtextured implants [85]. This potential of surface grooves to influence matrix and cell orientation and migration in areas immediately adjacent or not immediately in contact with the surface has been described before [57; 176].

Other research groups have seen no orientation along the surface grooves of textured surfaces and no difference between the capsules surrounding smooth or microgrooved implants [105; 106]. Neither have they seen a significant difference in tissue reaction influence around implants, which are either microgrooved, roughened or left smooth [53; 67; 68].

CELLS AND GRAVITATIONAL BIOLOGY

Gravity

Gravity is a force of attraction between all matters in the universe. It is the weakest known force in nature, but it still manages to hold galaxies and the solar system together, because it is always attractive and it can act over very large distances. The other fundamental forces include the strong nuclear force, the weak nuclear force, and electromagnetism, together they are responsible for all of the forces exchanged between matter particles.

Sir Isaac Newton (1642 - 1727) discovered that a force is required to change the speed or direction of movement of an object. He realized that the force called "gravity" must make an apple fall from a tree. Furthermore, he deduced that gravitational forces exist between all objects. Some objects require more force to move than others. The force needed to push an object at a given acceleration rate is proportional to the object's mass. Because of this relationship, gravity is commonly referred to as the resultant acceleration of a mass due to gravitational force (**info box 1**).

Info Box 1

The force of gravity that one body exerts on another can be expressed as:

$$F_{\text{gravity}} = (G * m_1 * m_2) / r^2 \quad [1]$$

F = Force of gravity experienced by bodies
G = Gravitational constant: $6.6726 * 10^{-11} \text{ m}^3 \text{ kg}^{-1} \text{ s}^{-2}$
m₁ = mass of body one
m₂ = mass of body two
r = radius of body

Newton's second law states that:

$$F = m * a \quad [2]$$

Substitute the 'F' in equation [1] with 'm * a' in equation [2]:

$$m * a = (G * m_1 * m_2) / r^2 \quad [3]$$

Divide both sides by m:

$$a = (G * m) / r^2 \quad [4]$$

At a 90 degree angle:

$$a = g \quad [5]$$

The new formula is:

$$g = (G * m) / r^2 \quad [6]$$

This gives the acceleration due to gravity.

Knowing the gravitational constant, the mass of the Earth, and the distance from the centre of the Earth, you can calculate the gravity of Earth.

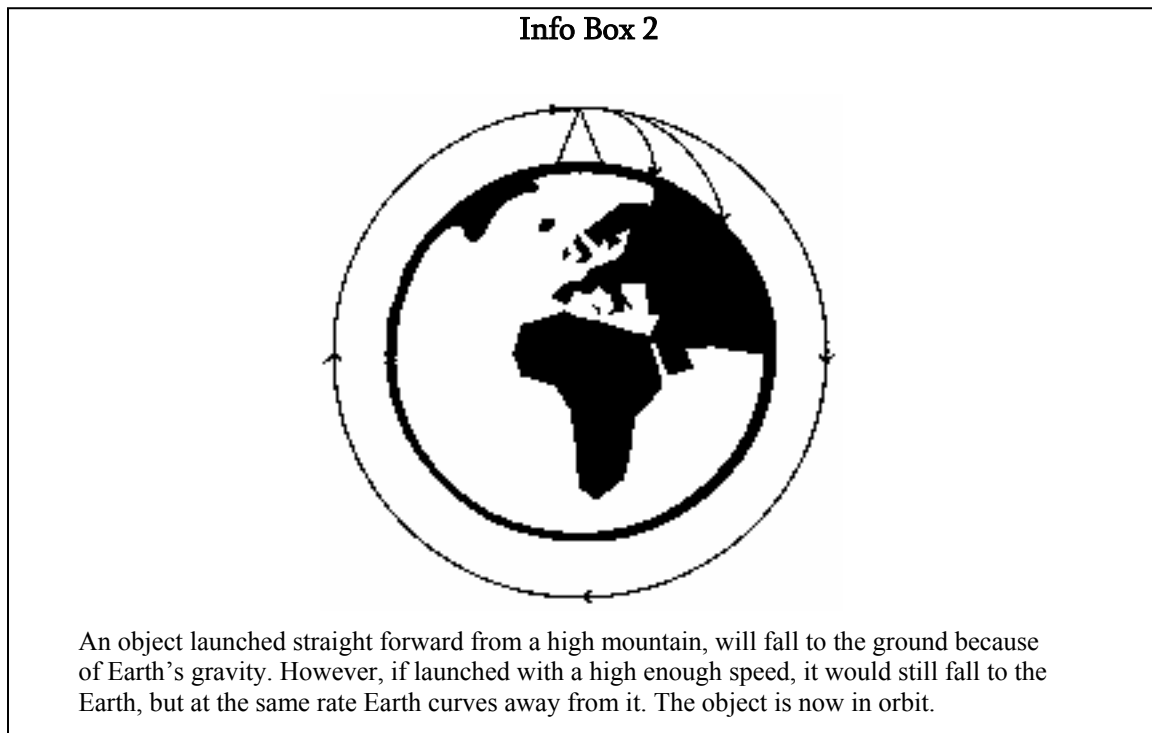
Satellites (e.g. the Moon) orbit around the Earth. The satellites move in a circular path around a centre point which is the Earth. The force holding the satellite in its circular path is the centripetal force (a.k.a. centrifugal force). However they also feel the gravitational pull of the Earth. The two forces are equal to each other:

$$F_{\text{centripetal}} = F_{\text{gravity}}$$
$$(m_1 * v^2) / r = (G * m_1 * m_2) / r^2 \quad [7]$$

When measured at sea level on the surface of Earth, an object experiences what is commonly referred to as "1 g" or "one Earth gravity." If an object was dropped, the resultant acceleration is approximately 9.81 meters per second squared (m/s²). In Earth's orbit, Earth's gravity force is counteracted by the spacecraft's motion around the earth (Centrifugal Force). The net force on the object is very close to zero. In practice, such accelerations range from about one percent of Earth's gravitational acceleration (onboard aircraft in parabolic flight) to approximately one part in a million (when orbiting the Earth).

Technically, an object is in free fall when gravity and only gravity is allowed to act on it. In other words, it is what most people generally refer to as falling. To really understand free fall one must also understand acceleration. Most people think acceleration is simply when an object increases speed. By its most exact definition however, acceleration is any change in an object's speed or

direction. Satellites orbiting Earth are also considered to be in free fall. To explain this, imagine that one is standing on top of a really tall mountain (**info box 2**). You throw a ball straight forward, the ball will fall to the ground, because Earth's gravitational force directed toward the centre of the Earth will pull it down. If you throw the ball really fast, it not only falls toward the Earth it also travels outward, over the Earth. If you could throw the ball fast enough it would travel so far over the ground that by the time it came down the ground would have curved away from it because the Earth is round. In this case the ball is a satellite orbiting Earth with nothing but gravity acting on it, hence the ball is in free fall.



Albert Einstein (1879 - 1955) presented in 1915 a revision of Newton's works in his general theory of relativity (a flaw was discovered in Newton's theory, concerning the orbit of Mercury, which was circling the Sun in a way Newton had not predicted). This work completely rewrote the way we look at gravity and even changed our understanding of the very structure of the universe. According to Albert Einstein, there is no difference between the acceleration of gravity and any other acceleration (principle of equivalence). No person or instrument in a closed box could tell the difference between the force of gravity and the force caused by a rocket engine accelerating the box at a uniform 9.81 m/s^2 .

Thus, g is the acceleration caused by the gravitational attraction of a body (e.g. a planet). The acceleration so derived has the same dimensions as the acceleration produced by uniform circular motion on a centrifuge. Experiments conducted on ground-based centrifuges indicate that centrifugation provides an excellent simulated gravity environment for gravitational biology research as long as the centrifuge is of sufficient diameter (radius of rotation) and capable of a sufficient rotation rate [202-207].

Physical phenomena

The effects of gravity on a cell can be divided in direct and indirect effects. Direct are the effects of acceleration onto the cells or the intracellular components. Indirect effects are effects on the cell environment, like the ECM or the tissue of which the cell is part of. The researcher should bare in

mind these indirect effects while interpreting the results of cell culture experiments. There are several phenomena which, especially at the cell *in vitro* level, play a considerable role in gravitational biological research, namely sedimentation, hydrostatic pressure, diffusion, convection, and buoyancy [208-210].

Sedimentation

Sedimentation is the downwards movement of a particle relative to its surrounding medium. During this downward movement the medium, such as fluid, there are three kinds of forces on the particle; downward gravity force, upward buoyancy, and upward resistance known as drag force. This drag force is behind the object due to viscosity and also turbulence behind the particle.

Sedimentation is an important difference between an experimental environment on Earth or in space. Statocytes, specialised cells in the root tip of plants, contain amyloplasts. These relatively big and heavy particles play a part in the positive gravitropism of plants. Gravitropism (sometimes called geotropism in older texts) is a key regulatory process, in response to gravity, in plants to insure that roots grow down and shoots grow up in developing seedlings [208; 209] .

Hydrostatic pressure

In situations of hypergravity part of the pressure which is acting on a surface area derives from the weight of the liquid column standing above these surfaces, like culture medium above a monolayer of cells.

Hydrostatic pressure is linearly proportional to g . Hydrostatic pressure due to weight is zero under weightlessness conditions obviously. During ground based hypergravity experiments not only the hydrostatic pressure derived from the liquid column on the surface of the culture plate should be taken into account but also the atmospheric pressure, which is about 100 kPa at sea level [208; 209].

Diffusion

Molecules in a gas or liquid continually move about and collide with each other. This process, diffusion, is better known as the Brownian movement of small particles in solution. Diffusion takes place in response to a concentration gradient. The flow of molecules/particles is opposite to the concentration gradient. Diffusion is not altered under microgravity. Therefore, in the absence of sedimentation, diffusion is under weightlessness conditions the most important remaining means to mix the fluid or gas [208; 209].

Convection

Differences in density also cause movement in a gas or liquid. This known as convection and it appears when a part of a liquid or gas heats up and, thus, expands. The density of the heated liquid or gas decreases. This heated part shall move upwards since it is lighter than its surroundings. This phenomenon is only present under gravity (acceleration) conditions and is absent in weightlessness. The absence of convection during *in vitro* experiments in space results that spent medium culture, metabolic waste products, as well as autocrine growth factors accumulate around the cells and tissues [208; 209; 211].

Diffusion/Convection

The effects of diffusion and convection differ considerably in magnitudes. Local differences in density of the extracellular medium at microgravity can no longer lead to convective currents around cells that are surrounded with free fluid as they would under normal gravity conditions. In the absence of microconvective flows, the mixing of gases, solutes, solvent molecules, and local

temperatures would depend predominantly on diffusion, and thus be reduced dramatically (**info box 3**).

From the info box it can be conceived that convective currents can cover a distance much faster than diffusion. In other words, we can expect that cells may “get stuck in their dirty bathwater” during prolonged exposures to microgravity. Some of the possible consequences of such poor mixing on cells are effects on their cytoskeleton, membrane potential, and cell behaviour [209].

Buoyancy

Buoyancy is the capacity to float in a liquid medium or even a gas. Buoyancy can also result in convection of a part of a liquid or gas to rise. Local changes in temperature or composition can result in density variations and can therefore cause convection. The force of buoyancy works opposite to gravity, and is proportional to the objects volume and the weight of the liquid. Buoyancy driven convection is not present in a weightlessness environment, making it an important difference between ground and space experiments [208; 209].

Info Box 3

A typical diffusion constant of salt in water (e.g. K⁺ ions in water) is $D = 0.001 \text{ mm}^2/\text{s}$.
In order to cover a distance $s = 2 \text{ mm}$ by diffusion, it would take the K⁺ ions approximately:

$$t = s^2/D$$

$$t = 4/0.001 = 4000 \text{ s} = 1.1 \text{ hrs}$$

s = displacement distance

D = diffusion constant

In contrast, convection currents that results from density differences can cover the same distance much faster. Assume a spherical particle with radius $r = 0.1 \text{ mm}$ in water. Water density of water $\rho = 1.0 \text{ g/cm}^3$ and the viscosity $\eta = 0.01 \text{ poise}$. Assume the specific gravity of the particle is 1% more than water, $\rho = 1.01 \text{ g/cm}^3$. At normal gravity of $g = 9.81 \text{ m/s}^2$ the particle will sink at speed v at which Stokes friction F equals the gravitational pull:

$$F = 6\pi r\eta v = 4/3\pi r^3(\rho_{\text{water}} - \rho)g$$

Consequently,

$$v = (2/9\eta)(\rho_{\text{water}} - \rho) r^2 g = 0.2 \text{ mm/s}$$

In other words, the K⁺ ions in a convective current that resulted from only a 1% difference in density would cover the distance of 2 mm in 10 s, which is 400 times faster as by diffusion alone. In short, convective currents, not diffusion, are responsible for the rapid mixing of gases and solvents.

On the use of ground-based machines or simulating hyper- & microgravity

There are several advantages and reasons to perform ground-based research studies prior to conducting experiments in space. Most ground based research facilities are readily available and the studies may be performed on a day to day basis and result in sound scientific data. Ground based research is interesting to perform basic acceleration studies and test the effects of

accelerations in preparation of real microgravity experiments onboard orbiting spacecraft, sounding rockets, or parabolic flight aircraft. Also, to define the future space-experiment setup, it is interesting to investigate more specifically, the parameters which might be involved in real microgravity conditions. Ground based studies are sometimes necessary to test hardware performance under simulated hypergravity conditions. Particularly, the effects of launch accelerations and vibrations on the test system whether or not in combination with the hardware [209; 212-214].

Ground facilities are differentiated in hypergravity and microgravity. In case of simulating hypergravity, the Medium Sized Centrifuge for Acceleration Research (MidiCAR) is a dedicated centrifuge in which cell or tissue samples may be exposed to accelerations up to 100 times Earth's gravity [215-217].

A more extended range of machines are available to simulate microgravity; The Random Positioning Machine (RPM), sometimes referred to as 3D-clinostat, simulates microgravity on the principle of gravity vector averaging. Since gravity is a vector (it has both a magnitude and a direction), constantly changing the samples position with regard to the Earth's gravity vector direction, the sample may experience this as a zero-gravity environment. The level of simulation within this RPM depends very much on the speed of rotation and the distance of the sample to the centre of rotation [218].

The Free Fall Machine (FFM) can simulate microgravity for long duration experiments. The system is based on the principle of free fall. The free fall periods are at a maximum of about 900 ms and are interrupted by an acceleration of around 20 x g for about 20-80 ms. The hypothesis, developed by Dr. Mesland, is that systems may experience the FFM as a continuous free fall environment if the gravity perception time in the FFM of the system is shorter than the intermediate period of 20-80 ms [219].

The working principle of a parabolic aircraft is exactly the same as that of a FFM, only the time courses are different. To create a microgravity environment the aircraft follows a trajectory: starting from a steady normal horizontal flight, then the aircraft pulls up for about 8 seconds. Engine thrust is then reduced strongly to set-in the parabolic flight. Microgravity is maintained for about 15 sec, after which the aircraft pulls up to come back to steady horizontal flight. The number of parabolas flown per flight hour is between 12 and 15, depending on the interval time between parabolas [209; 213; 214].

Cell response to changes in gravity (gravisensing)

The consequences of basic physics do not mean that it is impossible for cells to sense gravity. After all, they are biological systems of immense complexity that have evolved to expect gravity to be present at all times. Yet, there is no reasonable possibility for cells to sense gravity because all other forces (electrical, polymerisation, surface) in the cellular world are so much greater. Although, cells are indeed too small to experience gravity as a major force, the cellular environment is considerably larger, and it is influenced by gravity through the generation of pressure, and buoyancy-driven convective currents for example. The cells may sense the gravity-mediated changes in their environment, and thus may be able to detect gravity after all, albeit in an indirect way [220-226].

The term gravisensing means, ideally, the detection of the amplitude and direction of inertial acceleration. There are a very few direct ways for cells to detect the direction (to tell up from down) because their own weight is too small compared to other forces, but they are able to detect the amplitude of gravity. Some cells are equipped with specialised gravisensing organs or are specialised gravisensors themselves, like hair cells and statocytes in plant roots [227; 228]. Most

cells are not specialised for the task, but respond to microgravity conditions by indirect consequences of the lack of inertial acceleration.

Although it is clear that physical forces, such as those due to gravity, are fundamental regulators of tissue development, little is known about how living cells sense these signals and convert them into biochemical response. This transduction process, which is at the core of gravity sensation, is known as mechanotransduction [229; 230]. Mechanotransduction at work can be observed in the otoliths in the sensory cells of the inner ear. Another well known example is bone-resorption observed in space farers who undergo long term space flight. The change in loading pattern, caused by microgravity, results in immediate bone remodelling [128; 231]. Osteoblasts and osteoclasts, responsible for this remodelling do not possess statoliths, yet the bone cells and other cells within other tissues are sensitive to mechanical forces. A potential gravity sensor could be the nucleus of the eukaryotic cell. The packed DNA inside the nucleus makes the nucleus about 18% denser compared to the rest of the cell. This higher density makes the nucleus sink to the bottom of the cell in 1 g environment; however, the cytoskeleton actively maintains the nucleus in place. This process transfers a nuclear load to the cytoskeletal fibres adjacent to the nucleus and could be another way of transducing information about the direction and magnitude of the gravity field the cell is subjected to [208]. A molecular mechanism for sensing nuclear positioning is until now unknown.

Extensive research has been performed on the lymphocytes in microgravity [195; 232-235]. Depending whether the lymphocytes are free floating or adhered, the mitogenic response of the cells is reduced. It appears that Interleukin-1, -2 activated lymphocytes need to anchor and spread in order for a sound response [236; 237].

In case of fibroblasts, mechanical stress is an important and specific regulator of distinct extracellular matrix (ECM) components. There are different possibilities how genes for an ECM component are regulated by mechanical signals. In a primary response, a cellular mechanotransduction pathway activates available transcription factor, which in turn binds to “mechano-responsive” regulatory element in the ECM gene promoter. A secondary response would be a mechanical signal which induces the transcription and synthesis of nuclear factor, which transactivates an ECM gene (fibronectin is an ECM gene transactivated by transcription factor EGR-1, via the ras/Erk-1/2 pathway). A third possibility is that mechanical stress induces synthesis and/or secretion of growth factor, which indirectly regulates ECM gene expression via auto- or paracrine feedback loop of TGF- β . This latter possibility seems to be responsible for long term adaptive responses of connective tissues to mechanical stress. Gene array studies of the cells grown in microgravity show remarkable effects. There are increases and decreases of message levels for many genes in microgravity. This implies that cells are mounting a massive gene regulatory effort to acclimate to the microgravity environment and maintain homeostasis. Long term focusing on protein expression (proteomics) could supply information on the cells adjustment (acclimation) to the space environment [238].

The effects of altered gravity on the cell membrane and the cytoskeleton have been studied; the more extensive studies try to link the environment factor gravity (usually microgravity) with the functional status of membranes and elements of cytoskeleton. The involvement of membrane structures and cytoskeleton in the processes of reception and realization of gravitational stimulus allows us to evaluate the extent of the direct or indirect influence of gravity on cell functioning in the gravitational field [239; 240]. Gruener *et al.* [241] studied the effects of altered gravity on the aggregation of the nicotinic acetylcholine receptors and the structure of the cytoskeleton in cultured muscle cells. Marked changes were shown in the distribution and organization of actin filaments and a reduced incidence of acetylcholine receptor aggregates. Hence, they concluded that the sensitivity of synaptic receptor aggregation and cytoskeletal morphology suggests that

microgravity alters cell behaviour. Investigations more focussed have revealed changes in both the microfilament and microtubule network. Thinning and redistribution of MF [242] the loss of self-organisation and local disorders of MT as well as a general increase in apoptosis in the early phases of microgravity have all been described [235; 242-244]. Seitzer *et al.* [245] noticed in human fibroblasts a increase in collagen synthesis under microgravity conditions, while increasing g resulted in decreasing collagen production compared to 1 g controls. Croute *et al.* [246] had human dermal fibroblasts undergo hypergravity (2-20 g) for up to 8 days. Changes in cell shape (star shape with fine filopodia) and anchoring point arrangement appeared above 15 g. The centrosome was shown to migrate to the nucleus side compared to the above the nucleus position in 1 g controls. The fibronectin network thickened after 8 day of culture and collagen fibrils appeared linking ordered arrays of fibres. According to their observations hypergravity can induce change in fibroblast cell shape, migration way, and anchorage leading to reorganisation of ECM without a hampering cell proliferation. Recently, Tabony *et al.* [247] tackled the problem of molecular processes in biological systems affected by gravity. Since (bio)chemical reactions do not depend upon gravity, it is proposed that biological systems might depend on gravity by way of the bifurcation properties of certain non-linear chemical reactions [223; 244; 248]. By way of combining reaction and diffusion the homogenous solution spontaneously self-organises and may determine the morphology that develops. They found that MT shows this behaviour. Experiments carried out under low gravity conditions show that the presence of gravity at the bifurcation time actually triggers the self-organising process. This is an experimental demonstration of how a very simple biochemical system, containing only two molecules, can be gravity sensitive. As microtubule organisation is essential to cellular function, it is quite plausible that the type of processes described in that article provide an underlying explanation for the gravity dependence of living systems at a cellular level.

As already mentioned the cell-matrix adhesion contacts form the physical link from the ECM across the cell membrane to the cytoskeleton. Because of their strategic location, transmembrane proteins within cell-matrix contacts are good candidates for translating mechanical into chemical signals. Two such transmembrane components have been implicated: ion channels and integrins. In mechanosensory nerve and muscle cells, stretch sensitive cation channels are likely to be the actual strain gauges; they might be attached directly to the ECM and/or the cytoskeleton within matrix contacts. In non-excitable cells such as fibroblasts, ion channels could be involved in mechanotransduction as well, but in addition there are integrins which can work as stretch sensors themselves. Immediate consequences of ECM derived forces transmitted to integrins are the Rho-dependent assembly and growth of focal adhesion complexes at these sites, an increase in cytoskeletal tractional force, and a triggering of MAP kinase and NF- κ B pathways within the cell. Fibroblasts undergoing tension, within collagen matrices, induce transient activation of MAP kinase (p38 and ERK) indicate that MAP kinases can act as general, but unspecific, transducers of mechanical stress towards the cell interior [249].

Gravity alterations, being a physical environmental signal, causes shift in morphological cell characteristics. Although the direct influences of gravity are more pronounced in vitro and non-direct influences usually expresses themselves in unicellular organism in vivo. Morphogenesis processes like adhesion and locomotion are controlled by the cells' signal transduction systems. And gravity affects such processes. Minor disturbances in this system coming from the environment, due to amplification, may provide significant modulations of the signals. Research of this system at the level of molecular cell reception is of great importance and interest [250].

Like all living biological systems, a cell needs both energy and information in order to function. Gaining insight into the mechanisms responsible for cell gravisensitivity can be acquired by

solving the fundamental problem of molecular physiology. Morphological deformations are the result of spatial disposition changes of cells in the gravitation field. The cell shape is altered at one point [250]. Interaction between cell shape and functions present one of the most intriguing problems in biology. There is still a large discrepancy between the empirical use of mechanical forces in orthopaedics, dentistry and plastic surgery, and the theoretical understanding of the cellular and molecular mechanisms involved. Progress has been made in discovering the conversion of mechanical into chemical signals, triggering of intracellular signalling pathways, and the mechanisms of mechanically induced gene activation. However, many important details have to be solved. For instance, the biophysical mechanism which converts a mechanical stimulus into a chemical signal. Also the specificity of the cellular response to externally applied mechanical stress. Since forces propagate throughout the cell, any vector stress will be sensed as tension in one part and compression in another part of the cell. One stimulus triggers distinct signals in different locations, resulting in an array of signalling pathways [238]. Wherever a cell response occurs, one should look first of all for an extracellular cause, like a gravity dependent process. Secondly an intracellular, cytoskeletal, cause should be sought in the context of weak zones of the cytoskeleton.

RESEARCH OBJECTIVES

Summary

The components of the cytoskeleton and the focal adhesions of the cell are key players in the cells' adhesion and locomotion across the microtextured surface of substrates. The orientations and morphology of the cells are important, for these cells should resemble correct normal tissue as closely as possible if it wants to be effective in repairing or constructing tissue. Pattern formation or contact guidance is involved in meeting those requirements. Previous studies have expanded the knowledge and understanding how these surface topography principles work and have resulted in the development and improvement of biomaterials used in medical implants. With humans, slowly but steadily, expansion into space, new questions are raised and new problems are faced. Reports of involvement of the cytoskeleton and focal adhesions in relation to microgravity and the changes in cell morphology due to gravity have raised questions how this comes about. Do cells sense changes in gravity directly, what intracellular process and signalling pathways are involved? The field of gravitational cell biology will obtain that knowledge and comprehend the behaviour of cells in changed gravity circumstances. This knowledge could be used in helping the development and manufacturing of tissue engineered constructs suitable for use on this world or beyond.

Research Hypothesis

The response of cells *in vitro* towards micro-structured surfaces will drastically change when exposed to micro- and hyper-gravity conditions, and that this will be a useful tool in elucidating the cell mechanosensing process.

Therefore, the influence of hypergravity and simulated microgravity and substrate surface micro-morphology on cell appearance and differentiation will be investigated.

Research Questions

1. Does the cellular morphological behaviour *in vitro* to standardised, well characterised surfaces relate to the geometrical properties of these surfaces under different gravity conditions?

2. Do the intracellular cytoskeletal components orientation, organisation, and distribution differ between cells cultured on smooth and microtextured surfaces under different gravity conditions?
3. Is the cellular response to microtexture altered if different topography dimensions are used?
4. What intracellular signalling pathways are triggered under simulated microgravity conditions?
5. What genes are up/down-regulated under micro/hyper-gravity conditions?
6. To what topography dimension do cells still respond by adjusting their cell shape?
7. Can the MidiCAR centrifuge be used as a model to study inertial shear force?
8. Evaluation of the suitability of different ground-based machines designed for the simulation of micro/hyper-gravity. Are the results comparable with earlier findings in space?
9. Several scientific publications propose mechanisms for the response of cells to gravity alterations (gravisensing). Can any of these theories be proven true or denied?

REFERENCES

1. Alberts, B., Bray, D., Johnson, A., Lewis, J., Raff, M., Roberts, K., and Walter, P. (1998). "Essential Cell Biology," Garland Publishing, New York.
2. Alberts, B., Bray, D., Johnson, A., Lewis, J., Raff, M., Roberts, K., and Walter, P. (2002). "Molecular Biology of the Cell," 4th edition ed., Garland Publishing, New York, NY.
3. Lodish, H., Berk, A., Zipursky, S. L., Matsudaira, P., Baltimore, D., and Darnell, J. (2000). "Molecular Cell Biology," W.H. Freeman and Compnay, New York, NY.
4. Parsons, J. T. (2003). Focal adhesion kinase: the first ten years. *J Cell Sci* 116, 1409-16.
5. Heidemann, S. R., Kaech, S., Buxbaum, R. E., and Matus, A. (1999). Direct observations of the mechanical behaviors of the cytoskeleton in living fibroblasts. *J Cell Biol* 145, 109-22.
6. Geiger, B. and Bershadsky, A. (2001). Assembly and mechanosensory function of focal contacts. *Curr Opin Cell Biol* 13, 584-92.
7. Choquet, D., Felsenfeld, D. P., and Sheetz, M. P. (1997). Extracellular matrix rigidity causes strengthening of integrin-cytoskeleton linkages. *Cell* 88, 39-48.
8. Lee, T. Y. and Gotlieb, A. I. (2003). Microfilaments and microtubules maintain endothelial integrity. *Microsc Res Tech* 60, 115-27.
9. Traub, O. and Berk, B. C. (1998). Laminar shear stress: mechanisms by which endothelial cells transduce an atheroprotective force. *Arterioscler Thromb Vasc Biol* 18, 677-685.
10. Zamir, E. and Geiger, B. (2001). Molecular complexity and dynamics of cell-matrix adhesions. *J Cell Sci* 114, 3583-90.

11. Zamir, E., Katz, B. Z., Aota, S., Yamada, K. M., Geiger, B., and Kam, Z. (1999). Molecular diversity of cell-matrix adhesions. *J Cell Sci* 112 (Pt 11), 1655-69.
12. Shyy, J. Y. and Chien, S. (2002). Role of integrins in endothelial mechanosensing of shear stress. *Circ Res* 91, 769-775.
13. Vuori, K. (1998). Integrin signaling: tyrosine phosphorylation events in focal adhesions. *J Membr Biol* 165, 191-9.
14. Klemke, R. L., Leng, J., Molander, R., Brooks, P. C., Vuori, K., and Cheresch, D. A. (1998). CAS/Crk coupling serves as a "molecular switch" for induction of cell migration. *J Cell Biol* 140, 961-72.
15. Abassi, Y. A. and Vuori, K. (2002). Tyrosine 221 in Crk regulates adhesion-dependent membrane localization of Crk and Rac and activation of Rac signaling. *EMBO J* 21, 4571-82.
16. Hayashi, I., Vuori, K., and Liddington, R. C. (2002). The focal adhesion targeting (FAT) region of focal adhesion kinase is a four-helix bundle that binds paxillin. *Nat Struct Biol* 9, 101-6.
17. Wittmann, T. and Waterman-Storer, C. M. (2001). Cell motility: can Rho GTPases and microtubules point the way? *J Cell Sci* 114, 3795-803.
18. Mitchison, T. J. and Cramer, L. P. (1996). Actin-based cell motility and cell locomotion. *Cell* 84, 371-9.
19. Small, J. V., Kaverina, I., Krylyshkina, O., and Rottner, K. (1999). Cytoskeleton cross-talk during cell motility. *FEBS Lett* 452, 96-9.
20. Small, J. V. and Kaverina, I. (2003). Microtubules meet substrate adhesions to arrange cell polarity. *Curr Opin Cell Biol* 15, 40-7.
21. Beningo, K. A., Dembo, M., Kaverina, I., Small, J. V., and Wang, Y. L. (2001). Nascent focal adhesions are responsible for the generation of strong propulsive forces in migrating fibroblasts. *J Cell Biol* 153, 881-8.
22. Noren, N. K., Arthur, W. T., and Burridge, K. (2003). Cadherin engagement inhibits RhoA via p190RhoGAP. *J Biol Chem* 278, 13615-8.
23. Arthur, W. T. and Burridge, K. (2001). RhoA inactivation by p190RhoGAP regulates cell spreading and migration by promoting membrane protrusion and polarity. *Mol Biol Cell* 12, 2711-20.
24. Gauthier-Rouviere, C., Vignal, E., Meriane, M., Roux, P., Montcourier, P., and Fort, P. (1998). RhoG GTPase controls a pathway that independently activates Rac1 and Cdc42Hs. *Mol Biol Cell* 9, 1379-94.
25. Tsuji, T., Ishizaki, T., Okamoto, M., Higashida, C., Kimura, K., Furuyashiki, T., Arakawa, Y., Birge, R. B., Nakamoto, T., Hirai, H., and Narumiya, S. (2002). ROCK and mDia1 antagonize in Rho-dependent Rac activation in Swiss 3T3 fibroblasts. *J Cell Biol* 157, 819-30.
26. Kaverina, I., Krylyshkina, O., Gimona, M., Beningo, K., Wang, Y. L., and Small, J. V. (2000). Enforced polarisation and locomotion of fibroblasts lacking microtubules. *Curr Biol* 10, 739-42.
27. Yokoyama, K., Kaji, H., Nishimura, K., and Miyaji, M. (1990). The role of microfilaments and microtubules in apical growth and dimorphism of *Candida albicans*. *J Gen Microbiol* 136 (Pt 6), 1067-75.
28. Dugina, V. B., Svitkina, T. M., Vasil'ev, I. u. M., and Gel'fand, I. M. (1987). [Changes in the form and cytoskeleton of cultured fibroblasts as affected by 12-tetradecanoylphorbol-13-acetate]. *Tsitologiya* 29, 1138-43.
29. Uitto, V. J., Larjava, H., Peltonen, J., and Brunette, D. M. (1992). Expression of fibronectin and integrins in cultured periodontal ligament epithelial cells. *J Dent Res* 71, 1203-11.
30. Curtis, A. and Riehle, M. (2001). Tissue engineering: the biophysical background. *Phys Med Biol* 46, R47-65.

31. Ferber, D. (1999). Lab-grown organs begin to take shape. *Science* 284, 422-3, 425.
32. Strehl, R., Schumacher, K., de Vries, U., and Minuth, W. W. (2002). Proliferating cells versus differentiated cells in tissue engineering. *Tissue Eng* 8, 37-42.
33. Minuth, W. W., Sittinger, M., and Kloth, S. (1998). Tissue engineering: generation of differentiated artificial tissues for biomedical applications. *Cell Tissue Res* 291, 1-11.
34. Langer, R. and Vacanti, J. P. (1993). Tissue engineering. *Science* 260, 920-6.
35. Vacanti, J. P. and Langer, R. (1999). Tissue engineering: the design and fabrication of living replacement devices for surgical reconstruction and transplantation. *Lancet* 354 Suppl 1, S132-4.
36. Langer, R. S. and Vacanti, J. P. (1999). Tissue engineering: the challenges ahead. *Sci Am* 280, 86-9.
37. Hubbell, J. A. (1999). Bioactive biomaterials. *Curr Opin Biotechnol* 10, 123-9.
38. Hubbell, J. A. (1995). Biomaterials in tissue engineering. *Biotechnology (N Y)* 13, 565-76.
39. Lysaght, M. J., Nguy, N. A., and Sullivan, K. (1998). An economic survey of the emerging tissue engineering industry. *Tissue Eng* 4, 231-8.
40. Lysaght, M. J. and Reyes, J. (2001). The growth of tissue engineering. *Tissue Eng* 7, 485-93.
41. von Recum, A. F., Shannon, C.E., Cannon, C. E., Long, K. J., van Kooten, T. G., and Meyle, J. (1996). Surface roughness, porosity, and texture as modifiers of cellular adhesion. *Tissue Eng* 2, 241-53.
Notes: Presented at the 7th Taniguchi Conference on Polymer Chemistry, Tissue Engineering with the Use of Biomedical Polymers, Kyoto, Japan, November 7-12, 1995.
42. Curtis, A. and Wilkinson, C. (1997). Topographical control of cells. *Biomaterials* 18, 1573-83.
43. Meyle, J., Wolburg, H., and von Recum, A. F. (1993). Surface micromorphology and cellular interactions. *J Biomater Appl* 7, 362-74.
44. Clark, P., Connolly, P., Curtis, A. S., Dow, J. A., and Wilkinson, C. D. (1990). Topographical control of cell behaviour: II. Multiple grooved substrata. *Development* 108, 635-644.
45. Clark, P., Connolly, P., Curtis, A. S., Dow, J. A., and Wilkinson, C. D. (1987). Topographical control of cell behaviour. I. Simple step cues. *Development* 99, 439-448.
46. Walboomers, X. F., Croes, H. J., Ginsel, L. A., and Jansen, J. A. (1999). Contact guidance of rat fibroblasts on various implant materials. *J Biomed Mater Res* 47, 204-12.
47. Walboomers, X. F., Croes, H. J., Ginsel, L. A., and Jansen, J. A. (1998). Growth behavior of fibroblasts on microgrooved polystyrene. *Biomaterials* 19, 1861-1868.
48. Walboomers, X. F., Ginsel, L. A., and Jansen, J. A. (2000). Early spreading events of fibroblasts on microgrooved substrates. *J Biomed Mater Res* 51, 529-534.
49. Walboomers, X. F., Monaghan, W., Curtis, A. S., and Jansen, J. A. (1999). Attachment of fibroblasts on smooth and microgrooved polystyrene. *J Biomed Mater Res* 46, 212-20.
50. Yoshinari, M., Matsuzaka, K., Inoue, T., Oda, Y., and Shimono, M. (2003). Effects of multigrooved surfaces on fibroblast behavior. *J Biomed Mater Res* 65A, 359-368.
51. Matsuzaka, K., Walboomers, X. F., Yoshinari, M., Inoue, T., and Jansen, J. A. (2003). The attachment and growth behavior of osteoblast-like cells on microtextured surfaces. *Biomaterials* 24, 2711-9.

52. Walboomers, X. F., Dalton, B. A., Evans, M. D., Steele, J. G., and Jansen, J. A. (2002). Transforming growth factor-beta 1, 2, and 3 can inhibit epithelial tissue outgrowth on smooth and microgrooved substrates. *J Biomed Mater Res* 60, 445-51.
53. Walboomers, X. F., Croes, H. J., Ginsel, L. A., and Jansen, J. A. (1998). Microgrooved subcutaneous implants in the goat. *J Biomed Mater Res* 42, 634-41.
54. Dalby, M. J., Childs, S., Riehle, M. O., Johnstone, H. J., Affrossman, S., and Curtis, A. S. (2003). Fibroblast reaction to island topography: changes in cytoskeleton and morphology with time. *Biomaterials* 24, 927-35.
55. Dalby, M. J., Riehle, M. O., Johnstone, H. J., Affrossman, S., and Curtis, A. S. (2002). Polymer-Demixed Nanotopography: Control of Fibroblast Spreading and Proliferation. *Tissue Eng* 8, 1099-1108.
56. Dalby, M. J., Riehle, M. O., Johnstone, H., Affrossman, S., and Curtis, A. S. (2002). In vitro reaction of endothelial cells to polymer demixed nanotopography. *Biomaterials* 23, 2945-54.
57. Glass-Brudzinski, J., Perizzolo, D., and Brunette, D. M. (2002). Effects of substratum surface topography on the organization of cells and collagen fibers in collagen gel cultures. *J Biomed Mater Res* 61, 608-18.
58. Chesmel, K. D., Clark, C. C., Brighton, C. T., and Black, J. (1995). Cellular responses to chemical and morphologic aspects of biomaterial surfaces. II. The biosynthetic and migratory response of bone cell populations. *J Biomed Mater Res* 29, 1101-10.
59. Chesmel, K. D. and Black, J. (1995). Cellular responses to chemical and morphologic aspects of biomaterial surfaces. I. A novel in vitro model system. *J Biomed Mater Res* 29, 1089-1099.
60. Dalby, M. J., Yarwood, S. J., Riehle, M. O., Johnstone, H. J., Affrossman, S., and Curtis, A. S. (2002). Increasing fibroblast response to materials using nanotopography: morphological and genetic measurements of cell response to 13-nm-high polymer demixed islands. *Exp Cell Res* 276, 1-9.
61. Dewez, J. L., Lhoest, J. B., Detrait, E., Berger, V., Dupont-Gillain, C. C., Vincent, L. M., Schneider, Y. J., Bertrand, P., and Rouxhet, P. G. (1998). Adhesion of mammalian cells to polymer surfaces: from physical chemistry of surfaces to selective adhesion on defined patterns. *Biomaterials* 19, 1441-5.
62. Matsuzaka, K., Walboomers, F., de Ruijter, A., and Jansen, J. A. (2000). Effect of microgrooved poly-L-lactic (PLA) surfaces on proliferation, cytoskeletal organization, and mineralized matrix formation of rat bone marrow cells. *Clin Oral Implants Res* 11, 325-33.
63. Matsuzaka, K., Walboomers, X. F., de Ruijter, J. E., and Jansen, J. A. (1999). The effect of poly-L-lactic acid with parallel surface micro groove on osteoblast-like cells in vitro. *Biomaterials* 20, 1293-301.
64. Parker, J. A., Walboomers, X. F., Von Den Hoff, J. W., Maltha, J. C., and Jansen, J. A. (2003). Soft tissue reaction to microgrooved poly-L-lactic acid implants loaded with transforming growth factor beta(3). *Tissue Eng* 9, 117-26.
65. Parker, J. A., Brunner, G., Walboomers, X. F., Von den Hoff, J. W., Maltha, J. C., and Jansen, J. A. (2002). Release of bioactive transforming growth factor beta(3) from microtextured polymer surfaces in vitro and in vivo. *Tissue Eng* 8, 853-61.
66. Parker, J. A., Walboomers, X. F., Von den Hoff, J. W., Maltha, J. C., and Jansen, J. A. (2002). The effect of bone anchoring and micro-grooves on the soft tissue reaction to implants. *Biomaterials* 23, 3887-96.
67. Parker, J. A., Walboomers, X. F., Von den, H. J., Maltha, J. C., and Jansen, J. A. (2002). Soft tissue response to microtextured silicone and poly-L-lactic acid implants: fibronectin pre-coating vs. radio-frequency glow discharge treatment. *Biomaterials* 23, 3545-53.
68. Parker, J. A., Walboomers, X. F., Von den Hoff, J. W., Maltha, J. C., and Jansen, J. A. (2002). Soft-tissue response to silicone and poly-L-lactic acid implants with a periodic or random surface micropattern. *J Biomed Mater Res*

- 61, 91-8.
69. Beumer, G. J., van Blitterswijk, C. A., and Ponec, M. (1994). Degradative behaviour of polymeric matrices in (sub)dermal and muscle tissue of the rat: a quantitative study. *Biomaterials* 15, 551-9.
 70. Ranucci, C. S. and Moghe, P. V. (2001). Substrate microtopography can enhance cell adhesive and migratory responsiveness to matrix ligand density. *J Biomed Mater Res* 54, 149-61.
 71. Peter, S. J., Lu, L., Kim, D. J., Stamatias, G. N., Miller, M. J., Yaszemski, M. J., and Mikos, A. G. (2000). Effects of transforming growth factor beta1 released from biodegradable polymer microparticles on marrow stromal osteoblasts cultured on poly(propylene fumarate) substrates. *J Biomed Mater Res* 50, 452-62.
 72. Gombotz, W. R., Pankey, S. C., Bouchard, L. S., Phan, D. H., and Puolakkainen, P. A. (1994). Stimulation of bone healing by transforming growth factor-beta 1 released from polymeric or ceramic implants. *J Appl Biomater* 5, 141-50.
 73. Miller, D. C., Thapa, A., Haberstroh, K. M., and Webster, T. J. (2004). Endothelial and vascular smooth muscle cell function on poly(lactic-co-glycolic acid) with nano-structured surface features. *Biomaterials* 25, 53-61.
 74. Thapa, A., Webster, T. J., and Haberstroh, K. M. (2003). Polymers with nano-dimensional surface features enhance bladder smooth muscle cell adhesion. *J Biomed Mater Res* 67A, 1374-83.
 75. Thapa, A., Miller, D. C., Webster, T. J., and Haberstroh, K. M. (2003). Nano-structured polymers enhance bladder smooth muscle cell function. *Biomaterials* 24, 2915-26.
 76. Singhvi, R., Kumar, A., Lopez, G. P., Stephanopoulos, G. N., Wang, D. I., Whitesides, G. M., and Ingber, D. E. (1994). Engineering cell shape and function. *Science* 264, 696-8.
 77. Tschopp, A. and Cogoli, A. (1983). Hypergravity promotes cell proliferation. *Experientia* 39, 1323-9.
 78. Walboomers, F., Paquay, Y. C., and Jansen, J. A. (2001). A new titanium fiber mesh-cuffed peritoneal dialysis catheter: evaluation and comparison with a Dacron-cuffed tenckhoff catheter in goats. *Perit Dial Int* 21, 254-62.
 79. den Braber, E. T., Jansen, H. V., de Boer, M. J., Croes, H. J., Elwenspoek, M., Ginsel, L. A., and Jansen, J. A. (1998). Scanning electron microscopic, transmission electron microscopic, and confocal laser scanning microscopic observation of fibroblasts cultured on microgrooved surfaces of bulk titanium substrata. *J Biomed Mater Res* 40, 425-33.
 80. Scotchford, C. A., Ball, M., Winkelmann, M., Voros, J., Csucs, C., Brunette, D. M., Danuser, G., and Textor, M. (2003). Chemically patterned, metal-oxide-based surfaces produced by photolithographic techniques for studying protein- and cell-interactions. II: Protein adsorption and early cell interactions. *Biomaterials* 24, 1147-58.
 81. Winkelmann, M., Gold, J., Hauert, R., Kasemo, B., Spencer, N. D., Brunette, D. M., and Textor, M. (2003). Chemically patterned, metal oxide based surfaces produced by photolithographic techniques for studying protein- and cell-surface interactions I: Microfabrication and surface characterization. *Biomaterials* 24, 1133-45.
 82. Chehroudi, B. and Brunette, D. M. (2002). Subcutaneous microfabricated surfaces inhibit epithelial recession and promote long-term survival of percutaneous implants. *Biomaterials* 23, 229-37.
 83. Perizzolo, D., Lacefield, W. R., and Brunette, D. M. (2001). Interaction between topography and coating in the formation of bone nodules in culture for hydroxyapatite- and titanium-coated micromachined surfaces. *J Biomed Mater Res* 56, 494-503.
 84. Goto, T., Wong, K. S., and Brunette, D. M. (1999). Observation of fibronectin distribution on the cell undersurface using immunogold scanning electron microscopy. *J Histochem Cytochem* 47, 1487-94.
 85. Brunette, D. M. and Chehroudi, B. (1999). The effects of the surface topography of micromachined titanium substrata on cell behavior in vitro and in vivo. *J Biomech Eng* 121, 49-57.

86. Chou, L., Firth, J. D., Nathanson, D., Uitto, V. J., and Brunette, D. M. (1996). Effects of titanium on transcriptional and post-transcriptional regulation of fibronectin in human fibroblasts. *J Biomed Mater Res* 31, 209-17.
87. Qu, J., Chehroudi, B., and Brunette, D. M. (1996). The use of micromachined surfaces to investigate the cell behavioural factors essential to osseointegration. *Oral Dis* 2, 102-15.
88. Oakley, C. and Brunette, D. M. (1995). Response of single, pairs, and clusters of epithelial cells to substratum topography. *Biochem Cell Biol* 73, 473-89.
89. Oakley, C. and Brunette, D. M. (1993). The sequence of alignment of microtubules, focal contacts and actin filaments in fibroblasts spreading on smooth and grooved titanium substrata. *J Cell Sci* 106 (Pt 1), 343-54.
90. Brunette, D. M. (1986). Fibroblasts on micromachined substrata orient hierarchically to grooves of different dimensions. *Exp Cell Res* 164, 11-26.
91. Chehroudi, B., McDonnell, D., and Brunette, D. M. (1997). The effects of micromachined surfaces on formation of bonelike tissue on subcutaneous implants as assessed by radiography and computer image processing. *J Biomed Mater Res* 34, 279-90.
92. Jansen, J. A., von Recum, A. F., van der Waerden, J. P., and de Groot, K. (1992). Soft tissue response to different types of sintered metal fibre-web materials. *Biomaterials* 13, 959-68.
93. Eisenbarth, E., Linez, P., Biehl, V., Velten, D., Breme, J., and Hildebrand, H. F. (2002). Cell orientation and cytoskeleton organisation on ground titanium surfaces. *Biomol Eng* 19, 233-7.
94. Eisenbarth, E., Meyle, J., Nachtigall, W., and Breme, J. (1996). Influence of the surface structure of titanium materials on the adhesion of fibroblasts. *Biomaterials* 17, 1399-403.
95. de Oliveira, P. T. and Nanci, A. (2004). Nanotexturing of titanium-based surfaces upregulates expression of bone sialoprotein and osteopontin by cultured osteogenic cells. *Biomaterials* 25, 403-13.
96. Lind, M., Overgaard, S., Soballe, K., Nguyen, T., Ongpipattanakul, B., and Bunger, C. (1996). Transforming growth factor-beta 1 enhances bone healing to unloaded tricalcium phosphate coated implants: an experimental study in dogs. *J Orthop Res* 14, 343-50.
97. Webster, T. J., Ergun, C., Doremus, R. H., Siegel, R. W., and Bizios, R. (2001). Enhanced osteoclast-like cell functions on nanophase ceramics. *Biomaterials* 22, 1327-33.
98. Vuola, J., Bohling, T., Goransson, H., and Puolakkainen, P. (2002). Transforming growth factor beta released from natural coral implant enhances bone growth at calvarium of mature rat. *J Biomed Mater Res* 59, 152-9.
99. ter Brugge, P. J., Wolke, J. G., and Jansen, J. A. (2002). Effect of calcium phosphate coating crystallinity and implant surface roughness on differentiation of rat bone marrow cells. *J Biomed Mater Res* 60, 70-8.
100. den Braber, E. T., de Ruijter, J. E., Ginsel, L. A., von Recum, A. F., and Jansen, J. A. (1998). Orientation of ECM protein deposition, fibroblast cytoskeleton, and attachment complex components on silicone microgrooved surfaces. *J Biomed Mater Res* 40, 291-300.
101. den Braber, E. T., de Ruijter, J. E., Ginsel, L. A., von Recum, A. F., and Jansen, J. A. (1996). Quantitative analysis of fibroblast morphology on microgrooved surfaces with various groove and ridge dimensions. *Biomaterials* 17, 2037-44.
102. Green, A. M., Jansen, J. A., van der Waerden, J. P., and von Recum, A. F. (1994). Fibroblast response to microtextured silicone surfaces: texture orientation into or out of the surface. *J Biomed Mater Res* 28, 647-53.
103. von Recum, A. F. and van Kooten, T. G. (1995). The influence of micro-topography on cellular response and the implications for silicone implants. *J Biomater Sci Polym Ed* 7, 181-98.

104. den Braber, E. T., de Ruijter, J. E., Smits, H. T., Ginsel, L. A., von Recum, A. F., and Jansen, J. A. (1995). Effect of parallel surface microgrooves and surface energy on cell growth. *J Biomed Mater Res* 29, 511-8.
105. Walboomers, X. F. and Jansen, J. A. (2000). Microgrooved silicone subcutaneous implants in guinea pigs. *Biomaterials* 21, 629-36.
106. den Braber, E. T., de Ruijter, J. E., and Jansen, J. A. (1997). The effect of a subcutaneous silicone rubber implant with shallow surface microgrooves on the surrounding tissues in rabbits. *J Biomed Mater Res* 37, 539-47.
107. Gutierrez, J. A. and Perr, H. A. (1999). Mechanical stretch modulates TGF-beta1 and alpha1(I) collagen expression in fetal human intestinal smooth muscle cells. *Am J Physiol* 277, G1074-80.
108. Wang, J. H., Jia, F., Yang, G., Yang, S., Campbell, B. H., Stone, D., and Woo, S. L. (2003). Cyclic Mechanical Stretching of Human Tendon Fibroblasts Increases the Production of Prostaglandin E(2) and Levels of Cyclooxygenase Expression: A Novel In Vitro Model Study. *Connect Tissue Res* 44, 128-133.
109. Wang, J. H. and Grood, E. S. (2000). The strain magnitude and contact guidance determine orientation response of fibroblasts to cyclic substrate strains. *Connect Tissue Res* 41, 29-36.
110. Park, J. M., Borer, J. G., Freeman, M. R., and Peters, C. A. (1998). Stretch activates heparin-binding EGF-like growth factor expression in bladder smooth muscle cells. *Am J Physiol* 275, C1247-54.
111. Fray, T. R., Molloy, J. E., Armitage, M. P., and Sparrow, J. C. (1998). Quantification of single human dermal fibroblast contraction. *Tissue Eng* 4, 281-91.
112. Carano, A. and Siciliani, G. (1996). Effects of continuous and intermittent forces on human fibroblasts in vitro. *Eur J Orthod* 18, 19-26.
113. Kain, H. L. and Reuter, U. (1995). Release of lysosomal protease from retinal pigment epithelium and fibroblasts during mechanical stresses. *Graefes Arch Clin Exp Ophthalmol* 233, 236-43.
114. Wang, J. H., Goldschmidt-Clermont, P., and Yin, F. C. (2000). Contractility affects stress fiber remodeling and reorientation of endothelial cells subjected to cyclic mechanical stretching. *Ann Biomed Eng* 28, 1165-71.
115. Wang, J. H., Jia, F., Gilbert, T. W., and Woo, S. L. (2003). Cell orientation determines the alignment of cell-produced collagenous matrix. *J Biomech* 36, 97-102.
116. Wang, J. H., Yang, G., Li, Z., and Shen, W. (2003). Fibroblasts responses to cyclic mechanical stretching depend on cell orientation to the stretching direction. *J Biomech* 37, 573-6.
117. Basso, N. and Heersche, J. N. (2002). Characteristics of in vitro osteoblastic cell loading models. *Bone* 30, 347-51.
118. Butler, K., Benghuzzi, H., and Tucci, S. (2001). Tissue-implant response following soft tissue implantation of poly-L-lysine coated UHMW-polyethylene into adult male rats. *Biomed Sci Instrum* 37, 19-24.
119. Johnson, R., Harrison, D., Tucci, M., Tsao, A., Lemos, M., Puckett, A., Hughes, J. L., and Benghuzzi, H. (1997). Fibrous capsule formation in response to ultrahigh molecular weight polyethylene treated with peptides that influence adhesion. *Biomed Sci Instrum* 34, 47-52.
120. Schreuders, P. D., Salthouse, T. N., and von Recum, A. F. (1988). Normal wound healing compared to healing within porous Dacron implants. *J Biomed Mater Res* 22, 121-35.
121. von Recum, A. F., Opitz, H., and Wu, E. (1993). Collagen types I and III at the implant/tissue interface. *J Biomed Mater Res* 27, 757-61.
122. Rowland, S. A., Shalaby, S. W., Latour, R. A. Jr, and von Recum, A. F. (1995). Effectiveness of cleaning surgical implants: quantitative analysis of contaminant removal. *J Appl Biomater* 6, 1-7.

123. Chung, T. W., Liu, D. Z., Wang, S. Y., and Wang, S. S. (2003). Enhancement of the growth of human endothelial cells by surface roughness at nanometer scale. *Biomaterials* 24, 4655-61.
124. Naughton, B. A., Tjota, A., Sibanda, B., and Naughton, G. K. (1991). Hematopoiesis on suspended nylon screen-stromal cell microenvironments. *J Biomech Eng* 113, 171-7.
125. Neumann, T., Nicholson, B. S., and Sanders, J. E. (2003). Tissue engineering of perfused microvessels. *Microvasc Res* 66, 59-67.
126. Kaverina, I., Krylyshkina, O., Beningo, K., Anderson, K., Wang, Y. L., and Small, J. V. (2002). Tensile stress stimulates microtubule outgrowth in living cells. *J Cell Sci* 115, 2283-91.
127. Hughes-Fulford, M. (2001). Changes in gene expression and signal transduction in microgravity. *J Gravit Physiol* 8, P1-4.
128. Hughes-Fulford, M., Tjandrawinata, R., Fitzgerald, J., Gasuad, K., and Gilbertson, V. (1998). Effects of microgravity on osteoblast growth. *Gravit Space Biol Bull* 11, 51-60.
129. Farsi, J. M. and Aubin, J. E. (1984). Microfilament rearrangements during fibroblast-induced contraction of three-dimensional hydrated collagen gels. *Cell Motil* 4, 29-40.
130. Schmidt, J. A. and von Recum, A. F. (1992). Macrophage response to microtextured silicone. *Biomaterials* 13, 1059-69.
131. Wu, Z., Wong, K., Glogauer, M., Ellen, R. P., and McCulloch, C. A. (1999). Regulation of stretch-activated intracellular calcium transients by actin filaments. *Biochem Biophys Res Commun* 261, 419-25.
132. Matsuda, T. and Chung, D. J. (1994). Microfabricated surface designs for cell culture and diagnosis. *ASAIO J* 40, M594-7.
133. Wojciak-Stothard, B., Curtis, A., Monaghan, W., MacDonald, K., and Wilkinson, C. (1996). Guidance and activation of murine macrophages by nanometric scale topography. *Exp Cell Res* 223, 426-35.
134. Curtis, A. S., Casey, B., Gallagher, J. O., Pasqui, D., Wood, M. A., and Wilkinson, C. D. (2001). Substratum nanotopography and the adhesion of biological cells. Are symmetry or regularity of nanotopography important? *Biophys Chem* 94, 275-83.
135. Britland, S., Morgan, H., Wojciak-Stodart, B., Riehle, M., Curtis, A., and Wilkinson, C. (1996). Synergistic and hierarchical adhesive and topographic guidance of BHK cells. *Exp Cell Res* 228, 313-25.
136. Matsuzawa, M., Potember, R. S., Stenger, D. A., and Krauthamer, V. (1993). Containment and growth of neuroblastoma cells on chemically patterned substrates. *J Neurosci Methods* 50, 253-60.
137. Zimmermann, J., Bittner, K., Stark, B., and Mulhaupt, R. (2002). Novel hydrogels as supports for in vitro cell growth: poly(ethylene glycol)- and gelatine-based (meth)acrylamidopeptide macromonomers. *Biomaterials* 23, 2127-34.
138. Voigt, M., Andree, C., Kalt, T., Dormann, S., Schaefer, D. J., Walgenbach, K. J., and Stark, G. B. (2002). Human recombinant EGF protein delivered by a biodegradable cell transplantation system. *Tissue Eng* 8, 263-72.
139. Nehls, V. and Drenckhahn, D. (1995). A novel, microcarrier-based in vitro assay for rapid and reliable quantification of three-dimensional cell migration and angiogenesis. *Microvasc Res* 50, 311-22.
140. den Braber, E. T., de Ruijter, J. E., Smits, H. T., Ginsel, L. A., von Recum, A. F., and Jansen, J. A. (1996). Quantitative analysis of cell proliferation and orientation on substrata with uniform parallel surface microgrooves. *Biomaterials* 17, 1093-9.
141. Beumer, G. J., Van Blitterswijk, C. A., and Ponec, M. The use of gas plasma treatment to improve the cell-

- substrate properties of a skin substitute made of poly(ether)/poly(ester) copolymers. *J Mat Sc Mat Med* 5, 1-6. 94.
142. Matsuda, T., Miwa, H., Moghaddam, M. J., and Iida, F. (1993). Newly designed tissue adhesion prevention technology based on photocurable mucopolysaccharides. In vivo evaluation. *ASAIO J* 39, M327-31.
 143. Tateshita, T., Ono, I., and Kaneko, F. (2001). Effects of collagen matrix containing transforming growth factor (TGF)-beta(1) on wound contraction. *J Dermatol Sci* 27, 104-13.
 144. Vernon, R. B. and Gooden, M. D. (2002). New technologies in vitro for analysis of cell movement on or within collagen gels. *Matrix Biol* 21, 661-9.
 145. Sottile, J. and Hocking, D. C. (2002). Fibronectin polymerization regulates the composition and stability of extracellular matrix fibrils and cell-matrix adhesions. *Mol Biol Cell* 13, 3546-59.
 146. Huang, Q., Goh, J. C., Hutmacher, D. W., and Lee, E. H. (2002). In vivo mesenchymal cell recruitment by a scaffold loaded with transforming growth factor beta1 and the potential for in situ chondrogenesis. *Tissue Eng* 8, 469-82.
 147. Arora, P. D., Narani, N., and McCulloch, C. A. (1999). The compliance of collagen gels regulates transforming growth factor-beta induction of alpha-smooth muscle actin in fibroblasts. *Am J Pathol* 154, 871-82.
 148. Pandit, A., Ashar, R., and Feldman, D. (1999). The effect of TGF-beta delivered through a collagen scaffold on wound healing. *J Invest Surg* 12, 89-100.
 149. Yokozeki, M., Moriyama, K., Shimokawa, H., and Kuroda, T. (1997). Transforming growth factor-beta 1 modulates myofibroblastic phenotype of rat palatal fibroblasts in vitro. *Exp Cell Res* 231, 328-36.
 150. Chegini, N., Gold, L. I., and Williams, R. S. (1994). Localization of transforming growth factor beta isoforms TGF-beta 1, TGF-beta 2, and TGF-beta 3 in surgically induced endometriosis in the rat. *Obstet Gynecol* 83, 455-61.
 151. Krummel, T. M., Michna, B. A., Thomas, B. L., Sporn, M. B., Nelson, J. M., Salzberg, A. M., Cohen, I. K., and Diegelmann, R. F. (1988). Transforming growth factor beta (TGF-beta) induces fibrosis in a fetal wound model. *J Pediatr Surg* 23, 647-52.
 152. Lanning, D. A., Diegelmann, R. F., Yager, D. R., Wallace, M. L., Bagwell, C. E., and Haynes, J. H. (2000). Myofibroblast induction with transforming growth factor-beta1 and -beta3 in cutaneous fetal excisional wounds. *J Pediatr Surg* 35, 183-7; discussion 187-8.
 153. Uhal, B. D., Ramos, C., Joshi, I., Bifero, A., Pardo, A., and Selman, M. (1998). Cell size, cell cycle, and alpha-smooth muscle actin expression by primary human lung fibroblasts. *Am J Physiol* 275, L998-L1005.
 154. Lindahl, G. E., Chambers, R. C., Papakrivopoulou, J., Dawson, S. J., Jacobsen, M. C., Bishop, J. E., and Laurent, G. J. (2002). Activation of fibroblast procollagen alpha 1(I) transcription by mechanical strain is transforming growth factor-beta-dependent and involves increased binding of CCAAT-binding factor (CBF/NF-Y) at the proximal promoter. *J Biol Chem* 277, 6153-61.
 155. Dalby, M. J., Riehle, M. O., Yarwood, S. J., Wilkinson, C. D., and Curtis, A. S. (2003). Nucleus alignment and cell signaling in fibroblasts: response to a micro-grooved topography. *Exp Cell Res* 284, 274-82.
 156. Brunette, D. M. (1988). The effects of implant surface topography on the behavior of cells. *Int J Oral Maxillofac Implants* 3, 231-46.
 157. Zeichen, J., van Griensven, M., and Bosch, U. (2000). The proliferative response of isolated human tendon fibroblasts to cyclic biaxial mechanical strain. *Am J Sports Med* 28, 888-92.
 158. Skutek, M., van Griensven, M., Zeichen, J., Brauer, N., and Bosch, U. (2003). Cyclic mechanical stretching of human patellar tendon fibroblasts: activation of JNK and modulation of apoptosis. *Knee Surg Sports Traumatol*

Arthrosc 11, 122-9.

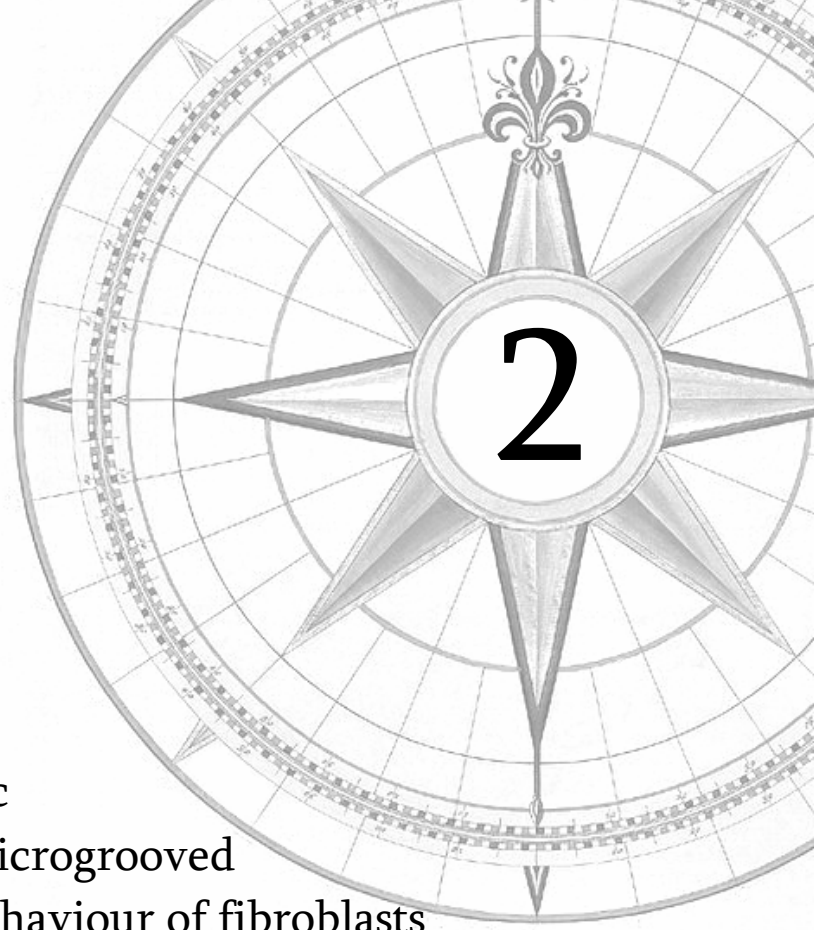
159. Howard, P. S., Kucich, U., Taliwal, R., and Korostoff, J. M. (1998). Mechanical forces alter extracellular matrix synthesis by human periodontal ligament fibroblasts. *J Periodontal Res* 33, 500-8.
160. Carver, W., Nagpal, M. L., Nachtigal, M., Borg, T. K., and Terracio, L. (1991). Collagen expression in mechanically stimulated cardiac fibroblasts. *Circ Res* 69, 116-22.
161. Lam, S., Verhagen, N. A., Strutz, F., van der Pijl, J. W., Daha, M. R., and van Kooten, C. (2003). Glucose-induced fibronectin and collagen type III expression in renal fibroblasts can occur independent of TGF-beta1. *Kidney Int* 63, 878-88.
162. Dalby, M. J., Riehle, M. O., Johnstone, H. J., Affrossman, S., and Curtis, A. S. (2003). Nonadhesive nanotopography: fibroblast response to poly(n-butyl methacrylate)-poly(styrene) demixed surface features. *J Biomed Mater Res* 67A, 1025-32.
163. Sato, A., Hamazaki, T., Oomura, T., Osada, H., Kakeya, M., Watanabe, M., Nakamura, T., Nakamura, Y., Koshikawa, N., Yoshizaki, I., Aizawa, S., Yoda, S., Ogiso, A., Takaoki, M., Kohno, Y., and Tanaka, H. (1999). Effects of microgravity on c-fos gene expression in osteoblast-like MC3T3-E1 cells. *Adv Space Res* 24, 807-13.
164. Neidlinger-Wilke, C., Grood, E. S., Wang JH-C, Brand, R. A., and Claes, L. (2001). Cell alignment is induced by cyclic changes in cell length: studies of cells grown in cyclically stretched substrates. *J Orthop Res* 19, 286-93.
165. Wang, J. H., Grood, E. S., Florer, J., and Wenstrup, R. (2000). Alignment and proliferation of MC3T3-E1 osteoblasts in microgrooved silicone substrata subjected to cyclic stretching. *J Biomech* 33, 729-35.
166. Neidlinger-Wilke, C., Wilke, H. J., and Claes, L. (1994). Cyclic stretching of human osteoblasts affects proliferation and metabolism: a new experimental method and its application. *J Orthop Res* 12, 70-8.
167. Buckley, M. J., Banes, A. J., and Jordan, R. D. (1990). The effects of mechanical strain on osteoblasts in vitro. *J Oral Maxillofac Surg* 48, 276-82; discussion 282-3.
168. Buckley, M. J., Banes, A. J., Levin, L. G., Sumpio, B. E., Sato, M., Jordan, R., Gilbert, J., Link, G. W., and Tran Son Tay, R. (1988). Osteoblasts increase their rate of division and align in response to cyclic, mechanical tension in vitro. *Bone Miner* 4, 225-36.
169. Price, R. L., Gutwein, L. G., Kaledin, L., Tepper, F., and Webster, T. J. (2003). Osteoblast function on nanophase alumina materials: Influence of chemistry, phase, and topography. *J Biomed Mater Res* 67A, 1284-93.
170. Beumer, G. J., van Blitterswijk, C. A., Bakker, D., and Ponec, M. (1993). Cell-seeding and in vitro biocompatibility evaluation of polymeric matrices of PEO/PBT copolymers and PLLA. *Biomaterials* 14, 598-604.
171. Lewis, L., Barrandon, Y., Green, H., and Albrecht-Buehler, G. (1987). The reorganization of microtubules and microfilaments in differentiating keratinocytes. *Differentiation* 36, 228-33.
172. Yoffe, B., Darlington, G. J., Soriano, H. E., Krishnan, B., Risin, D., Pellis, N. R., and Khaoustov, V. I. (1999). Cultures of human liver cells in simulated microgravity environment. *Adv Space Res* 24, 829-36.
173. ter Brugge, P. J. and Jansen, J. A. (2002). Initial interaction of rat bone marrow cells with non-coated and calcium phosphate coated titanium substrates. *Biomaterials* 23, 3269-77.
174. Yang, F. C., Atkinson, S. J., Gu, Y., Borneo, J. B., Roberts, A. W., Zheng, Y., Pennington, J., and Williams, D. A. (2001). Rac and Cdc42 GTPases control hematopoietic stem cell shape, adhesion, migration, and mobilization. *Proc Natl Acad Sci U S A* 98, 5614-8.
175. Chehroudi, B., Gould, T. R., and Brunette, D. M. (1988). Effects of a grooved epoxy substratum on epithelial cell behavior in vitro and in vivo. *J Biomed Mater Res* 22, 459-73.

176. Dalton, B. A., Walboomers, X. F., Dziegielewska, M., Evans, M. D., Taylor, S., Jansen, J. A., and Steele, J. G. (2001). Modulation of epithelial tissue and cell migration by microgrooves. *J Biomed Mater Res* 56, 195-207.
177. Clark, P., Connolly, P., and Moores, G. R. (1992). Cell guidance by micropatterned adhesiveness in vitro. *J Cell Sci* 103 (Pt 1), 287-92.
178. Clark, P., Connolly, P., Curtis, A. S., Dow, J. A., and Wilkinson, C. D. (1991). Cell guidance by ultrafine topography in vitro. *J Cell Sci* 99 (Pt 1), 73-7.
179. Helmke, B. P., Rosen, A. B., and Davies, P. F. (2003). Mapping mechanical strain of an endogenous cytoskeletal network in living endothelial cells. *Biophys J* 84, 2691-9.
180. Helmke, B. P., Thakker, D. B., Goldman, R. D., and Davies, P. F. (2001). Spatiotemporal analysis of flow-induced intermediate filament displacement in living endothelial cells. *Biophys J* 80, 184-94.
181. Helmke, B. P., Goldman, R. D., and Davies, P. F. (2000). Rapid displacement of vimentin intermediate filaments in living endothelial cells exposed to flow. *Circ Res* 86, 745-752.
182. Wang, J. H., Goldschmidt-Clermont, P., Wille, J., and Yin, F. C. (2001). Specificity of endothelial cell reorientation in response to cyclic mechanical stretching. *J Biomech* 34, 1563-72.
183. Wang, J. H., Goldschmidt-Clermont, P., Moldovan, N., and Yin, F. C. (2000). Leukotrienes and tyrosine phosphorylation mediate stretching-induced actin cytoskeletal remodeling in endothelial cells. *Cell Motil Cytoskeleton* 46, 137-45.
184. Hsu, P. P., Li, S., Li, Y. S., Usami, S., Ratcliffe, A., Wang, X., and Chien, S. (2001). Effects of flow patterns on endothelial cell migration into a zone of mechanical denudation. *Biochem Biophys Res Commun* 285, 751-9.
185. Spisni, E., Bianco, M. C., Griffoni, C., Toni, M., D'Angelo, R., Santi, S., Riccio, M., and Tomasi, V. (2003). Mechanosensing role of caveolae and caveolar constituents in human endothelial cells. *J Cell Physiol* 197, 198-204.
186. Chafik, D., Bear, D., Bui, P., Patel, A., Jones, N. F., Kim, B. T., Hung, C. T., and Gupta, R. (2003). Optimization of Schwann cell adhesion in response to shear stress in an in vitro model for peripheral nerve tissue engineering. *Tis Eng* 9, 233-41.
187. Kaech, S., Ludin, B., and Matus, A. (1996). Cytoskeletal plasticity in cells expressing neuronal microtubule-associated proteins. *Neuron* 17, 1189-99.
188. Petrov, V. V., Fagard, R. H., and Lijnen, P. J. (2002). Stimulation of collagen production by transforming growth factor-beta1 during differentiation of cardiac fibroblasts to myofibroblasts. *Hypertension* 39, 258-63.
189. Iwasaki, H., Yoshimoto, T., Sugiyama, T., and Hirata, Y. (2003). Activation of cell adhesion kinase beta by mechanical stretch in vascular smooth muscle cells. *Endocrinology* 144, 2304-10.
190. Guignandon, A., Usson, Y., Laroche, N., Lafage-Proust, M. H., Sabido, O., Alexandre, C., and Vico, L. (1997). Effects of intermittent or continuous gravitational stresses on cell- matrix adhesion: quantitative analysis of focal contacts in osteoblastic ROS 17/2.8 cells. *Exp Cell Res* 236, 66-75.
191. Ballestrem, C., Wehrle-Haller, B., Hinz, B., and Imhof, B. A. (2000). Actin-dependent lamellipodia formation and microtubule-dependent tail retraction control-directed cell migration. *Mol Biol Cell* 11, 2999-3012.
192. Ballestrem, C., Wehrle-Haller, B., and Imhof, B. A. (1998). Actin dynamics in living mammalian cells. *J Cell Sci* 111 (Pt 12), 1649-58.
193. Liu, C., Yao, J., Mercola, D., and Adamson, E. (2000). The transcription factor EGR-1 directly transactivates the fibronectin gene and enhances attachment of human glioblastoma cell line U251. *J Biol Chem* 275, 20315-23.

194. Wojciak-Stothard, B., Madeja, Z., Korohoda, W., Curtis, A., and Wilkinson, C. (1995). Activation of macrophage-like cells by multiple grooved substrata. Topographical control of cell behaviour. *Cell Biol Int* 19, 485-90.
195. Bechler, B., Cogoli, A., Cogoli-Greuter, M., Muller, O., Hunzinger, E., and Criswell, S. B. (1992). Activation of microcarrier-attached lymphocytes in microgravity. *Biotechnol Bioeng* 40, 991-6.
196. Curtis, A. S. and Wilkinson, C. D. (1998). Reactions of cells to topography. *J Biomater Sci Polym Ed* 9, 1313-29.
197. Teixeira, A. I., Abrams, G. A., Bertics, P. J., Murphy, C. J., and Nealey, P. F. (2003). Epithelial contact guidance on well-defined micro- and nanostructured substrates. *J Cell Sci* 116, 1881-92.
198. Curtis, A. and Wilkinson, C. (2001). Nanotechniques and approaches in biotechnology. *Trends Biotechnol* 19, 97-101.
199. Curtis, A. and Wilkinson, C. (1999). New depths in cell behaviour: reactions of cells to nanotopography. *Biochem Soc Symp* 65, 15-26.
200. Gehrke, T. A., Walboomers, X. F., and Jansen, J. A. (2000). Influence of transforming growth factor-beta3 on fibrous capsule formation around microgrooved subcutaneous implants in vivo. *Tissue Eng* 6, 505-17.
201. Shannon, C., Thull, R., and von Recum, A. (1997). Types I and III collagen in the tissue capsules of titanium and stainless-steel implants. *J Biomed Mater Res* 34, 401-8.
202. Halliday, D., Resnick, R., and Walker, J. (2000). "Extended, Fundamentals of Physics," 6th Edition ed., John Wiley and Sons, USA.
203. Morrison, D., Wolff, S., and Frankoi, A. (1995). "Exploration of the Universe," 7th Edition ed., Saunders College Publishing, USA.
204. Mariusz Kovler. Exploring Gravity. 2001.
205. NASA. Space Station Biological Research Project.
206. ThinkQuest Internet Challenge Library. From Apples to Orbits. 99.
207. John F. Hawley. Cosmology Key Terms. 99.
208. Todd, P. (1989). Gravity-dependent phenomena at the scale of the single cell. *ASGSB Bull* 2, 95-113.
209. Jack van Loon and JP Veldhuijzen. Dutch Experiment Support Center.
210. ASGSB. American Society for Gravitational and Space Biology.
211. Todd, P. (1992). Physical effects at the cellular level under altered gravity conditions. *Adv Space Res* 12, 43-9.
212. They, M., Pepin, A., Dressaire, E., Chen, Y., and Bornens, M. (2006). Cell distribution of stress fibres in response to the geometry of the adhesive environment. *Cell Motil Cytoskeleton* 63, 341-55.
213. Brown, A. H. (1992). Centrifuges: evolution of their uses in plant gravitational biology and new directions for research on the ground and in spaceflight. *ASGSB Bull* 5, 43-57.
214. Smith, A. H. (1992). Centrifuges: their development and use in gravitational biology. *ASGSB Bull* 5, 33-41.
215. van Loon, J. J., van den Bergh, L. C., Veldhuijzen, J. P., and Huijser, R. Development of a centrifuge for acceleration research in cell and developmental biology. In academic thesis: Effect of spaceflight and hypergravity on mineral metabolism in organ cultures of fetal mouse long bones. Appendix C. 95. Amsterdam, Free University Amsterdam.

216. Briegleb, W. (1992). Some qualitative and quantitative aspects of the fast-rotating clinostat as a research tool. *ASGSB Bull* 5, 23-30.
217. Cogoli, M. (1992). The fast rotating clinostat: a history of its use in gravitational biology and a comparison of ground-based and flight experiment results. *ASGSB Bull* 5, 59-67.
218. van Loon, J. J. W. A. (2007). Some history and use of the random positioning machine, RPM, in gravity related research. *Advances in Space Research* doi:10.1016/j.asr.2007.02.016.
219. Mesland, D. A., Anton, A. H., Willemsen, H., and van den Ende, H. (1996). The Free Fall Machine--a ground-based facility for microgravity research in life sciences. *Microgravity Sci Technol* 9, 10-4.
220. Albrecht-Buehler, G. (1991). Possible mechanisms of indirect gravity sensing by cells. *ASGSB Bull* 4, 25-34.
221. Block, I., Wolke, A., Briegleb, W., and Ivanova, K. (1995). Gravity perception and signal transduction in single cells. *Acta Astronaut* 36, 479-86.
222. Cogoli, A. and Gmunder, F. K. (1991). Gravity effects on single cells: techniques, findings, and theory. *Adv Space Biol Med* 1, 183-248.
223. Kondepudi, D. K. (1991). Detection of gravity through nonequilibrium mechanisms. *ASGSB Bull* 4, 119-24.
224. Kondrachuk, A. V. and Sirenko, S. P. (1996). The theoretical consideration of microgravity effects on a cell. *Adv Space Res* 17, 165-8.
225. Mesland, D. A. (1992). Possible actions of gravity on the cellular machinery. *Adv Space Res* 12, 15-25.
226. Mesland, D. A. (1992). Mechanisms of gravity effects on cells: are there gravity-sensitive windows? *Adv Space Biol Med* 2, 211-28.
227. Sievers, A. and Hejnowicz, Z. (1998). Graviperception in plants: the role of the cytoskeleton. *J Gravit Physiol* 5, P5-8.
228. Berquand, A., Xia, N., Castner, D. G., Clare, B. H., Abbott, N. L., Dupres, V., Adriaensen, Y., and Dufrene, Y. F. (2005). Antigen binding forces of single antilysozyme Fv fragments explored by atomic force microscopy. *Langmuir* 21, 5517-23.
229. Ingber, D. (1999). How cells (might) sense microgravity. *FASEB J* 13 Suppl, S3-15.
230. Ingber, D. E. (1997). Integrins, tensegrity, and mechanotransduction. *Gravit Space Biol Bull* 10, 49-55.
231. Hughes-Fulford, M. and Lewis, M. L. (1996). Effects of microgravity on osteoblast growth activation. *Exp Cell Res* 224, 103-9.
232. Schwarzenberg, M., Pippia, P., Meloni, M. A., Cossu, G., Cogoli-Greuter, M., and Cogoli, A. (1999). Signal transduction in T lymphocytes--a comparison of the data from space, the free fall machine and the random positioning machine. *Adv Space Res* 24, 793-800.
233. Cogoli, A. and Cogoli-Greuter, M. (1997). Activation and proliferation of lymphocytes and other mammalian cells in microgravity. *Adv Space Biol Med* 6, 33-79.
234. Pippia, P., Sciola, L., Cogoli-Greuter, M., Meloni, M. A., Spano, A., and Cogoli, A. (1996). Activation signals of T lymphocytes in microgravity. *J Biotechnol* 47, 215-22.
235. Schatten, H., Lewis, M. L., and Chakrabarti, A. (2001). Spaceflight and clinorotation cause cytoskeleton and mitochondria changes and increases in apoptosis in cultured cells. *Acta Astronaut* 49, 399-418.
236. Gmunder, F. K., Kiess, M., Sonnefeld, G., Lee, J., and Cogoli, A. (1990). A ground-based model to study the

- effects of weightlessness on lymphocytes. *Biol Cell* 70, 33-8.
237. Cogoli, A. (1997). Signal transduction in T lymphocytes in microgravity. *Gravit Space Biol Bull* 10, 5-16.
 238. Chiquet, M., Renedo, A. S., Huber, F., and Fluck, M. (2003). How do fibroblasts translate mechanical signals into changes in extracellular matrix production? *Matrix Biol* 22, 73-80.
 239. Guignandon, A., Lafage-Proust, M. H., Usson, Y., Laroche, N., Caillot-Augusseau, A., Alexandre, C., and Vico, L. (2001). Cell cycling determines integrin-mediated adhesion in osteoblastic ROS 17/2.8 cells exposed to space-related conditions. *FASEB J* 15, 2036-8.
 240. Tairbekov, M. G. (1996). Physico-chemical characteristics of biomembranes and cell gravisensitivity. *Adv Space Res* 17, 161-4.
 241. Gruener, R., Roberts, R., and Reitstetter, R. (1994). Reduced receptor aggregation and altered cytoskeleton in cultured myocytes after space-flight. *Biol Sci Space* 8, 79-93.
 242. Buravkova, L. B. and Romanov, Y. A. (2001). The role of cytoskeleton in cell changes under condition of simulated microgravity. *Acta Astronaut* 48, 647-50.
 243. Guignandon, A., Vico, L., Alexandre, C., and Lafage-Proust, M. H. (1995). Shape changes of osteoblastic cells under gravitational variations during parabolic flight--relationship with PGE2 synthesis. *Cell Struct Funct* 20, 369-75.
 244. Papaseit, C., Pochon, N., and Tabony, J. (2000). Microtubule self-organization is gravity-dependent. *Proc Natl Acad Sci U S A* 97, 8364-8.
 245. Seitzer, U., Bodo, M., Muller, P. K., Acil, Y., and Batge, B. (1995). Microgravity and hypergravity effects on collagen biosynthesis of human dermal fibroblasts. *Cell Tissue Res* 282, 513-7.
 246. Croute, F., Gaubin, Y., Pianezzi, B., and Soleilhavoup, J. P. (1995). Effects of hypergravity on the cell shape and on the organization of cytoskeleton and extracellular matrix molecules of in vitro human dermal fibroblasts. *Microgravity Sci Technol* 8, 118-24.
 247. Tabony, J., Glade, N., Papaseit, C., and Demongeot, J. (2002). Microtubule self-organisation and its gravity dependence. *Adv Space Biol Med* 8, 19-58.
 248. Kondepudi, D. K. and Storm, P. B. (1992). Gravity detection through bifurcation. *Adv Space Res* 12, 7-14.
 249. Lee, D. J., Rosenfeldt, H., and Grinnell, F. (2000). Activation of ERK and p38 MAP kinases in human fibroblasts during collagen matrix contraction. *Exp Cell Res* 257, 190-7.
 250. Tairbekov, M. G. (1996). The role of signal systems in cell gravisensitivity. *Adv Space Res* 17, 113-9.



The effect of combined cyclic
mechanical stretching and microgrooved
surface topography on the behaviour of fibroblasts

WA Loesberg, XF Walboomers, JJWA van Loon and JA Jansen

J Biomed Mater Res A. 75 (3), 723-732, 2005

INTRODUCTION

Previous studies have shown that connective tissue is responsive to mechanical loading. Various *in vitro* systems have been developed to study this phenomenon. One of such systems is based on mechanical loading by uni-axial stress [1; 2]. Under the influence of uni-axial stress, cultured fibroblasts have a tendency to orient themselves. Fibroblasts orientation begins within hours after initiation of stretch, and the cells remain oriented for several hours after cessation of stretch. The alignment is dependent on the cell type used, but in general is perpendicular to the stretch direction [1; 3-10]. Earlier studies have proven that similar cell alignment can also be induced by topographical clues. For instance, fibroblasts cultured on microgrooved culturing substrates align along the grooves [11-16]. Topography can actively direct cell shape, and spreading. The cells are capable of sensing the structural shape of their environment, and determine their form and function appropriately. In both situations, various biological responses have been studied: remodelling of actin cytoskeleton [6; 14; 17; 18], changes in cell proliferation [10; 17; 19-22], and changes in gene expression and protein synthesis [23-27].

It is understood that the cellular response to stretching and microgrooves can interact [5]. Still, numerous parameters have to be investigated to fully understand cell behaviour. Unknown is, whether the observed effects still apply when fibroblast cells are seeded on different microgroove dimensions, as used in the experiments by Brunette and co-workers [15], [28; 29] and by others [19]. These researchers reported favourable tissue responses along certain types of textures, in a range of animal studies. Simultaneous *in vitro* work showed that topographic features affect cellular alignment, direction of proliferation, cellular attachment, growth rate, metabolism, and cytoskeleton arrangement. Therefore, the production of extracellular matrix components of the fibroblasts (collagen type I, fibronectin), and integrins, will also be investigated in this study as to supply additional information.

The aim of this study is therefore to evaluate *in vitro* the differences in cellular behaviour, between fibroblast cells cultured on smooth and microgrooved substrates, which undergo cyclic stretching. Our hypothesis is that cellular shape and orientation is determined by the topographical clues on the substrates. To ensure comparison to previous work two different topographies were used: a 10 μm wide square-groove [30] [31] and a 40 μm wide V-groove [32; 33]. As controls, smooth substrates were used. Onto all substrates rat dermal fibroblasts (RDF) were cultured. After mechanical loading the morphological characteristics were compared using scanning electron microscopy to supply qualitative information on the spreading and orientation. Immuno-staining of filamentous actin was visualised with fluorescence microscopy and cell alignment was scored quantitatively. Finally, the expression of collagen type I, fibronectin, and $\alpha 1$ - and $\beta 1$ -integrin were investigated, as the primary molecules involved in cell- matrix adhesion.

MATERIALS AND METHODS

Substrates:

Silicone dishes were produced by mixing two-component polydimethylsiloxane (PMDS) Elastosil 601A en 601B (Wacker Chemie, Riemerling, Germany) in a ratio of 10:1. The silicone mixture was poured into an acrylic dish-mold. The mixture was left for one hour for air bubbles to escape, after which the mold was placed in an oven for 2 hours at 50 °C.

Microtextured patterns were photo-etched in a silicon wafer using lithographic and reactive ion etching techniques as described by Walboomers et al [11]. **Figure 1** shows the two different topographies which were used in this study: a 10 μm wide groove/ridge, 1 μm deep (square-groove) and a 40 μm wide groove, 5 μm wide ridge and 30 μm deep (V-groove). These silicon wafers were used as templates for the production of silicone culturing substrates. After mixing of the two components, pouring, and curing of the silicone, the silicone replicas were removed from

the template. The obtained silicone substrates were bonded to the bottoms of the silicone dishes described above, using room temperature vulcanising (RTV) silicone adhesive (Nusil Technology, Carpinteria, CA, USA). The grooved substrates were attached either parallel or perpendicular to the stretching direction (**Figure 2**). Smooth silicone substrates were prepared to serve as the control group. Subsequently, all dishes were washed in a 10% solution of Liqui-Nox Detergent (Alconox Inc., New York, NY, USA), sonificated in a 1% Liqui-Nox solution, rinsed extensively in MilliQ-water, and autoclaved for 15 min at 121 °C. Just before cell culture, a radio frequency glow-discharge (RFGD) treatment was applied for 10 min at a pressure of $2.0 \cdot 10^{-2}$ mbar (Harrick Scientific Corp., Ossining, NY, USA) to promote cell attachment by improving the wettability of the substrates [34-38].

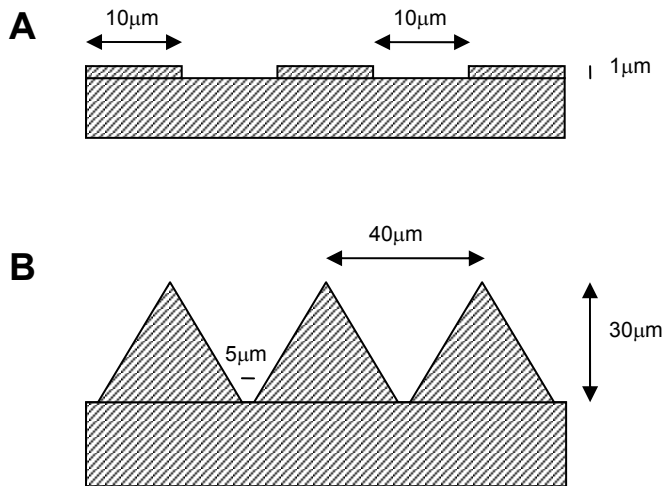


Figure 1: Graphical presentation of a cross section of template surface topographies used in this study: (A) 10 μm square groove, and (B) V-groove topography; here the wall and floor of the groove meet at angle of 120°. For clarity the drawings are not to scale.

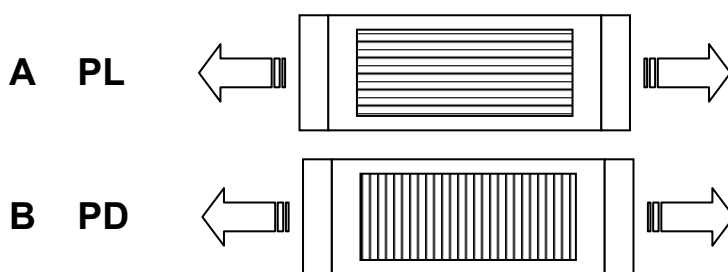


Figure 2: Silicone dishes with microgrooved substrates attached on the bottom. (A) Grooves parallel (PL), and (B) perpendicular (PD) to the stretching direction. The culture area of the microgrooved surfaces is 3 x 6 cm.

Cell culture:

RDFs were obtained from the ventral skin of male Wistar rats [39]. To ensure quick and constant availability, cells were cryo-preserved. Before experimentation, cells were thawed and cultured in α -Modified Eagles Medium (α -MEM) containing Earle's salts, L-glutamine, 10% foetal calf serum (FCS), and gentamicin (50 μ g/ml). Cells were cultured in a CO₂ incubator set at 37 °C in a humidified atmosphere. Experiments were performed with 6 - 8th culture generation cells. Onto all substrates, 1×10^4 cells/cm² were seeded. After incubation of 1 h, the silicone dishes were placed inside a custom-made stretching apparatus (**Figure 3**), as described previously [1; 3; 40; 41]. Different cyclic stretching magnitudes were applied: 0%, 4%, 8% at a 1 Hz frequency. Also, two different stretch durations were applied: 3 or 24h. Directly at the end of each experimental run, the RDF cell layers were washed three times with PBS and prepared for further analysis.

Scanning electron microscopy:

To assess cellular morphology of the fibroblasts, Scanning electron microscopy (SEM) was used. Directly after stretching, cells were fixed for 5 minutes in 2% glutaraldehyde, rinsed for 5 minutes

with 0.1 M sodium-cacodylate buffer (pH 7.4), dehydrated in a graded series of ethanol, and dried in tetramethylsilane to air. The specimens were sputter-coated with gold and examined and photographed using a Jeol 6310 SEM.

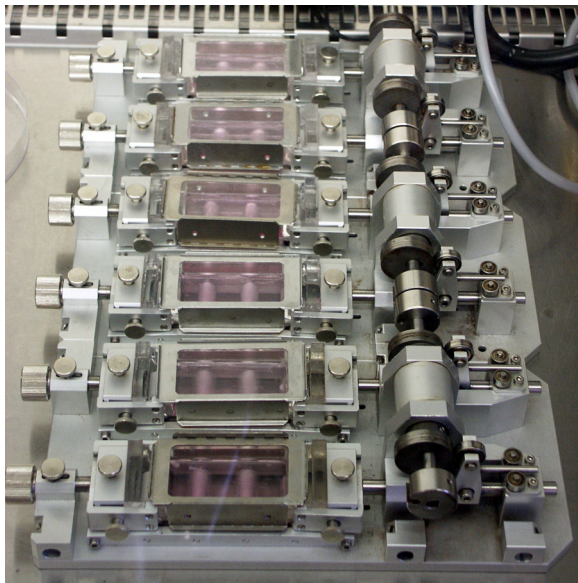


Figure 3: The stretching device that was used to apply a uniform cyclic strain of 4 or 8 % at 1 Hz for several hours.

Immunofluorescence

To observe the cytoskeleton, cells were fixed for 30 minutes in 2% paraformaldehyde, and permeabilised with 1% Triton X100 for 5 min. Then filamentous actin was stained with Alexa Fluor 568 phalloidin (Molecular Probes Inc., Eugene, OR, USA) diluted in PBS containing 1% Bovine Serum Albumin (BSA) to block non-specific epitopes, according to manufactures specifications. Finally, the specimens were examined with a Leica/Leitz DM RBE Microscope system at magnification of 10x. Cytoskeletal components were examined for their overall morphology as well as their orientation with respect to the groove direction as described below.

Image Analysis

The fluorescence micrographs were analyzed with Scion Image software (Beta Version 4.0.2, Scion Corp., Frederick, MD, USA). The orientation/distribution of the entire cell was examined. For each sample four fields were selected randomly. Within each field two criteria were used for cell selection: (1) the cell is not in contact with other cells and (2) cell is not in contact with the field perimeter. Thereafter, on each cell within the field the following parameters were examined: first, the maximum cell diameter was measured as the longest distance between two edges within the cell borders. Second, the angle between this axis and the grooves (or an arbitrarily selected line for smooth surfaces). This latter measurement will be termed the orientation angle. Using Clarks criteria [42], cells oriented at 0–10 degrees from the groove direction were regarded to be aligned.

RT-PCR analysis

Total RNA was isolated from the RDFs with a RNA isolation and stabilisation kit (QIAGEN, Hilden, Germany), and cDNA was synthesised from 1 mg of total RNA. After an initial denaturation for 2 min at 95°C, the samples were amplified for 35 cycles, consisting of annealing at 55 °C for 1 min, elongation at 72 °C for 2 min, and denaturation at 95 °C for 1 min. The duration of the final elongation reaction was increased to 10 min at 72 °C to permit completion of reaction products. The PCR products were separated on a 1.5% (w/v) agarose gel, and visualised by ethidium bromide staining. Semi-quantitative analysis of band intensity was performed using Quantity One 1-D analysis software for Windows (Version 4.5.0, Bio Rad, Hercules, California,

USA) The RT-PCR products value corresponding to collagen type I (only 24 hours samples), fibronectin, $\alpha 1$ integrin, $\beta 1$ integrin were divided by glyceraldehyde-3-phosphate dehydrogenase (GAPDH) value. The forward and reverse primer sequence can be found in **Table 1**.

	5' Primer (Forward)	3'Primer (Reverse)	Size (bp)
Collagen Type I	TGTTCGTGGTTCTCAGGGTAG	TTGTCGTAGCAGGGTTCTTTC	254
Fibronectin	CCTTAAGCCTTCTGCTCTGG	CGGCAAAAGAAAGCAGA AACT	301
$\alpha 1$ -Integrin	AGCTGGACATAGTCATCGTC	AGTTGTCATGCG ATTCTCCG	374
$\beta 1$ -Integrin	AATGTTTCAGTGCAGAGCC	TTGGGATGATGTCCGGAC	262
GAPDH	CGATGCTGGCGCTGAGTAC	CGTTCAGCTCAGGGATGACC	470

Table 1: Forward and reverse primer sequences used in this study.

Statistical analysis:

Acquired quantitative data were analysed using SPSS for Windows (Release 12.0.1, SPSS Inc., Chicago, USA). The effects of and the interaction between both time or force and surface were analysed using two-way analysis of variance (ANOVA). A probability (p) value less than or equal to 0.05 was considered significant.

RESULTS

Scanning Electron Microscopy

SEM revealed that the pattern of grooves and ridges were perfectly reproduced in the silicone rubber substrata (**Figure 4**). As observed earlier by Walboomers et al. [11], the ridges appear to have an additional roughness due to the etching process, which is used to fabricate the original silicon wafers. This roughness also was faithfully replicated onto the silicone substrata, indicating the accuracy of the casting process.

When analysing cell morphology, SEM showed that the RDF cells aligned along the groove direction on all grooved surfaces. On the smooth substrata (control) cells were spread out in a random fashion. Cells cultured on the substrates with the more pronounced grooves (V-groove substrate) seemed to be more clearly aligned than compared to square-groove substrates. The same applied for cells cultured for the longer time period (24h) in comparison to the 3h culturing. The cells cultured on square-groove substrate have a flat appearance and were able to descend into the grooves, whereas the cells cultured on V-groove substrate were nearly always found on top of the ridges. Their cell bodies frequently crossed over to the adjacent ridge, forming a bridge between them.

Fluorescence microscopy and Image Analysis

Fluorescence microscopy clearly showed the actin filaments stained with phalloidin-TRITC (**Figure 5**). Subsequent image analysis confirmed the cellular behaviour, as seen under the SEM, i.e. while the RDFs cultured on grooved substrates in general show alignment along the grooves; the smooth control samples do not induce any form of alignment. The quantified results for cell alignment are presented as box-whisker plots (**Figure 6**). Such a graph shows the distribution midpoint, the first and third quartile (boxes), and the largest and smallest observation (whiskers). The effects of the main parameters are expressed as an alignment percentage of the total number of cells, and are displayed in **Table 2**. Due to poor sample recovery no data was available for groups S3H8, PDSQ3H4, and PLV24H0.

An ANOVA was performed on the data, for all main parameters: groove type, groove orientation, stretch force, and time. In this analysis, all parameters proved significant, except stretch force. Regarding groove type 82% of the cells were aligned along the V-grooves, combined with prolonged culture time, and 76% of the cells in square grooves, compared to 19% of the smooth substrates.

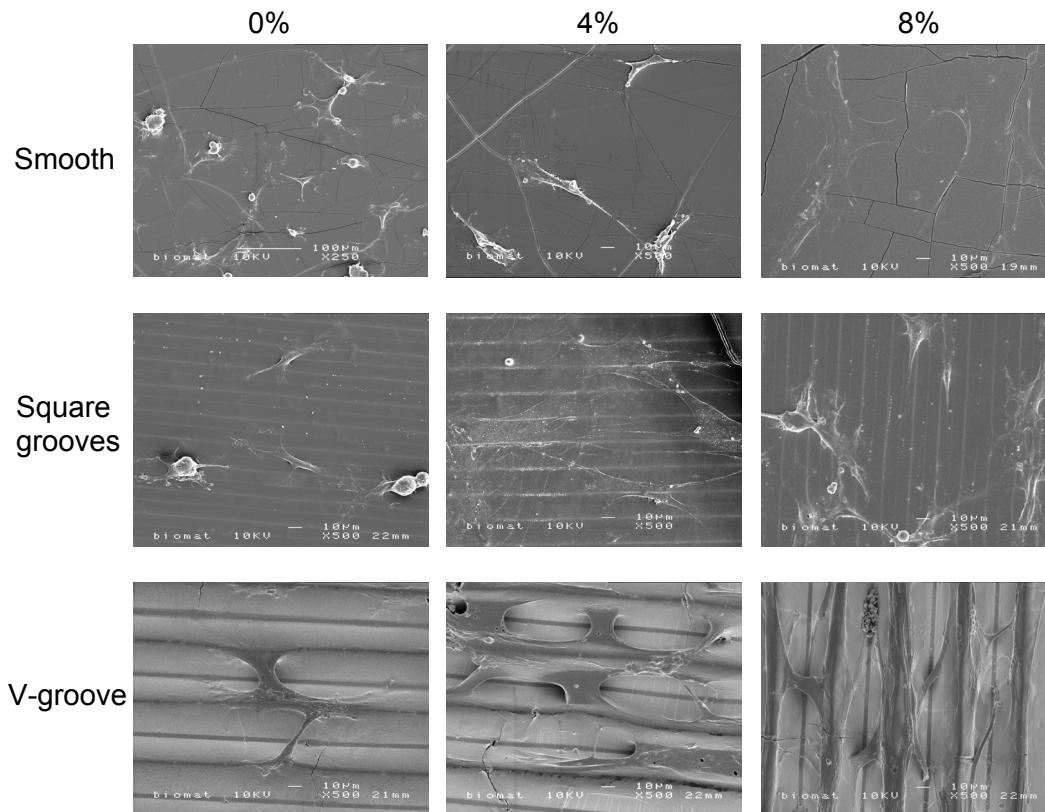


Figure 4: SEM micrographs of RDFs cultured under various circumstances. Top row: smooth substrates, 0% stretch force (left), 4% stretch force (centre), and 8% stretch force (left). Middle row: square-groove substrates, 0% parallel (left), 8% parallel (centre), 8% perpendicular (right). Bottom row: V-groove substrates, 0% parallel (left), 8% parallel (centre), 8% perpendicular (right). All micrographs were taken from 24 hrs samples.

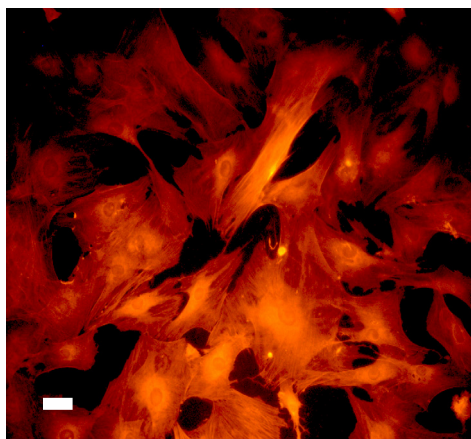


Figure 5: Phalloidin-TRITC fluorescence staining of the actin filaments of rat dermal fibroblasts cultured on a smooth silicone substrate. Magnification x20. Bar size = 10 micron.

With regard to groove direction; microgrooves perpendicular to the stretch direction elicit a better alignment: 82% of the cells aligned on perpendicular orientation compared to 57% on parallel orientation on V-grooves. On square grooves the percentages increased from 36% (parallel) to 77% (perpendicular).

The amount of stretching force does not influence cell alignment along the grooved topography. The effect of stretch force from 0% to 4%, or from 4% to 8% is marginal. The percentages of aligned cells are close to each other, average percentage differences are about 3-5%.

Finally, the effect of time on the alignment percentage is minimal, but significant. 24 hour samples show a higher alignment compared to their 3 hour counterparts; in smooth samples there is a 4% increase in time, on V-grooves and square-grooves this is 9% and 22% respectively. It should be noted that interaction of the parameters groove type and groove orientation makes exact interpretation difficult.

<i>Degree subgroups</i>	<i>0 - 10</i>	<i>11 - 45</i>	<i>46-90</i>
<i>Sample group</i>			
PLSQ3H0	35.4	39.8	24.8
PLSQ24H0	47.8	40.7	11.5
PDSQ3H0	38.0	44.8	17.2
PDSQ24H0	57.4	38.0	4.6
PLV3H0	66.9	27.4	5.7
PLV24H0	n/a	n/a	n/a
PDV3H0	75.7	21.8	2.5
PDV24H0	85.0	15.0	0
PLSQ3H4	23.8	39.1	37.1
PLSQ24H4	31.1	44.8	24.1
PDSQ3H4	n/a	n/a	n/a
PDSQ24H4	59.9	35.7	4.4
PLV3H4	53.5	37.8	8.7
PLV24H4	80.3	17.6	2.1
PDV3H4	76.9	18.5	4.6
PDV24H4	89.3	10.0	0.7
PLSQ3H8	14.9	32.2	52.9
PLSQ24H8	34.3	33.4	32.3
PDSQ3H8	58.6	34.7	6.7
PDSQ24H8	61.7	38.1	3.2
PLV3H8	55.7	31.6	12.7
PLV24H8	79.4	17.1	3.5
PDV3H8	72.5	23.4	4.1
PDV24H8	77.6	16.3	6.1
S3H0	15.3	34.8	49.9
S24H0	15.3	40.9	43.8
S3H4	16.8	49.0	34.2
S24H4	24.2	51.6	24.2
S3H8	n/a	n/a	n/a
S24H8	25.0	52.4	22.6

Table 2: Percentages of aligned cells divided in three subgroups. See Figure 6 for explanation of abbreviations.

RT-PCR

The mRNA expression for α 1-, and β 1-integrins, fibronectin, and collagen type I of the RDF cells was examined after each experimental run. An example of the visualised samples, separated on agarose gel, can be found in **Figure 7**, while all RT-PCR sample product ratios are listed in **Table 3**. With respect to the grooved samples; β 1 levels in the 0% stretch force were lower than those in the stretched samples. The Collagen Type I levels increased with higher stretch force. The smooth control samples showed that most product values were equal to the household gene, except the β 1-integrin subunit in samples experiencing either 4% or 8%, stretch force. Also the α 1-integrin subunit decreased with higher stretch magnitude.

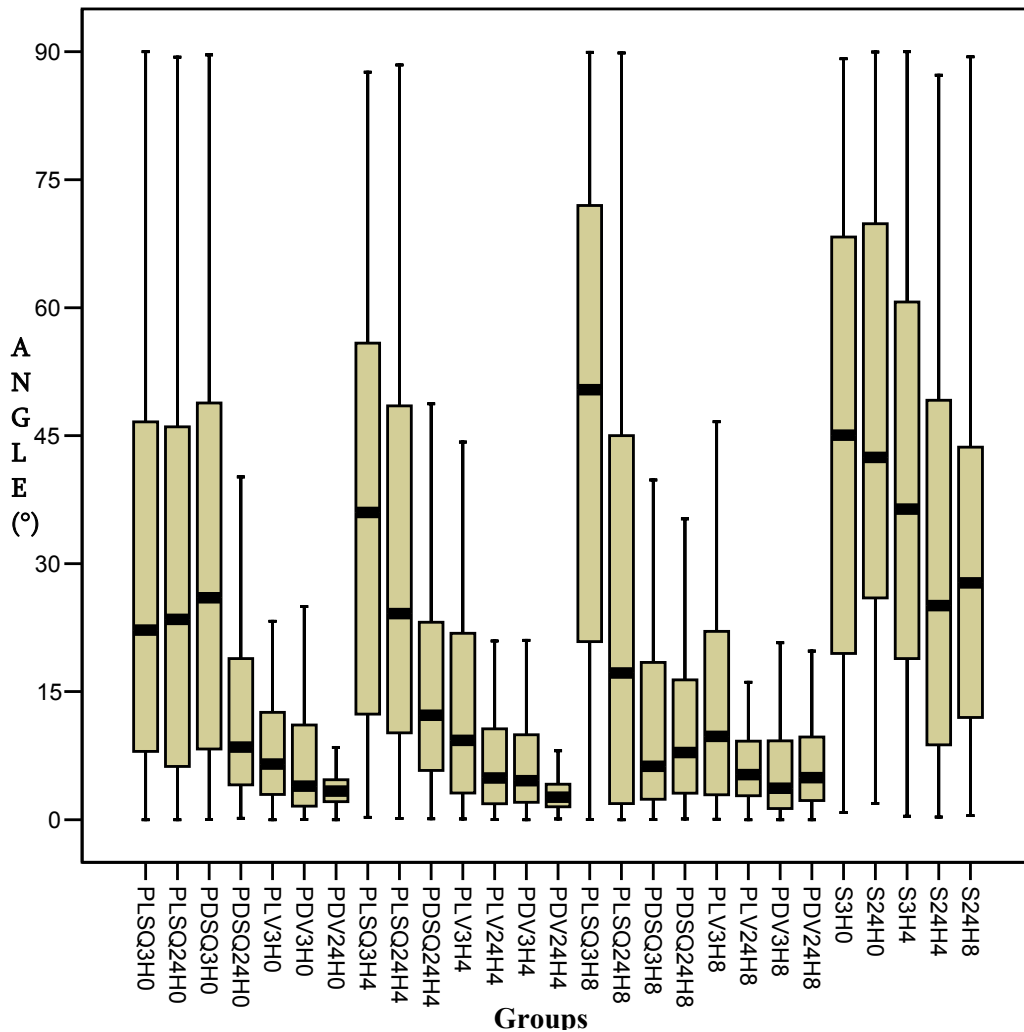


Figure 6: Box-whisker plot showing the distribution of cellular orientation. Note that no orientation is observed on the smooth samples and that orientation on grooved samples is dependent on the groove type. PL = parallel, PD = perpendicular, SQ = square groove, V = V-groove, 3H and 24H stands for the experiment time, and 0, 4, and 8 stands for the applied stretch force. For each parameter at least 300 individual cells were analysed.

DISCUSSION

The aim of this study was to evaluate *in vitro* the differences in cellular behaviour, between fibroblast cells, cultured on smooth and microgrooved substrates, which undergo cyclic stretching. From our data it could be concluded that independent of the stretch magnitude or whether the microgrooves are oriented parallel or perpendicular to the stretching direction, the fibroblasts primarily adjust their shape according to substrate surface (micro) features, whilst a secondary role is played by mechanical loading.

Scanning electron microscopy, immunofluorescence staining, and subsequent image analysis all confirmed that fibroblasts were oriented on both types of microgrooved surfaces. The shapes of the groove surfaces were based on earlier studies. Although the exact confirmation of the grooves differed, the rate of cellular orientation mainly was determined by increasing groove depth. This is in accordance with earlier work of Clark et al. [42; 43]. There it was concluded that groove depth is much more important in alignment of cells than the spacing of the grooves. Even when patterns of nanometer scale were used, an increase in groove depth led to better orientation [16].

Group	PL	PL	PD	PD	PL	PL	PD	PD	PL	PL	PD	PD	PL	PL	PD	PD
	SQ	SQ	SQ	SQ	V	V	V	V	SQ	SQ	SQ	SQ	V	V	V	V
	3H	24H	3H	24H	3H	24H	3H	24H	3H	24H	3H	24H	3H	24H	3H	24H
	0	0	0	0	0	0	0	0	4	4	4	4	4	4	4	4
$\alpha 1$	0.87	0.98	n/a	0.91	1	1	0.84	0.78	0.90	0.98	1	0.96	1	n/a	1	1
$\beta 1$	0.43	0.51	n/a	0.55	0.33	0.18	0.21	0.36	0.58	0.63	0.71	0.49	0.79	n/a	0.65	0.75
Fibro	0.88	0.61	n/a	0.98	0.80	0.86	0.94	0.67	0.99	1	0.40	1	1	n/a	0.99	0.99
Coll I	n/a	0.61	n/a	0.57	n/a	0.58	n/a	0.58	n/a	0.76	n/a	0.78	n/a	n/a	n/a	0.94

n/a: not available

Group	PL	PL	PD	PD	PL	PL	PD	PD	S	S	S	S	S	S
	SQ	SQ	SQ	SQ	V	V	V	V	3H	24H	3H	24H	3H	24H
	3H	24H	3H	24H	3H	24H	3H	24H	0	0	4	4	8	8
	8	8	8	8	8	8	8	8						
$\alpha 1$	1	0.95	n/a	n/a	1	0.3	0.42	1	1	1	1	0.28	1	0.76
$\beta 1$	1	0.96	n/a	n/a	1	0.91	0.58	0.78	1	1	1	0.86	0.84	0.72
Fibro	1	1	n/a	n/a	1	0.92	1	1	1	1	1	1	1	1
Coll I	n/a	0.96	n/a	n/a	n/a	0.87	n/a	0.99	n/a	1	n/a	0.96	n/a	1

Table 3: RT-PCR semiquantitative analysis. Displayed are the ratios between the gene of interest and the household gene GAPDH. See Figure 6 for explanation of group abbreviations.

In the current study, it was seen that cells on square-groove substrates were able to reach the bottom of the 1 μ m deep grooves, whereas on the substrates with V-grooves the cells lost contact with the bottom of the grooves. The cellular extensions probing the V-groove substrate surface only find the top ridge, resulting in extension of the cellular body along these ridges. This difference in behaviour might explain the variation in the orientation between the different groove depths. Orientation is almost independent of groove spacing. There is only a small dependency, probably caused by the fact that sometimes cells cross-over to other top ridges, where part of the cell is extending in the same direction.

In our study, after 3 hours of stretch cellular orientation starts to commence, and after 24 hours the cells have aligned themselves almost entirely along the grooves. This observation was also noted by Neidlinger-Wilke and co-workers [3], studying only the exposure to cyclic stretch (i.e. no surface texturing was applied). These researchers found that the degree of cell alignment continued to improve up to 24 hours. Similarly, Walboomers *et al* [18] described early events displayed by fibroblast cells on textured surfaces. In that particular study, it was found that cell orientation on microtextures starts with the formation of abundant membrane extensions. These are probable signs of exploration and probing of the surface by the cells. Since the cell is lacking

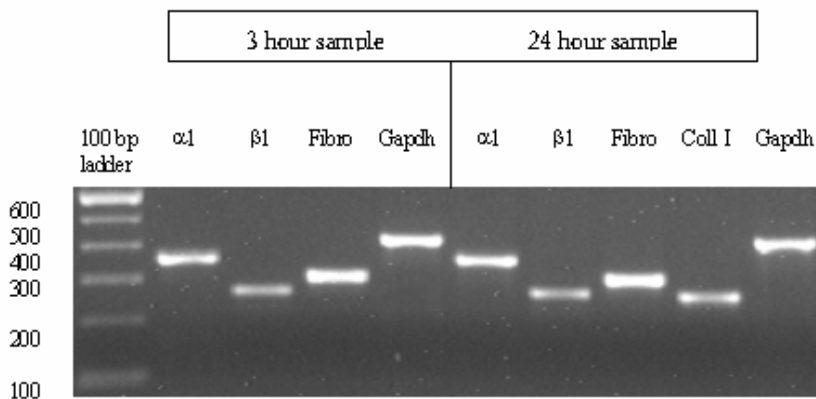


Figure 7: RT-PCR sample example of parallel oriented square-type grooves with 4% stretch force, visualised on agarose gel.

natural ECM, and neighbouring cells, these extensions are formed in all directions. Within hours, the presence of suitable attachment sites is confirmed and contacts are established with deposited ECM material. The cell flattens and spreads, and active filaments form longitudinal stress fibres

[44]. In this study, it was evident that cellular orientation occurred immediately during the cell spreading, and always was parallel to the grooves.

Cell movements or orientation as reaction to mechanical stress might be based on a comparable mechanisms. But in contrast to the responses to microtextures as described above, the reaction towards the mechanical loading can only occur after cell has attached and spread out over the surface, and after the cell has established an inter-connective system of ECM, integrins, and cytoskeleton. From our RT-PCR results it is clear that the production of these components is vital for cells, so they have a mechanically resistant attachment support. This is indicated by the fact that cells under mechanical stimulation show enhanced β 1-integrin and collagen-I levels. The cell-matrix interactions in cultured fibroblasts cells are almost solely mediated via receptors of the integrin family. Upon recognition of the extracellular ligand, integrins start to cluster and become activated, which results in recruitment of an array of proteins and the formation of the focal adhesion complex (FAC), containing both cytoskeletal and signalling molecules [44-47]. Activation results in repeated (de)polymerisation series of actin, and finally the formation of stress fibres. These structures establish a physical link between the ECM components and the cytoskeleton via the integrins, thereby offering a continuous path acting as a mechanotransducer. This “mechanosensing connection” is used by the cells to perform their mechanical functions as for instance the orientation changes as response to the stretching. In vitro, cells are geared towards a mechanical equilibrium between the tension of the ECM support and the stress in the cells, since application of external tension or relaxation to the support is rapidly compensated by cell relaxation or traction [45; 46].

From the image analysis it also became clear that substrates with microgrooves perpendicular to the stretch direction elicit a better cell alignment. This is to be expected, since cells align along the grooves, and their orientation is increased by turning away from the stretch direction. This is a new finding, as Wang et al [5] recently reported that cyclic stretching of fibroblasts on microgrooved surfaces did not result in changes of alignment regardless of the stretching direction. In contrast, in our study we did see an additional effect of stretch vs. orientation. Probably, if grooves are made small enough, there is a point where mechanical loading can overrule clues delivered to the cells in the form of surface texturing. However, further research will be required to establish such a threshold dimension for the grooves, as it will necessitate the development of textures at a nanometer level. Such development is currently underway [48]. Several research groups did describe the effects of nanotopography, like Wojciak-Stothard *et al* [7] who used microfabricated grooves and steps, 30-282 nm deep. Teixeira *et al* [49; 50] used grooves with varying pitches between 400 nm and 4 μ m, which were either 150 or 600 nm deep. Still, true nanotechnology to achieve 1-20 nanometer patterns simultaneously in groove width, spacing, and depth, needs to be developed yet.

Some of the issues that remain to be investigated are, whether the cytoskeleton or the cell responses to environmental stimuli occur earlier. Cell orientation should be considered separate from orientation of e.g. actin microfilaments. Shirinsky and co-workers [51] observed that actin cytoskeleton is closely involved in the orientation process, yet when the orientation is completed, the cells are no longer dependent upon that system to maintain their position. Moreover, the relationship between the cytoskeleton and the intracellular signalling is a field in which further research has to be conducted. It is known that the cytoskeleton is constantly remodelling to provide a rapid reaction system for the cell to respond to changes in their mechanical environment, and to supply the best possible way to maintain equilibrium with their environment. For understanding cell reactions, we first need to understand when the reaction is initiated, and in what cell parts: i.e. the focal adhesion complex with its membrane receptors, the cytoskeletal components, or the interacting proteins of the cellular signalling.

CONCLUSION

We can maintain our hypothesis, as microgrooved topography is most effective in applying strains relative to the long axis of the cell. Actin microfilament rearrangement may predetermine the subsequent alignment and elongation of the fibroblasts, which in turn can regulate fibroblast attachment via the intracellular signalling pathways to the underlying membrane receptors. It is here that the secondary effects of stretch force take place. How the mechanotransduction, responsible for the cell orientation, actually works remains to be fully solved. The different forces of uni-axial cyclic stretching combined with the two different loading conditions with respect to the cells long axes may activate different mechano-transduction mechanisms, but the net result is the same: i.e. reduction of mechanical resistance on the cells. The cell will choose the path of least resistance, and adjust its shape to the strongest environmental clue.

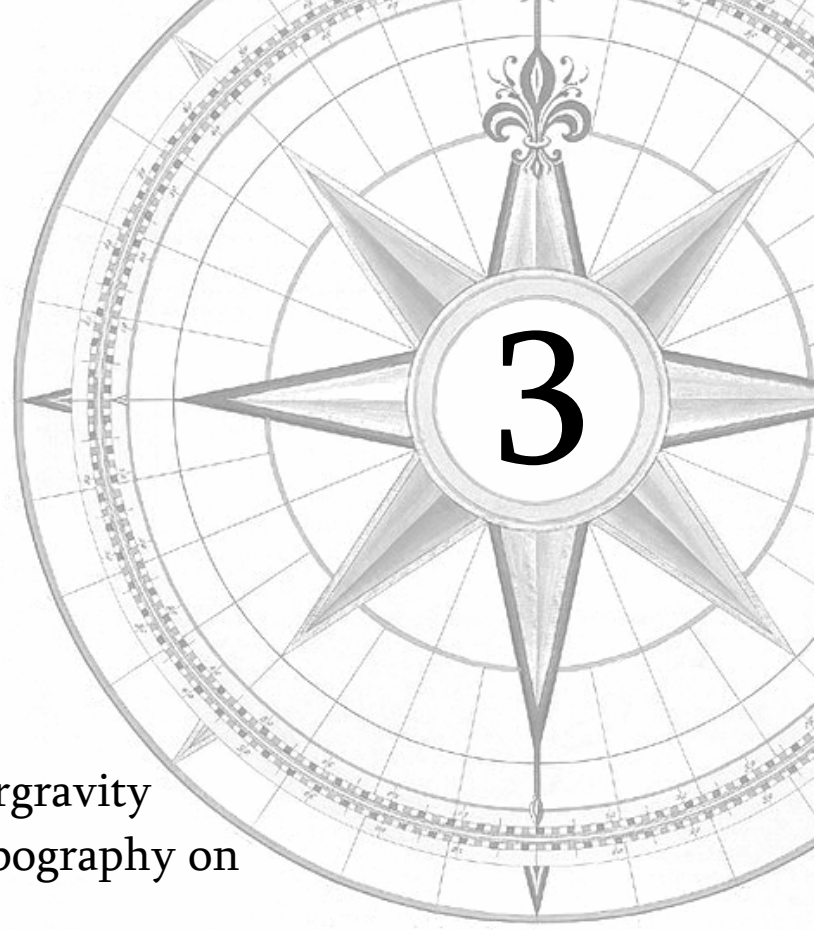
REFERENCES

1. Neidlinger-Wilke, C., Grood, E. S., Wang JH-C, Brand, R. A., and Claes, L. Cell alignment is induced by cyclic changes in cell length: studies of cells grown in cyclically stretched substrates. *J Orthop Res* 2001, 286-93, 2001.
2. Winter, L. C., Walboomers, X. F., Bumgardner, J. D., and Jansen, J. A. Intermittent versus continuous stretching effects on osteoblast-like cells in vitro. *J Biomed Mater Res* 2003, 1269-75, 2003.
3. Neidlinger-Wilke, C., Grood, E., Claes, L., and Brand, R. Fibroblast orientation to stretch begins within three hours. *J Orthop Res* 2002, 953-6, 2002.
4. Wang, J. H., Jia, F., Gilbert, T. W., and Woo, S. L. Cell orientation determines the alignment of cell-produced collagenous matrix. *J Biomech* 2003, 97-102, 2003.
5. Wang, J. H., Yang, G., Li, Z., and Shen, W. Fibroblasts responses to cyclic mechanical stretching depend on cell orientation to the stretching direction. *J Biomech* 2003, 573-6, 2003.
6. Pender, N. and McCulloch, C. A. Quantitation of actin polymerization in two human fibroblast sub-types responding to mechanical stretching. *J Cell Sci* 1991, 187-93, 1991.
7. Wojciak-Stothard, B., Curtis, A., Monaghan, W., MacDonald, K., and Wilkinson, C. Guidance and activation of murine macrophages by nanometric scale topography. *Exp Cell Res* 1996, 426-35, 1996.
8. Wojciak-Stothard, B., Madeja, Z., Korohoda, W., Curtis, A., and Wilkinson, C. Activation of macrophage-like cells by multiple grooved substrata. Topographical control of cell behaviour. *Cell Biol Int* 1995, 485-90, 1995.
9. den Braber, E. T., Jansen, H. V., de Boer, M. J., Croes, H. J., Elwenspoek, M., Ginsel, L. A., and Jansen, J. A. Scanning electron microscopic, transmission electron microscopic, and confocal laser scanning microscopic observation of fibroblasts cultured on microgrooved surfaces of bulk titanium substrata. *J Biomed Mater Res* 1998, 425-33, 1998.
10. den Braber, E. T., de Ruijter, J. E., Smits, H. T., Ginsel, L. A., von Recum, A. F., and Jansen, J. A. Quantitative analysis of cell proliferation and orientation on substrata with uniform parallel surface micro-grooves. *Biomaterials* 1996, 1093-9, 1996.
11. Walboomers, X. F., Croes, H. J., Ginsel, L. A., and Jansen, J. A. Growth behavior of fibroblasts on microgrooved polystyrene. *Biomaterials* 1998, 1861-1868, 1998.
12. Walboomers, X. F., Monaghan, W., Curtis, A. S., and Jansen, J. A. Attachment of fibroblasts on smooth and microgrooved polystyrene. *J Biomed Mater Res* 1999, 212-20, 1999.
13. Clark, P., Connolly, P., and Moores, G. R. Cell guidance by micropatterned adhesiveness in vitro. *J Cell Sci* 1992, 287-92, 1992.

14. Oakley, C., Jaeger, N. A., and Brunette, D. M. Sensitivity of fibroblasts and their cytoskeletons to substratum topographies: topographic guidance and topographic compensation by micromachined grooves of different dimensions. *Exp Cell Res* 1997, 413-24, 1997.
15. Brunette, D. M. Fibroblasts on micromachined substrata orient hierarchically to grooves of different dimensions. *Exp Cell Res* 1986, 11-26, 1986.
16. Clark, P., Connolly, P., Curtis, A. S., Dow, J. A., and Wilkinson, C. D. Cell guidance by ultrafine topography in vitro. *J Cell Sci* 1991, 73-7, 1991.
17. Matsuzaka, K., Walboomers, F., de Ruijter, A., and Jansen, J. A. Effect of microgrooved poly-l-lactic (PLA) surfaces on proliferation, cytoskeletal organization, and mineralized matrix formation of rat bone marrow cells. *Clin Oral Implants Res* 2000, 325-33, 2000.
18. Walboomers, X. F., Ginsel, L. A., and Jansen, J. A. Early spreading events of fibroblasts on microgrooved substrates. *J Biomed Mater Res* 2000, 529-534, 2000.
19. von Recum, A. F. and van Kooten, T. G. The influence of micro-topography on cellular response and the implications for silicone implants. *J Biomater Sci Polym Ed* 1995, 181-98, 1995.
20. Neidlinger-Wilke, C., Wilke, H. J., and Claes, L. Cyclic stretching of human osteoblasts affects proliferation and metabolism: a new experimental method and its application. *J Orthop Res* 1994, 70-8, 1994.
21. Buckley, M. J., Banes, A. J., Levin, L. G., Sumpio, B. E., Sato, M., Jordan, R., Gilbert, J., Link, G. W., and Tran Son Tay, R. Osteoblasts increase their rate of division and align in response to cyclic, mechanical tension in vitro. *Bone Miner* 1988, 225-36, 1988.
22. Yoshinari, M., Matsuzaka, K., Inoue, T., Oda, Y., and Shimono, M. Effects of multigrooved surfaces on fibroblast behavior. *J Biomed Mater Res* 2003, 359-368, 2003.
23. Hughes-Fulford, M. and Gilbertson, V. Osteoblast fibronectin mRNA, protein synthesis, and matrix are unchanged after exposure to microgravity. *FASEB J* 1999, S121-7, 1999.
24. Chiquet, M., Renedo, A. S., Huber, F., and Fluck, M. How do fibroblasts translate mechanical signals into changes in extracellular matrix production? *Matrix Biol* 2003, 73-80, 2003.
25. Leung, D. Y., Glagov, S., and Mathews, M. B. Cyclic stretching stimulates synthesis of matrix components by arterial smooth muscle cells in vitro. *Science* 1976, 475-7, 1976.
26. Carver, W., Nagpal, M. L., Nachtigal, M., Borg, T. K., and Terracio, L. Collagen expression in mechanically stimulated cardiac fibroblasts. *Circ Res* 1991, 116-22, 1991.
27. Kessler, J. O. The internal dynamics of slowly rotating biological systems. *ASGSB Bull* 1992, 11-21, 1992.
28. Brunette, D. M. and Chehroudi, B. The effects of the surface topography of micromachined titanium substrata on cell behavior in vitro and in vivo. *J Biomech Eng* 1999, 49-57, 1999.
29. Chehroudi, B., Gould, T. R., and Brunette, D. M. Effects of a grooved epoxy substratum on epithelial cell behavior in vitro and in vivo. *J Biomed Mater Res* 1988, 459-73, 1988.
30. Matsuzaka, K., Walboomers, X. F., Yoshinari, M., Inoue, T., and Jansen, J. A. The attachment and growth behavior of osteoblast-like cells on microtextured surfaces. *Biomaterials* 2003, 2711-9, 2003.
31. Parker, J. A., Walboomers, X. F., Von den Hoff, J. W., Maltha, J. C., and Jansen, J. A. Soft-tissue response to silicone and poly-L-lactic acid implants with a periodic or random surface micropattern. *J Biomed Mater Res* 2002, 91-8, 2002.
32. Chehroudi, B. and Brunette, D. M. Subcutaneous microfabricated surfaces inhibit epithelial recession and

- promote long-term survival of percutaneous implants. *Biomaterials* 2002, 229-37, 2002.
33. Chehroudi, B., McDonnell, D., and Brunette, D. M. The effects of micromachined surfaces on formation of bonelike tissue on subcutaneous implants as assessed by radiography and computer image processing. *J Biomed Mater Res* 1997, 279-90, 1997.
 34. Walboomers, X. F., Croes, H. J., Ginsel, L. A., and Jansen, J. A. Contact guidance of rat fibroblasts on various implant materials. *J Biomed Mater Res* 1999, 204-12, 1999.
 35. den Braber, E. T., de Ruijter, J. E., Ginsel, L. A., von Recum, A. F., and Jansen, J. A. Quantitative analysis of fibroblast morphology on microgrooved surfaces with various groove and ridge dimensions. *Biomaterials* 1996, 2037-44, 1996.
 36. Parker, J. A., Walboomers, X. F., Von den, H. J., Maltha, J. C., and Jansen, J. A. Soft tissue response to microtextured silicone and poly-L-lactic acid implants: fibronectin pre-coating vs. radio-frequency glow discharge treatment. *Biomaterials* 2002, 3545-53, 2002.
 37. Beumer, G. J., Van Blitterswijk, C. A., and Ponec, M. The use of gas plasma treatment to improve the cell-substrate properties of a skin substitute made of poly(ether)/poly(ester) copolymers. *J Mat Sc Mat Med* 5, 1-6. 94.
 38. Amstein, C. F. and Hartman, P. A. Adaptation of plastic surfaces for tissue culture by glow discharge. *J Clin Microbiol* 1975, 46-54, 1975.
 39. Freshney, R. I. Culture of animal cells: a multimedia guide. 99. Chichester, John Wiley & Sons Ltd.
 40. Wang, H., Ip, W., Boissy, R., and Grood, E. S. Cell orientation response to cyclically deformed substrates: experimental validation of a cell model. *J Biomech* 1995, 1543-52, 1995.
 41. Walboomers, X. F., Habraken, W. J., Feddes, B., Winter, L. C., Bumgardner, J. D., and Jansen, J. A. Stretch-mediated responses of osteoblast-like cells cultured on titanium-coated substrates in vitro. *J Biomed Mater Res* 2004, 131-9, 2004.
 42. Clark, P., Connolly, P., Curtis, A. S., Dow, J. A., and Wilkinson, C. D. Topographical control of cell behaviour. I. Simple step cues. *Development* 1987, 439-448, 1987.
 43. Clark, P., Connolly, P., Curtis, A. S., Dow, J. A., and Wilkinson, C. D. Topographical control of cell behaviour: II. Multiple grooved substrata. *Development* 1990, 635-644, 1990.
 44. Hynes, R. O. and Destree, A. T. Relationships between fibronectin (LETS protein) and actin. *Cell* 1978, 875-86, 1978.
 45. Lambert, Ch. A., Nusgens, B. V., and Lapiere, Ch. M. Mechano-sensing and mechano-reaction of soft connective tissue cells. *Adv Space Res* 1998, 1081-91, 1998.
 46. Hynes, R. O. Cell adhesion: old and new questions. *Trends Cell Biol* 1999, M33-7, 1999.
 47. Burridge, K. and Fath, K. Focal contacts: transmembrane links between the extracellular matrix and the cytoskeleton. *Bioessays* 1989, 104-8, 1989.
 48. Curtis, A. and Wilkinson, C. New depths in cell behaviour: reactions of cells to nanotopography. *Biochem Soc Symp* 1999, 15-26, 1999.
 49. Teixeira, A. I., Abrams, G. A., Bertics, P. J., Murphy, C. J., and Nealey, P. F. Epithelial contact guidance on well-defined micro- and nanostructured substrates. *J Cell Sci* 2003, 1881-92, 2003.
 50. Teixeira, A. I., Nealey, P. F., and Murphy, C. J. Responses of human keratocytes to micro- and nanostructured substrates. *J Biomed Mater Res* 2004, 369-76, 2004.

51. Shirinsky, V. P., Antonov, A. S., Birukov, K. G., Sobolevsky, A. V., Romanov, Y. A., Kabaeva, N. V., Antonova, G. N., and Smirnov, V. N. Mechano-chemical control of human endothelium orientation and size. *J Cell Biol* 1989, 331-9, 1989 .



The effect of combined hypergravity
and microgrooved surface topography on
the behaviour of fibroblasts

WA Loesberg, XF Walboomers, JJWA van Loon and JA Jansen

Cell Motil Cytoskeleton. 63 (7), 384-394, 2006

INTRODUCTION

Cells cultured on textured substrata are very responsive to surface micro- and nanometre features [1-5]. For example, remodelling of the cytoskeleton [4; 6; 7], cell proliferation [6; 8; 9], gene expression and protein synthesis [10] have been shown to be affected by substratum surface geometrical conditions [11]. Also, it is known that surface topography can actively direct cell shape and spreading [10-17]. Evidently, cells are capable of sensing the structural shape of their environment, and determine their form and function appropriately.

How cell behaviour is guided by texture is well known, and it seems that the underlying principle is similar to the processes occurring when mechanical forces are applied to cells. Mechanotransduction of stationary (texture) and dynamic (mechanical strain) forces has led to research in a new topic: interaction between different forces. One of those forces that can be used to study this interaction is gravity. In a laboratory environment, it is very well possible to simulate conditions of altered gravity by using centrifuges for hypergravity and random rotation for microgravity. Although cells seem too small to experience gravity as a major force, cells may sense gravity-mediated changes in their environment [18-20]. Small changes might be integrated or amplified thus generating the various changes as seen under micro- or hyper-gravity conditions [21]. Much research has been conducted on lymphocytes and their behaviour in microgravity [22-26]. Marked differences were found in proliferation, apoptosis, production of cytokines, etc. In case of fibroblasts, mechanical stress is an important regulator of distinct cell shape and extracellular matrix component production [27-29]. Some more theoretical studies have argued against cells sensing gravity or changes therein [30; 31]. Nevertheless, a limited number of studies has been performed to examine cell shape changes under various gravity conditions [23; 32-36]. A change in cell shape measured under varying g levels contributes to the idea of direct effects of gravity onto cells.

Although each force affecting cell behaviour separately is relatively well studied *in vitro*, in the living organism always multiple forces will be present. The interaction between forces however remains poorly understood [37; 38]. Therefore, the two aforementioned parameters: topography and (hyper)gravity will be investigated in this study. Thus, this study evaluates *in vitro* the differences in morphological behaviour between fibroblast cells cultured on polystyrene substrata, both smooth and microgrooved, which are placed in a hypergravity environment. In addition, the up regulation of several proteins involved in cell-surface interaction will be investigated. The underlying aim is to discern which parameter is more important in determining final cell response. Our hypothesis is that cellular shape and orientation is determined by the topographical cues on the substrata and gravity increases the cellular attachment to these substrata. As controls fibroblast cells will be cultured on similar substrata which will remain at normal (Earth) gravity.

MATERIALS AND METHODS

Substrata:

Microtextured patterns were etched in a silicon wafer using lithographic and ion etching techniques as described by Walboomers *et al.* [1]. Ridge- and groove widths were 1, 2, 5, or 10 μm , with a uniform depth of 1.0 μm . Smooth substrata were prepared to serve as the control group. These silicon wafers were used as templates for the production of polystyrene (PS) substrata for cell culturing [39]. Replicas were equipped with 18mm diameter cylinders to obtain culture dishes (**Figure 1**). Before use a radio frequency glow-discharge (RFGD) treatment was applied for 5 min at a pressure of 2.0×10^{-2} mbar (Harrick Scientific Corp., Ossining, NY, USA) to improve wettability of the substrata [40-44].

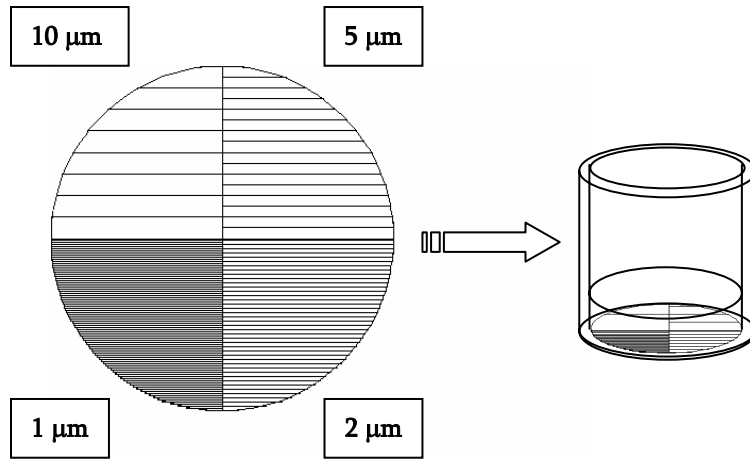


Figure 1. Graphical presentation of a top view of the template surface topography featuring the different groove types and the complete culture dish used in this study (height: 18 mm, width: 18 mm, surface: 269 mm², medium level during experimentation: 4.4 mm). For clarity the drawings are not to scale.

Cell culture:

Rat dermal fibroblasts (RDFs) were obtained from the ventral skin of male Wistar rats [45]. To ensure quick and constant availability, cells were cryo-preserved. Before experimentation, cells were thawed and cultured in α -Modified Eagles Medium (α -MEM) containing Earle's salts, L-glutamine, 10% foetal calf serum (FCS), and gentamicin (50 μ g/ml). Cells were cultured in a 5% CO₂ incubator set at 37°C in a humidified atmosphere. Experiments were performed with 6 - 8th culture generation cells. Onto all substrata, 1.5×10^4 cells/cm² were seeded. After pre-incubation of 1 h, the culture dishes were inserted into a 12-wells plate for support. The wells plate was placed inside aluminium culture boxes with a humidified atmosphere. These culture boxes in turn were hung into brackets enabling the boxes to tilt/swing so the hypergravity was perpendicular to the surface. Before running, the culture boxes were provided with an appropriate volume of CO₂ to ensure pH stability.

The medium size centrifuge for acceleration research (MidiCAR) was used in this study to simulate hypergravity (**Figure 2**). The centrifuge is housed inside a temperature controlled cabinet and contains a control sample compartment enabling the control samples to undergo the same circumstances, yet at 1 g (Earth) gravity. The culture dishes with a grooved substratum were placed at random inside the 12-wells plate. Previous pilot studies revealed no differences on a cellular level whether the grooves were placed horizontally or vertically with respect to the rotation axis. Centrifuge setting ranges were: 10, 25 or 50 g for two different time periods: 4 or 24 hours. [46-48]. Directly at the end of each time period, the RDF cell layers were washed three times with PBS, fixed, and prepared for further analysis.

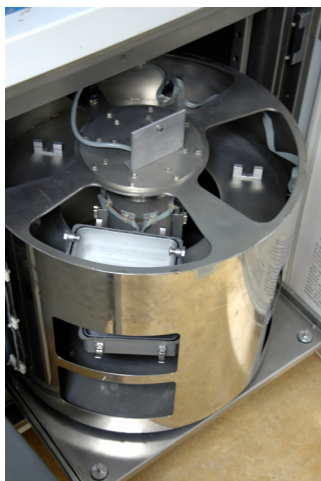


Figure 2. The Medium Size Centrifuge for Acceleration Research (MidiCAR) used to simulate hypergravity, in which the samples were subjected up to 10, 25 or 50 times Earth's gravity. The MidiCAR is equipped with a computerised temperature and motor control. The control samples are placed in the upper (non-spinning) compartment of the centrifuge, while the other samples are placed in brackets in the mid and lower section.

Scanning electron microscopy:

To assess cellular morphology of the fibroblasts (n = 4 dishes), scanning electron microscopy (SEM) was used. Cells were washed, fixed for 5 minutes in 2% glutaraldehyde, rinsed for 5 minutes with 0.1 M sodium-cacodylate buffer (pH 7.4), dehydrated in a series of ethanol, and dried in tetramethylsilane. Specimens were sputter coated with gold and examined with a Jeol 6310 SEM.

Immunofluorescence

To observe the cytoskeleton, cells (n = 4 dishes) were fixed for 30 minutes in 2% paraformaldehyde, and permeabilised with 1% Triton X100 for 5 min. Filamentous actin was stained with Alexa Fluor 568 phalloidin (Molecular Probes Inc., Eugene, OR, USA) diluted in PBS/1% Bovine Serum Albumin (BSA) to block non-specific epitopes. Vinculin was stained with mouse monoclonal primary antibodies to vinculin (Sigma, V-9131), followed by labelling with Alexa Fluor 488 goat anti-mouse secondary antibodies IgG. Finally, the specimens were examined with a Biorad MRC 1000 confocal laser scanning microscope (CLSM) system at magnification of 10x.

For quantitative image analysis samples (n = 4 dishes) were stained with Phalloidin-TRITC (Sigma, P-1951), followed by examination with a Leica/Leitz DM RBE Microscope at magnification of 10x.

Image Analysis

The digital immunofluorescence images acquired with the CLSM were loaded into Confocal Assistant (version 4.02) to create overlay images. The Phalloidin-TRITC fluorescence micrographs were analyzed with Scion Image software (Beta Version 4.0.2, Scion Corp., Frederick, MY, USA). The orientation of the cell on the surface was examined. For each sample four fields of view were selected randomly. Within each field two criteria were used for cell selection: (1) the cell is not in contact with other cells and (2) cell is not in contact with the field perimeter. Thereafter, on each cell within the field the following parameters were examined: first, the maximum cell diameter was measured as the longest distance between two edges within the cell borders. Second, the angle between this axis and the grooves (or an arbitrarily selected line for smooth surfaces). This latter measurement will be termed the orientation angle. Cell extensions like filopodia, which could confound the alignment measurement, were not included when assessing the cell orientation. Using Clarks criteria [13], cells oriented at 0–10 degrees from the groove direction were regarded to be aligned.

RT-PCR analysis

Total RNA was isolated from the RDFs with an isolation and stabilisation kit (QIAGEN, Hilden, Germany), and cDNA was synthesised from 1 mg of total RNA (n = 3 x 4 dishes). After initial denaturation for 2 min at 95°C, the samples were amplified for 35 cycles (annealing 55°C 1 min, elongation 72°C 2 min, denaturation 95°C 1 min). The duration of the final elongation reaction was increased to 10 min at 72°C to permit completion of reaction products. The PCR products were separated on a 1.5% (w/v) agarose gel, and visualised by ethidium bromide staining. Semi-quantitative analysis of band intensity was performed using Quantity One 1-D analysis software for Windows (Version 4.5.0, Bio Rad, Hercules, California, USA). The collagen type I (only 24 hours samples), fibronectin, $\alpha 1$ integrin, $\beta 1$ integrin gene expressions were normalised to glyceraldehyde-3-phosphate dehydrogenase (GAPDH) values. Forward and reverse primer sequences are shown in **Table 1**.

	5' Primer (Forward)	3'Primer (Reverse)	Size (bp)
Collagen Type I	TGTTTCGTGGTTCTCAGGGTAG	TTGTCGTAGCAGGGTTCTTTC	254
Fibronectin	CCTTAAGCCTTCTGCTCTGG	CGGCAAAAGAAAGCAGAAGT	301
α 1-Integrin	AGCTGGACATAGTCATCGTC	AGTTGTCATGCGATTCTCCG	374
β 1-Integrin	AATGTTTCAGTGCAGAGCC	TTGGGATGATGTCGGGAC	262
GAPDH	CGATGCTGGCGCTGAGTAC	CGTTCAGCTCAGGGATGACC	470

Table 1: Forward and reverse primer sequences used in this study.

Statistical analysis:

Acquired quantitative data were analysed using SAS for Windows (Release 9, SAS Institute Inc., Cary, North Carolina, USA). The effects of and the possible interaction between both time or gravity and surface were analysed using two-way analysis of variance (ANOVA) with Scheffé post-test. A probability (p) value less than or equal to 0.05 was considered significant.

RESULTS

Scanning Electron Microscopy

SEM illustrated the accurate reproduction of grooves and ridges in the polystyrene substrata (**Figure 3**). The accuracy of the casting process was apparent in the additional roughness on the ridges of the polystyrene substrata due to the etching process, which was used to fabricate the original silicon wafers. When analysing cell morphology (**Figure 4A & B**), SEM showed that on smooth substrata (control) cells were spread out in a random fashion, while RDF cells aligned along the groove direction on all grooved surfaces. Cells cultured on the substratum quadrants with the smaller grooves (1 and 2 micron, **Figure 4C**) seemed to be more clearly aligned than compared to wider grooved parts of the substrata (5 and 10 micron, **Figure 4D**). The same applied for cells cultured for the shorter time period (4 hours, **Figure 4E**) in comparison to the 24 hours culturing (**Figure 4F**). Although better alignment was observed on most 4 hours samples, some showed a similar alignment with the 24 hours samples. The cells cultured on widely spaced grooved substrata ($>5\mu\text{m}$) had a flat appearance, and were able to descend into the grooves, whereas the cells cultured on small grooved substratum were nearly always found on top of the ridges (**Figure 4G & H**). In the latter, cellular extensions probing the substratum surface only find the top ridge, resulting in extension of the cellular body along these small ridges.

The cytoskeleton was investigated by staining filamentous actin and vinculin anchor points of the cell focal adhesions. **Figure 5A** shows a 1g smooth substratum sample, the observed cell shape and spreading and random orientation was similar to SEM micrographs. Red staining is that of the actin filaments, which were running parallel and in the long axis of cells. Vinculin staining resulted in a considerable background around the nucleus. Vinculin spots were visible in some photos, positioned at the end of actin bundles, and extended in the direction of the actin bundle. RDFs cultured on grooved surfaces displayed a similar view, as was found on smooth surfaces; however there was clear orientation of the cells and their cytoskeleton (**Figure 5B**). The overall view of cells cultured on smooth surfaces at increased g-load did not change notably (**Figure 5C**). This is in contrast to the cells cultured on grooved substrata: with increasing g force the alignment of the cells increased, reaching its optimum at 25g (**Figure 5B, D, E**). At 50 g the cells changed their shape and tended to spread out more, which was not observed for the smooth controls. **Figure 5F** reveals an abundant staining of vinculin in the micrographs, while actin filament staining in several cells was reduced.

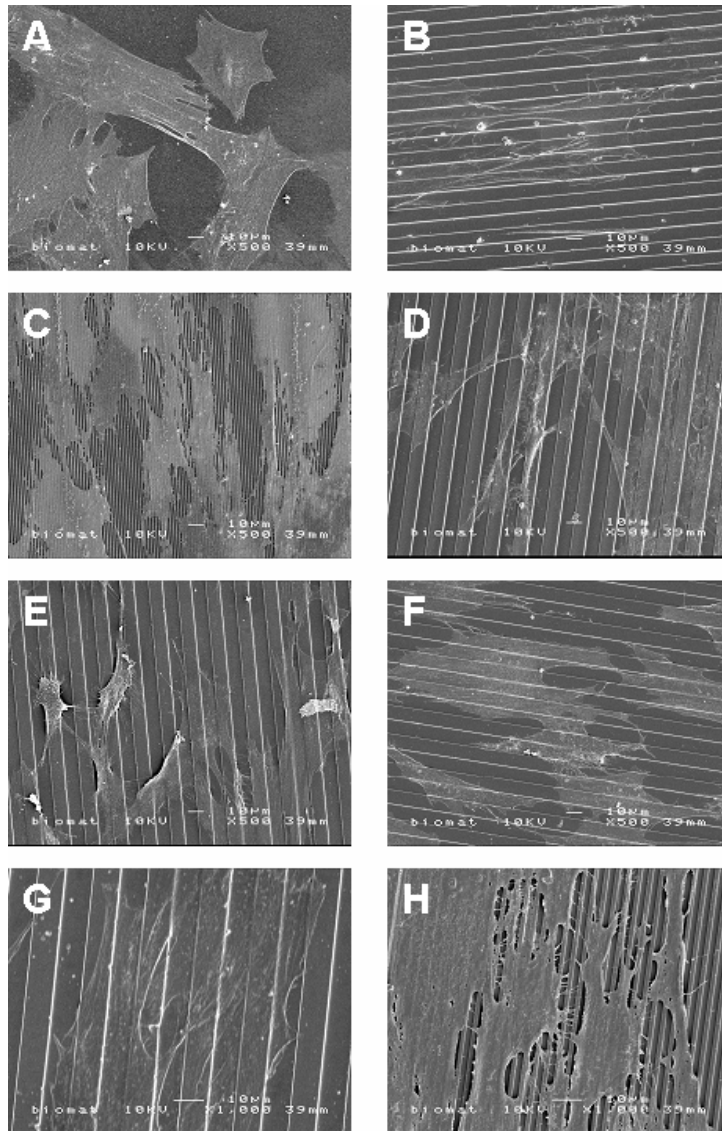


Figure 4. SEM micrographs of RDFs cultured under various conditions. (A) smooth substratum with cells in a random fashion, (B) 10 μm wide grooved substratum displaying aligned cells. Increased alignment of cells cultured on smaller grooves (C, 1 μm wide) in comparison to wide grooves (D, 10 μm wide). After 4 hours of centrifugation, cells display alignment (E, 10 μm wide), after 24 hours however the alignment becomes more apparent as can be seen in cell narrowness (F, 10 μm wide). Cells cultured on wide grooves (10 μm) are spread out in appearance (G) while on smaller grooves (2 μm) the cells can be found on top of the ridges (H). All micrographs were taken from 24 hrs samples, unless otherwise stated (magnification A till F = x500, G,H = x1000)).

Image Analysis

The actin filaments stained with phalloidin-TRITC were clearly visible in fluorescence microscopy. Image analysis confirmed the cellular orientation behaviour, as was seen with the SEM, *i.e.* while the RDFs cultured on grooved substrata in general showed alignment along the grooves; the smooth control samples did not induce any form of alignment. The quantified results for cell alignment are presented as box-whisker plots (**Figure 6**). Such a graph shows the distribution midpoint, the 25th and 75th percentile (boxes), and the largest and smallest observation (whiskers).

Because of the obvious significant differences between smooth and grooved surfaces, it was decided to analyse within both groups instead of between both groups. **Figure 7** depicts the mean angles of RDFs cultured on either smooth or grooved substrata divided over time. On smooth surfaces (**Figure 7A**) no significant change in alignment could be measured with increasing neither gravitational force nor time. The mean angle of cells cultured on grooved surfaces significantly decreased (thus alignment increased) with increasing g-force until it reached a turning point between 25 and 50g where it displayed an increase in mean angle value (**Figure 7B**). This pattern was shown consistently in both subgroups of 4 and 24 hours. The elevated mean angle in the 24 hours subgroups revealed a gravity dependency for this behaviour.

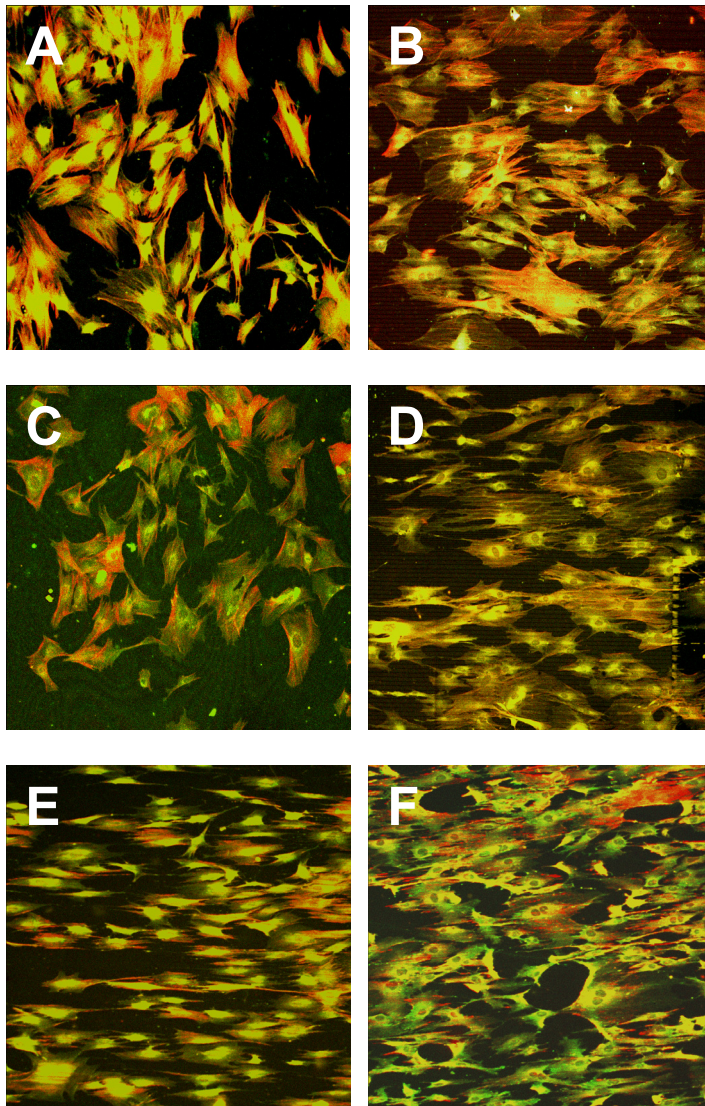


Figure 5. CLSM micrographs of RDFs cultured under several conditions. (A) Smooth substratum showing random orientated cells at normal gravity after 24 hours. (B) Aligned cells on a grooved substratum (10 μm wide) at 1 g. (C) 24 hours at 50 g on a smooth surface results in very little changes to alignment compared to A). Micrograph D is a 24hours/10g sample with 2 μm wide grooves while E is that of a 4hours/25g sample with 1 μm wide grooves, together with B the increased cell alignment with increasing gravitational force is evident, reaching its optimum at 25g. After 24 hours at 50g (F) cells alter their shape and display less alignment and cell surface area is wider (5 μm wide grooves). Colour figure on page 162.

Statistical analysis using an ANOVA was performed on the data, for all main parameters: topography, gravity force, and time. In this analysis, all parameters proved significant. Regarding topography a maximum of 89% of the cells were aligned along the grooved substrata compared to 12% of the smooth substrata.

The amount of gravitational force did influence cell alignment along the grooved topography. Although the effect of gravity from 1 to 10g was not significant, the increase from 10 to 25g and the decrease from 25 to 50g were significant.

As suggested from the graphs shown in **Figure 7**, statistics confirmed that there was no interaction between time and gravity, but over time gravity force became an increasingly important factor affecting cellular alignment. Finally, the effect of time on the alignment percentage was low, but significant. 24 hour samples showed a lower alignment rates compared to their 4 hour counterparts; on grooved substrata this was 63% and 76% respectively.

RT-PCR

The mRNA expression for $\alpha 1$ -, and $\beta 1$ -integrins, fibronectin, and collagen type I of the RDF cells was examined after each experimental run. An example of the visualised samples, separated on agarose gel, is shown in **Figure 8**, while all RT-PCR sample product ratios are listed in **Table 2**. With respect to all samples, gene expression levels were influenced by both time and gravity.

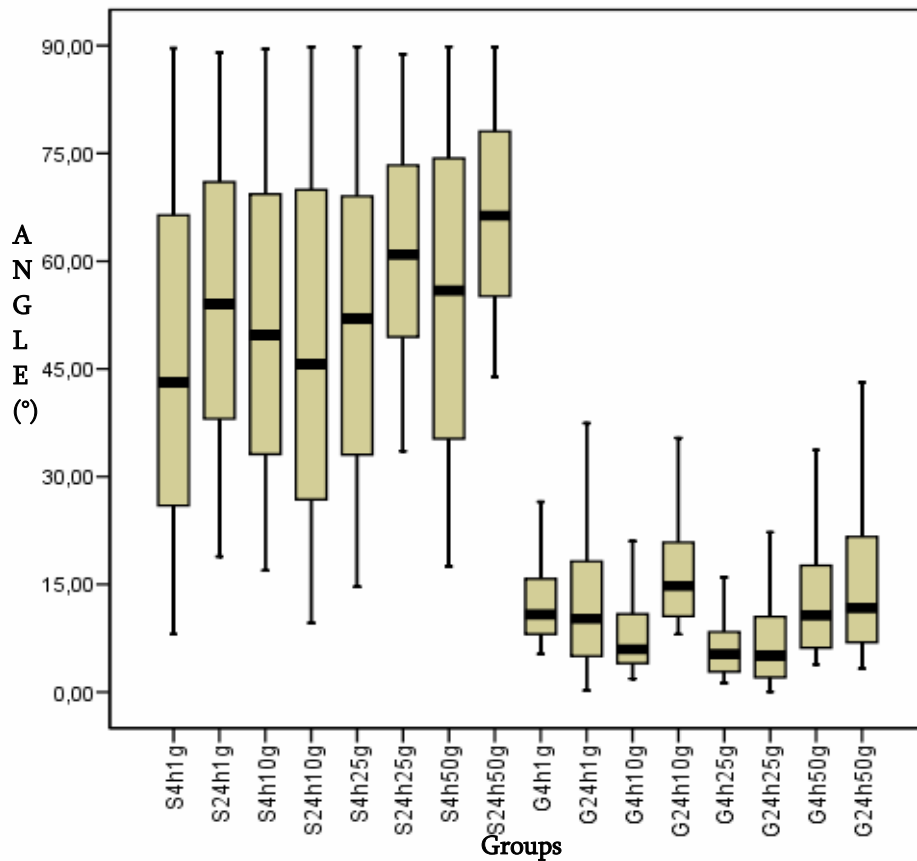


Figure 6. Box-whisker plot showing the distribution of cellular orientation. This graph shows the distribution midpoint, the first and third quartile (boxes), and the largest and smallest observation (whiskers). Of special note are the extreme differences in alignment between smooth and grooved surfaces. This led to investigate within both groups instead of between both groups. For each sample at least 200 individual cells were analysed. S = smooth, G = grooved (all groove widths combined), 4h and 24h stands for the experiment time, and 1, 10, 25 and 50 stands for the applied g-force.

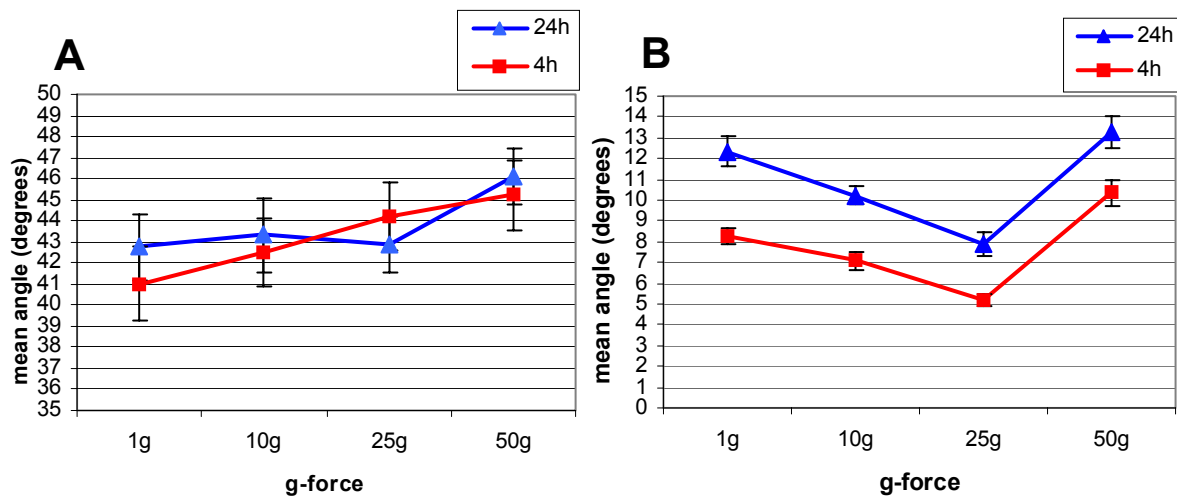


Figure 7. The mean angle and standard error of the mean for both smooth (A) and grooved (B) surfaces divided over time.

Most gene levels were reduced in time as can be seen in the 1g control group; in addition, hypergravity reduced the expression levels even further. The smooth control samples showed that most product values were equal to the housekeeping gene, except the $\beta 1$ -integrin subunit in samples experiencing either 25 or 50 g. The α -1 integrin depression in the 4h/10g group was notable, as it suggested adaptation to changes in environment; however, this was not reflected in its smooth control group. Both collagen type 1 and fibronectin were seemingly unaffected by time or force. Whenever there are reductions of collagen synthesis, there was also substantial decrease of β -1 integrin up-regulation.

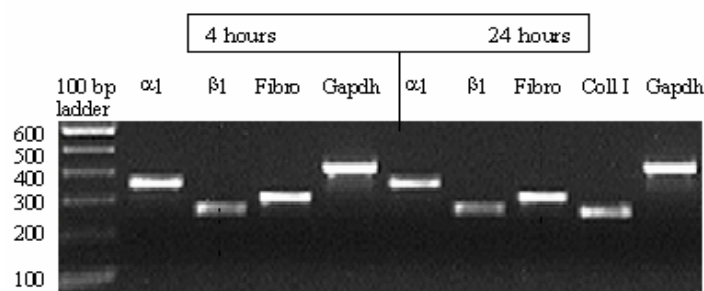


Figure 8. Example of PCR results of cells cultured on a grooved substratum undergoing 25g, visualised on agarose gel.

Group	G4h1g	G24h1g	G4h10g	G24h10g	G4h25g	G24h25g	G4h50g	G24h50g
alpha1	1,00	0,94	0,74	1,00	1,00	0,96	1,00	0,96
beta1	0,96	0,88	0,96	0,89	0,82	0,73	0,84	0,80
fibro	1,00	0,99	1,27	1,00	1,00	0,99	1,00	0,99
coll type 1	n/a	0,96	n/a	0,99	n/a	0,96	n/a	0,99
GAPDH	1,00	1,00	1,00	1,00	1,00	1,00	1,00	1,00

Group	S4h1g	S24h1g	S4h10g	S24h10g	S4h25g	S24h25g	S4h50g	S24h50g
alpha1	0,97	1,00	0,97	1,01	1,00	1,00	1,00	1,00
beta1	0,76	0,67	0,72	0,50	1,00	0,94	0,99	0,98
fibro	1,01	1,00	0,99	0,98	1,00	1,00	1,00	1,00
coll type 1	n/a	0,84	n/a	0,86	n/a	1,00	n/a	1,00
GAPDH	1,00	1,00	1,00	1,00	1,00	1,00	1,00	1,00

n/a: not available

Table 2: RT-PCR semiquantitative analysis. Shown are the ratios between the gene of interest and the housekeeping gene GAPDH. See Figure 6 for explanation of group abbreviations.

DISCUSSION

This study evaluated *in vitro* the differences in cellular behaviour between fibroblast cells cultured on smooth and microgrooved substrata, which experience artificial hypergravity by centrifugation. From our data it can be concluded that the fibroblasts primarily adjust their shape according to substratum surface (topographical) features. Nevertheless, also apparent effects of the applied hypergravity conditions were measured.

When regarding our study set up, several remarks can be made. Of course, as in any *in vitro* model, the number of experimental conditions that could be applied is limited. In a real hypergravity environment such as would be present during space flight, cells would experience simultaneous effects of temperature changes, vibration, irradiation, angle between the cell and the direction of acceleration, pH changes, etc. These parameters are all interrelated but too complicated to investigate within one study set-up. Also, in our model possibly enhanced gas solubility in the medium during the centrifugation could arise due to the pressure in the

centrifuge system, and can have led to biochemical effects that are thus not direct, but secondary effects of gravity acting on the cells.

The dimensions of the groove features were based on earlier studies [1; 6; 7; 40]. Scanning electron microscopy, immunofluorescence staining, and subsequent image analysis confirmed that fibroblasts were oriented on the microgrooved surfaces. It was seen that cells on the 10 and 5 micron wide grooved parts were able to reach the bottom of the 1 μ m deep grooves, whereas on the parts with 2 and 1 micron wide grooves the cells lost contact with the bottom of the grooves. The mechanism behind cell orientation has been postulated in literature [1; 4; 46; 49]. Cell orientation on (microtextured) surfaces starts with the formation of multiple membrane extensions. The cell is probing and exploring the surface in order to adhere and come to a mechanical equilibrium with its environment. Since the immediate surroundings is lacking natural extracellular matrix (ECM) and the relatively low seeding density results in isolated cells, the aforementioned membrane extensions are formed in all directions. Once appropriate attachment sites are found the cell will deposit ECM material (*e.g.* collagen). The cell changes its spherical appearance, spreads on the surface, and active filaments form longitudinal stress fibres [50]. In this study, it was evident that cellular orientation indeed occurred immediately during the cell spreading, and always parallel to the grooves.

Cell movement or orientation as reaction to mechanical stresses, like the hypergravity applied here, might be based on a comparable mechanisms. However, in contrast to the responses to microtextures as described above, the mechanical force (hypergravity) was introduced after the cell has attached and spread out over the surface, and after the cells had most likely established an inter-connective system of ECM, integrins, and cytoskeleton. The subsequent effects of gravity might be primary or secondary: The primary effects of gravity are those which directly affect the inside of the cell and internal components of the cell, while secondary effects are effects of the environment onto cells. These latter effects are the physical phenomena, which appear in an altered gravity situation, where hydrostatic pressure derived from the liquid column on the surface of the culture is linearly proportional to gravity force. In addition the acceleration from a centrifuge increases with increasing distance from the centre of rotation, thus creating a gravity gradient. Regardless of these differences, centrifugation provides an excellent simulated gravity environment for cell biology research as long as the centrifuge (MidiCAR used in this study) is of sufficient diameter in relation to the sample studied.

The SEM and CLSM results, confirmed that on smooth substrata no notable differences were seen on cell shape. The microtextures elicited the main effect on cell behaviour. The possible effects of gravity were less evident but still present, as increased gravity did affect cell shape. The CLSM overview micrographs showed considerable background staining around the nucleus, a phenomenon known to others as well [1; 51]. The magnification was chosen at 10x so that cell alignment measurements were possible over a large number of cells (at least 200 measurements per group). Actin filaments followed cellular alignment and focal adhesions, as shown by vinculin staining, were always located at the end of the actin filament.

The image analysis proved that substrata with microgrooves elicit cell alignment. Because of the obvious differences between smooth and grooved surfaces, study groups were split up and the grooved surfaces were investigated more closely. Concerning alignment there was no significant difference between 1 and 10g. However, gravitational force above 10g significantly enhances cellular orientation and this effect increased when cells are subjected to prolonged exposure of gravity independent of force magnitude. Since cell-cell contact was scarce, which might disrupt cellular orientation along the grooves, the described differences could indeed be assigned to prolonged exposure to gravity. This points to that, although actin cytoskeleton is closely involved in the orientation process, when the orientation is completed the cells are no longer dependent

upon that system to maintain their position. However, hypergravity is still present and exerts a continuous influence making the cytoskeleton respond and provide the cell with the means to maintain equilibrium with its environment. Such an assumption could be further tested in experiments with cytoskeleton inhibitors such as cytochalasin.

For our RT-PCR the production of components vital for cellular attachment was evaluated. Differences in gene expression of fibronectin on grooved versus smooth surfaces have previously been published by Chou et al. [52]. Our results indicated that cells under hypergravitational stimulation showed decreased β 1-integrin and collagen-I levels. Generally speaking a lower up-regulation of these components led to a situation of decreased orientation. Combining the statistical analysis of the effects of gravity and the semi-quantitative results of our genes of interest we concluded that over time gravity becomes more apparent resulting in down regulation of certain proteins. Nonetheless, at higher g forces, the 25 g sample groups display the most profound orientation, yet with lowered values of β 1-integrin. We could speculate that fibroblasts could rely on another anchor protein member of the β -integrin family in order to help them align, although many other explanations could be given. With increasing gravity (50g) this other pathway also becomes affected. Similar adaptive behaviour of integrin expression has also been described by others [53]. The statistical analysis performed on the fluorescence micrographs revealed two turning points signifying that anchor proteins are up- or down-regulated at different g-forces. The decreased alignment in the 1 g sample groups might be explained by the fact that these cells are only experiencing environmental cues in the shape of microtexture without the additional effect of altered gravity. The increase of β -1 in the 4 hours sample group might be correlated to the enhanced alignment in comparison with 24 hours sample groups.

CONCLUSIONS

Like all living biological systems, a cell needs both energy and information in order to function. Information regarding the mechanisms responsible for cell sensitivity to gravity is gradually being acquired. There is still a large discrepancy between the empirical use of mechanical forces in orthopaedics, dentistry and plastic surgery, and the theoretical understanding of the cellular and molecular mechanisms involved. Progress has been made in discovering the conversion of mechanical into chemical signals, triggering of intracellular signalling pathways, and the mechanisms of mechanically induced gene activation. However, the specificity of cellular responses to externally applied mechanical stress and the interaction between various environmental cues requires more in depth research. From our study, we conclude that the fibroblasts primarily adjust their shape according to morphological environmental cues like substratum surface whilst a secondary, but significant, role is played by hypergravity forces.

REFERENCES

1. Walboomers, X. F., Croes, H. J., Ginsel, L. A., and Jansen, J. A. Growth behavior of fibroblasts on microgrooved polystyrene. *Biomaterials* 1998, 1861-1868, 1998.
2. Walboomers, X. F., Monaghan, W., Curtis, A. S., and Jansen, J. A. Attachment of fibroblasts on smooth and microgrooved polystyrene. *J Biomed Mater Res* 1999 , 212-20, 1999.
3. Clark, P., Connolly, P., Curtis, A. S., Dow, J. A., and Wilkinson, C. D. Cell guidance by ultrafine topography in vitro. *J Cell Sci* 1991, 73-7, 1991.
4. Oakley, C., Jaeger, N. A., and Brunette, D. M. Sensitivity of fibroblasts and their cytoskeletons to substratum topographies: topographic guidance and topographic compensation by micromachined grooves of different dimensions. *Exp Cell Res* 1997, 413-24, 1997.

5. Brunette, D. M. Fibroblasts on micromachined substrata orient hierarchically to grooves of different dimensions. *Exp Cell Res* 1986, 11-26, 1986.
6. Matsuzaka, K., Walboomers, F., de Ruijter, A., and Jansen, J. A. Effect of microgrooved poly-l-lactic (PLA) surfaces on proliferation, cytoskeletal organization, and mineralized matrix formation of rat bone marrow cells. *Clin Oral Implants Res* 2000, 325-33, 2000.
7. Walboomers, X. F., Ginsel, L. A., and Jansen, J. A. Early spreading events of fibroblasts on microgrooved substrates. *J Biomed Mater Res* 2000, 529-534, 2000.
8. den Braber, E. T., de Ruijter, J. E., Smits, H. T., Ginsel, L. A., von Recum, A. F., and Jansen, J. A. Quantitative analysis of cell proliferation and orientation on substrata with uniform parallel surface micro-grooves. *Biomaterials* 1996, 1093-9, 1996.
9. von Recum, A. F. and van Kooten, T. G. The influence of micro-topography on cellular response and the implications for silicone implants. *J Biomater Sci Polym Ed* 1995, 181-98, 1995.
10. Chiquet, M., Renedo, A. S., Huber, F., and Fluck, M. How do fibroblasts translate mechanical signals into changes in extracellular matrix production? *Matrix Biol* 2003, 73-80, 2003.
11. Carver, W., Nagpal, M. L., Nachtigal, M., Borg, T. K., and Terracio, L. Collagen expression in mechanically stimulated cardiac fibroblasts. *Circ Res* 1991, 116-22, 1991.
12. Wojciak-Stothard, B., Madeja, Z., Korohoda, W., Curtis, A., and Wilkinson, C. Activation of macrophage-like cells by multiple grooved substrata. Topographical control of cell behaviour. *Cell Biol Int* 1995, 485-90, 1995.
13. Clark, P., Connolly, P., Curtis, A. S., Dow, J. A., and Wilkinson, C. D. Topographical control of cell behaviour. I. Simple step cues. *Development* 1987, 439-448, 1987.
14. Dalby, M. J., Riehle, M. O., Yarwood, S. J., Wilkinson, C. D., and Curtis, A. S. Nucleus alignment and cell signaling in fibroblasts: response to a micro-grooved topography. *Exp Cell Res* 2003, 274-82, 2003.
15. Curtis, A. and Wilkinson, C. New depths in cell behaviour: reactions of cells to nanotopography. *Biochem Soc Symp* 1999, 15-26, 1999.
16. Dalby, M. J., Giannaras, D., Riehle, M. O., Gadegaard, N., Affrossman, S., and Curtis, A. S. Rapid fibroblast adhesion to 27nm high polymer demixed nano-topography. *Biomaterials* 2004, 77-83, 2004.
17. Flemming, R. G., Murphy, C. J., Abrams, G. A., Goodman, S. L., and Nealey, P. F. Effects of synthetic micro- and nano-structured surfaces on cell behavior. *Biomaterials* 1999, 573-88, 1999.
18. They, M., Pepin, A., Dressaire, E., Chen, Y., and Bornens, M. Cell distribution of stress fibres in response to the geometry of the adhesive environment. *Cell Motil Cytoskeleton* 2006, 341-55, 2006.
19. Cogoli, A. and Gmunder, F. K. Gravity effects on single cells: techniques, findings, and theory. *Adv Space Biol Med* 1991, 183-248, 1991.
20. Block, I., Wolke, A., Briegleb, W., and Ivanova, K. Gravity perception and signal transduction in single cells. *Acta Astronaut* 1995, 479-86, 1995.
21. Kondepudi, D. K. Detection of gravity through nonequilibrium mechanisms. *ASGSB Bull* 1991, 119-24, 1991.
22. Schwarzenberg, M., Pippia, P., Meloni, M. A., Cossu, G., Cogoli-Greuter, M., and Cogoli, A. Signal transduction in T lymphocytes--a comparison of the data from space, the free fall machine and the random positioning machine. *Adv Space Res* 1999, 793-800, 1999.
23. Cogoli, A. and Cogoli-Greuter, M. Activation and proliferation of lymphocytes and other mammalian cells in microgravity. *Adv Space Biol Med* 1997, 33-79, 1997.

24. Pippia, P., Sciola, L., Cogoli-Greuter, M., Meloni, M. A., Spano, A., and Cogoli, A. Activation signals of T lymphocytes in microgravity. *J Biotechnol* 1996, 215-22, 1996.
25. Schatten, H., Lewis, M. L., and Chakrabarti, A. Spaceflight and clinorotation cause cytoskeleton and mitochondria changes and increases in apoptosis in cultured cells. *Acta Astronaut* 2001, 399-418, 2001.
26. Cogoli, A. Signal transduction in T lymphocytes in microgravity. *Gravit Space Biol Bull* 1997, 5-16, 1997.
27. Croute, F., Gaubin, Y., Pianezzi, B., and Soleilhavoup, J. P. Effects of hypergravity on the cell shape and on the organization of cytoskeleton and extracellular matrix molecules of in vitro human dermal fibroblasts. *Microgravity Sci Technol* 1995, 118-24, 1995.
28. Seitzer, U., Bodo, M., Muller, P. K., Acil, Y., and Batge, B. Microgravity and hypergravity effects on collagen biosynthesis of human dermal fibroblasts. *Cell Tissue Res* 1995, 513-7, 1995.
29. Buravkova, L. B. and Romanov, Y. A. The role of cytoskeleton in cell changes under condition of simulated microgravity. *Acta Astronaut* 2001, 647-50, 2001.
30. Kondrachuk, A. V. Theoretical considerations of plant gravisensing. *Adv Space Res* 2001, 907-14, 2001.
31. Kondrachuk, A. V. and Sirenko, S. P. The theoretical consideration of microgravity effects on a cell. *Adv Space Res* 1996, 165-8, 1996.
32. Searby, N. D., Steele, C. R., and Globus, R. K. Influence of increased mechanical loading by hypergravity on the microtubule cytoskeleton and prostaglandin E2 release in primary osteoblasts. *Am J Physiol Cell Physiol* 2005, C148-158, 2005.
33. Boonstra, J. Growth factor-induced signal transduction in adherent mammalian cells is sensitive to gravity. *FASEB J* 1999, S35-42, 1999.
34. Rijken, P. J., Boonstra, J., Verkleij, A. J., and de Laat, S. W. Effects of gravity on the cellular response to epidermal growth factor. *Adv Space Biol Med* 1994, 159-88, 1994.
35. Sciola, L., Cogoli-Greuter, M., Cogoli, A., Spano, A., and Pippia, P. Influence of microgravity on mitogen binding and cytoskeleton in Jurkat cells. *Adv Space Res* 1999, 801-5, 1999.
36. Erkut, S. and Can, G. Effects of glow-discharge and surfactant treatments on the wettability of vinyl polysiloxane impression materials. *J Prosthet Dent* 2005, 356-63, 2005.
37. Wang, J. H., Yang, G., Li, Z., and Shen, W. Fibroblasts responses to cyclic mechanical stretching depend on cell orientation to the stretching direction. *J Biomech* 2003, 573-6, 2003.
38. Loesberg, W. A., Walboomers, X. F., van Loon, J. J., and Jansen, J. A. The effect of combined cyclic mechanical stretching and microgrooved surface topography on the behavior of fibroblasts. *J Biomed Mater Res A* 2005, 723-732, 2005.
39. Chesmel, K. D. and Black, J. Cellular responses to chemical and morphologic aspects of biomaterial surfaces. I. A novel in vitro model system. *J Biomed Mater Res* 1995, 1089-1099, 1995.
40. Walboomers, X. F., Croes, H. J., Ginsel, L. A., and Jansen, J. A. Contact guidance of rat fibroblasts on various implant materials. *J Biomed Mater Res* 1999, 204-12, 1999.
41. den Braber, E. T., de Ruijter, J. E., Ginsel, L. A., von Recum, A. F., and Jansen, J. A. Quantitative analysis of fibroblast morphology on microgrooved surfaces with various groove and ridge dimensions. *Biomaterials* 1996, 2037-44, 1996.
42. Parker, J. A., Walboomers, X. F., Von den, H. J., Maltha, J. C., and Jansen, J. A. Soft tissue response to microtextured silicone and poly-L-lactic acid implants: fibronectin pre-coating vs. radio-frequency glow

- discharge treatment. *Biomaterials* 2002, 3545-53, 2002.
43. Beumer, G. J., Van Blitterswijk, C. A., and Ponec, M. The use of gas plasma treatment to improve the cell-substrate properties of a skin substitute made of poly(ether)/poly(ester) copolymers. *J Mat Sc Mat Med* 5, 1-6. 94.
 44. Amstein, C. F. and Hartman, P. A. Adaptation of plastic surfaces for tissue culture by glow discharge. *J Clin Microbiol* 1975, 46-54, 1975.
 45. Freshney, R. I. Culture of animal cells: a multimedia guide. 99. Chichester, John Wiley & Sons Ltd.
 46. Neidlinger-Wilke, C., Grood, E., Claes, L., and Brand, R. Fibroblast orientation to stretch begins within three hours. *J Orthop Res* 2002, 953-6, 2002.
 47. Wang, H., Ip, W., Boissy, R., and Grood, E. S. Cell orientation response to cyclically deformed substrates: experimental validation of a cell model. *J Biomech* 1995, 1543-52, 1995.
 48. Walboomers, X. F., Habraken, W. J., Feddes, B., Winter, L. C., Bumgardner, J. D., and Jansen, J. A. Stretch-mediated responses of osteoblast-like cells cultured on titanium-coated substrates in vitro. *J Biomed Mater Res* 2004, 131-9, 2004.
 49. Clark, P., Connolly, P., and Moores, G. R. Cell guidance by micropatterned adhesiveness in vitro. *J Cell Sci* 1992, 287-92, 1992.
 50. Hynes, R. O. and Destree, A. T. Relationships between fibronectin (LETS protein) and actin. *Cell* 1978, 875-86, 1978.
 51. den Braber, E. T., Jansen, H. V., de Boer, M. J., Croes, H. J., Elwenspoek, M., Ginsel, L. A., and Jansen, J. A. Scanning electron microscopic, transmission electron microscopic, and confocal laser scanning microscopic observation of fibroblasts cultured on microgrooved surfaces of bulk titanium substrata. *J Biomed Mater Res* 1998, 425-33, 1998.
 52. Chou, L., Firth, J. D., Uitto, V. J., and Brunette, D. M. Substratum surface topography alters cell shape and regulates fibronectin mRNA level, mRNA stability, secretion and assembly in human fibroblasts. *J Cell Sci* 1995, 1563-73, 1995.
 53. ter Brugge, P. J., Dieudonne, S., and Jansen, J. A. Initial interaction of U2OS cells with noncoated and calcium phosphate coated titanium substrates. *J Biomed Mater Res* 2002, 399-407, 2002.



The effect of combined simulated
microgravity and microgrooved surface
topography on fibroblasts

WA Loesberg, XF Walboomers, EM Bronkhorst, JJWA van Loon and JA Jansen

Cell Motil Cytoskeleton. 64 (3), 174-185, 2007

INTRODUCTION

Mechanosensitivity of fibroblast cells towards static forces, e.g. stress provided by a microgrooved surface onto which the cells are cultured or dynamic stress in the shape of for instance substratum deformation by stretch or fluid shear have been well documented. Mechanical stress is an important and specific director of cell shape and stimulus for extracellular matrix component production. [1-9]. On the other hand, cells can also experience mechanical unloading by removing the, at cell level, very weak, but most constant force in nature: gravity. Morphological and functional studies have shown that many cells like osteoblast-like cells and lymphocytes are highly sensitive to altered gravity [10-17].

Although it is generally accepted that the response to environmental stimuli is multi-factorial, research towards the interaction of cells cultured on substratum texture (nano-, micropatterns) and mechanical force is sparse. Such studies are necessary to serve as baseline values for further research aimed at understanding of observed cell response phenomena on a molecular basis [18-22]. Ground based research to simulate microgravity conditions by means of a random positioning machine (RPM), also referred to as 3D clinostat, provides an excellent means to conduct gravitational studies. The RPM is a microweight (microgravity) simulator that is based on the principle of 'gravity-vector-averaging'. Gravity is a vector, i.e. it has a magnitude and direction. During an experimental run in the RPM the sample position with regard to the Earth's gravity vector direction is constantly changing, and as a result the samples will experience a near-weightlessness environment [23-28].

In this study we evaluated in vitro the differences in morphological behaviour between fibroblast cells cultured on polystyrene substrata, both smooth and with a surface microtopography, which were placed in a simulated microgravity environment. In addition to microscopy analysis, the transcription of several proteins involved in cell-surface interaction was investigated, as well as, proteins of the mitogen activated protein kinases (MAPK) pathway which are involved in cell adhesion and motility. The underlying aim was to understand which parameter is more important in determining cell response. Our hypothesis is that cellular shape and orientation is determined by the topographical cues, and a simulated microgravity environment will decrease the cellular orientation to these substrata. As controls fibroblast cells were cultured on similar substrata, which remained at normal (Earth) gravity.

MATERIALS AND METHODS

Substrata:

Microgrooved patterns were made, using a photo lithographic technique and subsequent etching in a silicon wafer as described by Walboomers et al. [1]. This wafer is divided into 4 quadrants with a ridge- and groove width of 1, 2, 5, or 10 μm , with a uniform depth of 0.5 μm . Wafers with a planar surface were used as controls. The silicon wafer was used as template for the production of polystyrene (PS) substrata for cell culturing. PS was solvent cast in manner described by Chesmel and Black [29]. Polystyrene replicas were attached to 18 mm diameter cylinders with polystyrene-chloroform adhesive. Shortly before use a radio frequency glow-discharge (RFGD) treatment was applied for 5 minutes at a pressure of 2.0×10^{-2} mbar (Harrick Scientific Corp., Ossining, NY, USA) to promote cell attachment by improving the wettability of the substrata.

Cell culture:

Rat dermal fibroblasts (RDF) were obtained from the ventral skin of male Wistar rats as described by Freshney [30]. Cells were cultured in CO_2 -independent α -MEM containing Earle's salts (Gibco, Invitrogen Corp., Paisley, Scotland), L-glutamine, 10% FCS, gentamicin (50 $\mu\text{g}/\text{ml}$), in an incubator set at 37 °C with a humidified atmosphere. Experiments were performed with 4 - 8th culture

generation cells. Onto the various substrata, 1.0×10^4 cells/cm² were seeded. Cells were cultured for 4h, after which they were placed in a 12 wells plate for support. Custom made silicone caps closed each well and the tissue culture dish therein (**Figure 1**). Using a type 22G1 needle and applying a little pressure while adding additional medium, air bubbles were removed to prevent unwanted shear force and turbulence during rotation. In this system with only one specific density fluid and absent air bubbles no fluid motion was to be expected, since the media was moving with the same velocity as the cell monolayer. The well plates containing the samples were secured onto the experiment platform. From previous studies it is known that fibroblasts need approximately 4 hours to commence adapting their morphology to a new environment[31]. Therefore experiment times were chosen of 4 and 24 hours.

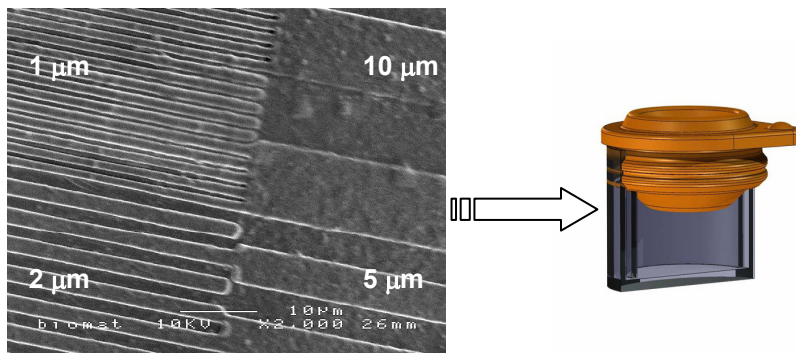


Figure 1. SEM micrograph of a grooved substratum, showing in detail the accurate production of the 4 different groove widths into the polystyrene. Clockwise, starting in upper left: 1, 10, 5, and 2 micron wide and uniform 0.5 micron deep grooves. At right a graphical presentation of a complete polystyrene culture dish used in this study with silicone closing cap securing the insert snug into the well of a 12 wells plate and providing an air bubble free environment.

Simulated microgravity:

The RPM is shown in **Figure 2**. One of the first versions was developed by T. Hoson et al. [32]. We used a similar system, manufactured by Dutch Space (formerly Fokker Space, Leiden, The Netherlands). The outer frame rotated perpendicular to the inner frame, which caused the samples to move randomly in 3 axis. The rotational movement of both frames was powered by two servomotors. A PC user interface with dedicated software controlled the two servomotors onset, rate, and duration of rotation. The rotational velocity of both frames was randomised with a maximum of 60°/sec, direction, and interval was set at random. The samples were fixed in the centre of the inner frame, the largest radius was 57.8 mm to the outermost well. The RPM was accommodated in a temperature-controlled incubator set at 37 °C and capable to be supplied with a 5% CO₂/air gas mixture [33].

For the experiments the cell layers were washed three times with Phosphate Buffered Saline (PBS) and prepared for further analysis immediately after retrieval from the RPM machine.

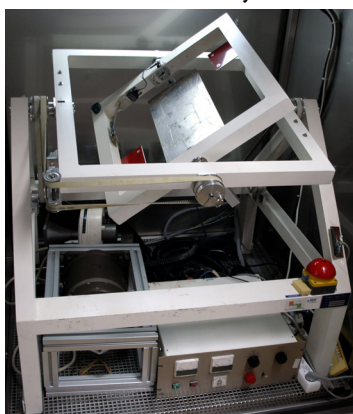


Figure 2. The Random Positioning Machine (RPM) used in this study to simulate weightlessness. The RPM is equipped with a computerised temperature and motor control. The control samples are secured on one of the machine support struts, while experimental samples are placed on the inner frame of the clinostat.

Scanning electron microscopy (SEM):

To assess overall morphology of the fibroblasts, SEM was performed (n = 4). Cells were rinsed, fixed in for 5 minutes in 2% glutaraldehyde, followed by 5 minutes in 0.1 M sodium-cacodylate buffer (pH 7.4), dehydrated in a graded series of ethanol, and dried in tetramethylsilane to air. Specimens were sputter-coated with gold and examined with a Jeol 6310 SEM (Tokyo, Japan).

Immunofluorescence

Components of the cytoskeleton were made visible using fluorescent staining techniques. RDF cells, cultured on microgrooved substrata were rinsed in PBS, pH7.2, fixed for 30 minutes in 2% paraformaldehyde, and permeabilised with 1% Triton X100 for 5 min. Filamentous actin was stained with Alexa Fluor 568 phalloidin (Molecular Probes, A-12380, Leiden, The Netherlands) diluted in 1% Bovine Serum Albumin/PBS to block non-specific epitopes. Vinculin was stained with rabbit polyclonal primary antibodies to vinculin (Santa Cruz, sc-5573), followed by labelling with goat anti-rabbit secondary antibodies IgG with Alexa Fluor 488 (Molecular Probes, A-11034). Finally, the specimens were examined with a Biorad (Hercules, CA, USA) MRC 1024 confocal laser scanning microscope (CLSM) system with a krypton-argon laser at magnification of 40x. The digital immunofluorescence images acquired with the CLSM were loaded into Confocal Assistant (version 4.02, Todd Clark Brelje, USA) to create overlay images. Cytoskeletal components were examined for their overall morphology as well as their orientation with respect to the groove direction. For quantitative image analysis samples were stained with Phalloidin-TRITC (Sigma, P-1951, St. Louis, MO, USA), followed by examination with a Leica/Leitz DM RBE Microscope (Wetzlar, Germany) at magnification of 10x.

Image Analysis

The Phalloidin-TRITC fluorescence micrographs were analyzed with Scion Image software (Beta Version 4.0.2, Scion Corp., Frederick, MY, USA). The orientation of fibroblasts was examined and photographed. For each sample six fields of view were selected randomly. The criteria for cell selection were (1) the cell is not in contact with other cells and (2) the cell is not in contact with the image perimeter. The maximum cell diameter was measured as the longest distance between two edges within the cell borders. The angle between this axis and the grooves (or an arbitrarily selected line for smooth surfaces) was termed the orientation angle. If the average angle was 45 degrees, cells were supposed to lie in an at random orientation. Cell extensions like filopodia, which could confound the alignment measurement, were not included when assessing the cell orientation. Using Clarks criteria [34; 35], cells oriented at 0–10 degrees from the groove direction were regarded to be aligned. The distribution of cytoskeletal patterns with time, gravity force in view of the type of microgrooves and groove direction was described by the percentage of cells in the sample that displayed each pattern.

Cellular surface area was measured with the aforementioned image analyses software. Applying the same criteria for cell selection; cell areas were determined and displayed as μm^2 . Between 850 - 1010 cells were measured per group for both orientation and surface area.

RT-PCR

Total RNA was isolated from fibroblasts with an RNA isolation and stabilisation kit (QIAGEN, Hilden, Germany) and cDNA was synthesised from 1 μg of total RNA with an RT-PCR kit. After initial denaturation for 2 min at 95°C, the samples were amplified for 35 cycles (annealing 55 °C 1 min, elongation 72 °C 2 min, denaturation 95 °C 1 min). The duration of the final elongation reaction was increased to 10 min at 72 °C to permit completion of reaction products. PCR products were separated on a 2% (w/v) agarose gel and visualised by ethidium bromide staining. RT-PCR

products ratios were the result of three replicates and were semi-quantified by band intensity analysis using Quantity One 1-D analysis software for Windows (Version 4.5.0, Bio Rad, Hercules, California, USA). The collagen type I (only 24 hours samples), fibronectin, $\alpha 1$ integrin, $\beta 1$ integrin gene expressions were normalised to glyceraldehyde-3-phosphate dehydrogenase (GAPDH) values. The forward and reverse primer sequences are listed in **Table 1**.

	5' Primer (Forward)	3'Primer (Reverse)	Size (bp)
Collagen Type I	TGTTTCGTGGTTCTCAGGGTAG	TTGTCGTAGCAGGGTTCTTTC	254
Fibronectin	CCTTAAGCCTTCTGCTCTGG	CGGCAAAAGAAAGCAGAACT	301
$\alpha 1$ -Integrin	AGCTGGACATAGTCATCGTC	AGTTGTCATGCGATTCTCCG	374
$\beta 1$ -Integrin	AATGTTTCAGTGCAGAGCC	TTGGGATGATGTCGGGAC	262
GAPDH	CGATGCTGGCGCTGAGTAC	CGTTCAGCTCAGGGATGACC	407

Table 1: Forward and reverse primer sequences used in this study

Statistical analysis:

Acquired data from the fluorescence micrographs of cell alignment were analysed using SPSS for Windows (Release 12.0.1, SPSS Inc., Chicago, USA). The effects of and the interaction between both time and/or force and surface were analysed using ANOVA, including a modified least significant difference (Bonferroni) multiple range test to detect significant differences between two distinct groups. Probability (p) value ≤ 0.05 was considered significant.

RESULTS

Scanning Electron Microscopy

The micro topography pattern of grooves and ridges was accurately reproduced in the polystyrene substrata. When observing cell morphology, RDFs cultured on smooth substrata displayed a cell spreading which was considered random (**Figure 3A**), while a orientation along the groove direction was observed when cells were cultured on microgrooved substrata (**Figure 3B**). Upon visual inspection no noticeable difference were seen with regards to cell orientation when comparing the different groove sizes. **Figure 3C** shows a grooved substratum section, which features 1 micron (left side), as well as, 10 micron (right side) wide grooves, both 0.5 micron deep. This micrograph shows clearly that the cells or part of cells on the wider grooves (5 μm and above) were flatter in appearance and were able to descend to the bottom of the grooves, while on the more narrow textures cells remained on top of the ridges, bridging the gaps between the ridges and extending their cell bodies. Although the visual differences were quite small, most 4 hour samples (**Figure 3D**) seemed to showed a better cell alignment towards the grooves when compared to 24 hour samples (**Figure 3E**). In addition, cells cultured on smooth surfaces revealed a larger cell area, especially those which experienced the short experiment time.

Fluorescence microscopy (CLSM)

The cytoskeleton was investigated by staining filamentous actin and vinculin anchor points of the cell focal adhesions. **Figure 4A** shows a 1g smooth substratum sample; the observed cell shape, spreading, and random orientation were similar to SEM micrographs. Red staining is that of the actin filaments, which were always running parallel with the long axis of cells. Vinculin staining for focal adhesions resulted in a considerable background around the nucleus. Vinculin spots were visible in some samples, positioned at the end of actin bundles, and always extended in the direction of the actin bundle. RDFs cultured on grooved surfaces displayed a similar view, as was found on smooth surfaces; however there was clear orientation of the cells and their cytoskeleton (**Figure 4B**). The overall view of cells cultured on smooth surfaces in the RPM did change not notably (**Figure 4C & D**).

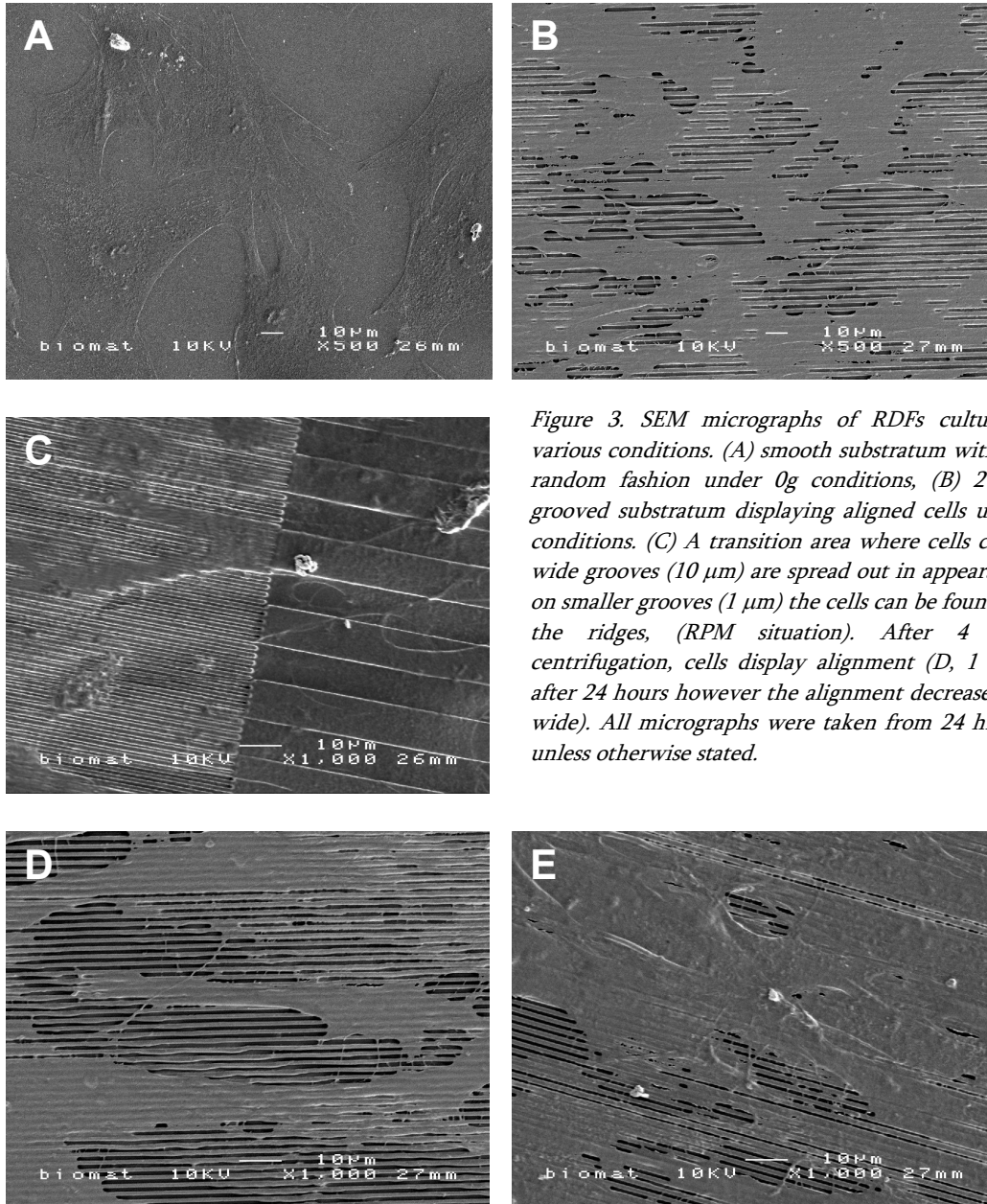


Figure 3. SEM micrographs of RDFs cultured under various conditions. (A) smooth substratum with cells in a random fashion under 0g conditions, (B) 2 μm wide grooved substratum displaying aligned cells under RPM conditions. (C) A transition area where cells cultured on wide grooves (10 μm) are spread out in appearance while on smaller grooves (1 μm) the cells can be found on top of the ridges, (RPM situation). After 4 hours of centrifugation, cells display alignment (D, 1 μm wide), after 24 hours however the alignment decreases (E, 1 μm wide). All micrographs were taken from 24 hrs samples, unless otherwise stated.

This is in contrast to the cells cultured on grooved substrata: in the RPM the alignment of the cells evidently decreased. Under simulated microgravity after 24 hours the cells changed their shape and tended to spread out more, which was not observed for the smooth controls (**Figure 4E & F**).

Image Analysis

Image analysis of the phalloidin-TRITC stained actin filaments showed that cellular orientation of RDFs cultured on all grooved substrata was profound (**Figure 5**). Cells cultured on smooth samples revealed a random orientation in cell spreading. The quantified results for cell orientation are presented in **Figure 6**. No significant differences in alignment were found within the smooth groups neither in time or in gravity. However, besides the obvious significant difference between smooth and grooved substrata, significant differences existed (**Figure 7A**) within the grooved groups as was shown by ANOVA performed on the data. In this analysis all main parameters: topography, gravity, and time proved significant.

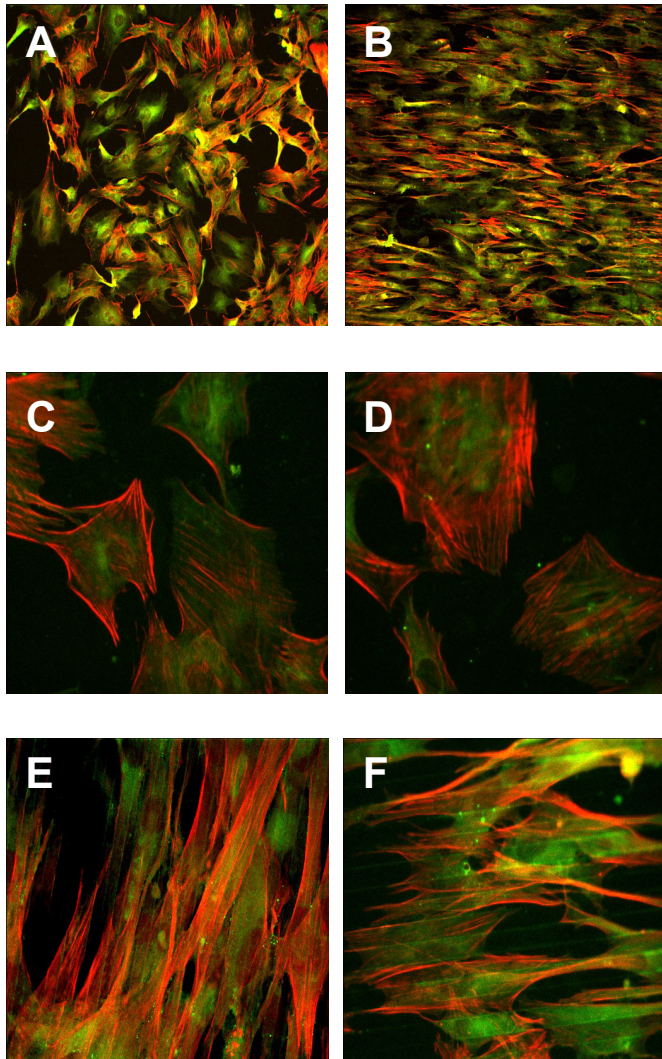


Figure 4. CLSM micrographs of RDFs cultured under several conditions. (A) Smooth substratum showing random orientated cells at normal gravity after 4 hours. (B) Aligned cells on a grooved substratum (5 μm wide) at 1g. (C) Cells cultured on planar substratum after 24 hours in RPM results in little changes in cell shape compared to a 24hours/1g sample (D). In contrast, on topographic substrata cells displayed decreased orientation towards the grooves under near weightlessness conditions; E shows cellular alignment after 4 hours in RPM, while F shows cell orientation after 24 hours. Colour figure on page 163.

Regarding topography, around 75% of the cells cultured on grooved substrata were considered aligned compared to 14% on smooth surfaces. The effect of gravitational loading, although small, is significant. Under simulated microgravity conditions the mean angle of cells cultured on grooved substrata increased, thus overall alignment decreased. This was shown particularly in the 4 hour time groups where alignment decreased from 84 to 78%.

Time played an important role in the cellular orientation: 24 hour groups always showed a significantly decreased alignment towards the grooves. Around 70% of cells were still aligned after 24 hours compared to 81% after 4 hours of culturing.

Comparable to the orientation of the RDFs, there was a significant difference in cell area between smooth and grooved substrata, but also within both groups. Quantified results for cell area are presented in **Figure 7B**. On grooved surfaces overall cell area was about 2480 μm^2 compared to 3700 μm^2 overall on smooth surfaces. In the smooth group the time parameter is of major influence on cell area. Cellular surface decreased over time from 4060 μm^2 to around 3250 μm^2 . An additional effect of simulated microgravity could not be determined in the smooth group. However, within the grooved group, after prolonged culturing, an additional effect was found in cell area: the increase to 2800 μm^2 was significant compared to the other grooved samples which averaged at 2350 μm^2 .

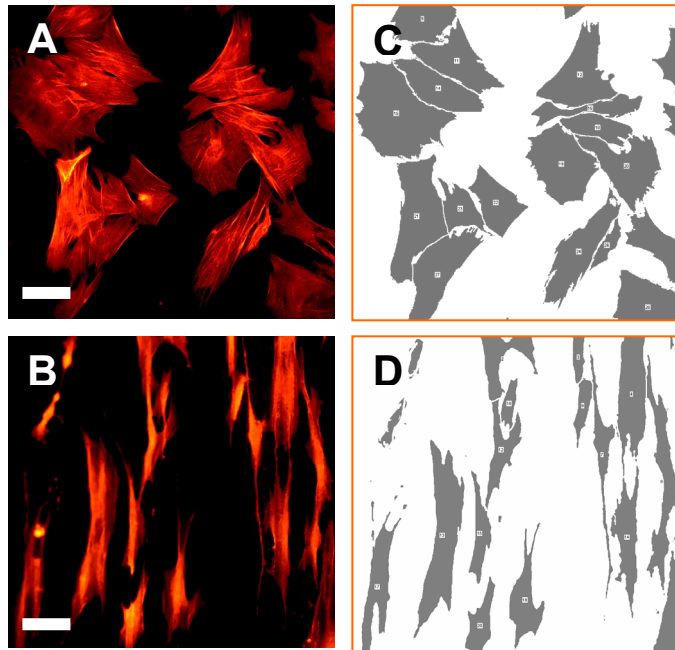


Figure 5. Fluorescence staining with Phalloidin-TRITC of the actin filaments of rat dermal fibroblasts cultured on a smooth (A) and 5 μm wide grooved (B) polystyrene substratum. C and D are examples of digitised threshold images as used for image analysis. Both samples: 24 hours, RPM. Magnification x20. Bar size = 10 μm .

RT-PCR

After each experimental run, samples were recovered and the mRNA expression for $\alpha 1$ -, and $\beta 1$ -integrins, fibronectin, and collagen type I of the fibroblasts was analysed. An example of the visualised samples, separated on agarose gel, is shown in **Figure 8**. The RT-PCR sample product ratios are listed in **Table 2**. Gene expression was influenced by both time and modelled gravity. All gene levels were reduced in time; 24 hours groups showed a down regulation of the genes of interest when compared to the 4 hours groups. Simulated microgravity additionally reduced the expression levels, particularly those of $\beta 1$ -integrin and fibronectin. While fibroblasts cultured on smooth substrata for 24 hours displayed a reduction of expression, the levels were higher compared with fibroblasts cultured for 24 hours on grooved substrata. However, under simulated microgravity conditions the reverse was seen; cells cultured on grooved substrata showed a higher expression level in comparison to the smooth control group.

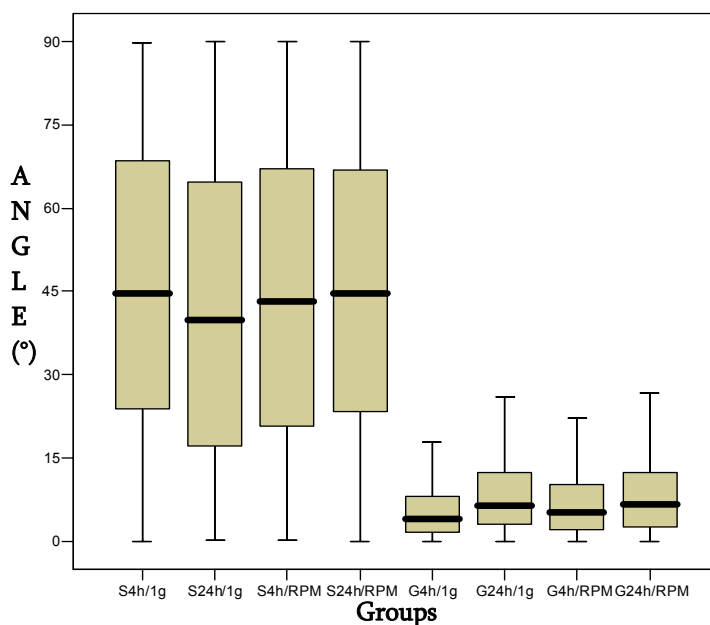


Figure 6. Box-whisker plot showing the distribution of cellular orientation. This graph shows the distribution midpoint, the first and third quartile (boxes), and the largest and smallest observation (whiskers). Of special note are the extreme differences in alignment between smooth and grooves surfaces. This led to investigate within both groups instead of between both groups. For each sample at least 850 individual cells were analysed. S = smooth, G = grooved (all groove widths combined), 4h and 24h stands for the experiment time, and 1g and RPM stands for the applied gravitational force.

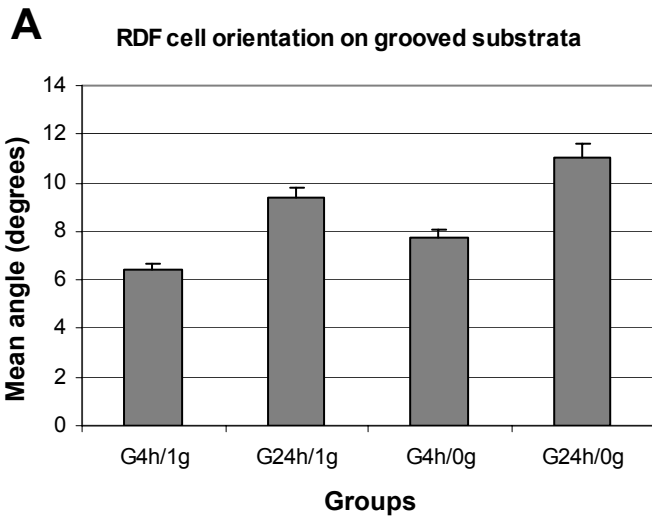


Figure 7. The mean angle and standard error of the mean for both orientation (A) and area (B) of fibroblasts subjected to various parameters. See Figure 6 for explanation of abbreviations.

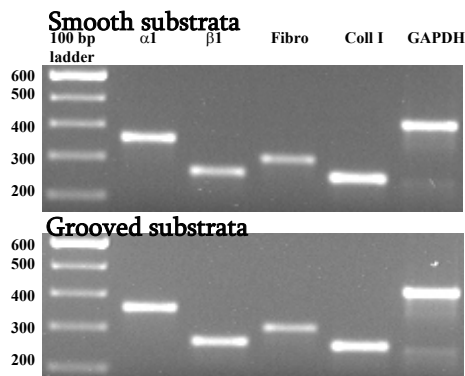
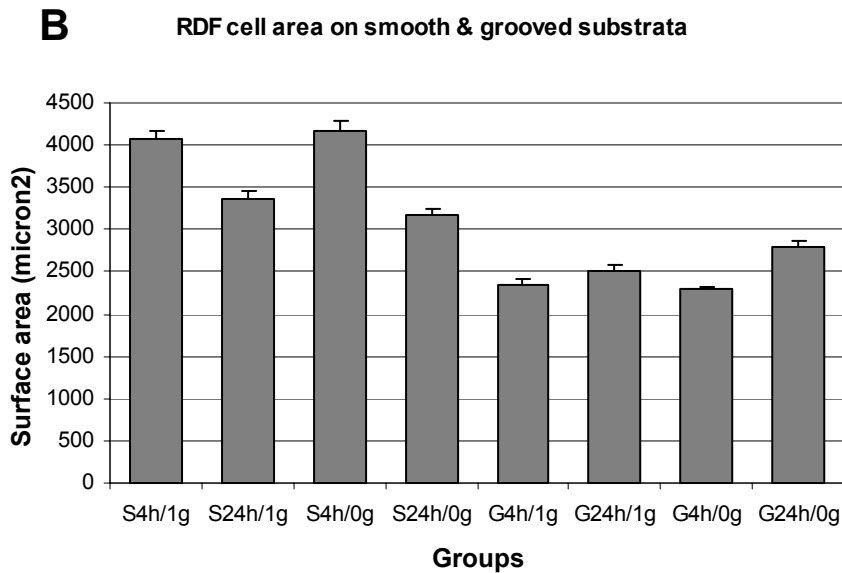


Figure 8. Example of representative PCR results of cells cultured on a smooth (top) and grooved (bottom) substratum subjected to 0g for 24 hours, visualised on agarose gel.

DISCUSSION

The aim of this study was to understand what is essential in determining morphological cell response to substrata and simulated microgravity. Fibroblasts cells were cultured on polystyrene substrata, both planar and topographic, which were mounted inside the RPM which simulated a microgravity environment. Besides studying the morphological cell response like shape and

orientation, the expression of several proteins involved in cell-surface interaction was also investigated.

From our data it can be concluded that RDFs adjust their shape according to micro-topographical features, a secondary, yet significant, role is played by simulated microgravity, particular in combination with prolonged culturing. Under simulated microgravity in the RPM, cells tend to rely more on the stresses encountered from the remaining environmental parameter, i.e. the substratum. It seems that the grooves enhance the cellular-substratum interface.

Regarding the used study design several publications on the use of the RPM or 3-axis clinostat have not only pointed out the usefulness of this research tool to evaluate whether organisms or cells may be sensitive to gravity changes, but also that behaviour of cells to simulated μg conditions on Earth are similar to those found in space flight [10; 24; 36]. Still, it has to be noted that magnitude in simulated microgravity is less pronounced than in true microgravity. The rotation velocity of 60 degrees per second as used in this RPM is recommended for in vitro cell samples. The short radial distance from the cells to both rotational axis and the adequate rotational speed makes it possible to compensate for any perception of gravity stimulus. However, another publication [37] has pointed out that a major characteristic of true microgravity is the absence of buoyancy-driven convective currents. Under microgravity conditions, liquid or gaseous domains which have different temperature or composition cannot rely on convective currents to equalise their density and composition. In contrast, they rely on diffusion, which is a very slow process. The rotation of the samples mounted onto the RPM generates internal motion, which increases the mixing of the sample environment comparable to the levels of normal gravity convection. Another point of concern is the interaction of gravity and thermal fluctuations. Both give rise to changes in cell component behaviour independently of each other. This interaction is difficult to calculate due to the flexibility of the cytoskeleton [27]. Other changes of cell function observed on the RPM might be induced by rotation through the Earth's magnetic field and induction of electric currents. Effects of this theoretically existing influence may make it necessary to shield off the RPM or samples. Stress associated with 3-axis clinorotation needs to be distinguished from effects of simulated microgravity. Still, by using static controls inside the RPM cabinet, we could ensure that the observed alterations were induced by weightlessness. Samples received identical treatment before the start of the experiment and were randomised for 3D clinostat or 1g control. Nevertheless, essential results obtained on the RPM would ideally have to be verified via space experiments, and vice versa, especially to obtain better statistics.

In a rotating set-up such as the RPM, air bubbles present within the closed environment of the cell culture can cause havoc on the cell viability via shear stress [38-40]. The simple, yet effective, solution was the use of a silicone closing cap for each individual well/insert. Combined with CO₂ independent culture medium this resulted in zero air bubbles before and after rotation. Although this design works well in short period experiments, lengthy culturing will require medium changing, and thus other hardware.

<i>Group</i>	<i>G4h1g</i>	<i>G24h1g</i>	<i>G4hRPM</i>	<i>G24hRPM</i>	<i>S4h1g</i>	<i>S24h1g</i>	<i>S4hRPM</i>	<i>S24hRPM</i>
Alpha-1	0,97	0,86	0,99	0,98	1,00	0,88	0,98	0,82
Beta-1	0,96	0,93	0,81	0,76	0,98	0,93	0,95	0,69
Fibro	1,00	0,90	0,98	0,81	0,99	0,80	0,99	0,68
Coll-1	n/a	0,72	n/a	0,83	n/a	0,86	n/a	0,64
GAPDH	1,00	1,00	1,00	1,00	1,00	1,00	1,00	1,00

n/a: not available

Table 2: *RT-PCR semi-quantitative analysis. Shown are the ratios between the gene of interest and the housekeeping gene GAPDH. See Figure 6 for explanation of group abbreviations.*

In comparison with other studies, several comments can be made, particularly on the expression of certain genes of interest and their importance in cellular function in altered gravitational circumstances; Seitzer et al. [41] reported an increase in collagen synthesis by fibroblasts cultured on thermanox coverslips under real microgravity conditions, although after 20 hours of culturing this increase was reduced to 10% compared to control (1g) samples. Our data show that prolonged culturing will negate such amplifications. This is also seen by Saito et al. [16] who observed an decrease of collagen synthesis (both mRNA and protein) by osteoblast-like cells after 72 hours of simulated microgravity.

Arase et al [17], who compared gene expression levels in human fibroblasts with 3D-clinostat treatment, showed that gene levels of ErbB-2, a proto-oncogene that regulates cell proliferation, was down-regulated. Since several integrins, including β -1, are associated with ErbB-2 [42] and our results show a down-regulation of beta-1 integrin in a microgravity environment, it is therefore possible that altered expression levels of ErbB-2 may play a role in the 3D-clinostat dependent signaling cascade. This finding emphasizes the importance of changed integrin binding in (the absence of) mechanical stress.

As a final remark, we have to emphasize that it makes a considerable difference if the cellular machinery itself would be sensitive to gravity, than if cells simply react to a changed chemical environment due to cessation of gravity-induced convection flows. In the former, gravity would be a fundamental feature at least at some moment of cellular function, and microgravity an important instrument to study its mechanisms of operation. Aside from the immediate consequences for manned space exploration, new insights may be expected in the function and evolution of cell molecular systems. In the latter, novel discoveries could hardly be found and similar experimental results may well be obtained in Earth-based investigations. Therefore, the problem of whether or not effects found in real microgravity experiments are due to direct action on cells is an important question which the RPM may help solve [43].

CONCLUSIONS

Our hypothesis was that topographical cues determine cellular shape and orientation, even if simulated microgravity decreases cellular adherence. Regarding all study results, we conclude that our hypothesis holds. However, the effects of simulated microgravity in the long run will become more apparent on cellular function. RPM resulted in the reduced expression of proteins involved in the cell-surface interface and decreased cellular alignment. Research which includes intracellular signalling will be necessary to further understand the behaviour on the level of cell molecular machinery. We concluded from our data that fibroblasts primarily adjust their shape according to morphological environmental cues, like the substrata surface, thereby underscoring the importance of adhesion in cell behaviour. Simulated microgravity plays a secondary, but significant role.

REFERENCES

1. Walboomers, X. F., Croes, H. J., Ginsel, L. A., and Jansen, J. A. Growth behavior of fibroblasts on microgrooved polystyrene. *Biomaterials* 1998, 1861-1868, 1998.
2. den Braber, E. T., de Ruijter, J. E., Smits, H. T., Ginsel, L. A., von Recum, A. F., and Jansen, J. A. Quantitative analysis of cell proliferation and orientation on substrata with uniform parallel surface micro-grooves. *Biomaterials* 1996, 1093-9, 1996.
3. Clark, P., Connolly, P., Curtis, A. S., Dow, J. A., and Wilkinson, C. D. Cell guidance by ultrafine topography in vitro. *J Cell Sci* 1991, 73-7, 1991.
4. Ingber, D. E. Tensegrity I. Cell structure and hierarchical systems biology. *J Cell Sci* 2003, 1157-73, 2003.

5. Ingber, D. E. Integrins, tensegrity, and mechanotransduction. *Gravit Space Biol Bull* 1997, 49-55, 1997.
6. Curtis, A. and Wilkinson, C. New depths in cell behaviour: reactions of cells to nanotopography. *Biochem Soc Symp* 1999, 15-26, 1999.
7. Brunette, D. M. and Chehroudi, B. The effects of the surface topography of micromachined titanium substrata on cell behavior in vitro and in vivo. *J Biomech Eng* 1999, 49-57, 1999.
8. Oakley, C., Jaeger, N. A., and Brunette, D. M. Sensitivity of fibroblasts and their cytoskeletons to substratum topographies: topographic guidance and topographic compensation by micromachined grooves of different dimensions. *Exp Cell Res* 1997, 413-24, 1997.
9. Chou, L., Firth, J. D., Uitto, V. J., and Brunette, D. M. Substratum surface topography alters cell shape and regulates fibronectin mRNA level, mRNA stability, secretion and assembly in human fibroblasts. *J Cell Sci* 1995, 1563-73, 1995.
10. Uva, B. M., Masini, M. A., Sturla, M., Prato, P., Passalacqua, M., Giuliani, M., Tagliafierro, G., and Strollo, F. Clinorotation-induced weightlessness influences the cytoskeleton of glial cells in culture. *Brain Res* 2002, 132-9, 2002 .
11. Schwarzenberg, M., Pippia, P., Meloni, M. A., Cossu, G., Cogoli-Greuter, M., and Cogoli, A. Signal transduction in T lymphocytes--a comparison of the data from space, the free fall machine and the random positioning machine. *Adv Space Res* 1999, 793-800, 1999.
12. Cogoli, A. and Cogoli-Greuter, M. Activation and proliferation of lymphocytes and other mammalian cells in microgravity. *Adv Space Biol Med* 1997, 33-79, 1997.
13. Rijken, P. J., Boonstra, J., Verkleij, A. J., and de Laat, S. W. Effects of gravity on the cellular response to epidermal growth factor. *Adv Space Biol Med* 1994, 159-88, 1994.
14. Schatten, H., Lewis, M. L., and Chakrabarti, A. Spaceflight and clinorotation cause cytoskeleton and mitochondria changes and increases in apoptosis in cultured cells. *Acta Astronaut* 2001, 399-418, 2001.
15. Grigoryan, E. N., Anton, H. J., and Mitashov, V. I. Microgravity effects on neural retina regeneration in the newt. *Adv Space Res* 1998, 293-301, 1998.
16. Saito, M., Soshi, S., and Fujii, K. Effect of hyper- and microgravity on collagen post-translational controls of MC3T3-E1 osteoblasts. *J Bone Miner Res* 2003, 1695-1705, 2003.
17. Arase, Y., Nomura, J., Sugaya, S., Sugita, K., Kita, K., and Suzuki, N. Effects of 3-D clino-rotation on gene expression in human fibroblast cells. *Cell Biol Int* 2002, 225-33, 2002.
18. Boonstra, J. Growth factor-induced signal transduction in adherent mammalian cells is sensitive to gravity. *FASEB J* 1999, S35-42, 1999.
19. Wang, J. H., Yang, G., Li, Z., and Shen, W. Fibroblasts responses to cyclic mechanical stretching depend on cell orientation to the stretching direction. *J Biomech* 2003, 573-6, 2003.
20. Sciola, L., Cogoli-Greuter, M., Cogoli, A., Spano, A., and Pippia, P. Influence of microgravity on mitogen binding and cytoskeleton in Jurkat cells. *Adv Space Res* 1999, 801-5, 1999.
21. Loesberg, W. A., Walboomers, X. F., van Loon, J. J., and Jansen, J. A. The effect of combined cyclic mechanical stretching and microgrooved surface topography on the behavior of fibroblasts. *J Biomed Mater Res A* 2005, 723-732, 2005.
22. Searby, N. D., Steele, C. R., and Globus, R. K. Influence of increased mechanical loading by hypergravity on the microtubule cytoskeleton and prostaglandin E2 release in primary osteoblasts. *Am J Physiol Cell Physiol* 2005, C148-158, 2005.

23. They, M., Pepin, A., Dressaire, E., Chen, Y., and Bornens, M. Cell distribution of stress fibres in response to the geometry of the adhesive environment. *Cell Motil Cytoskeleton* 2006, 341-55, 2006.
24. Cogoli, M. The fast rotating clinostat: a history of its use in gravitational biology and a comparison of ground-based and flight experiment results. *ASGSB Bull* 1992, 59-67, 1992.
25. Kessler, J. O. The internal dynamics of slowly rotating biological systems. *ASGSB Bull* 1992, 11-21, 1992.
26. Kondrachuk, A. V. and Sirenko, S. P. The theoretical consideration of microgravity effects on a cell. *Adv Space Res* 1996, 165-8, 1996.
27. Briegleb, W. Some qualitative and quantitative aspects of the fast-rotating clinostat as a research tool. *ASGSB Bull* 1992, 23-30, 1992.
28. Sievers, A. and Hejnowicz, Z. How well does the clinostat mimic the effect of microgravity on plant cells and organs? *ASGSB Bull* 1992, 69-75, 1992.
29. Chesmel, K. D. and Black, J. Cellular responses to chemical and morphologic aspects of biomaterial surfaces. I. A novel in vitro model system. *J Biomed Mater Res* 1995, 1089-1099, 1995.
30. Freshney, R. I. Culture of animal cells: a multimedia guide. 99. Chichester, John Wiley & Sons Ltd.
31. Walboomers, X. F., Ginsel, L. A., and Jansen, J. A. Early spreading events of fibroblasts on microgrooved substrates. *J Biomed Mater Res* 2000, 529-534, 2000.
32. Hoson, T., Kamisaka, S., Masuda, Y., and Sievers, A. Changes in plant growth processes under microgravity conditions simulated by a three-dimensional clinostat. *Botanical Mag* 1992, 53-70, 1992.
33. Mesland, D. A. Novel ground-based facilities for research in the effects of weight. *ESA Microgravity News* 1996, 5-10, 1996.
34. Clark, P., Connolly, P., Curtis, A. S., Dow, J. A., and Wilkinson, C. D. Topographical control of cell behaviour: II. Multiple grooved substrata. *Development* 1990, 635-644, 1990.
35. Clark, P., Connolly, P., Curtis, A. S., Dow, J. A., and Wilkinson, C. D. Topographical control of cell behaviour. I. Simple step cues. *Development* 1987, 439-448, 1987.
36. Villa, A., Versari, S., Maier, J. A. M., and Bradamante, S. Cell behaviour in simulated microgravity: a comparison of results obtained with RWV and RPM. *Grav Space Biol* 2005, 89-90, 2005.
37. Albrecht-Buehler, G. The simulation of microgravity conditions on the ground. *ASGSB Bull* 1992, 3-10, 1992.
38. Hammond, T. G. and Hammond, J. M. Optimized suspension culture: the rotating-wall vessel. *Am J Physiol Renal Physiol* 2001, F12-25, 2001.
39. Cherry, R. S. and Hulle, C. T. Cell death in the thin films of bursting bubbles. *Biotechnol Prog* 1992, 11-8, 1992.
40. Kleis, S. J., Schreck, S., and Nerem, R. M. A viscous pump bioreactor. *Biotech Bioeng* 1990, 771-777, 1990.
41. Seitzer, U., Bodo, M., and Muller, P. K. Gravity effects on connective tissue biosynthesis by cultured mesenchymal cells. *Adv Space Res* 1995, 235-8, 1995.
42. Falcioni, R., Antonini, A., Nistico, P., Di Stefano, S., Crescenzi, M., Natali, P. G., and Sacchi, A. Alpha 6 beta 4 and alpha 6 beta 1 integrins associate with ErbB-2 in human carcinoma cell lines. *Exp Cell Res* 1997, 76-85, 1997.
43. Mesland, D. A. Possible actions of gravity on the cellular machinery. *Adv Space Res* 1992, 15-25, 1992.



Simulated microgravity activates
MAPK pathways in fibroblasts cultured on
microgrooved surface topography

WA Loesberg, XF Walboomers, JJWA van Loon and JA Jansen

Cell Motil Cytoskeleton, *in press*, 2008

INTRODUCTION

For fibroblasts, mechanical stress is an important and specific director of cell shape and stimulus for extracellular matrix component production. For instance, stress provided by a microgrooved pattern onto which the cells are seeded, as well as, stresses from substratum deformation are well documented [1-9]. On the other hand, cells can also experience mechanical unloading by removing the, at cell level, very weak, but ever present force in nature: gravity. Morphological and functional studies have shown that many cells like osteoblast-like cells and lymphocytes are highly sensitive to altered gravity conditions [10-17]. Although it is generally accepted that the response to environmental stimuli is multi-factorial in origin, research towards the interaction of cells cultured on substratum texture (nano-, micropatterns) and mechanical force is sparse. Such studies are necessary to serve as baseline values for further research aimed at understanding of observed cell response phenomena on a molecular basis [18-22]. For instance, what signalling cascades are important in mediating the cellular response (e.g. mRNA expression; cytoskeleton (de)polymerisation) towards their environment. A familiar signalling pathway is the mitogen activated protein kinase (MAPK) pathways which transmits environmental signals from the cell membrane to the nucleus through phosphorylation cascades, resulting in gene expression regulation (**Figure 1**). Three subgroups of MAPKs are known: extracellular signal-regulated kinases (ERK1/2), jun N-terminal kinase/stress-activated protein kinase (JNK/SAPK), and p38^{MAPK} (p38). Although it has been shown that these kinases respond to a range of stimuli, little is known about the cellular response to altered gravity circumstances [23-26]. Upstream from ERK1/2 and JNK/SAPK is a family of proteins commonly known as Rho GTPases. Members include, besides Rho, Rac and Cdc42. Rho mediates the formation of cytoskeletal stress fibres, while Rac mediates the formation of membrane ruffles, and Cdc42 mediates the formation of peripheral filopodia. Rho exerts its distinct actions through interactions with ROCK, a serine/threonine protein kinase. Cdc42/Rac operates via p65 activated kinase (PAK). While separate Cdc42/Rac and Rac/Rho hierarchies exist, these might not extend into a linear form since Cdc42 and Rho activities are competitive. ROCK promotes the formation of Rho-induced actin stress fibres and focal-adhesion complexes, to which the ends of the stress fibres attach. On the other hand, Cdc42-induced peripheral filopodia formation is accompanied by Rac-induced membrane ruffles, which together with PAK, which stimulates the disassembly of stress fibres, play a role in cell movement. PAK also fosters loss of focal-adhesion complexes [27-30]. This cooperation and antagonism between different Rho GTPases in their role of reorganisation of the actin cytoskeleton under microgravity has received little attention.

Ground based research to simulate microgravity by means of a Random Positioning Machine (RPM) provides excellent means to conduct gravitational studies. The RPM is a microweight (microgravity) simulator that is based on the principle of 'gravity-vector-averaging'. Gravity is a vector, *i.e.* it has a magnitude and direction. During an experimental run in the RPM the sample position with regard to the Earth's gravity vector is constantly and randomly changing, and as a result the samples will experience a simulated weightlessness environment [31-34].

In this study we evaluated *in vitro* the differences in morphological behaviour between fibroblast cells cultured on polystyrene substrata, both planar and with a surface microtopography, which were placed in a simulated microgravity environment. In addition, the mRNA transcription of several proteins involved in cell-surface interaction was investigated. The underlying aim was to understand which parameter is more important in determining cell response. Our hypothesis is that cellular shape and orientation is determined by the topographical cues, and a simulated microgravity environment will decrease the cellular orientation to these substrata. As control fibroblast cells were cultured on similar substrata, which remained at normal (Earth) gravity.

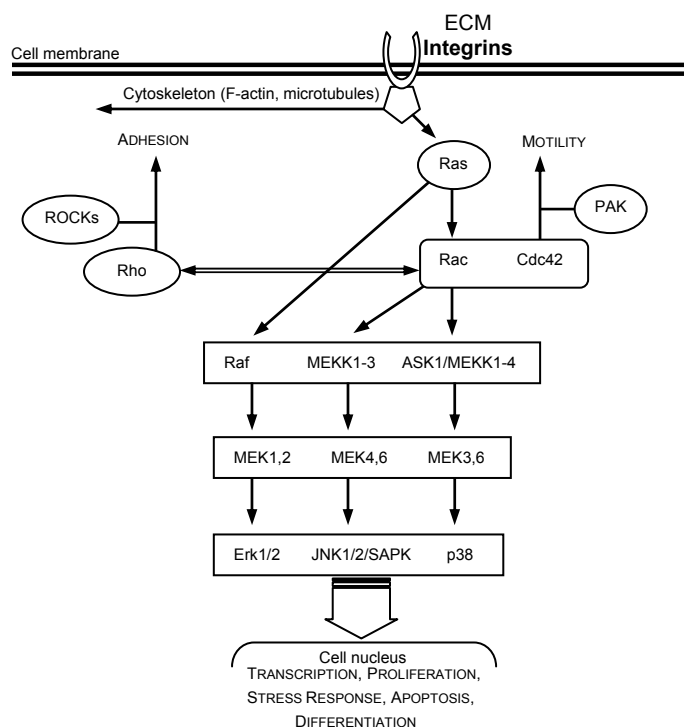


Figure 1. Mitogen Activated Protein Kinases (MAPK) intracellular signalling pathways. A simplified schematic of the three major MAPK pathways and the members of the Rho family of small GTPases.

MATERIALS AND METHODS

Substrata:

Microgrooved patterns were made, using a photo lithographic technique and subsequent etching in a silicon wafer as described by Walboomers *et al.* [1]. The dimensions of the microgrooved topography were a ridge- and groove width of 1 μm ; with a uniform depth of 0.25 μm . Wafers with a planar surface were used as controls. The silicon wafer was used as template for the production of polystyrene (PS) substrata for cell culturing. PS substrates were solvent cast in a manner described by Chesmel and Black [35] and were attached to 18 mm diameter cylinders with polystyrene-chloroform adhesive. Shortly before use a radio frequency glow-discharge (RFGD) treatment was applied for 5 minutes at a pressure of 2.0×10^{-2} mbar and a power of 200 W (Harrick Scientific Corp., Ossining, NY, USA) in order to sterilize the dishes, as well as, promote cell attachment by improving the wettability of the substrata.

Cell culture:

Rat dermal fibroblasts (RDF) were obtained from the ventral skin of male Wistar rats as described by Freshney [36]. Cells were cultured in CO_2 -independent α -MEM containing Earle's salts (Gibco, Invitrogen Corp., Paisley, Scotland), L-glutamine, 10% FCS, gentamicin (50 $\mu\text{g}/\text{ml}$), in an incubator set at 37 $^\circ\text{C}$ with a humidified atmosphere. Experiments were performed with 4 - 8th culture generation cells. Onto the various substrata, 1.5×10^4 cells/ cm^2 were seeded. Cells were pre-cultured for 4h, after which they were placed in a 12 wells plate for support. Custom made silicone caps closed each well and the tissue culture dish therein (**Figure 2**). Using a type 22G1 needle and applying a little pressure while adding additional medium, air bubbles were removed to prevent unwanted shear force and turbulence during rotation in the RPM. In this system with only one specific density fluid and absence of air bubbles no fluid motion was to be expected, since the media was moving with the same velocity as the cell monolayer. The well plates containing the samples were secured onto the platform. From previous studies it is known that fibroblasts need approximately 4 hours to begin adapting their morphology to a new environment [37]. Therefore experimental times were chosen of 30 and 120 minutes and 48 hours to obtain

information on the cell behaviour from an early time period until a state of equilibrium between the cells and their environment.

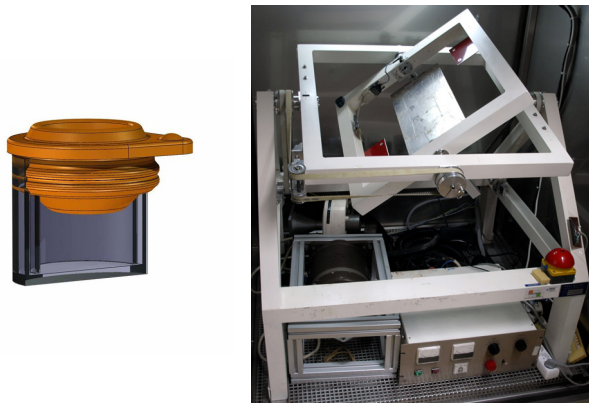


Figure 2. At left a graphical cross section of a polystyrene culture dish used in this study with silicone closing cap securing the insert snug into the well of a 12 wells plate and providing an air bubble free environment. On the right the Random Positioning Machine (RPM) used in this study to simulate weightlessness. The RPM is equipped with a computerised temperature and motor control. The control samples are secured on one of the machine support struts, while experimental samples are placed on the inner frame of the clinostat.

Simulated microgravity:

The RPM is shown in **Figure 2**. One of the first versions was developed by T. Hoson *et al.* [38]. We used a similar system, manufactured by Dutch Space (formerly Fokker Space, Leiden, The Netherlands). The outer frame rotated independently from the inner frame, which caused the samples to move in 3 axis. The rotational movement of both frames was powered by two servomotors. A PC user interface with dedicated software controlled the random movements of the two servomotors with regard to: onset, rate, and duration of rotation. The rotational velocity of both frames was randomised with a maximum of 60°/sec, direction, and interval was set at random. The samples were fixed in the centre of the inner frame; the largest radius was 57.8 mm to the outermost well (residual g is between 10^{-3} and 10^{-2} g, [34]). The RPM was accommodated in a temperature-controlled incubator set at 37°C [33]. For the experiments the cell layers were washed three times with Phosphate Buffered Saline (PBS) and prepared for further analysis immediately after retrieval from the RPM machine.

Scanning electron microscopy (SEM):

To assess overall morphology of the fibroblasts, SEM was performed ($n = 4$). Cells were rinsed, fixed for 5 minutes in 2% glutaraldehyde, followed by 5 minutes in 0.1 M sodium-cacodylate buffer (pH 7.4), dehydrated in a graded series of ethanol, and dried in tetramethylsilane to air. Specimens were sputter-coated with gold and examined with a Jeol 6310 SEM (Tokyo, Japan).

Immunofluorescence

Components of the cytoskeleton were made visible using fluorescent staining techniques. RDF cells, cultured on microgrooved substrata were rinsed in PBS, pH7.2, fixed for 30 minutes in 2% paraformaldehyde, and permeabilised with 1% Triton X100 for 5 min. Filamentous actin was stained with Alexa Fluor 568 phalloidin (Molecular Probes, A-12380, Leiden, The Netherlands) diluted in 1% Bovine Serum Albumin/PBS to block non-specific epitopes. Vinculin was stained with rabbit polyclonal primary antibodies to vinculin (sc-5573, Santa Cruz biotechnology Inc., Santa Cruz, CA, USA), followed by labelling with goat anti-rabbit secondary antibodies IgG with Alexa Fluor 488 (Molecular Probes, A-11034). Finally, the specimens were examined with a Biorad (Hercules, CA, USA) MRC 1024 confocal laser scanning microscope (CLSM) system with a krypton-argon laser at magnification of 40x. The digital immunofluorescence images acquired with the CLSM were loaded into Image J (version 1.5.0, Wayne Rasband, NIH, USA) to create

overlay images. Cytoskeletal components were examined for their overall morphology as well as their orientation with respect to the groove direction.

Image Analysis

For quantitative image analysis samples were stained with phalloidin-TRITC (Sigma, P-1951, St. Louis, MO, USA), followed by examination with a Leica/Leitz DM RBE Microscope (Wetzlar, Germany) at magnification of 10x. The phalloidin-TRITC fluorescence micrographs were analyzed with Scion Image software (Beta Version 4.0.2, Scion Corp., Frederick, MD, USA). The orientation of fibroblasts was examined and photographed. For each sample six fields of view were selected randomly. The criteria for cell selection were (1) the cell was not in contact with other cells and (2) the cell was not in contact with the image perimeter. The maximum cell diameter was measured as the longest straight line between two edges within the cell borders. The angle between this axis and the grooves (or an arbitrarily selected line for smooth surfaces) was termed the orientation angle. If the average angle was 45 degrees, cells were supposed to have a random orientation. Cell extensions like filopodia, which could confound the alignment measurement, were not included when assessing the cell orientation. Using Clarks criteria [39; 40], cells oriented at 0–10 degrees from the groove direction were regarded to be aligned. The distribution of cytoskeletal patterns with time, gravity force in view of the type of microgrooves and groove direction was described by the percentage of cells in the sample that displayed each pattern. Between 500 and 800 cells were measured per group for both orientation and surface area.

Cellular surface area was measured with the aforementioned image analyser software. Applying the same criteria for cell selection; cell areas were determined and displayed as μm^2 . Between 350 - 500 cells were measured per group for both orientation and surface area.

Quantitative-PCR

Total RNA was isolated from fibroblasts with an RNA isolation and stabilisation kit (QIAGEN, Hilden, Germany) and cDNA was synthesised with reverse transcription in 11 μl aliquots of total RNA with an RT-PCR kit (Invitrogen, Carlsbad, CA, USA).

After RNA isolation and stabilisation and cDNA amplification; 12.5 μl of iQ SYBR Green SuperMix (Bio-Rad, Hercules, CA, USA) was added to each well of an optical 96 wells plate, 1.5 μl of both forward and reverse primer were added, as well as, 4.5 μl DEPC and 5 μl of 10 times diluted cDNA sample. The wells plate was covered and centrifuged shortly to remove air bubbles, following PCR quantification using cycling parameters: 95 °C x3 min; 95 °C x15 seconds → 60 °C x30 seconds followed by 72 °C x30 seconds for 40 cycles. All samples were analysed in triplicate. The comparative Ct-values method was used to calculate the relative quantity of $\alpha 1$ -, $\beta 1$ -, and $\beta 3$ -integrin, and Collagen Type I and GAPDH [41]. Expression of the housekeeping gene glyceraldehyde-3-phosphate dehydrogenase (GAPDH) was used as an internal control to normalise results.

SDS-PAGE and Western Blot analysis

For preparing total protein extracts; cells were washed 3 times with ice cold PBS. Cells were harvested by scraping followed by disruption with 500 μl ice-cold lysis buffer (50 mM Tris (pH 7.4), 250 mM NaCl, 5 mM EDTA, 50 mM NaF, 1mM Na_3VO_4 , 1% Nonidet P40 (BioSource, Camarillo, CA, USA) supplemented with 1 mM Phenylmethanesulfonyl fluoride (PMSF, P7626, Sigma-Aldrich, Steinheim, Germany) and Protease Inhibitor Cocktail (P2714, Sigma-Aldrich). Samples were cleared of cellular debris and concentrated by centrifugation for 65 minutes, 4°C at 12,000 rpm (Amicon Microcon YM-10 centrifugal filter tube, Millipore, Billerica, MA, USA). The protein concentrations in the retentate were determined, and equal amounts of protein were

dissolved in 10 μ l of 2x reducing sample buffer (4% SDS, 100mM Tris (pH 6.0), 10% β -mercaptoethanol, 20% Glycerol) and heated at 95°C for 5 minutes and electrophoresed on 12.5% SDS-Acrylamide minislab gels and transferred to (polyvinylidene difluoride) PVDF membranes (Immobilon-P, Millipore). After protein transfer, the membranes were blocked in 4% powdered milk in TBST (0.05% Tween 20 in TBS) overnight at room temperature. Immunological blots were then performed at room temperature for 1 hour in 2% skim milk in TBST buffer containing specific primary antibodies (see below).

Antibodies for Western Blot analysis

Western blots were probed with the following antibodies: Anti-ERK 1/2 (C-16; sc-93), JNK1 (C-17; sc-474), p38 MAPK (C-20; sc-535), α PAK (H-300; sc-11394), RhoA (119; sc-179), Rac1 (T-17; sc-6084), Cdc42 (P1; sc-87). Phosphorylated (i.e. active) proteins were investigated with anti-active p-ERK 1/2 (E-4; sc-7383), p-JNK (G-7; sc-6254), and p-p38 (D-8; sc-7973). All antibodies were obtained from Santa Cruz Biotechnology.

After membranes were washed with TBST, they were incubated with appropriate secondary antibody IgG with alkaline phosphatase conjugate and immunoreactive bands were visualized using Nitroblue Tetrazolium (NBT) and 5-bromo-4-chloro-3-indolyl phosphate (BCIP) chemiluminescence reagents (Bio-Rad Laboratories Hercules, CA, USA).

Statistical analysis:

Acquired data from the fluorescence micrographs of cell alignment, as well as, QPCR data were analysed using SPSS for Windows (Release 12.0.1, SPSS Inc., Chicago, USA). The effects of and the interaction between both time and/or force and surface were analysed using analysis of variance (ANOVA), including a modified least significant difference (Tukey) multiple range test to detect significant differences between two distinct groups. Probability (p) values of ≤ 0.05 were considered significant.

RESULTS

Scanning Electron Microscopy

The microtopography pattern of grooves and ridges was accurately reproduced in the polystyrene substrata. When observing cell morphology, RDFs cultured on smooth substrata showed a cell spreading, which was not only considered random but also displayed the different stages of cell spreading; from round cells with abundance amounts of filopodia to flat stretched out cells with large cell surface areas (**Figure 3A-C**). RDFs seeded onto grooved substrata already showed alignment from an early time point onward although their cell bodies were still rather wide. In later stages the fibroblasts had stretched out into elongated cells with narrow cell width and high alignment (**Figure 3D-F**).

When subjected to simulated microgravity, RDFs cultured on smooth surfaces at first appeared to differ only minimally in cellular behaviour (**Figure 3G**). However, after 120 minutes cells displayed cell membrane ruffles, but retained their spindle shape (**Figure 3H**). After 48 hours fibroblasts appeared as long spindle-shaped cells (**Figure 3I**). RDFs seeded onto grooved surface in the RPM appeared similar in their cell morphology when compared to their 1g counterparts, although cell widths were not as narrow. This became more apparent after 48 hours of culturing under simulated microgravity conditions (**Figure 3J-L**).

Fluorescence microscopy (CLSM)

The cytoskeleton was investigated by staining filamentous actin and vinculin containing anchor points of the cell focal adhesions. **Figure 4A-C** shows 1g smooth substratum samples for 3 time

points; the observed cell shape, spreading, and random orientation were similar to SEM micrographs. Actin filaments (red), were always running in the direction of the long axis of cells. Vinculin staining for focal adhesions resulted in a non-specific staining around the nucleus.

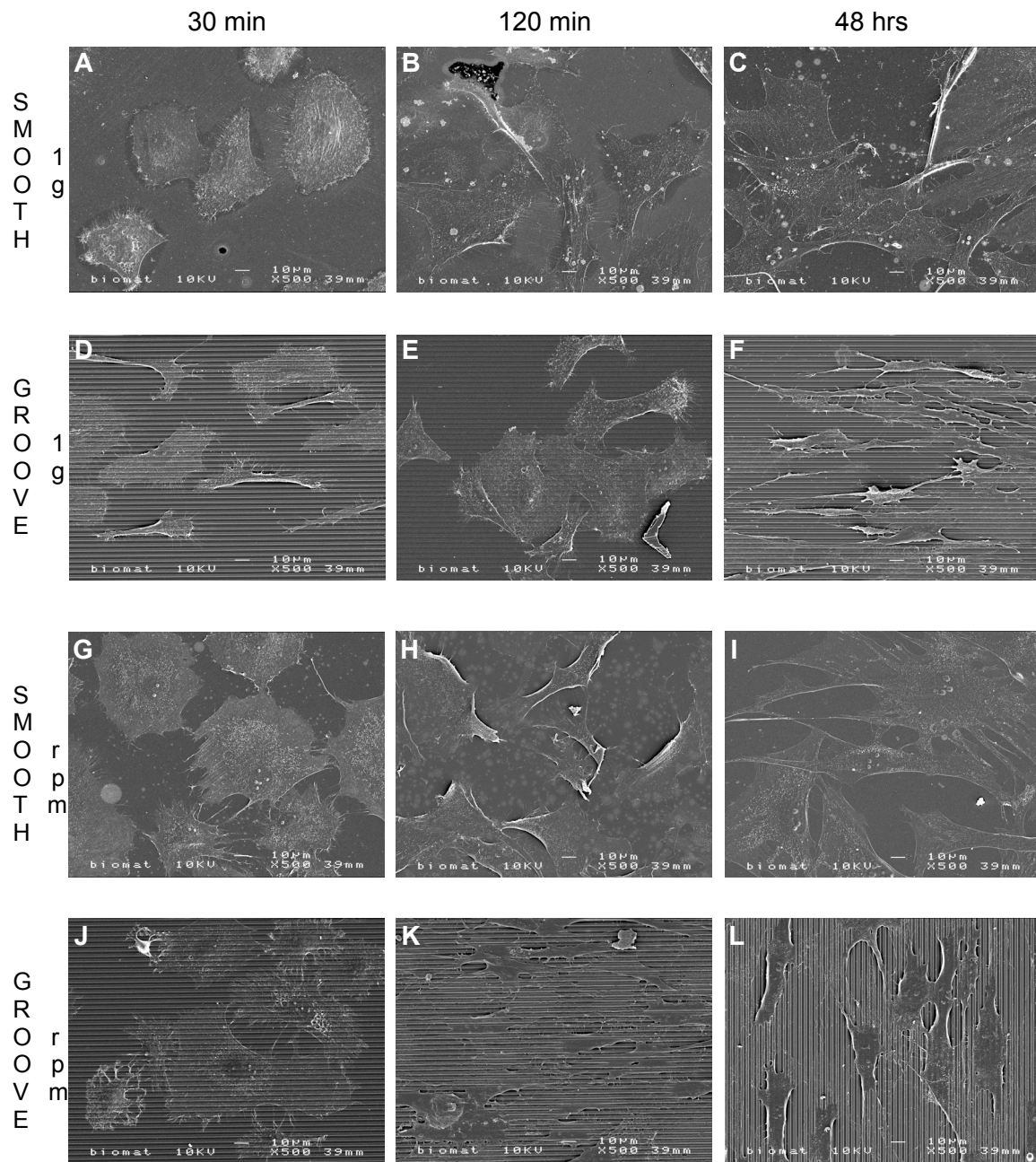


Figure 3. SEM micrographs of RDFs cultured under various conditions. Normal gravity: (A) Smooth substratum, 30 minutes, (B) Smooth, 120 minutes, (C) Smooth, 48 hours and (D) Grooved surface, 30 minutes, (E) Groove, 120 minutes, (F) Groove, 48 hours. Microgravity: (G) Smooth 30 minutes, (H) Smooth, 120 minutes, (I) Smooth, 48 hours and (J) Groove surface, 30 minutes, (K) Groove, 120 minutes, (L) Groove, 48 hours (magnification x500).

Vinculin spots (green) were visible in some samples, positioned at the end of actin bundles, and always extended in the direction of the actin bundle. RDFs cultured on grooved surfaces displayed a similar morphology, as found on smooth surfaces; however, there was increased orientation of the cells and their cytoskeleton with time (**Figure 4D-F**).

Cell morphology and cytoskeleton (CSK) distribution of RDFs cultured on smooth substrata in the RPM appeared to remain the same, although after 30 minutes the F-actin bundles seem to be more

pronounced (**Figure 4G**). After 2 hours of RPM, F-actin bundles had become thinner (**Figure 4H**). After 48 hours under simulated weightlessness conditions, RDFs cultured in smooth surfaces appeared in all shapes and sizes, however, elongated cells seemed to be more abundant. Their CSK was clearly defined, and focal adhesion points were lavishly present (**Figure 4I**).

RDFs cultured on grooved substrata in the RPM as shown in **Figure 4J & K** revealed a comparable cellular alignment towards the grooves when compared to the 1g control groups. Fibroblasts cytoskeleton showed round cells with F-actin in the long axis of the cells, and vinculin anchor points at the end of these thick actin bundles. After 48 hours of simulated microgravity cells had recuperated and appeared to be highly aligned, although their cell bodies were wider, as seen in the clearly visible actin filaments and vinculin staining (**Figure 4L**).

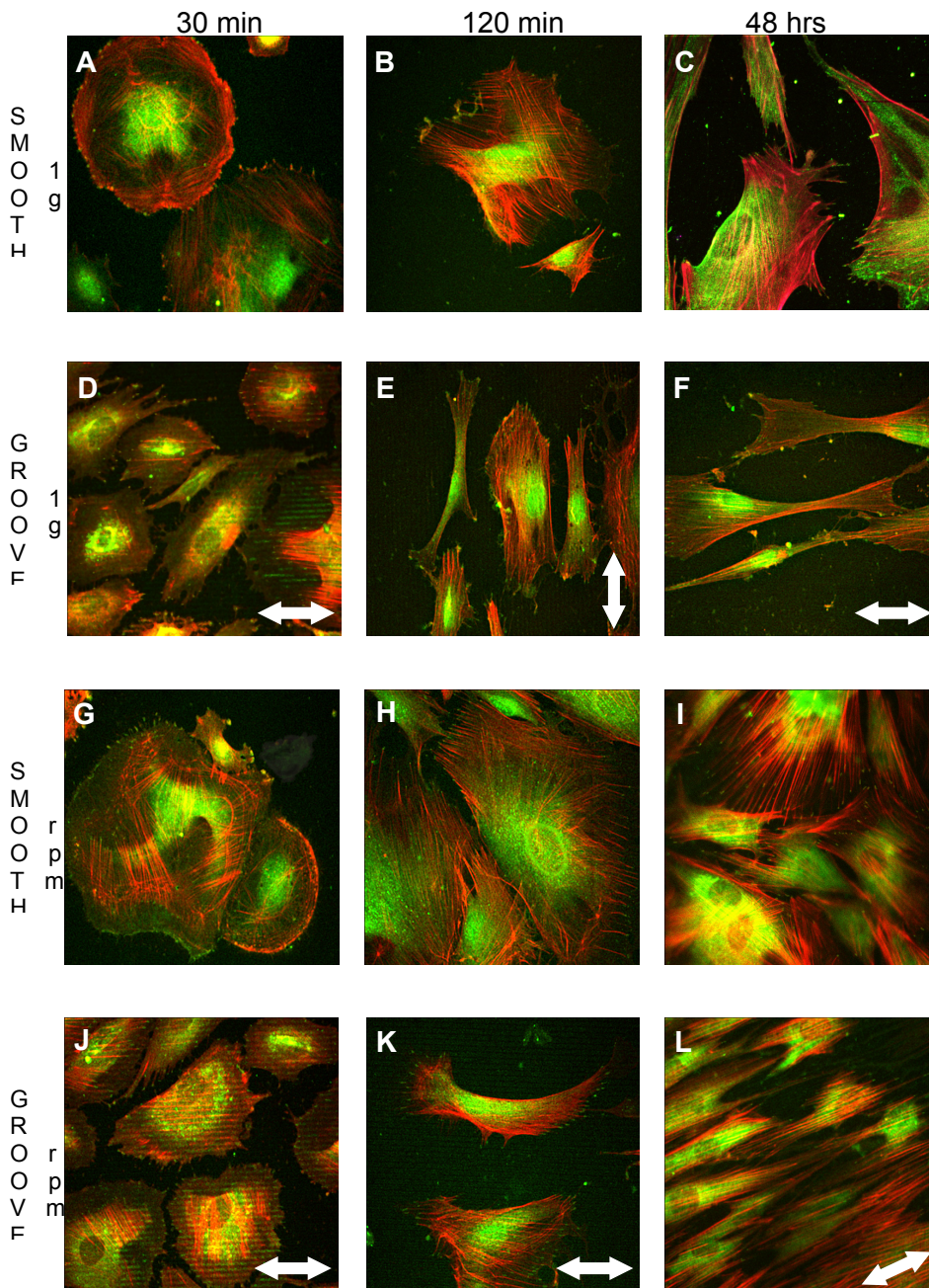


Figure 4. CLSM micrographs of RDFs cultured under several conditions. Normal gravity: (A) Smooth substratum, 30 minutes, (B) Smooth, 120 minutes, (C) Smooth, 48 hours and (D) Grooved surface, 30 minutes, (E) Groove, 120 minutes, (F) Groove, 48 hours. Simulated microgravity: (G) Smooth 30 minutes, (H) Smooth, 120 minutes, (I) Smooth, 48 hours and (J) Groove surface, 30 minutes, (K) Groove, 120 minutes, (L) Groove, 48 hours. Double ended arrow groove direction. Colour figure on page 166.

Image Analysis

Actin filaments were stained with Phalloidin-TRITC and image analysis was conducted, which showed that RDFs orientation was profound on all grooved substrata. RDFs seeded onto smooth

surfaces displayed a random orientation in cell alignment. The quantified results for cellular alignment are presented in **Figure 5**. Within the smooth groups the mean angle remained stable in time and/or gravity, and thus no significant differences were found. There were significant differences between the smooth and grooved groups obviously, but more important were the differences within the grooved groups as was proven by analysis of variance (ANOVA) multiple comparison test. In this analysis the main parameters: topography, gravity, and time proved significant in all but one case.

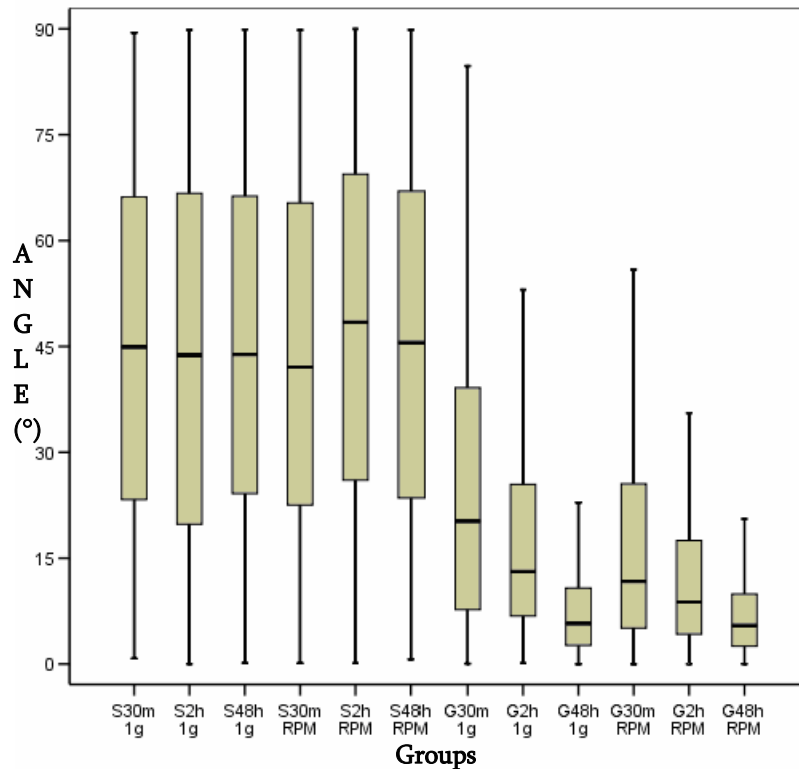


Figure 5. Box-whisker plot showing the distribution of cellular orientation of fibroblasts under various circumstances of mechanical loading. While the smooth substrata elicit random orientation as seen by the mean angle around 45 degrees, the groove patterns make fibroblast align and with time enhance their orientation towards the grooves as shown by the decreasing mean angle. Within the grooved sample groups all differences in mean angle are significant except those for the 48 hours groups. For each sample at least 500 individual cells were analysed. S = smooth, G = grooved, 30m, 2h, and 48h stands for the experiment time, and 1g and RPM stands for the applied gravitational force.

Regarding topography, around 80% of the cells cultured on grooved substrata were considered aligned compared to 13% on smooth surfaces.

The effects of gravitational unloading is significant, under simulated microgravity the mean angle of fibroblasts on grooved surfaces decreased compared to 1g control groups, thus the overall alignment increased. Particularly in the earlier time points, cells in the RPM, on average, had a mean angle 6 degrees below that of the 1g control groups, in addition a higher proportion (averaging an additional 20%) of the cells were aligned. After 48 hours there were no significant differences to any further extent between the 1g and RPM grooved groups. The mean angle levelled out to around 8-9 degrees for 80 percent of all fibroblast cells at 48 hours.

Time played an important role in the cellular orientation: 48 hour groups always showed a significantly increased alignment towards the grooves. Up to 80% of cells were aligned after 48 hours compared to 40% and 52% after respectively, 30 and 120 minutes of culturing.

Comparable to the orientation of the RDFs, there was a significant difference in cell area between smooth and grooved substrata, but also among the control and RPM treated groups (**Figure 6**). On grooved surfaces overall cell area was about $2580 \pm 180 \mu\text{m}^2$ compared to $3230 \pm 265 \mu\text{m}^2$ overall on smooth surfaces. In the RPM, fibroblasts cultured on smooth surfaces for 30 minutes compared to fibroblasts cultured on grooved surfaces for 30 minutes had a significant difference in cell surface area ($4267 \pm 530 \mu\text{m}^2$ and $3345 \pm 242 \mu\text{m}^2$, respectively). After 48 hours in RPM cell surface area in the grooved groups decreased significantly to $1798 \pm 175 \mu\text{m}^2$, while smooth groups settle around $2968 \pm 295 \mu\text{m}^2$.

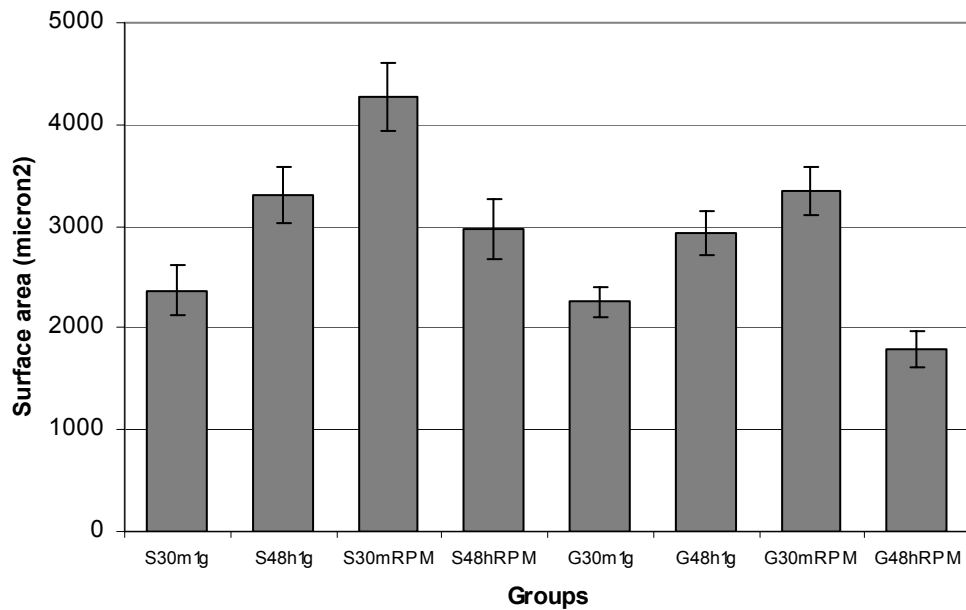


Figure 6. Bar graphs showing the mean and standard error of the for cell surface area of fibroblasts subjected to various parameters. The pattern in both smooth and grooved groups are the same, although the average cell area value for grooved groups is lower. See Figure 5 for explanation of abbreviations.

Quantitative-PCR

Real-time PCR analysis was performed to quantify the mRNA expression of α 1-, β 1-, and β 3-integrins, and collagen type I in fibroblasts. **Figure 7** shows the relative changes in gene expression of the various mRNA transcripts. Transcripts were normalised to the internal control gene GAPDH, and were computed relative to the expression in the smooth or the grooved 1g control group.

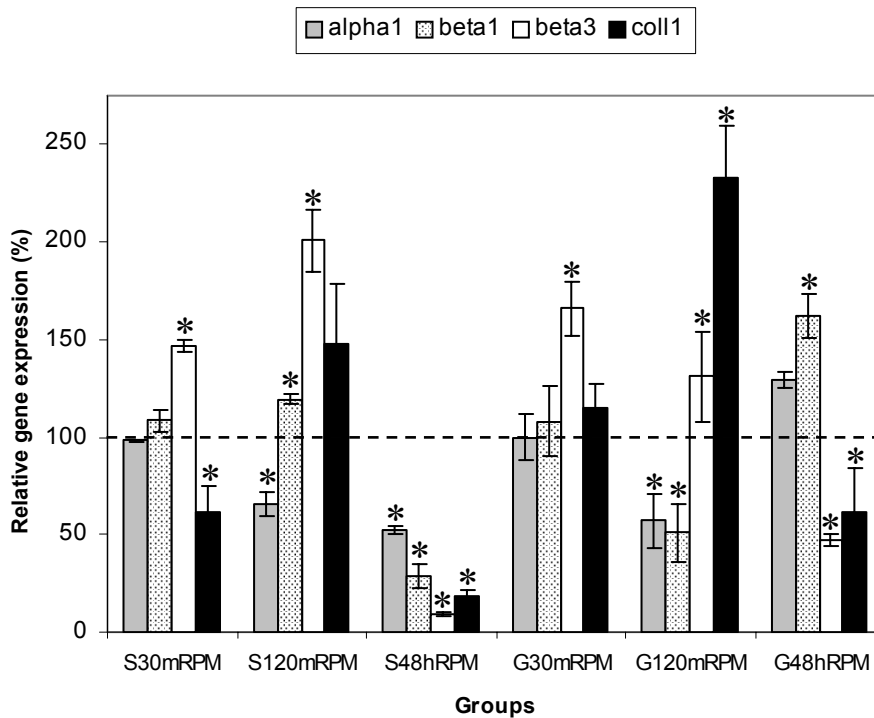


Figure 7. Relative mRNA levels of alpha-1, beta-1, beta-3 integrins, and collagen type I of fibroblast in microgravity setting, cultured for 30 min, 120 min, and 4 hours on either smooth or grooved surfaces. Total RNA was isolated after gravitational loading and Q-PCR performed. For the internal standard the respective 1g smooth or 1g grooved substrate was used. S = Smooth, G = Groove. 30m, 120m, and 48h are the experimental times, and RPM the type of applied gravity. Dashed line represents no difference/control group. Data are expressed as mean \pm SD, n = 3. *Significant difference (p < 0.05).

Alpha-1 gene expression in smooth experimental samples was down-regulated from two hours of culturing onward. Beta-1 and beta-3 integrin expression were initially elevated, at 48 hours however, both were significantly decreased. Collagen type I was up-regulated at two hours, after two days gene expression was severely reduced.

Within the grooved groups, alpha-1 integrin expression is down-regulated at first, but is restored after 48 hours. Beta-1 integrin showed a similar pattern. After 2 days of culturing in RPM, beta-1 is significantly up-regulated. Beta-3 integrin expression was initially increased, the last time point showed a significant decrease. Collagen type I gene expression is markedly up-regulated at two hours of experiencing RPM.

SDS-PAGE and Western Blot analysis

All three major signaling pathways within the Mitogen Activated Protein Kinase (MAPK) pathway were present: ERK-1/2, JNK/SAPK-1/2, and p38 MAPK. Also, their active (phosphorylated) form, could be detected in most groups (**Figure 8 A-C**). ERK-1/2 protein was present in all groups, and particularly in the 1g control groups, active ERK-1/2 protein could be detected in the all groups, although an increase was found after 48 hours in the 1g control group. While p-ERK-1/2 appeared predominantly in the 1g control groups, JNK/SAPK and p38 showed increased presence in both total and active protein in the 0g experiment groups. Especially during the early time points (30 and 120 minutes) larger bands were visible.

Upstream of the ERK pathway, RhoA and ROCK1/2 were detected (**Figure 9A&B**). These proteins, which are important in cell adhesion showed overall an improved presence with an increase in time and a decrease in gravity. Closely linked to RhoA, are Cdc42 and Rac1 fusion protein (**Figure 9 C&D**). These proteins are involved with cell motility and their presence was also increased in time and appeared to be up-regulated under microgravity conditions. PAK protein, a downstream effector of Cdc42 and Rac1, was also present. It appeared more in the grooved substrata groups than smooth, and microgravity resulted in an increase. The detection of PAK was hampered by the fact that the primary antibody not only bound to α -PAK, but also detected β - and γ -PAK, resulting in a smudged appearance (**Figure 9E**).

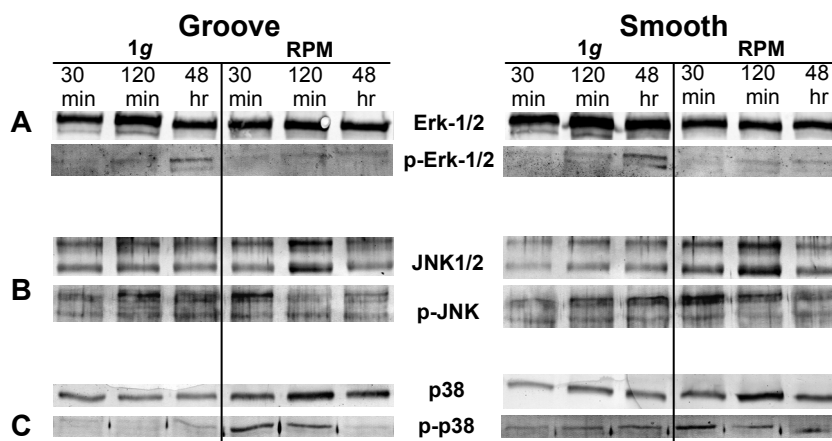


Figure 8. Western blots analysis of MAPK signalling pathways from whole cell lysates prepared from primary fibroblasts. Equal amount of protein were probed with antibodies specific to total ERK1/2 (A, top row) and phospho-ERK1/2 (A, bottom row) followed by immuno-staining with IgA Alkaline Phosphate conjugate. The whole cell extracts as described in panel A were analyzed by Western blotting. Samples were probed with antibodies specific for total JNK1/2 (B, top row) and phospho-JNK1/2 (B, bottom row), total p38 (C, top row) and phospho-p38 (C, bottom row).

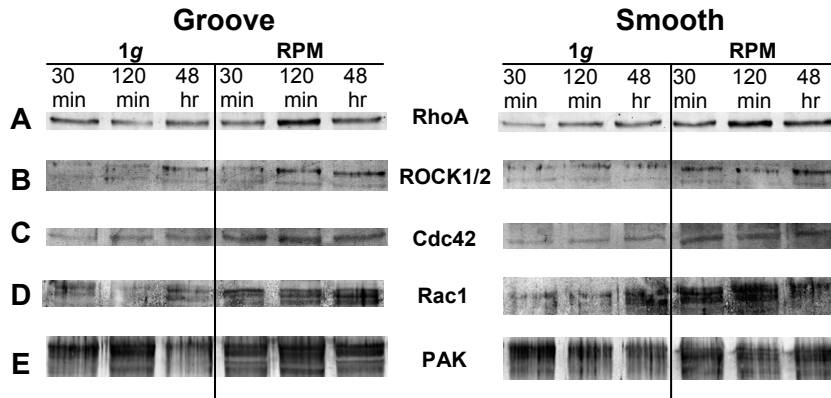


Figure 9. Western blots analysis of small GTPases family members from whole cell extracts prepared from primary fibroblasts. Equal amount of protein were probed with antibodies specific to total RhoA (A), ROCK1/2 (B), Cdc42 (C), Rac1 fusion protein (D), and $\alpha/\beta/\gamma$ PAK (E) followed by immuno-staining with IgA Alkaline Phosphate conjugate. The whole cell extracts were analyzed by Western blotting.

DISCUSSION

The aim of this study was to identify what is essential in determining morphological cell response to substrata and simulated microgravity. Fibroblasts were cultured on polystyrene substrata, both smooth and grooved, which were mounted inside the RPM. The mechanotransduction of these forces onto the cells were investigated from several angles: morphological cell responses like shape and orientation, and related to that the cytoskeleton of the cells; as well as the expression of several proteins involved in cell-surface interaction using Q-PCR. Finally, proteins of the MAPK intracellular signalling kinase pathways were visualised. From our data we concluded that RDFs adjust their shape according to micro-topographical features. In addition, microgravity plays a significant role on the cells response to outside environmental factors. Under simulated microgravity in the RPM, cells tend to rely more on the stresses encountered from the remaining environmental parameter, i.e. the substratum. It seems that the grooves enhance the cellular-substratum interface. This is reflected by the presence and/or activation of the several proteins involved in the MAPK pathways which control cell adhesion during exposure to simulated microgravity.

Our random positioning machine model to study microgravity has been reviewed by a number of publications, which have pointed out the usefulness of the RPM as a research tool to simulate space flight conditions in order to elucidate how living systems respond to this impact [10; 34; 42-46]. With a rotation of 60 degrees per second the residual g is between 10^{-3} and 10^{-2} g. Although an increased distance from the centre of rotation at the same speed will result in increased accelerations at the outer edges of the sample, we made the radial distance from the cell samples to both rotational axis as small as possible and thereby compensating as much as possible for any perception of gravity stimulus. A key principle in RPM use is that by increasing the frequency of rotation the travelling distance gets smaller. By performing this rotation constantly, a circular path is generated and by increasing the rate, cells will rotate around their own axis. This controlled rotation not only applies to the cells but also its surrounding liquid phase. It is argued that the coupling between the cells and the static surrounding liquid is the main reason for this microgravity simulation paradigm [34; 47]. However, a publication by Albrecht-Buehler [48] narrates that a true microgravity characteristic is the absence of buoyancy-driven convective currents. Under weightlessness circumstances, liquid or gaseous regions which have different temperature or composition cannot rely on convective currents to equalise their density and composition. In contrast, they rely on diffusion, which is a very slow process. The rotation of the samples mounted onto the RPM generates internal motion, which increases the mixing of the sample environment comparable to the levels of normal gravity convection. Within the RPM

gravity compensation occurs, which even if completely effective does not remove chronic gravitational stimulation. This stimulation might be perceived by mechanosensors within a cell and could initiate the mechanotransduction process. In attached cells this residual g may not be regarded as regular gravity applied to the cells. It is in fact an inertial shear force and directed perpendicular as compared to gravity generated by Earth. Cells undergoing RPM might display a small, perhaps significant, displacement of their total mass or intracellular structures [34].

True zero g , that is not to experience any gravitational pull, can only be achieved if an object would be infinitely far from any gravitating body (gravity may be a weak force; however, it has a long reach). All other conditions of weightlessness result from a net sum of all present forces equalling zero, not from an absence of gravity. This is impossible to achieve; we can only effectively isolate an experiment from the attraction of gravity while remaining in our solar system. Since attraction decreases non-linearly with increasing distance from the source, even a spacecraft in Low Earth Orbit experiences approximately 90% of the gravitational acceleration that exists at the surface of the Earth. From an analytical point of view regarding the RPM, it is necessary to identify all relevant gravity dependent variables in the system in order to resolve the extent to which the altered inertial environment created via rotation mimics the specific underlying cause-and-effect interactions that occur in a weightlessness environment [47]. However, from a researcher's perspective it might be better if efforts are spent in optimizing the system in order to attain a better end product. In our study all samples received identical treatment before the start of the experiment and were randomised for RPM or control. Also, to prevent shear stress caused by air bubbles within the contained surroundings of the cell culture which can be disastrous for cell viability [49-51], we used silicone closing caps which attached snug on each well/insert combination. This resulted in the absence of air bubbles before and after rotation. Nevertheless, essential results obtained with the RPM as a simulated microgravity model would ideally have to be confirmed via space experiments.

Combined with previous work [52], several interesting observations concerning cellular alignment on microgrooved topography can be made: within the first 4 hours after cell adhesion, fibroblast orientation rapidly increases. Cells demonstrate a mean angle as low 5 degrees. Fibroblasts in a simulated microgravity environment perform better than those cultured under normal gravity values. On average, cells in the RPM have mean angles around 14°; 6 degrees lower than the 1g control groups. Nevertheless, from 24 hours onward no difference can be distinguished between both 1g and RPM groups. Mean angles of fibroblasts after 48 hours of culturing on microgrooved surfaces, slightly increases before levelling off to 8 degrees.

QPCR data on proteins which are involved in cellular adhesion revealed an interesting development: collagen type I, an ECM component as deposited by the cells in order to adhere to their environment, was greatly reduced in samples run experiencing simulated microgravity conditions, as opposed to control (1g) samples. This seems to contradict Seitzer *et al.* [53], who reported an increase in collagen synthesis by fibroblasts cultured on thermanox coverslips under real microgravity conditions. However, they also showed that after 20 hours of culturing this increase was reduced to 10% compared to control samples. In previous research we have shown that prolonged culturing will counteract such up-regulations [52], which corroborates with Saito *et al.* [16] who also observed an decrease of collagen synthesis (both mRNA and protein) by osteoblast-like cells after 72 hours of simulated microgravity.

The up-regulation of beta-3 integrin of fibroblasts which underwent simulated microgravity during the early stages underscores that this subunit is an important functional receptor for ECM components (e.g., collagen). Combined with alpha-1 subunits, this beta-3 integrin mediates cell spreading on fibrillar type I collagen [54]. Recent studies [55; 56] observed that talin, an intracellular protein involved in focal adhesion anchorage, which binds to the beta-3 integrin

cytoplasmic tails is directly responsible for “inside-out” activation of beta-3. Quiescence of stable adhered cells might result in a slow recycling of integrins and explain that after 48 hours the beta-3 expression plummets in favour of beta-1 integrin, which throughout the different groups remained by and large unchanged or slightly elevated. The notable exception in beta-3 integrin gene expression occurs in cells cultured for 48 hours under RPM conditions, there beta-3 are severely down-regulated. This performance of beta-1, and alpha-1, corresponds with previous work [52; 57] and denotes the importance of these subunits in long-term interaction between a cell and its environment.

Elevated phosphorylation levels of JNK/SAPK and p38 indicate that these two major pathways, which are commonly activated by stressful conditions, were also activated by microgravity. As mentioned below, upstream $\alpha/\beta/\gamma$ PAK which activates JNK is also increased under RPM conditions. Upstream to PAK, the small GTPases Rac, Cdc42 also expresses increased activation after microgravity exposure.

Total ERK1/2 did not change for cells cultured on groove patterns under simulated microgravity. Although it could be argued that a small reduction exists for total ERK1/2 on the smooth substrate, it is clear that phosphorylated-ERK1/2 is obviously reduced in both the planar and the topographic surfaces. Meyers *et al.* [57] also reported ERK reduction in osteoblast cells; there the discontinued activation of ERK1/2 affected the Runx2 activation, an essential transcription factor for osteoblastic differentiation. Active-ERK1/2 in fibroblast cells is required for growth-factor-induced cell motility responses. A reduction might suggest that cells hunker down and stop moving altogether. This leads to increased surface area on these substrates, which increases the probability of fibroblasts forming stable attachments. This increase in adhesion results in more intracellular signaling cascades, which is reflected by an increase in activity of the members of the Rho GTPases family during exposure to simulated microgravity. This increase is present throughout, and demonstrates the interactions which exist at this intracellular level. It also reveals that fibroblasts are actively engaged with their environment. The morphological appearance of fibroblasts in the RPM underscores this observation: cells are outstretched, and display a proper cytoskeleton, however an increase in vinculin anchor points around the nucleus is also visible and fibroblast cell shape under zero g is markedly different compared to their 1g control counterparts.

CONCLUSIONS

There are suggestions that mechanical and physical forces may be sensed at the outset as local deformations or stimulation of the cell surface and those mechano-sensitive systems might promote changes in cell-signalling pathways, which are transformed subsequently into molecular responses. Another point of view is that the triggering element results from the intracellular polarised displacement of their total mass or intracellular structures/components. Notwithstanding the nature of the sensors, the “impact” of weightlessness is probably related narrowly to the functional state of cell membranes and contractible elements of the cytoskeleton. The involvement of these cell components may be crucial in the processes of reception and realisation of gravitational stimuli, as demonstrated by the clear alterations in the molecular organization of membranes and cytoskeleton under altered gravity conditions on a variety of cells.

Our results are consistent with the aforementioned observation that utilisation of microgravity to primary fibroblast cells encourages them to change their morphological appearance, and their expression of cell-substratum proteins through the MAPK intracellular signalling pathways. Our hypothesis is partially true: cells do orientate along the grooves, however simulated microgravity enhances fibroblast orientation on grooved substrates.

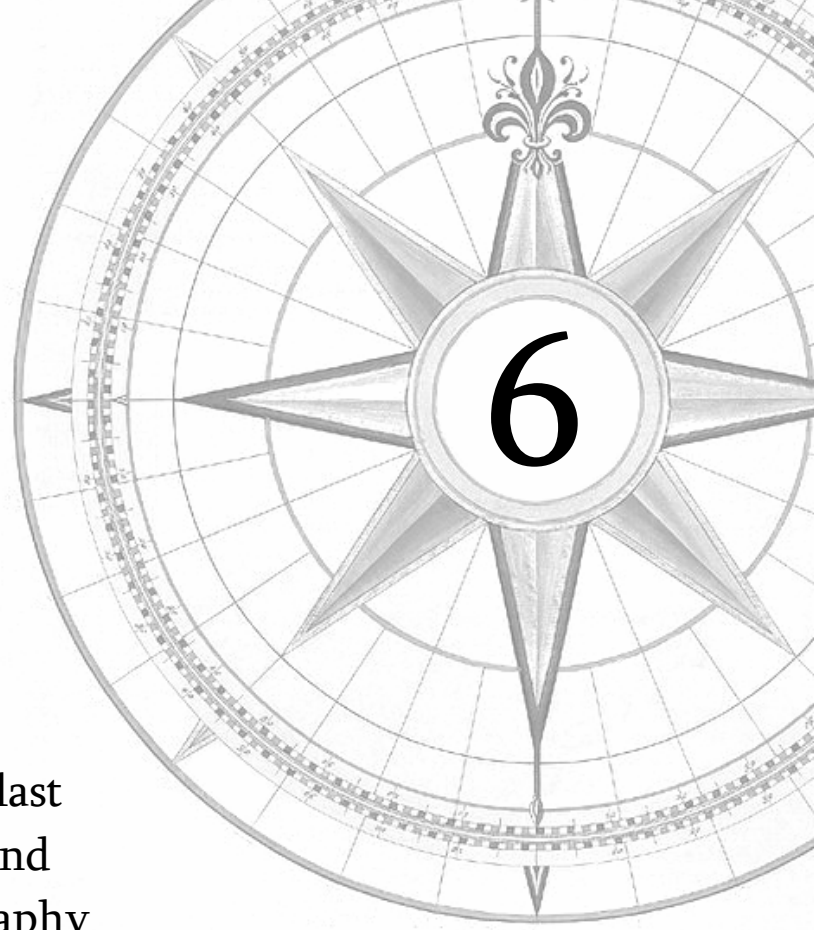
REFERENCES

1. Walboomers, X. F., Croes, H. J., Ginsel, L. A., and Jansen, J. A. Growth behavior of fibroblasts on microgrooved polystyrene. *Biomaterials* 1998, 1861-1868, 1998.
2. den Braber, E. T., de Ruijter, J. E., Smits, H. T., Ginsel, L. A., von Recum, A. F., and Jansen, J. A. Quantitative analysis of cell proliferation and orientation on substrata with uniform parallel surface micro-grooves. *Biomaterials* 1996, 1093-9, 1996.
3. Clark, P., Connolly, P., Curtis, A. S., Dow, J. A., and Wilkinson, C. D. Cell guidance by ultrafine topography in vitro. *J Cell Sci* 1991, 73-7, 1991.
4. Ingber, D. E. Tensegrity I. Cell structure and hierarchical systems biology. *J Cell Sci* 2003, 1157-73, 2003.
5. Ingber, D. E. Integrins, tensegrity, and mechanotransduction. *Gravit Space Biol Bull* 1997, 49-55, 1997.
6. Curtis, A. and Wilkinson, C. New depths in cell behaviour: reactions of cells to nanotopography. *Biochem Soc Symp* 1999, 15-26, 1999.
7. Brunette, D. M. and Chehroudi, B. The effects of the surface topography of micromachined titanium substrata on cell behavior in vitro and in vivo. *J Biomech Eng* 1999, 49-57, 1999.
8. Oakley, C., Jaeger, N. A., and Brunette, D. M. Sensitivity of fibroblasts and their cytoskeletons to substratum topographies: topographic guidance and topographic compensation by micromachined grooves of different dimensions. *Exp Cell Res* 1997, 413-24, 1997.
9. Chou, L., Firth, J. D., Uitto, V. J., and Brunette, D. M. Substratum surface topography alters cell shape and regulates fibronectin mRNA level, mRNA stability, secretion and assembly in human fibroblasts. *J Cell Sci* 1995, 1563-73, 1995.
10. Uva, B. M., Masini, M. A., Sturla, M., Prato, P., Passalacqua, M., Giuliani, M., Tagliaferro, G., and Strollo, F. Clinorotation-induced weightlessness influences the cytoskeleton of glial cells in culture. *Brain Res* 2002, 132-9, 2002 .
11. Schwarzenberg, M., Pippia, P., Meloni, M. A., Cossu, G., Cogoli-Greuter, M., and Cogoli, A. Signal transduction in T lymphocytes--a comparison of the data from space, the free fall machine and the random positioning machine. *Adv Space Res* 1999, 793-800, 1999.
12. Cogoli, A. and Cogoli-Greuter, M. Activation and proliferation of lymphocytes and other mammalian cells in microgravity. *Adv Space Biol Med* 1997, 33-79, 1997.
13. Rijken, P. J., Boonstra, J., Verkleij, A. J., and de Laat, S. W. Effects of gravity on the cellular response to epidermal growth factor. *Adv Space Biol Med* 1994, 159-88, 1994.
14. Schatten, H., Lewis, M. L., and Chakrabarti, A. Spaceflight and clinorotation cause cytoskeleton and mitochondria changes and increases in apoptosis in cultured cells. *Acta Astronaut* 2001, 399-418, 2001.
15. Grigoryan, E. N., Anton, H. J., and Mitashov, V. I. Microgravity effects on neural retina regeneration in the newt. *Adv Space Res* 1998, 293-301, 1998.
16. Saito, M., Soshi, S., and Fujii, K. Effect of hyper- and microgravity on collagen post-translational controls of MC3T3-E1 osteoblasts. *J Bone Miner Res* 2003, 1695-1705, 2003.
17. Arase, Y., Nomura, J., Sugaya, S., Sugita, K., Kita, K., and Suzuki, N. Effects of 3-D clino-rotation on gene expression in human fibroblast cells. *Cell Biol Int* 2002, 225-33, 2002.
18. Boonstra, J. Growth factor-induced signal transduction in adherent mammalian cells is sensitive to gravity. *FASEB J* 1999, S35-42, 1999.

19. Wang, J. H., Yang, G., Li, Z., and Shen, W. Fibroblasts responses to cyclic mechanical stretching depend on cell orientation to the stretching direction. *J Biomech* 2003, 573-6, 2003.
20. Sciola, L., Cogoli-Greuter, M., Cogoli, A., Spano, A., and Pippia, P. Influence of microgravity on mitogen binding and cytoskeleton in Jurkat cells. *Adv Space Res* 1999, 801-5, 1999.
21. Loesberg, W. A., Walboomers, X. F., van Loon, J. J., and Jansen, J. A. The effect of combined cyclic mechanical stretching and microgrooved surface topography on the behavior of fibroblasts. *J Biomed Mater Res A* 2005, 723-732, 2005.
22. Searby, N. D., Steele, C. R., and Globus, R. K. Influence of increased mechanical loading by hypergravity on the microtubule cytoskeleton and prostaglandin E2 release in primary osteoblasts. *Am J Physiol Cell Physiol* 2005, C148-158, 2005.
23. Aplin, A. E. and Juliano, R. L. Integrin and cytoskeletal regulation of growth factor signaling to the MAP kinase pathway. *J Cell Sci* 1999, 695-706, 1999.
24. Yuge, L., Hide, I., Kumagai, T., Kumei, Y., Takeda, S., Kanno, M., Sugiyama, M., and Kataoka, K. Cell differentiation and p38(MAPK) cascade are inhibited in human osteoblasts cultured in a three-dimensional clinostat. *In Vitro Cell Dev Biol Anim* 2003, 89-97, 2003.
25. Nebreda, A. R. and Porras, A. p38 MAP kinases: beyond the stress response. *Trends Biochem Sci* 2000, 257-260, 2000.
26. Porras, A., Zuluaga, S., Black, E., Valladares, A., Alvarez, A. M., Ambrosino, C., Benito, M., and Nebreda, A. R. P38 alpha mitogen-activated protein kinase sensitizes cells to apoptosis induced by different stimuli. *Mol Biol Cell* 2004, 922-933, 2004.
27. Tang, Y., Yu, J., and Field, J. Signals from the Ras, Rac, and Rho GTPases converge on the Pak protein kinase in Rat-1 fibroblasts. *Mol Cell Biol* 1999, 1881-1891, 1999.
28. He, H., Pannequin, J., Tantiogco, J. P., Shulkes, A., and Baldwin, G. S. Glycine-extended gastrin stimulates cell proliferation and migration through a Rho- and ROCK-dependent pathway, not a Rac/Cdc42-dependent pathway. *Am J Physiol Gastrointest Liver Physiol* 2005, G478-488, 2005.
29. Lim, L., Manser, E., Leung, T., and Hall, C. Regulation of phosphorylation pathways by p21 GTPases. The p21 Ras-related Rho subfamily and its role in phosphorylation signalling pathways. *Eur J Biochem* 1996, 171-185, 1996.
30. Manser, E. Small GTPases take the stage. *Dev Cell* 2002, 323-328, 2002.
31. Mesland, D. A. Mechanisms of gravity effects on cells: are there gravity-sensitive windows? *Adv Space Biol Med* 1992, 211-28, 1992.
32. Hoson, T., Kamisaka, S., Buchen, B., Sievers, A., Yamashita, M., and Masuda, Y. Possible use of a 3-D clinostat to analyze plant growth processes under microgravity conditions. *Adv Space Res* 1996, 47-53, 1996.
33. Mesland, D. A. Novel ground-based facilities for research in the effects of weight. *ESA Microgravity News* 1996, 5-10, 1996.
34. van Loon, J. J. W. A. Some history and use of the random positioning machine, RPM, in gravity relayed research. *Advances in Space Research* 2007, 2007.
35. Chesmel, K. D. and Black, J. Cellular responses to chemical and morphologic aspects of biomaterial surfaces. I. A novel in vitro model system. *J Biomed Mater Res* 1995, 1089-1099, 1995.
36. Freshney, R. I. Culture of animal cells: a multimedia guide. 99. Chichester, John Wiley & Sons Ltd.

37. Walboomers, X. F., Ginsel, L. A., and Jansen, J. A. Early spreading events of fibroblasts on microgrooved substrates. *J Biomed Mater Res* 2000, 529-534, 2000.
38. Hoson, T., Kamisaka, S., Masuda, Y., and Sievers, A. Changes in plant growth processes under microgravity conditions simulated by a three-dimensional clinostat. *Botanical Mag* 1992, 53-70, 1992.
39. Clark, P., Connolly, P., Curtis, A. S., Dow, J. A., and Wilkinson, C. D. Topographical control of cell behaviour: II. Multiple grooved substrata. *Development* 1990, 635-644, 1990.
40. Clark, P., Connolly, P., Curtis, A. S., Dow, J. A., and Wilkinson, C. D. Topographical control of cell behaviour. I. Simple step cues. *Development* 1987, 439-448, 1987.
41. Livak, K. J. and Schmittgen, T. D. Analysis of relative gene expression data using real-time quantitative PCR and the $2^{-\Delta\Delta C(T)}$ Method. *Methods* 2001, 402-8, 2001.
42. Cogoli, M. The fast rotating clinostat: a history of its use in gravitational biology and a comparison of ground-based and flight experiment results. *ASGSB Bull* 1992, 59-67, 1992.
43. Villa, A., Versari, S., Maier, J. A. M., and Bradamante, S. Cell behaviour in simulated microgravity: a comparison of results obtained with RWV and RPM. *Grav Space Biol* 2005, 89-90, 2005.
44. Kraft, T. F., van Loon, J. J., and Kiss, J. Z. Plastid position in Arabidopsis columella cells is similar in microgravity and on a random-positioning machine. *Planta* 2000, 415-22, 2000.
45. Vassy, J., Portet, S., Beil, M., Millot, G., Fauvel-Lafeve, F., Karniguian, A., Gasset, G., Irinopoulou, T., Calvo, F., Rigaut, J. P., and Schoevaert, D. The effect of weightlessness on cytoskeleton architecture and proliferation of human breast cancer cell line MCF-7. *FASEB J* 2001, 1104-6, 2001.
46. Hughes-Fulford, M. Signal transduction and mechanical stress. *Sci STKE* 2004, RE12, 2004.
47. Klaus, D. M. Clinostats and bioreactors. *Gravit Space Biol Bull* 2001, 55-64, 2001.
48. Albrecht-Buehler, G. The simulation of microgravity conditions on the ground. *ASGSB Bull* 1992, 3-10, 1992.
49. Hammond, T. G. and Hammond, J. M. Optimized suspension culture: the rotating-wall vessel. *Am J Physiol Renal Physiol* 2001, F12-25, 2001.
50. Cherry, R. S. and Hulle, C. T. Cell death in the thin films of bursting bubbles. *Biotechnol Prog* 1992, 11-8, 1992.
51. Kleis, S. J., Schreck, S., and Nerem, R. M. A viscous pump bioreactor. *Biotech Bioeng* 1990, 771-777, 1990.
52. Loesberg, W. A., Walboomers, X. F., Bronkhorst, E. M., van Loon, J. J., and Jansen, J. A. The effect of combined simulated microgravity and microgrooved surface topography on fibroblasts. *Cell Motil Cytoskeleton* 2007, 174-185, 2007.
53. Seitzer, U., Bodo, M., Muller, P. K., Acil, Y., and Batge, B. Microgravity and hypergravity effects on collagen biosynthesis of human dermal fibroblasts. *Cell Tissue Res* 1995, 513-7, 1995.
54. Jokinen, J., Dadu, E., Nykvist, P., Kapyla, J., White, D. J., Ivaska, J., Vehvilainen, P., Reunanen, H., Larjava, H., Hakkinen, L., and Heino, J. Integrin-mediated cell adhesion to type I collagen fibrils. *J Biol Chem* 2004, 31956-63, 2004.
55. Nayal, A., Webb, D. J., and Horwitz, A. F. Talin: an emerging focal point of adhesion dynamics. *Curr Opin Cell Biol* 2004, 94-8, 2004.
56. Zou, Z., Chen, H., Schmaier, A. A., Hynes, R. O., and Kahn, M. L. Structure-function analysis reveals discrete beta3 integrin inside-out and outside-in signaling pathways in platelets. *Blood* 2007, 3284-3290, 2007.

57. Meyers, V. E., Zayzafoon, M., Gonda, S. R., Gathings, W. E., and McDonald, J. M. Modeled microgravity disrupts collagen I/integrin signaling during osteoblastic differentiation of human mesenchymal stem cells. *J Cell Biochem* 2004, 697-707, 2004.



Mechanosensitivity of fibroblast
towards inertial shear force and
microgrooved surface topography

WA Loesberg, XF Walboomers, JA Jansen, and JJWA van Loon

Annals of Biomechanical Engineering, submitted, 2008

INTRODUCTION

The effects of fluid shear force on cell structure and function have been investigated in several studies. Especially, the effects of laminar flow and the associated wall shear stress on cells have been researched, since fluid shear is an important physiological phenomenon in blood vessels [1-4]. Besides endothelial cells, mechano-sensing and adaptation of bone is also often described to be governed by fluid shear forces [5-7]. A number of parameters have been measured: reorganisation of F-actin and intermediate filaments structures [8-12], extracellular matrix production (vinculin, fibronectin, integrin, collagen) [13; 14], the involvement of RhoA, the role of ion channels (Na⁺), and associated increases in ERK1/2 stimulation [15].

On a cellular level both fluid and inertial shear forces may use the same mechanotransduction pathways, whereby cells undergo changes in morphology as a response to mechanical signals. Inertial shear force can easily be generated under laboratory conditions in a fixed angle centrifuges. In standard centrifuges, either in regular laboratories or as control samples in space flight experiments, an essential difference between inertial shear force and gravity force is that inertial shear acts perpendicular to the gravity acceleration vector [16].

Force transmission from the extracellular matrix to the cell interior occurs through a chain of proteins, the focal adhesion sites, that are comprised of an integrin-extracellular matrix bond (e.g. vitronectin and fibronectin), integrin-associated proteins on the intracellular side (paxilin, tensin), and proteins linking the focal adhesion complex to the cytoskeleton (talin, vinculin). Stresses transmitted through adhesion receptors and distributed throughout the cell could cause conformational changes in individual force transmitting proteins, any of which would be a candidate for force transduction into a biochemical signal [17]. These integrin/focal adhesion mediated assemblies vice versa are dependant upon the activities of these signals, particularly the activity of the Rho family of GTPases. By subtly modulating pathways via soluble growth factors and differentiation factors, integrins also exerts their action through an indirect way. Antibody mediated engagement and clustering of integrins leads to activation of the Mitogen Activated Protein Kinase pathways, which are key effectors of these processes [18-20] (**Figure1**).

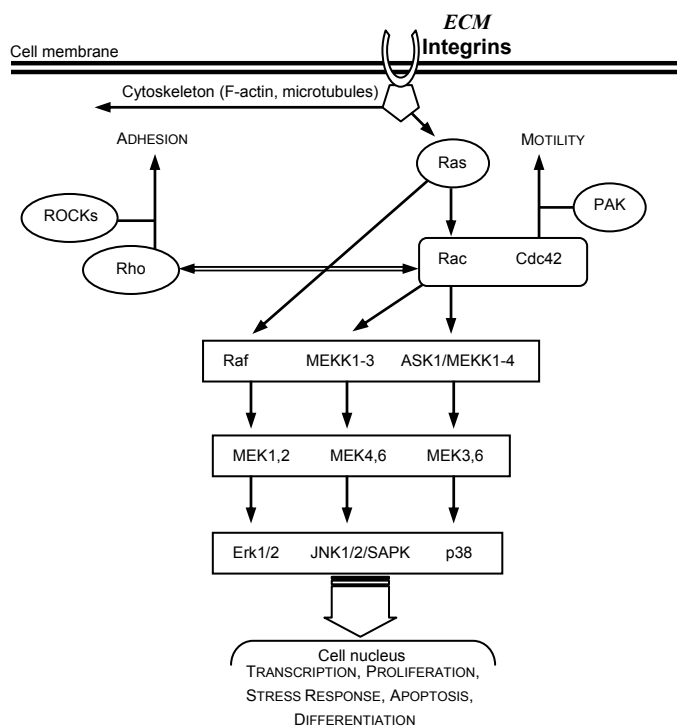


Figure 1. Mitogen Activated Protein Kinases (MAPK) intracellular signalling pathways. A simplified schematic of the three major MAPK pathways and the members of the Rho family of small GTPases.

Altered acceleration circumstances might have an effect on focal adhesion and actin polymerisation, both associated with integrins, which in turn control the signalling to MAPK. Although it has been shown that these kinases respond to a range of stimuli, little is known about the cellular response to changed shear conditions [21-23] [24-27]. In this study we applied a range of inertial shear forces on fibroblasts cultures on various micro-structured substrata. To ascertain the impact of inertial shear force we looked both at a morphological (scanning electron and fluorescence microscopy) and molecular level (mRNA transcription and Western blotting). The underlying aim was to understand to what extent inertial shear forces can alter directed cell behaviour, such as seen on microtextured substrates, and in addition, what parameter is more important in determining cell response.

MATERIALS & METHODS

Substrata:

Microgrooved patterns were made, using a photo lithographic technique and subsequent etching in a silicon wafer as described by Walboomers *et al.* [28]. The dimensions of the microgrooved topography were a ridge- and groove width of 1 μm , with a uniform depth of 0.25 μm . Wafers with a planar surface were used as controls. The silicon wafer was used as template for the production of polystyrene (PS) substrata for cell culturing. PS was solvent cast in manner described by Chesmel and Black [29]. Polystyrene replicas were attached to 18 mm diameter cylinders with polystyrene-chloroform adhesive, creating small culture dishes. Shortly before use a radio frequency glow-discharge (RFGD) treatment was applied for 5 minutes at a pressure of 2.0×10^{-2} mbar and a power of 200 W (Harrick Scientific Corp., Ossining, NY, USA) in order to promote cell attachment by improving the wettability of the substrata and to sterilise the culture dishes.

Cell culture:

Rat dermal fibroblasts (RDF) were obtained from the ventral skin of male Wistar rats as described by Freshney [30]. Cells were cultured in CO_2 -independent α -MEM containing Earle's salts (Gibco, Invitrogen Corp., Paisley, Scotland), L-glutamine, 10% FCS, gentamicin (50 $\mu\text{g}/\text{ml}$), in an incubator set at 37 $^\circ\text{C}$ with a humidified atmosphere. Experiments were performed with 4 - 8th culture generation cells. Onto the various substrata, 2.0×10^4 cells/ cm^2 were seeded. Cells were pre-cultured for 4h in the culture dishes, after which they were placed in a 12 wells plate for support. Custom-made silicone caps closed each well and the tissue culture dish therein. Using a type 22G1 needle and applying a little pressure while adding additional medium removed air bubbles. In this system with only one specific density fluid and absent air bubbles no fluid motion was to be expected, since the media was moving with the same velocity as the cell monolayer. The well plates containing the samples were inserted into aluminium culture boxes inside the centrifuge [31]. From previous studies it is known that fibroblasts need approximately 4 hours to commence adapting their morphology to a new environment [32]. Therefore experiment times were chosen of 0.5 and 2 and 4 hours to obtain information on the cells behaviour from an early time period until a state of stability between the cells and their environment.

Inertial shear:

The medium size centrifuge for acceleration research (MidiCAR) was used in this study to induce inertial shear stress as has been described earlier (**Figure 2**). In short, the centrifuge is housed inside a temperature controlled cabinet and contains a control sample compartment enabling the control samples to undergo the same environmental conditions, yet at 1 g (Earth) gravity. The culture dishes with a grooved substratum were placed with the grooves perpendicular to the radial

axis of rotation inside the 12-wells plate). Wells plates were placed inside a culture box which was hung in brackets inside the MidiCAR. The boxes were prevented from tilting by inserting wedges between the box top and the swivel point of the bracket. This setup results in a force parallel to the cell substratum instead of on top of the cells as in a regular swing-out centrifuge, and allows us to investigate the effects of inertial shear magnitude. Centrifuge programmed ranges were: 1 (control), 44 or 88 *g*. For calculations we presume the following “ideal” cell: half a sphere with a diameter of 10 μm , a height of 5 μm and a density of 1050 $\text{kg}\cdot\text{m}^{-3}$. Contents: $(4/3\pi r^3)/2 = 2.618 \times 10^{-16} \text{ m}^3$. Diameter through the cell centre $(\pi r^2)/2 = 7.854 \times 10^{-11} \text{ m}$. Solving for cell mass we get: $2.618 \times 10^{-16} \text{ m}^3 \times 1050 \text{ kg}\cdot\text{m}^{-3} = 2.749 \times 10^{-13} \text{ kg}$. At 1 *g*: $F = ma \Rightarrow 2.749 \times 10^{-13} \text{ kg} \times 9.81 \text{ ms}^{-2} = 2 \text{ pN}$. At 44 *g* (consists of 43 *g* centrifuge program + 1 *g* Earth gravity) = 118 pN, and 88 *g* = 237 pN. These Newton values are similar to frequently used Pascal values in fluid shear force studies: if we take the cross-section of a cell (perpendicular to the surface) = $7.854 \times 10^{-11} \text{ m}$, then $2.697 \times 10^{-12} \text{ N} \div 7.854 \times 10^{-11} \text{ m} = 0.0343 \text{ Pascal (N}\cdot\text{m}^{-2})$. For 1.5 Pa follows: $1.5 \div 0.0343 \cong 44 \text{ g}$, for 3.0 Pa follows: $3.0 \div 0.0343 \cong 88 \text{ g}$.

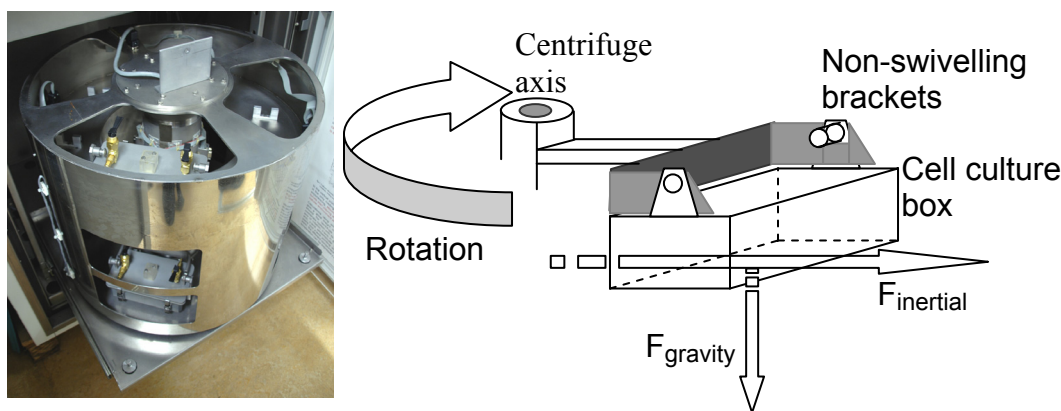


Figure 2. The Medium Size Centrifuge for Acceleration Research (MidiCAR) used to generate inertial shear force, in which the samples were subjected up to 1, 44 or 88 times Earth's gravity. The MidiCAR is equipped with a computerised temperature and motor control. The control samples are placed in the upper (non-spinning) compartment of the centrifuge, while the experimental samples are placed in brackets in the lower section. The brackets have wedges installed, preventing them from tilting. Graphical presentation of a secured rotating culture box, showing the direction in which inertial shear force acts on the cells.

Similar values are used in fluid shear studies with endothelial cells [33] or for bone cells [34]. Since it has been suggested that the rate (determined by the frequency and amplitude) rather than the magnitude of the applied loading stimulus alone is more important in evoking cellular responses, an intermittent setting was applied [34]. The force was sinusoidal with a period of 12 seconds for 44 *g* and 18 seconds for 88 *g*. Immediately after the end of each experiment run, the samples were retrieved from the centrifuge and the cells were washed three times with Phosphate Buffered Saline (PBS) and prepared for further analysis.

Scanning electron microscopy (SEM):

To assess overall morphology of the fibroblasts, SEM was performed. Cells were rinsed, fixed for 5 minutes in 2% glutaraldehyde, followed by 5 minutes in 0.1 M sodium-cacodylate buffer (pH 7.4), dehydrated in a graded series of ethanol, and dried in tetramethylsilane to air. Specimens were sputter-coated with gold and examined with a JEOL 6330 Field Emission SEM (Tokyo, Japan).

Immunofluorescence

Components of the cytoskeleton were made visible using fluorescent staining techniques. RDF cells, cultured on microgrooved substrata were rinsed in PBS, pH 7.2, fixed for 30 minutes in 3% paraformaldehyde/0.02% glutaraldehyde, and permeabilised with 1% Triton X100 for 5 min.

Filamentous actin was stained with Alexa Fluor 568 phalloidin (Molecular Probes, A-12380, Leiden, The Netherlands) diluted in 1% Bovine Serum Albumin/0.1% Tween-20 in PBS to block non-specific epitopes. Vinculin was stained with rabbit polyclonal primary antibodies to talin (Santa Cruz Biotechnology Inc., Santa Cruz, CA, USA), followed by labelling with goat anti-rabbit secondary antibodies IgG with Alexa Fluor 488 (Molecular Probes, A-11034) diluted in 1% BSA in PBS (1:400). Finally, the specimens were examined with a Biorad (Hercules, CA, USA) MRC 1024 confocal laser scanning microscope (CLSM) system with a krypton-argon laser at magnification of 40x. The digital immunofluorescence images acquired with the CLSM were loaded into Image J (version 1.5.0, Wayne Rasband, NIH, USA) to create overlay images. Cytoskeletal components were examined for their overall morphology as well as their orientation with respect to the groove direction. For quantitative image analysis samples were stained with Phalloidin-TRITC (Sigma, P-1951, St. Louis, MO, USA), followed by examination with a Leica/Leitz DM RBE Microscope (Wetzlar, Germany) at magnification of 10x.

Image Analysis

The Phalloidin-TRITC fluorescence micrographs were analyzed with Scion Image software (Beta Version 4.0.2, Scion Corp., Frederick, MD, USA). The orientation of fibroblasts was examined and photographed. For each sample six fields of view were selected randomly. The criteria for cell selection were (1) the cell is not in contact with other cells and (2) the cell is not in contact with the image perimeter. The maximum cell diameter was measured as the longest straight line between two edges within the cell borders. The angle between this axis and the grooves (or an arbitrarily selected line for smooth surfaces) was termed the orientation angle. If the average angle was 45 degrees, cells were supposed to lie in an at random orientation. Cell extensions like filopodia, which could confound the alignment measurement, were not included when assessing the cell orientation. Using Clarks criteria [35; 36], cells oriented at 0–10 degrees from the groove direction were regarded to be aligned. The distribution of cytoskeletal patterns with time, shear force in view of the type of microgrooves and groove direction was described by the percentage of cells in the sample that displayed each pattern. Between 500 - 800 cells were measured per group. Closely linked to cell orientation: cellular surface area and cell shape ratio were also measured with the aforementioned image analysis software to obtain information on cell spreading and elongation. Applying the same criteria for cell selection; cell areas were determined and displayed as μm^2 . Cell shape ratio were calculated as the ratio of the major to the minor dimension of a cell, by dividing the lengths of the major axis by the minor axis of the best fitting ellipse. A value of 1 corresponds to a perfect circle, while higher values correspond to more elongated cells. Between 250 - 500 cells were measured per group for orientation, area, and shape.

Quantitative-PCR

Total RNA was isolated from fibroblasts with an RNA isolation and stabilisation kit (QIAGEN, Hilden, Germany) and cDNA was synthesised with reverse transcription from 2 ng aliquots of total RNA with an RT-PCR kit (Invitrogen, Carlsbad, CA, USA).

After RNA isolation, stabilisation, and cDNA amplification; 12.5 μl of iQ SYBR Green SuperMix (Bio-Rad, Hercules, CA, USA) is added to each well of an optical 96 wells plate, 1.5 μl of both forward and reverse primer is added, as well as, 4.5 μl DEPC and 5 μl of 10 times diluted cDNA sample. The wells plate is covered and centrifuged shortly to remove air bubbles, following PCR quantification using cycling parameters: 95 °C x3 min; 95 °C x15 seconds → 60 °C x30 seconds followed by 72 °C x30 seconds for 40 cycles. All samples were assayed in triplicate. The comparative Ct-values method was used to calculate the relative quantity of $\alpha 1$ -, $\beta 1$ -, and $\beta 3$ -integrin, and Collagen Type I and glyceraldehyde-3-phosphate dehydrogenase (GAPDH).

Expression of the housekeeping gene (GAPDH) was used as an internal control to normalise results [37].

SDS-PAGE and Western Blot analysis

For preparing total protein extracts; cells were washed 3 times with ice cold PBS. Cells were harvested by scraping followed by disruption with 500 μ l ice-cold lysis buffer (50 mM Tris (pH 7.4), 250 mM NaCl, 5 mM EDTA, 50 mM NaF, 1mM Na₃VO₄, 1% Nonidet P40 (BioSource, Camarillo, CA, USA) supplemented with 1 mM Phenylmethanesulfonyl fluoride (PMSF, P7626, Sigma-Aldrich, Steinheim, Germany) and Protease Inhibitor Cocktail (P2714, Sigma-Aldrich). Samples were cleared of cellular debris and concentrated by centrifugation for 65 minutes, 4°C at 12,000 rpm (Amicon Microcon YM-10 centrifugal filter tube, Millipore, Billerica, MA, USA). The protein concentrations in the retentate were determined, and equal amounts of protein were dissolved in 10 μ l of 2x reducing sample buffer (4% SDS, 100mM Tris (pH 6.0), 10% β -mercaptoethanol, 20% Glycerol) and heated at 95°C for 5 minutes and electrophoresed on 12.5% SDS-Acrylamide minislab gels and transferred to (polyvinylidene difluoride) PVDF membranes (Immobilon-P, Millipore). After protein transfer, the membranes were blocked in 4% skim milk in TBST (0.05% Tween 20 in TBS) overnight at room temperature. Immunological blots were then performed at room temperature for 1 hour in 2% skim milk in TBST buffer containing specific primary antibodies.

Antibodies for Western Blot analysis

Western blots were probed with the following antibodies: Anti-ERK 1/2 (C-16; sc-93), JNK1 (C-17; sc-474), p38 MAPK (C-20; sc-535), α PAK (H-300; sc-11394), RhoA (119; sc-179), Rac1 (T-17; sc-6084), Cdc42 (P1; sc-87). Anti-active p-ERK 1/2 (E-4; sc-7383), p-JNK (G-7; sc-6254), p-p38 (D-8; sc-7973). All antibodies were obtained from Santa Cruz Biotechnology .

After membranes were washed with TBST, they were incubated with appropriate secondary antibody IgG with alkaline phosphatase conjugate and immuno-reactive bands were visualized using Nitroblue Tetrazolium (NBT) and 5-bromo-4-chloro-3-indolyl phosphate (BCIP) chemiluminescence reagents (Bio-Rad Laboratories Hercules, CA, USA).

Statistical analysis:

Acquired data from the fluorescence micrographs on cell alignment and QPCR data were analysed using SPSS for Windows (Release 12.0.1, SPSS Inc., Chicago, USA). The effects of and the interaction between both time and/or force and surface were analysed using analysis of variance (ANOVA), including a modified least significant difference (Tukey) multiple range test to detect significant differences between two distinct groups. Probability (p) values of ≤ 0.05 were considered significant.

RESULTS

Scanning electron microscopy

The micro topography pattern of grooves and ridges was accurately reproduced in the polystyrene substrata, down to the nano roughness along the edges of the ridges (data not shown). When examining cell morphology, RDFs cultured on smooth substrata showed a recognisable cell spreading associated with the early stages of cell adherence: from round cells with abundant amounts of filopodia to flat outstretched cells with large cell surface areas. The spreading pattern itself is considered random, since common cellular orientation could not be distinguished (**Figure 3A-C**). RDFs seeded onto grooved substrata already demonstrated orientation along the grooves from an early time point onward although their cell bodies were still rather wide. Since the

groove/ridge pitch is too small for the cells to descend to the bottom of the grooves they were always found on top of the ridges. Cellular extensions probing the substratum surface only find the top ridge, resulting in extension of the cellular body along these small ridges. In later stages the fibroblasts had stretched out themselves into elongated cells with narrow cell width and are highly aligned (**Figure 3D-F**).

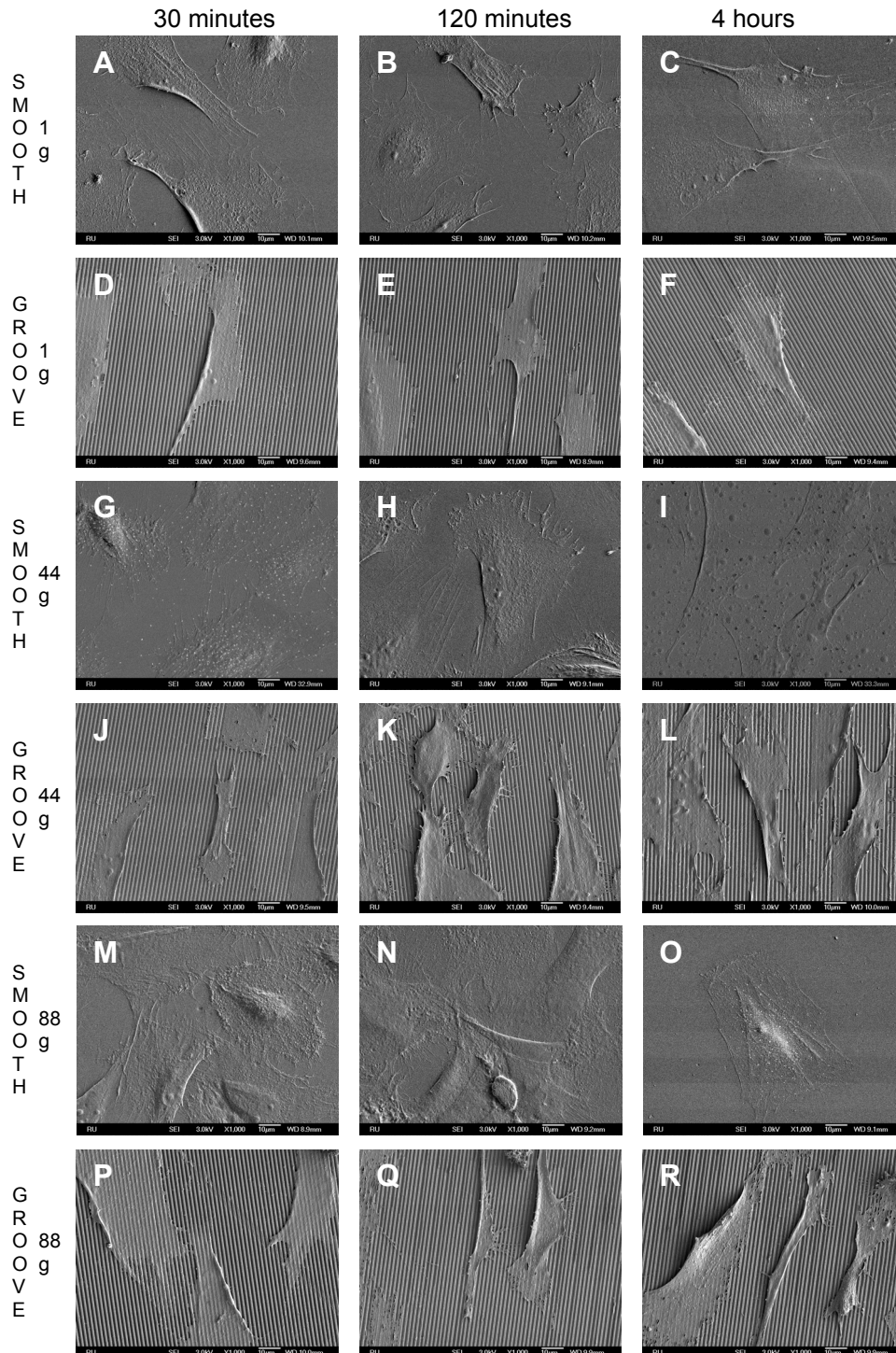


Figure 3. SEM micrographs of RDFs cultured under various conditions. Columns represent time; from left to right: 0.5, 2 and 4 hours. Rows represent a combination of topography and amount of shear force applied. First two rows: 1 g, Smooth and Grooved. Next two rows: 44 g, last two rows: 88 g (magnification x1000).

When subjected to inertial shear force, RDFs cultured on smooth topography remained morphologically quite similar compared to controls (**Figure 3G, H, M, & N**): round cells with numerous filopodia at the early stages. After 4 hours fibroblasts appeared as long, flat, shaped cells (**Figure 3I, O**). RDFs seeded onto grooved surface exposed to 44 g intermittent shear appeared

dissimilar in their cell morphology when compared to their 1 *g* counterparts (**Figure 3J-L**). Fibroblast after 2 and 4 hours of experiencing shear stress had heightened cell bodies and displayed membrane ruffles. Cellular morphology under 44 *g* resulted in cells appearing less orientated along the grooves on the whole, displaying membrane ruffles, and many filopodia stretching in all directions. Also cell surface area seems larger, due to wider cell bodies. When subjected to 88 *g* (**Figure 3P-R**), fibroblasts at first display wide cell bodies, but gradually became more narrow and more aligned compared to their control group.

Fluorescence microscopy

The cytoskeleton was investigated by staining filamentous actin and talin anchor points of the cell focal adhesions. **Figure 4A-C** shows 1 *g* smooth substratum samples for 3 time points; the observed cell shape, spreading, and random orientation were comparable to SEM micrographs. F-actin filaments (red staining) were running in the direction of not only the long axis of cells, but also around the cell membrane, and crossing over the cell nucleus. Talin (green) for focal adhesions resulted in a staining around the nucleus, and talin spots were visible in some samples, positioned at the end of actin bundles, and always extended in the direction of the actin bundle. RDFs cultured on grooved surfaces displayed a comparable morphology with SEM, however, there seems to be a more pronounced orientation of the cells and their cytoskeleton in time (**Figure 4D-F**). Cells are most stretched out and slender after 2 hours of culturing. Before that, cells are rounder and after 4 hours still aligned, yet their cell bodies were wider.

In **Figure 4G, H, & I**, RDFs can be observed cultured on a smooth surfaces and subjected to 44 *g* intermittent inertial shear force. It was striking that the actin filaments appeared thicker and more numerous. In addition, cells were not as round as one would expect during these early time points. After 4 hours, they displayed abundant actin filaments, not only in the direction of the long axis, but also perpendicular to the axis. Fibroblasts on grooved substrates experiencing 44 *g* inertial shear force displayed a shape and alignment pattern as observed within the control group (**Figure 4J-L**).

In contrast to the 44 *g* inertial shear force, 88 *g* resulted in cells, cultured on smooth substrates, remaining their round shape for a longer period (**Figure 4M, N**). After 4 hours of intermittent shear force, cells display a disturbed cytoskeleton; actin filaments were thin, albeit abundant, and talin anchor points are reduced in number and seemed to concentrate around the cell nucleus (**Figure 4O**). Copious amounts of actin filaments were seen in RDFs seeded onto grooved substrata experiencing 88 *g*. They seemed to be able to stay aligned, although after 4 hours the orientation along the grooves seemed to decrease, comparable to the other experiment and control group. The focal anchor points as visualised by the talin immuno-staining were predominantly centered around the cell core (**Figure 4P-R**).

Image analysis

The actin filaments stained with Phalloidin-TRITC were plainly visible and fibroblast cellular orientation corroborated with the SEM: RDFs cultured on grooved substrata displayed alignment along the ridges, while smooth surfaces did not bring about any form of alignment. The quantified results for cell orientation are presented as mean angle and standard error of the mean in **Figure 5**. Averaging around 45 degrees, smooth substrata did not induce any cellular orientation compared to their grooved equivalents, which, all groups combined, averaged around 12 degrees. Within the smooth groups no significant change in mean angle occurred, however, differences were observed among the various grooved substrate groups. Most striking was the significant decrease in mean angle (thus an increase in alignment) after 2 hours and the increase in mean angle at 4 hours. This reoccurring pattern took place in all groups.

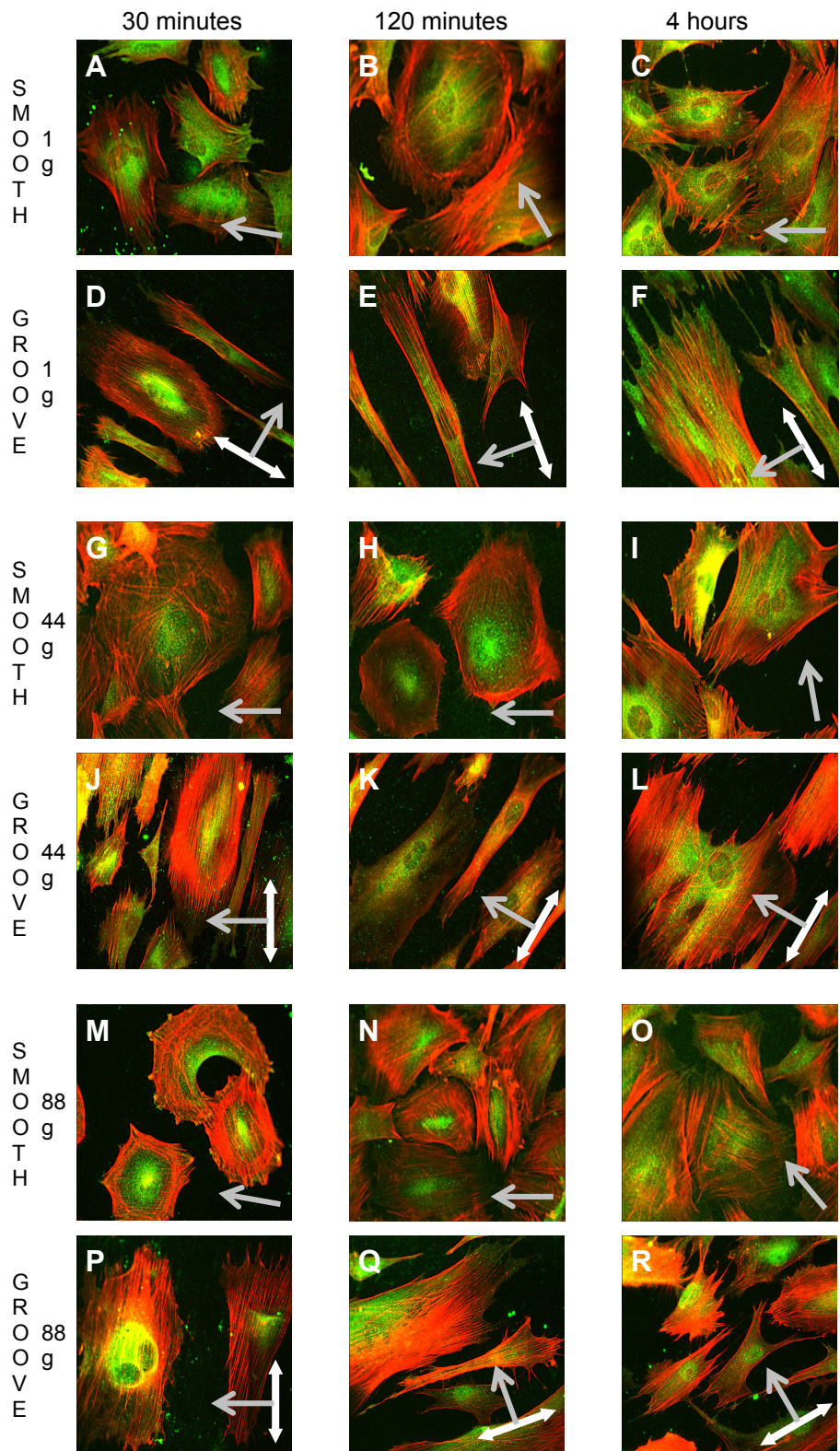


Figure 4. CLSM micrographs of RDFs cultured under several conditions. Columns represent time; from left to right: 30, 120 minutes and 4 hours. Rows represent a combination of topography and amount of shear force applied. First two rows: 1 g, Smooth and Grooved. Next two rows: 44 g, last two rows: 88 g. Double ended white arrow denotes groove direction, single grey arrow denotes shear direction. Colour figure on page 166.

Analysis of variance multiple comparison test (ANOVA) analysis of the main parameters: topography, inertial shear force, and time all proved significant. Regarding topography; combining all groups: 65% of the cells were aligned along the grooved substrata compared to 13% on smooth substrata. Inertial shear force significantly influences cellular orientation along grooved surfaces: 44 g resulted in a higher mean angle and a reduced total number of cells matching the alignment criteria (average: 16 degrees for 53% of the cells) compared to the control and 88 g groups,

respectively 10° - 70%, and 13° - 68%. Finally, the effects of time on fibroblast orientation was significant in all 2 hours sample groups showing a higher percentage of cells aligned and a subsequent lower mean angle independently of the inertial shear force applied. On the whole, within the grooved 2 hours group; 75% of the cells aligned to around 9°, compared to 16°- 56% (30 min group) and 14° - 59% (4 hours experiment group).

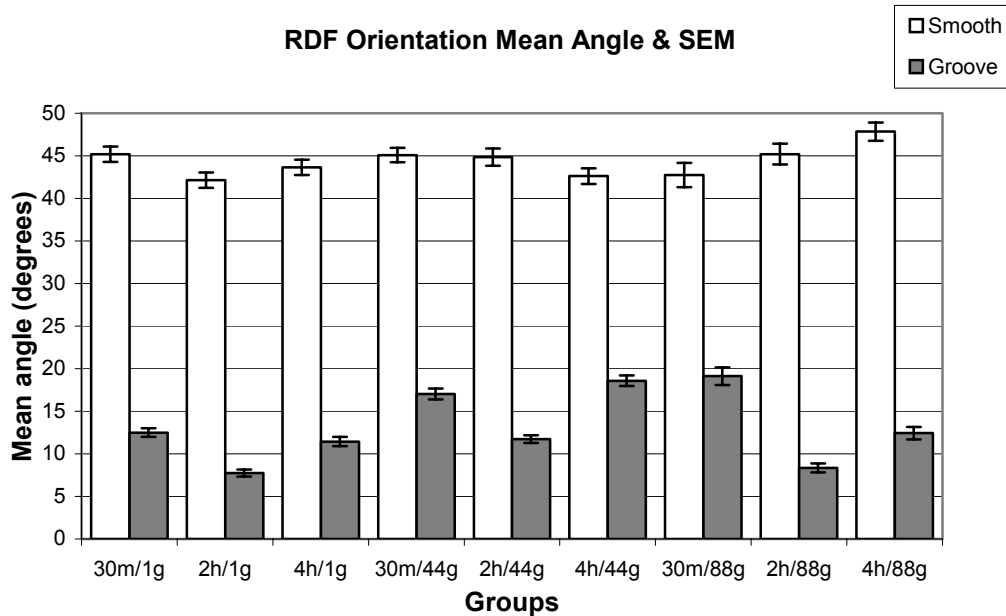


Figure 5. Bar graphs showing the distribution of cellular orientation of fibroblasts under various circumstances of inertial shear. Smooth substrata results in random spread of cells, as indicated by a mean angle around 45 degrees for all experiment groups. Grooved surfaces elicit cellular alignment. The lowest mean angle is reached after 2 hours of culturing, after which a slight increase happens. For each sample at least 500 individual cells were analysed. 30m, 2h and 4h stands for the experiment time, and 1, 44, and 88 g stands for the applied inertial shear force.

Cell surface area measurements revealed an interesting cellular response of fibroblasts towards shear stress (Figure 6). On smooth substrates non loaded cells appeared round (30 minutes) and gradually became more spindle shaped (4 hours), their overall cell area averaged around 2900 μm^2 . However, from 4 hours at 44 g onward, cell surface area jumps to 5307 μm^2 and remains at this level throughout 88 g groups. While smooth 4 hr/44 g still had spindle shaped cells, their cell bodies are wider with more protrusions compared to their 4 hr/1 g counterparts. Fibroblasts exposed to 88 g had a round shape and never attained a spindle shape. Cells cultured on a grooved substrate had an overall cell surface area between 1600-2100 μm^2 (1 and 44 g groups only). Cells cultured for 4 hours were in the high end of this range. A significant increase in cell area was measured in the 88 g groups: cells exposed to 88 g for 30 minutes had areas of 2704 μm^2 . After 4 hours at 88 g this had increased to 3575 μm^2 .

Finally, cell shape ratios were calculated to investigate fibroblast elongation (Figure 7). Under normal gravity circumstances fibroblast cultured on grooved surface had higher ratios compared to cells cultured on smooth surfaces. Thus, their cell bodies were more elongated/ellipse shaped. During both 44 and 88 g within the smooth groups there is a small, yet significant rise in shape ratio when comparing 30 minutes and 4 hours. Within the grooved group a significant peak is measured at 2 hours, followed by a decrease at 4 hours. The higher absolute ratios after 2 and 4 hours within the 88 g group compared to their 44 g counterparts proved to be no more than a trend.

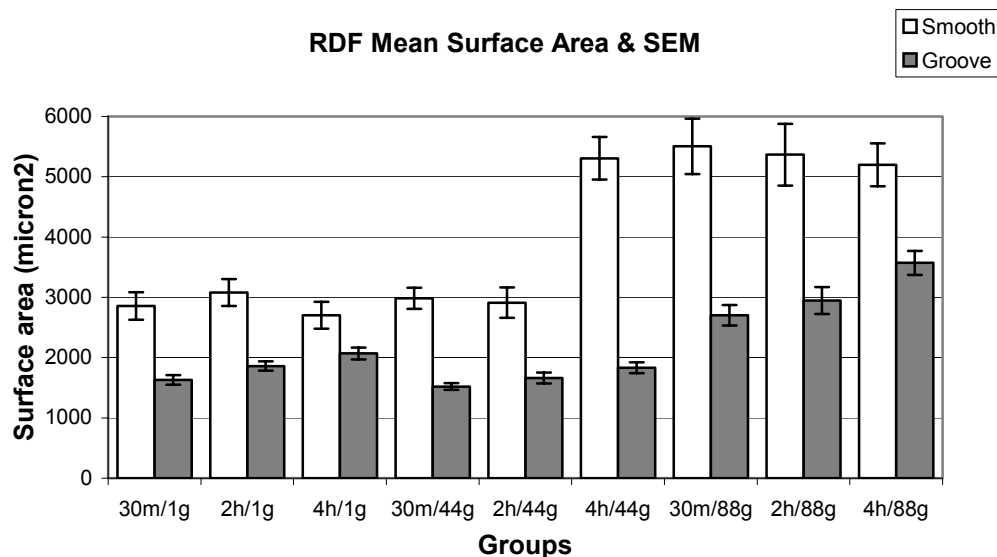


Figure 6. Bar graphs showing the mean and standard error of the mean for cell surface area of fibroblasts subjected to various conditions. S = smooth, G = grooved, 30m, 2h, and 4h stands for the experiment time, and 1, 44, and 88 g stands for the applied inertial shear force. For each sample at least 250 individual cells were analysed.

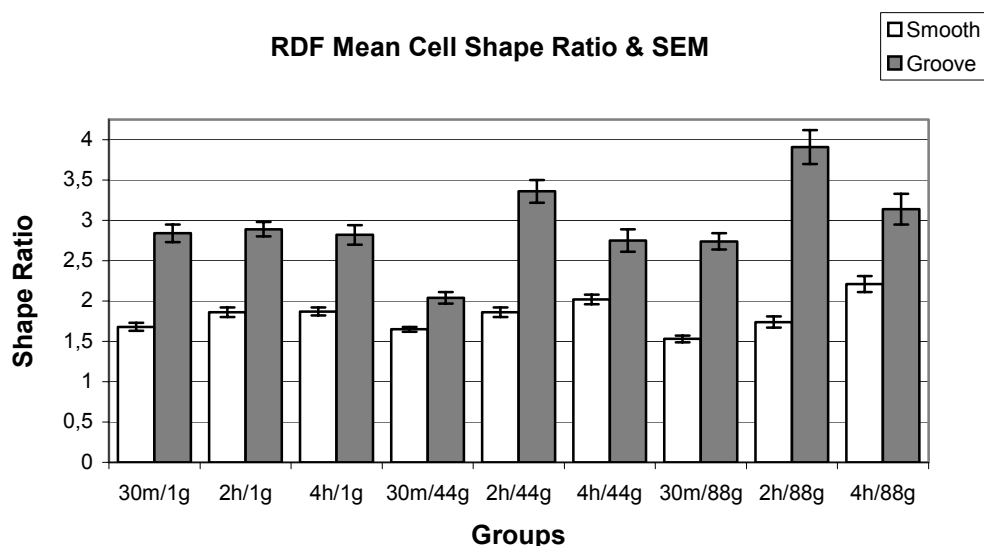


Figure 7. Bar graphs showing the mean and standard error of the mean for cell shape ratio of fibroblasts subjected to various conditions. S = smooth, G = grooved, 30m, 2h, and 4h stands for the experiment time, and 1, 44, and 88 g stands for the applied inertial shear force. For each sample at least 250 individual cells were analysed.

Quantitative-PCR

Real-time PCR analysis was conducted to quantify mRNA expression of $\alpha 1$, $\beta 1$ - and $\beta 3$ -integrins, and collagen type I. **Table 1** shows the amounts of the various transcripts relative to GAPDH, and data were normalised to the expression of the genes of interest in the respective control (1 g) groups (so called $2^{-\Delta\Delta CT}$ method).

Expression of these proteins, which are involved in the cellular interface with the environment, were influenced by both time and inertial shear force independently, even though both parameters interacted with each other. The latter remark was clearly visible in the 4 hours groups.

On the whole, fibroblast cultured on smooth surfaces which received 88 *g* of shear force responded much stronger than those cells cultured on grooved surfaces undergoing the same force. Alpha-1, beta-1, and beta-3 integrin expression was severely reduced in all but the 4 hours experiment groups. In those groups a significant up-regulation was shown, particularly by fibroblast cultured in smooth substrata en being subjected to 88 *g* of shear force. Of the three integrins, beta-1 integrin responded most intensely to both time and inertial shear, the relative mRNA levels were highest after 4 hours. Collagen type I revealed an up-regulation after 30 minutes and at 4 hours, while after 2 hours a significant down-regulation was seen. The sole exception being the 88 *g* groove group which showed an increase at 2 hours, but none at 4 hours.

Groups	alpha-1	beta-1	beta-3	collagen I
S 30m 44g	0.5 (0,4-0,6)	0.6 (0,5-0,9)	0.6 (0,4-0,7)	3.6 (2,4-5,5)
S 2h 44g	0.2 (0,2-0,4)	0.5 (0,3-0,9)	0.2 (0,1-0,4)	0.6 (0,4-0,9)
S 4h 44g	5.0 (2,2-11,2)	3.2 (1,7-6,1)	4.2 (2,1-8,3)	0.2 (0,1-0,4)
S 30m 88g	0.5 (0,3-0,7)	1.0 (0,6-1,6)	0.5 (0,3-0,8)	1.5 (1,1-2,0)
S 2h 88g	0.7 (0,4-1,1)	0.8 (0,5-1,5)	0.5 (0,3-0,9)	0.3 (0,2-0,5)
S 4h 88g	12.4 (5,4-28,5)	5.6 (2,9-11,1)	11.7 (5,5-24,8)	0.4 (0,2-0,9)
G 30m 1g	0,1 (0,0-0,9)	0,9 (0,2-3,1)	0,3 (0,1-1,2)	1,7 (0,6-4,5)
G 2h 1g	0,1 (0,0-0,5)	0,2 (0,1-0,9)	0,2 (0,1-0,7)	0,5 (0,2-1,0)
G 4h 1g	1,6 (0,2-10,3)	6,2 (1,5-25,8)	3,5 (0,7-17,9)	0,9 (0,4-2,3)
G 30m 44g	0,5 (0,2-1,1)	0,9 (0,4-2,2)	0,6 (0,2-1,8)	2,2 (1,1-4,2)
G 2h 44g	0,2 (0,1-0,4)	0,4 (0,2-0,6)	0,2 (0,1-0,3)	0,4 (0,2-0,6)
G 4h 44g	5,7 (2,5-13,0)	5,5 (3,2-9,2)	3,0 (1,4-6,5)	0,4 (0,2-0,9)
G 30m 88g	0,5 (0,5-0,7)	0,8 (0,7-0,9)	0,3 (0,3-0,3)	2,1 (1,4-3,2)
G 2h 88g	0,1 (0,0-0,3)	0,2 (0,1-0,4)	0,3 (0,2-0,5)	4,0 (2,4-6,6)
G 4h 88g	6,6 (4,5-9,6)	8,1 (5,4-12,1)	6,5 (4,5-9,6)	0,1 (0,1-0,2)

Table 1. *Effects of surface, time, and shear force on the relative gene expression of alpha-1, beta-1, beta-3-integrins, and collagen type I was analysed by quantitative PCR. Data are expressed as 2^{ΔΔCT} and range, n = 4. Values were relative to internal control gene GAPDH and normalised to Smooth 1g. Significantly different samples (p < 0.05) are in bold face.*

Immunoblot analysis

Western blot analysis showed that within the Mitogen Activated Protein Kinase (MAPK) pathways, all three major signalling pathways were present: ERK-1/2, JNK/SAPK-1/2, and p38^{MAPK}. The presence of both total and active protein could be detected (**Figure 8 A-C**). ERK-1/2 protein appeared in all groups, especially ERK-1 was clearly up-regulated at 30 and 120 minutes within the grooved groups. Phosphorylated (active) Erk-1/2 is most present in the early stages, and seemed to be particularly increased at the control groups and the 88 *g* groups, be it grooved or smooth. JNK-1/2 and p38^{MAPK} presence was evenly distributed within the groups. Their active components appeared most strongly in those groups which are subjected to 44 *g* inertial shear. Although p-JNK and p-p38 emerge throughout the different time points, they most often displayed more obvious bands at earlier (30 and 120 minutes) measurements.

In addition to the three pathways, several proteins which play essential roles in cellular attachment to and movement across substrates were investigated. RhoA, an upstream element of the ERK pathway, was found to be present under inertial shear conditions independently from surface topography (**Figure 9A**). Together with its downstream effector ROCK1/2, RhoA induces actin stress fibres and focal-adhesion complexes, to which the ends of the stress fibres attach. Upstream of the JNK/SAPK pathway and intimately linked to RhoA, are Cdc42 and Rac1. These two proteins stimulate the formation of Cdc42 induced filopodia with Rac1 induced membrane ruffles leading to cell movement. Cdc42 was found in both topographical groups, and appears to be continuously up-regulated within the fibroblast. The Rac1 fusion protein too was present in the various experiment groups. Larger bands of this protein were visible in the static control groups and the early time points (30 minutes) of the experiment groups (**Figure 9B, C**).

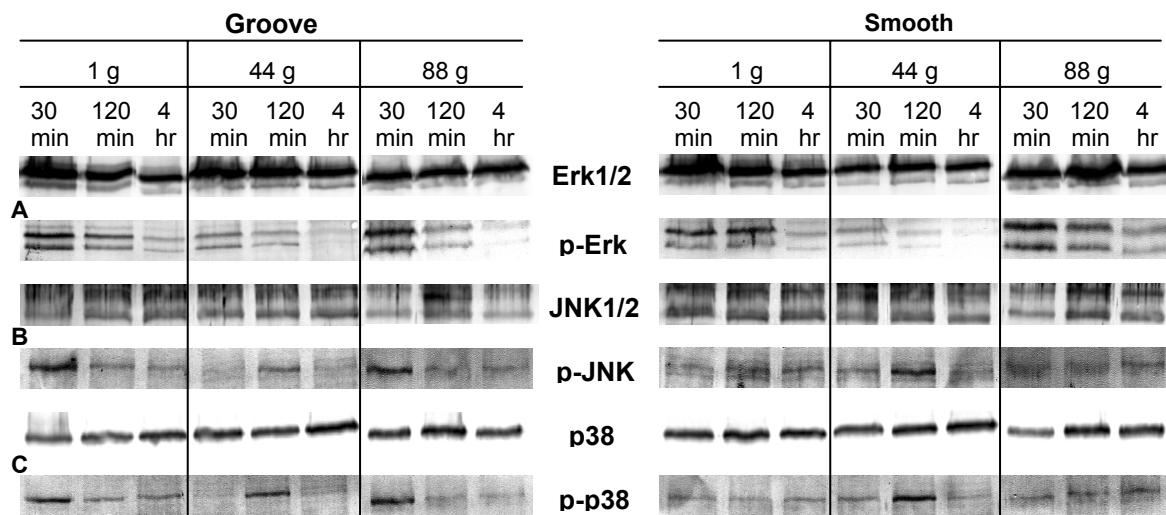


Figure 8. Western blots analysis of MAPK signalling pathways from whole cell lysates prepared from primary fibroblasts. Equal amount of protein were probed with antibodies specific to total ERK1/2 (A, top row) and phospho-ERK1/2 (A, bottom row) followed by immuno-staining with IgA Alkaline Phosphate conjugate. The whole cell extracts as described in panel A were analyzed by Western blotting. Samples were probed with antibodies specific for total JNK1/2 (B, top row) and phospho-JNK1/2 (B, bottom row), total p38 (C, top row) and phospho-p38 (C, bottom row).

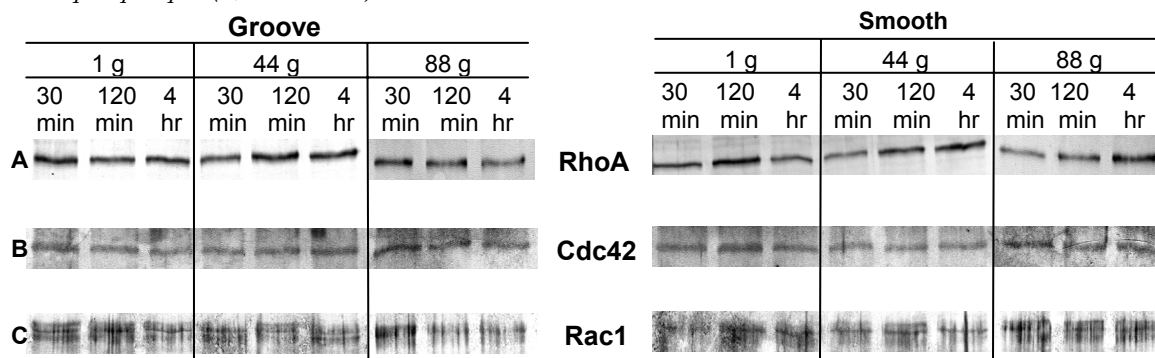


Figure 9. Western blots analysis of small GTPases family members from whole cell extracts prepared from primary fibroblasts. Equal amount of protein were probed with antibodies specific to total RhoA (A), Cdc42 (B), Rac1 fusion protein (C), followed by immuno-staining with IgA Alkaline Phosphate conjugate. The whole cell extracts were analyzed by Western blotting.

Discussion

In this *in vitro* study we shed, for the first time, some light on the magnitude of inertial shear forces on fibroblast cells cultured on both smooth and microgrooved polystyrene substrata placed inside a centrifuge setting. The underlying aim was to understand to what extent shear forces can alter cell behaviour and if inertial shear could be utilized as a model to explain possible phenomena as found in experiments which use centrifuges to investigate mechanotransduction in mammalian cells, particularly to study the signalling mechanisms and stress responses. The mechanotransduction of these static and dynamic forces transferred onto the cells were investigated: morphological cell responses like shape and orientation and related to that the cytoskeleton of the cells; the expression of several proteins involved in cell-surface interaction by means of Q-PCR were also investigated. Finally, proteins of the MAPK intracellular signalling kinase pathways were visualised. From our data we concluded that fibroblast adjust their shape according to micro-topographical features. Even so, inertial shear force plays a significant role in the response by RDFs to external loads. Although cells, in relation to their morphology, have a tendency to rely more on the static stresses encountered from the substratum, cellular behaviour

on a molecular level (i.e. mRNA transcripts and intracellular signalling pathways), as well as, whole cell colony performance are markedly influenced by inertial shear force.

Adherent cells will experience a large inertial shear acceleration and will lead to cell deformation (strain). In our study this strain on individual cells is visible as cells appearing less aligned along the microgrooves. The cell surface in general has increased, signalling the probability of fibroblasts forming stable attachments in order to withstand the inertial shear force better. Combined with the polymerization of abundant thicker actin filament bundles in the long axis of the fibroblast, but also in the short axis points to fibroblast able to sense inertial shear and respond to it in such a way as to minimize the stress on their cytoskeleton. In initial observation we noted a displacement of large numbers of cells towards the outer limits of the culture dish might indicate that even minimum low levels of shear force can relocate the bulk of the cell colony.

Inertial shear stress as a cell body force model to study mechanical and biological responses of cells is useful in understanding activation of the various pathways after mechanical stimulus. Explicitly, the model can identify the region within which forces or deformations are of sufficient magnitude to potentially elicit a biological response. Currently, much is known about the signalling pathways that are initiated when cells are subjected to a mechanical stress. However the process of mechanotransduction by which the mechanical disturbance is transformed into a biochemical signal is poorly understood.

The inertial shear force paradigm could possibly aid in linking mechanotransduction phenomena to mechanically-induced alterations in the molecular conformation of proteins [38]. These changes in conformation can lead to altered binding affinities of proteins, and ultimately initiating an intracellular signalling cascade or lead to changes in the proteins localized to regions of high stress. This hypothesis represents an alternative to transmembrane signalling via receptor-ligand interactions providing the cell with a means of reacting to changes in its mechanical, as opposed to biochemical, environment. By applying inertial shear as means to study conformational changes in the load-bearing regions of focal adhesion complexes for instance or the cytoskeleton, a more general quantitative description of mechanotransduction pathways should be possible [17; 39-43]. Fibroblasts are clearly affected by inertial shear force; their morphology under normal and shear conditions are markedly different. Cells subjected to shear display many filopodia, membrane ruffles, and thinner actin filaments, this corresponds with the up-regulation of beta-1 integrin, and the down-regulation of beta-3. Integrin recycling regulates cell migration, and especially beta-3 recycling influences the cell's decision to migrate with persistence or to move randomly [44] [45]. The displacement/migration of a substantial part of the cell colony to the outer rim of the culture dish away from the inertial shear force, and the continuous presence of both Cdc42 and Rac1 fusion protein are signs that cell body forces assert their stress onto the cellular structures [39]. JNK/SAPK and p38^{MAPK}, proteins which are activated downstream of the Rac1/Cdc42, are present within the shear experiment groups, combined with the reduction in Erk1/2. Thus, it appears cells are under significant stress and are sensitized to apoptosis via the up-regulation of p38 and the reduced regulation of survival pathways [46; 47]. Nonetheless, Erk1/2 is still largely present and so is RhoA. Fibroblasts obviously are trying to manage the situation created by inertial shear force. With Erk1/2, a survival pathway, up-regulated, and the strong presence of RhoA, which mediates the formation and maturation of focal adhesion complexes on the basal surface of the cell, fibroblasts sense the stress and are active in achieving a state of mechanical equilibrium (balance of forces). The cytoskeleton near the cortical surface does not necessarily sense the same stress. This hypothesis is supported by related studies that show release of prostaglandins in response to fluid shear stress being mediated by focal adhesion, and proteoglycans in the glycocalyx (associated plasma proteins of glycosaminoglycans) that have a transmembrane domain that can interact with the apical cytoskeleton [43; 48]. Key issue in adherent cellular survival is

the presence of extracellular matrix components and a means to interact. From previous research we have learned that fibronectin and collagen type I are unaffected by hypergravity [45]. Although integrins are down-regulated in the short run, up-regulation at 4 hours onwards safeguards the cells survival in the long run. Prolonged culturing (24 - 48 hours) will most likely lead to an augmentation of mechanical equilibrium between the cell and its environment.

CONCLUSIONS

In conclusion, we might state that topography emerges as the more dominant parameter for cellular response. However, adaptations of the cytoskeleton, the presence of intracellular proteins, and overall cell morphology point towards a competition between static and dynamic forces and results in an active cell response. A combination of inertial shear force and a nano-scale grooved pattern with longer culture times will elucidate to what extend each parameter can assert its influence on cell behaviour. This novel concept of inertial shear force is an appropriate and straightforward model to apply body forces onto cells.

REFERENCES

1. Zhang, W., Liu, Y., and Kassab, G. S. Flow-induced shear strain in intima of porcine coronary arteries. *J Appl Physiol* 2007, 2007.
2. Park, S. W., Byun, D., Bae, Y. M., Choi, B. H., Park, S. H., Kim, B., and Cho, S. I. Effects of fluid flow on voltage-dependent calcium channels in rat vascular myocytes: Fluid flow as a shear stress and a source of artifacts during patch-clamp studies. *Biochem Biophys Res Commun* 2007, 1021-7, 2007.
3. Meng, H., Wang, Z., Hoi, Y., Gao, L., Metaxa, E., Swartz, D. D., and Kolega, J. Complex hemodynamics at the apex of an arterial bifurcation induces vascular remodeling resembling cerebral aneurysm initiation. *Stroke* 2007, 1924-31, 2007.
4. Schneider, S. W., Nuschele, S., Wixforth, A., Gorzelanny, C., Alexander-Katz, A., Netz, R. R., and Schneider, M. F. Shear-induced unfolding triggers adhesion of von Willebrand factor fibers. *Proc Natl Acad Sci U S A* 2007, 7899-903, 2007.
5. Zernicke, R., MacKay, C., and Lorincz, C. Mechanisms of bone remodeling during weight-bearing exercise. *Appl Physiol Nutr Metab* 2006, 655-60, 2006.
6. McGarry, J. G., Klein-Nulend, J., and Prendergast, P. J. The effect of cytoskeletal disruption on pulsatile fluid flow-induced nitric oxide and prostaglandin E2 release in osteocytes and osteoblasts. *Biochem Biophys Res Commun* 2005, 341-8, 2005.
7. Klein-Nulend, J., Bacabac, R. G., and Mullender, M. G. Mechanobiology of bone tissue. *Pathol Biol (Paris)* 2005, 576-80, 2005.
8. Brown, T. D. Techniques for mechanical stimulation of cells in vitro: a review. *J Biomech* 2000, 3-14, 2000.
9. Nerem, R. M. Shear force and its effect on cell structure and function. *ASGSB Bull* 1991, 87-94, 1991.
10. Traub, O. and Berk, B. C. Laminar shear stress: mechanisms by which endothelial cells transduce an atheroprotective force. *Arterioscler Thromb Vasc Biol* 1998, 677-685, 1998.
11. Helmke, B. P. and Davies, P. F. The cytoskeleton under external fluid mechanical forces: hemodynamic forces acting on the endothelium. *Ann Biomed Eng* 2002, 284-296, 2002.
12. Helmke, B. P., Goldman, R. D., and Davies, P. F. Rapid displacement of vimentin intermediate filaments in living endothelial cells exposed to flow. *Circ Res* 2000, 745-752, 2000.
13. Shyy, J. Y. and Chien, S. Role of integrins in endothelial mechanosensing of shear stress. *Circ Res* 2002, 769-775,

- 2002.
14. Marschel, P. and Schmid-Schonbein, G. W. Control of fluid shear response in circulating leukocytes by integrins. *Ann Biomed Eng* 2002, 333-343, 2002.
 15. Traub, O., Ishida, T., Ishida, M., Tupper, J. C., and Berk, B. C. Shear stress-mediated extracellular signal-regulated kinase activation is regulated by sodium in endothelial cells. Potential role for a voltage-dependent sodium channel. *J Biol Chem* 1999, 274:20144-20150, 1999.
 16. van Loon, J. J., Folgering, E. H., Bouten, C. V., Veldhuijzen, J. P., and Smit, T. H. Inertial shear forces and the use of centrifuges in gravity research. What is the proper control? *J Biomech Eng* 2003, 342-346, 2003.
 17. Kaazempur-Mofrad, M. R., Abdul-Rahim, N. A., Karcher, H., Mack, P. J., Yap, B., and Kamm, R. D. Exploring the molecular basis for mechanosensation, signal transduction, and cytoskeletal remodeling. *Acta Biomater* 2005, 281-293, 2005.
 18. Lee, D. J., Rosenfeldt, H., and Grinnell, F. Activation of ERK and p38 MAP kinases in human fibroblasts during collagen matrix contraction. *Exp Cell Res* 2000, 260:190-7, 2000.
 19. Wang, J. G., Miyazu, M., Matsushita, E., Sokabe, M., and Naruse, K. Uniaxial cyclic stretch induces focal adhesion kinase (FAK) tyrosine phosphorylation followed by mitogen-activated protein kinase (MAPK) activation. *Biochem Biophys Res Commun* 2001, 275:356-61, 2001.
 20. Howe, A. K., Aplin, A. E., and Juliano, R. L. Anchorage-dependent ERK signaling--mechanisms and consequences. *Curr Opin Genet Dev* 2002, 12:30-5, 2002.
 21. Aplin, A. E. and Juliano, R. L. Integrin and cytoskeletal regulation of growth factor signaling to the MAP kinase pathway. *J Cell Sci* 1999, 112:695-706, 1999.
 22. Yuge, L., Hide, I., Kumagai, T., Kumei, Y., Takeda, S., Kanno, M., Sugiyama, M., and Kataoka, K. Cell differentiation and p38(MAPK) cascade are inhibited in human osteoblasts cultured in a three-dimensional clinostat. *In Vitro Cell Dev Biol Anim* 2003, 39:89-97, 2003.
 23. Nebreda, A. R. and Porras, A. p38 MAP kinases: beyond the stress response. *Trends Biochem Sci* 2000, 25:257-260, 2000.
 24. Tang, Y., Yu, J., and Field, J. Signals from the Ras, Rac, and Rho GTPases converge on the Pak protein kinase in Rat-1 fibroblasts. *Mol Cell Biol* 1999, 19:1881-1891, 1999.
 25. He, H., Pannequin, J., Tantiogco, J. P., Shulkes, A., and Baldwin, G. S. Glycine-extended gastrin stimulates cell proliferation and migration through a Rho- and ROCK-dependent pathway, not a Rac/Cdc42-dependent pathway. *Am J Physiol Gastrointest Liver Physiol* 2005, 289:G478-488, 2005.
 26. Lim, L., Manser, E., Leung, T., and Hall, C. Regulation of phosphorylation pathways by p21 GTPases. The p21 Ras-related Rho subfamily and its role in phosphorylation signalling pathways. *Eur J Biochem* 1996, 238:171-185, 1996.
 27. Manser, E. Small GTPases take the stage. *Dev Cell* 2002, 3:323-328, 2002.
 28. Walboomers, X. F., Croes, H. J., Ginsel, L. A., and Jansen, J. A. Growth behavior of fibroblasts on microgrooved polystyrene. *Biomaterials* 1998, 19:1861-1868, 1998.
 29. Chesmel, K. D. and Black, J. Cellular responses to chemical and morphologic aspects of biomaterial surfaces. I. A novel in vitro model system. *J Biomed Mater Res* 1995, 29:1089-1099, 1995.
 30. Freshney, R. I. Culture of animal cells: a multimedia guide. 99. Chichester, John Wiley & Sons Ltd.
 31. van Loon, J. J., van den Bergh, L. C., Veldhuijzen, J. P., and Huijser, R. Development of a centrifuge for

- acceleration research in cell and developmental biology. In academic thesis: Effect of spaceflight and hypergravity on mineral metabolism in organ cultures of fetal mouse long bones. Appendix C. 95. Amsterdam, Free University Amsterdam.
32. Walboomers, X. F., Ginsel, L. A., and Jansen, J. A. Early spreading events of fibroblasts on microgrooved substrates. *J Biomed Mater Res* 2000, 529-534, 2000.
 33. Patrick, C. W., Sampath, R., and McIntire, L. V. Fluid Shear Stress Effects on Cellular Function. 1626-1645. 95. CRC Press Inc. Biomedical Research Handbook: Tissue Engineering Section. B. Palsson and J.A. Hubbell.
 34. Bacabac, R. G., Smit, T. H., Mullender, M. G., Van Loon, J. J., and Klein-Nulend, J. Initial stress-kick is required for fluid shear stress-induced rate dependent activation of bone cells. *Ann Biomed Eng* 2005, 104-110, 2005.
 35. Clark, P., Connolly, P., Curtis, A. S., Dow, J. A., and Wilkinson, C. D. Topographical control of cell behaviour: II. Multiple grooved substrata. *Development* 1990, 635-644, 1990.
 36. Clark, P., Connolly, P., Curtis, A. S., Dow, J. A., and Wilkinson, C. D. Topographical control of cell behaviour. I. Simple step cues. *Development* 1987, 439-448, 1987.
 37. Livak, K. J. and Schmittgen, T. D. Analysis of relative gene expression data using real-time quantitative PCR and the $2^{-\Delta\Delta C(T)}$ Method. *Methods* 2001, 402-8, 2001.
 38. van Loon, J. J. W. A. Micro-gravity and mechanomics. *Gravitational and Space Biology* 20(2), 3-18. 2007.
 39. Tarbell, J. M., Weinbaum, S., and Kamm, R. D. Cellular fluid mechanics and mechanotransduction. *Ann Biomed Eng* 2005, 1719-1723, 2005.
 40. Lemmon, C. A., Sniadecki, N. J., Ruiz, S. A., Tan, J. L., Romer, L. H., and Chen, C. S. Shear force at the cell-matrix interface: enhanced analysis for microfabricated post array detectors. *Mech Chem Biosyst* 2005, 1-16, 2005.
 41. Karcher, H., Lammerding, J., Huang, H., Lee, R. T., Kamm, R. D., and Kaazempur-Mofrad, M. R. A three-dimensional viscoelastic model for cell deformation with experimental verification. *Biophys J* 2003, 3336-3349, 2003.
 42. Kamm, R. D. and Kaazempur-Mofrad, M. R. On the molecular basis for mechanotransduction. *Mech Chem Biosyst* 2004, 201-209, 2004.
 43. Norvell, S. M., Ponik, S. M., Bowen, D. K., Gerard, R., and Pavalko, F. M. Fluid shear stress induction of COX-2 protein and prostaglandin release in cultured MC3T3-E1 osteoblasts does not require intact microfilaments or microtubules. *J Appl Physiol* 2004, 957-966, 2004.
 44. White, D. P., Caswell, P. T., and Norman, J. C. $\alpha_3\beta_3$ and $\alpha_5\beta_1$ integrin recycling pathways dictate downstream Rho kinase signaling to regulate persistent cell migration. *J Cell Biol* 2007, 515-525, 2007.
 45. Loesberg, W. A., Walboomers, X. F., van Loon, J. J., and Jansen, J. A. The effect of combined hypergravity and microgrooved surface topography on the behaviour of fibroblasts. *Cell Motil Cytoskeleton* 2006, 384-394, 2006.
 46. Teramoto, H., Coso, O. A., Miyata, H., Igishi, T., Miki, T., and Gutkind, J. S. Signaling from the small GTP-binding proteins Rac1 and Cdc42 to the c-Jun N-terminal kinase/stress-activated protein kinase pathway. A role for mixed lineage kinase 3/protein-tyrosine kinase 1, a novel member of the mixed lineage kinase family. *J Biol Chem* 1996, 27225-27228, 1996.
 47. Porras, A., Zuluaga, S., Black, E., Valladares, A., Alvarez, A. M., Ambrosino, C., Benito, M., and Nebreda, A. R. P38 alpha mitogen-activated protein kinase sensitizes cells to apoptosis induced by different stimuli. *Mol Biol Cell* 2004, 922-933, 2004.
 48. Secomb, T. W., Hsu, R., and Pries, A. R. Effect of the endothelial surface layer on transmission of fluid shear

stress to endothelial cells. *Biorheology* 2001, 143-150, 2001.



The threshold at which substrate
nanogroove dimensions may influence
fibroblast alignment and adhesion

WA Loesberg, J te Riet, FCMJM van Delft, P Schön, CG Figdor,
S Speller, JJWA van Loon, XF Walboomers and JA Jansen

Biomaterials. 28 (27), 3944-3951, 2007

INTRODUCTION

Biomaterials for tissue and cell engineering are successfully incorporated into neighbouring tissue when they not only match the tissue's mechanical properties, but also bring forth specific cell responses, thus controlling or guiding the tissue formation in contact with the biomaterial. The cellular response to a biomaterial may be enhanced by mimicking the surface topography formed by the extra cellular matrix (ECM) components of natural tissue [1]. This could be beneficiary in the field of tissue engineering, which aims at the (re)generation of new and functional tissues. These ECM components are of nanometre scale and a first step in this quest is the production of nano(metre scale) topography. Previous studies have already addressed cellular reactions to larger micrometer scale topography. Predominantly groove and ridge patterns were studied, on which cells responded by altering morphology, orientation, adhesion, and gene regulation. Nanogroove patterns of 10-100 nm thus far have not yet been studied, although Teixeira *et al* [2] have studied cell behaviour on ridges 70 nm wide, with a pitch of 400 nm however, and a depth of 600 nm, and found cellular alignment along these grooves. Previous *in vitro* research has investigated nanocolumns produced by colloidal lithography or polymer demixing which caused changes in cell morphology, filopodia production, migration, and cytokine release [3]. From these studies, it has become clear that topography in the nanometre scale may be of importance in cell guiding [1; 3-5]. Despite the amount of control over the dimensions created by these techniques, however, they remain largely random. In addition, it is unknown to what extent cells will sense and adapt their morphology to an ordered topography if the dimensions become exceedingly small.

In this study, a nanogroove topography formed by electron beam lithography has been investigated. In order not to deviate too far from previously used patterns [6-9] ten nanogroove/ridge patterns with a 1:1 pitch ratio have been selected and compared to smooth controls.

We hypothesised that, if the topography is small enough, a cellular "point break" is reached, where cells no longer display contact guidance along nanogroove patterns. In order to verify this hypothesis, cell responses to such nanotopography fields have been investigated from a morphology point of view, using light microscopy and scanning electron microscopy, and subsequent image analysis.

MATERIALS AND METHODS

Substrata

Silicon wafers, 15 cm (6 inch) across, were spin coated with hydrogen silsesquioxane (HSQ) solutions in methyl isobutyl ketone (MIBK) (FOX-12, Dow Corning Corp., Midland, MI, USA) on a Karl Suss spinner at 1000 rpm during 10 s with closed lid, resulting in 100 nm thick HSQ layers. The wafers were exposed in a JEOL Electron Beam Pattern Generator (JBX-9300FS) to a 100 kV beam with a 500 pA beam current (4 nm spot size) using a 4 nm beam step size. The field patterns consisted of squares of $500 \times 500 \mu\text{m}^2$ containing 1:1 lines and spaces at various pitches. The wafers were developed by manual immersion at 20 °C in a 0.26 M tetra methyl ammonium hydroxide developer (TMA238WA), rinsed in 1:9 v:v TMA238WA:H₂O, rinsed in demineralised water and blown dry with N₂ [10-12]. For obtaining higher master structures, the e-beam patterned HSQ was used as a mask in a Reactive Ion Etching (RIE) process for silicon using a CF₄/O₂ plasma.

One 250 nm deep groove pattern, with a 2 μm pitch, was made using a photolithographic technique and subsequent etching in a silicon wafer as described by Walboomers *et al.* [6]. Wafers with a smooth surface were used as controls. In all instances, the silicon wafers were used as template for the production of polystyrene (PS) substrata for cell culturing. Polystyrene was solvent cast in a manner described by Chesmel and Black [13]. The dimensions of all substrata are

shown in Table 1. Polystyrene replicas were attached to 20 mm diameter cylinders with polystyrene-chloroform adhesive to create a cell culture dish. Shortly before use a radio frequency glow-discharge (RFGD) treatment using Argon was applied for 3 minutes at a pressure of 2.0×10^{-2} mbar (Harrick Scientific Corp., Ossining, NY, USA) and a power of 200 W in order to sterilise and promote cell attachment by improving the wettability of the substrata.

Cell culture

Rat dermal fibroblasts (RDF) were obtained from the ventral skin of male Wistar rats as described by Freshney [14]. Cells were cultured in Dulbecco's MEM containing Earle's salts (Gibco, Invitrogen Corp., Paisley, Scotland), L-glutamine, 10% FCS, gentamicin (50 $\mu\text{g}/\text{ml}$), in an incubator set at 37 °C with a humidified atmosphere. Cell passage 4 - 6th was used during the experiments. Onto the various substrata, 3.5×10^4 cells/cm² were seeded into the culture dishes. For the analysis, after 4 or 24 hours, the cell layers were washed three times with phosphate buffered saline (PBS) and prepared for further analysis immediately after retrieval.

Atomic Force Microscopy

Surface topography was quantitatively evaluated using a Dimension atomic force microscope (AFM; Dimension 3100, Veeco, Santa Barbara, CA). Tapping in ambient air was performed with 118 μm long silicon cantilevers (NW-AR5T-NCHR, NanoWorld AG, Wetzlar, Germany) with average nominal resonant frequencies of 317 kHz and average nominal spring constants of 30 N/m. This type of AFM probe has a high aspect ratio (7:1) portion of the tip with a nominal length of >2 μm and a half-cone angle of $<5^\circ$. Nominal radius of curvature of the AFM probe tip was less than 10 nm. The probes are especially suited to characterize the manufactured nanogrooves.

Height images of each field/sample were captured in ambient air at 50% humidity at a tapping frequency of 266.4 kHz. The analysed field was scanned at a scan rate of 0.5 Hz and 512 scanning lines. Nanoscope imaging software (version 6.13r1, Veeco) was used to analyze the resulting images. Surface roughness (root mean squared (RMS), nm) and depth (nm) were obtained and averaged for three random fields per substrate.

Scanning electron microscopy (SEM)

SEM graphs of the HSQ master structures were made using a Philips XL40 FEG-SEM. To assess overall morphology of the fibroblasts, SEM was also performed. Cells were rinsed, fixed for 5 minutes in 2% glutaraldehyde, followed by 5 minutes in 0.1 M sodium-cacodylate buffer (pH 7.4), dehydrated in a graded series of ethanol, and dried in tetramethylsilane to air. Specimens were sputter-coated with gold and examined with a Jeol 6310 SEM (Tokyo, Japan). Multiple micrographs were taken of cells on each nanopattern.

Image Analysis

For quantitative image analysis, samples were fixed in paraformaldehyde and stained with Methylene blue followed by examination with a Leica/Leitz DM RBE Microscope (Wetzlar, Germany) with magnification of 20x.

Methylene blue micrographs were analysed with Scion Image software (Beta Version 4.0.2, Scion Corp., Frederick, MD, USA). In several cases, due to low contrast between cell staining and background, the orientation was determined manually with a Falmouth Marine three-limb Course Protractor with a 5-minute accuracy. The orientation of fibroblasts on the different fields and patterns was examined and photographed. The criteria for cell selection were (1) the cell is not in contact with other cells and (2) the cell is not in contact with the image perimeter. The maximum cell diameter was measured as the longest distance between two edges within the cell borders. The

angle between this axis and the grooves (or an arbitrarily selected line for smooth surfaces) was termed the orientation angle. If the average angle was 45 degrees or more, cells were supposed to lie in a random orientation. Cell extensions like filopodia, which could confound the alignment measurement, were not included when assessing the cell orientation. For statistic analysis, cells oriented at $<10^\circ$ from the groove direction were considered to be aligned [15; 16]. The number of cells that were measured per sample group ranged from 24 to 290.

Statistical analysis:

Data acquired from the micrographs of cell alignment were analysed using SPSS for Windows (Release 12.0.1, SPSS Inc., Chicago, USA). The effects of, and the interaction between both time and surface were analysed using analysis of variance (ANOVA), including a modified least significant difference (Bonferroni) multiple range test to detect significant differences between two distinct groups. Probability (p) value ≤ 0.05 was considered to be significant.

Field	Pitch (nm, ratio 1:1)	Depth (nm \pm SE)	Roughness (nm \pm SE)
A	1000	37.8 \pm 0.6	17.3 \pm 0.2
B	600	37.3 \pm 0.7	16.3 \pm 0.1
C	400	34.6 \pm 1.4	14.9 \pm 0.6
D	300	33.8 \pm 1.6	13.5 \pm 0.1
E	200	30.6 \pm 1.1	11.6 \pm 0.1
F	160	30.5 \pm 1.1	9.4 \pm 0.1
G	100	17.9 \pm 1.0	6.7 \pm 0.4
H	80	11.0 \pm 0.6	4.8 \pm 0.1
I	60	7.8 \pm 0.6	4.5 \pm 0.3
J	40	4.4 \pm 0.5	3.6 \pm 0.1
K	1000	153.3 \pm 2.7	69.1 \pm 1.0
L	600	158.0 \pm 3.2	64.4 \pm 0.7
M	400	149.2 \pm 1.2	53.9 \pm 1.8
N	300	119.9 \pm 2.6	36.7 \pm 1.3
O	200	77.4 \pm 4.1	22.0 \pm 0.5
P	160	51.9 \pm 3.4	15.3 \pm 0.3
Q	100	17.2 \pm 3.5	9.2 \pm 0.7
R	80	15.3 \pm 1.9	8.7 \pm 0.9
S	60	11.6 \pm 1.1	8.3 \pm 0.1
T	40	10.9 \pm 1.1	6.6 \pm 0.4
μ m-Groove	2000	353.9 \pm 8.2	163.3 \pm 10.5
Smooth	n/a	n/a	1.24 \pm 0.14

Table 1. Feature dimensions of topographically patterned substrata.

RESULTS

Atomic force microscopy

In **Table 1**, the dimension, depth, and roughness as measured by AFM of the patterns in all polystyrene duplicates are given. The nano fields are designated A till T, while the microgrooved and smooth surfaces are designated by their own names. **Figure 1** shows a number of representative images. What can be seen in these images is, that although groove/ridge widths were fairly preserved at the top, at deeper levels the grooves became concave or even V-shaped. The smooth sample has no distinguishable pattern other than a RMS roughness of 1.2 ± 0.1 nm, occasionally a spike is present on the surface, probably the result of blemishes on the original wafer.

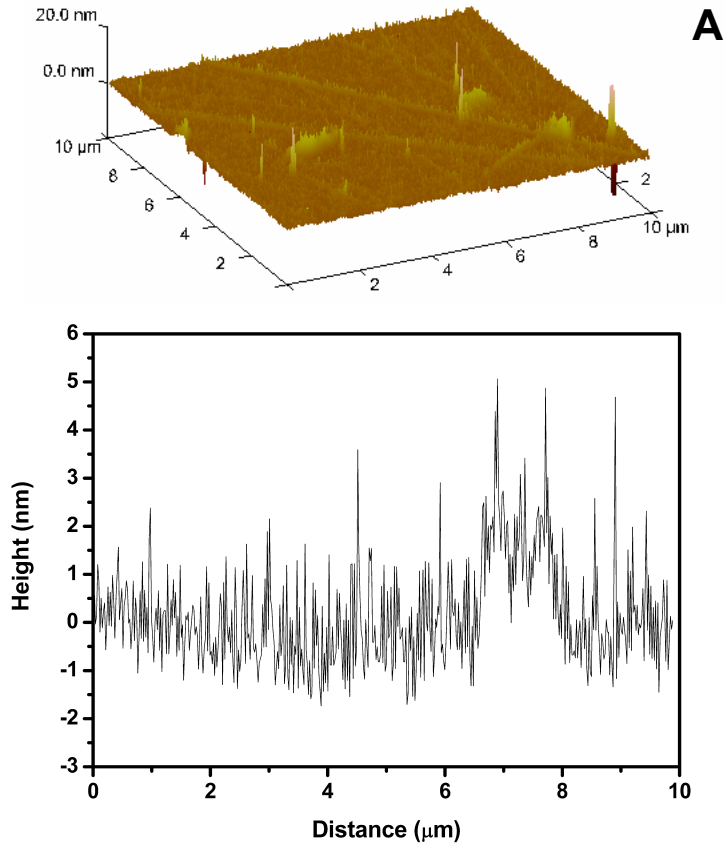
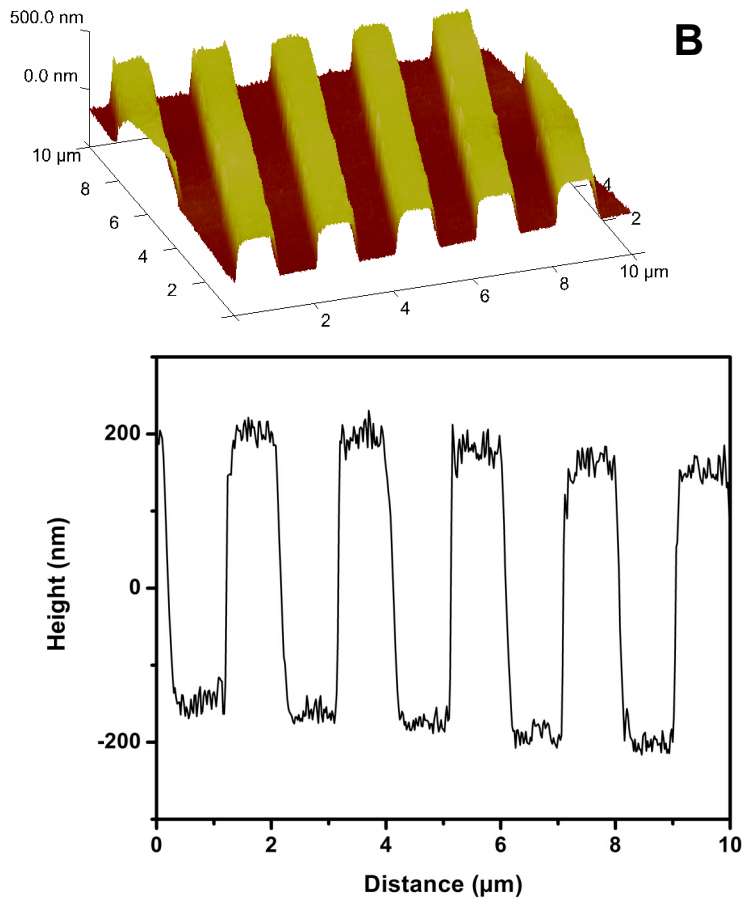
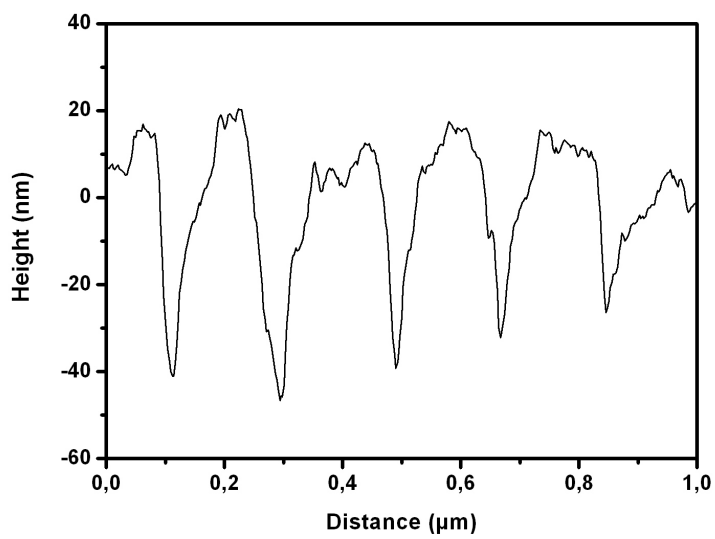
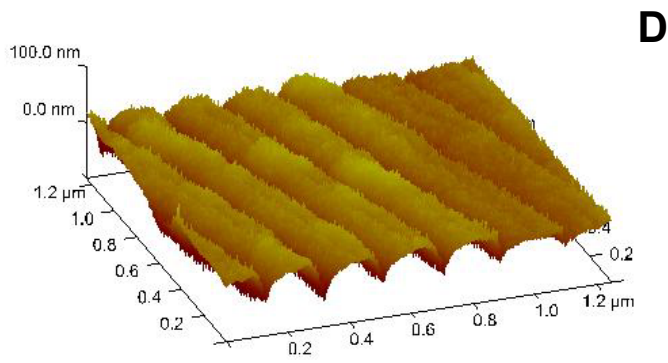
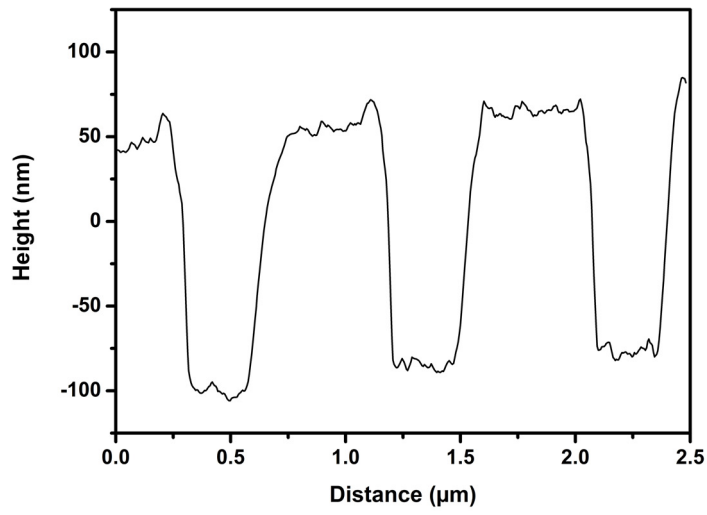
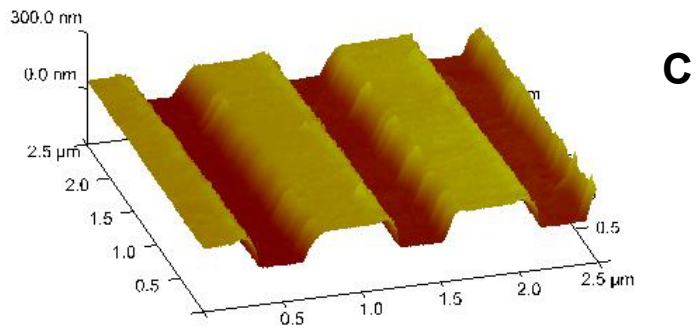


Figure 1. AFM graphs of topographies and height profiles of smooth (A), microgrooved (B), and nanogrooved substrates Field K and P (C and D, respectively).





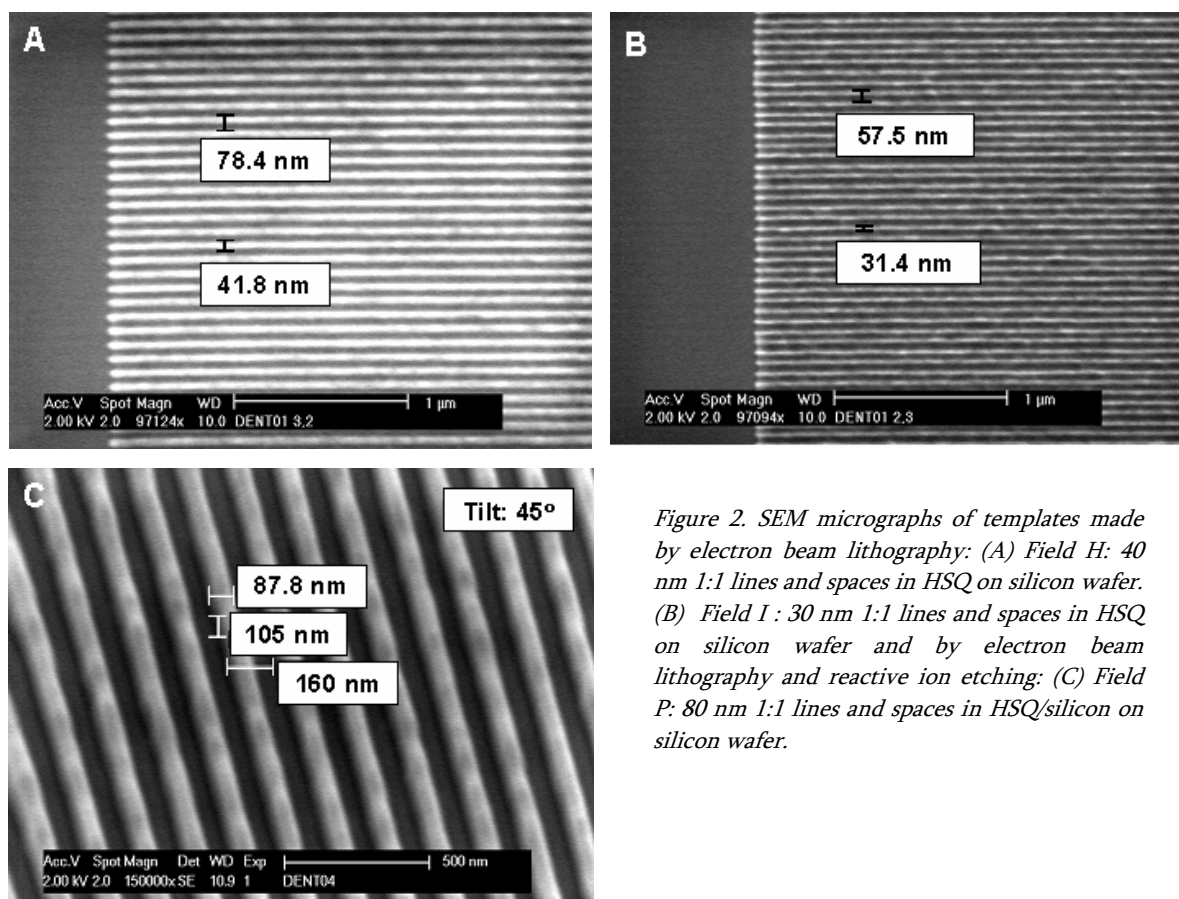


Figure 2. SEM micrographs of templates made by electron beam lithography: (A) Field H: 40 nm 1:1 lines and spaces in HSQ on silicon wafer. (B) Field I : 30 nm 1:1 lines and spaces in HSQ on silicon wafer and by electron beam lithography and reactive ion etching: (C) Field P: 80 nm 1:1 lines and spaces in HSQ/silicon on silicon wafer.

Scanning electron microscopy

Figure 2 shows a number of representative SEM graphs of the HSQ on silicon template structures as made by means of electron beam lithography (and Reactive Ion Etching).

The various nano topographies were accurately replicated in the polystyrene substrata. When observing cell morphology, fibroblasts cultured on smooth substrata displayed a cell spreading which is considered random (**Figure 3A**), while an orientation along the groove direction was observed when cells are cultured on micro-groove substrata (**Figure 3B**). With decreasing pitch visual inspection made it clear that alignment was reduced. From field K to N, alignment of cells was still observed (**Figure 3C**), on fields O till Q however cellular orientation was observed only rarely. Fields with the smallest pitch values (R, S, and T) resulted in cell morphology undistinguishable from the cells growing on the planar surface surrounding the textured fields, or the smooth control samples (**Figure 3D**). Fibroblast alignment on fields A to J was virtually non-existent as opposed to, fields with the deeper groove depth (K, etcetera) that did elicit alignment. Interestingly, time had a beneficiary effect on cellular alignment; in all cases increased culture times (24 hrs vs. 4 hrs) lead to an increase in orientation and/or more fields triggering alignment on the cell population (Field A in **Figure 3E & F**).

Image analysis

Image analysis and subsequent statistical analysis performed confirmed that topography and culturing time were both significant factors in eliciting cellular orientation. **Figure 4** lists the various patterns and the mean angle of orientation they enticed to the fibroblasts. To designate the turning point after which alignment does not occur anymore, polynomic trend lines were drawn in the figures and the steepest parts were calculated.

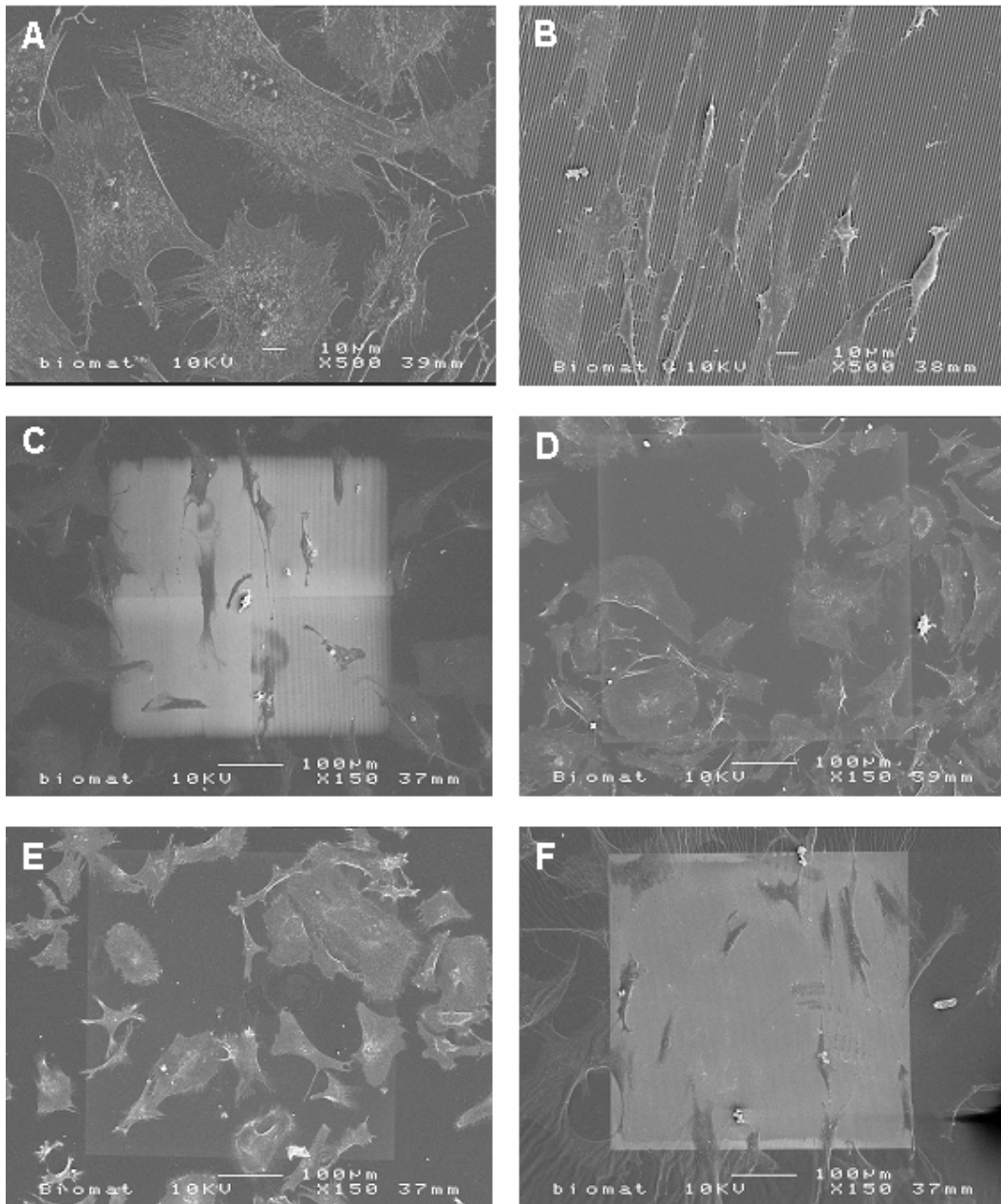


Figure 3. SEM micrographs of RDFs cultured under various conditions. (A) smooth substratum with cells in a random fashion, (B) 1 μm wide (350 nm deep) grooved substratum displaying aligned cells. (C) Field N (width 150 nm, depth 120 nm) still elicits cellular alignment to a majority of the cells compared to (D) Field R (width 40 nm, depth 15 nm) on which cells lay randomly spread. (E) Field A (width 500 nm, depth 35 nm) after 4 hours of culturing and Field A after 24 hours of culturing (F). All micrographs were taken from 24 hrs samples, unless otherwise stated.

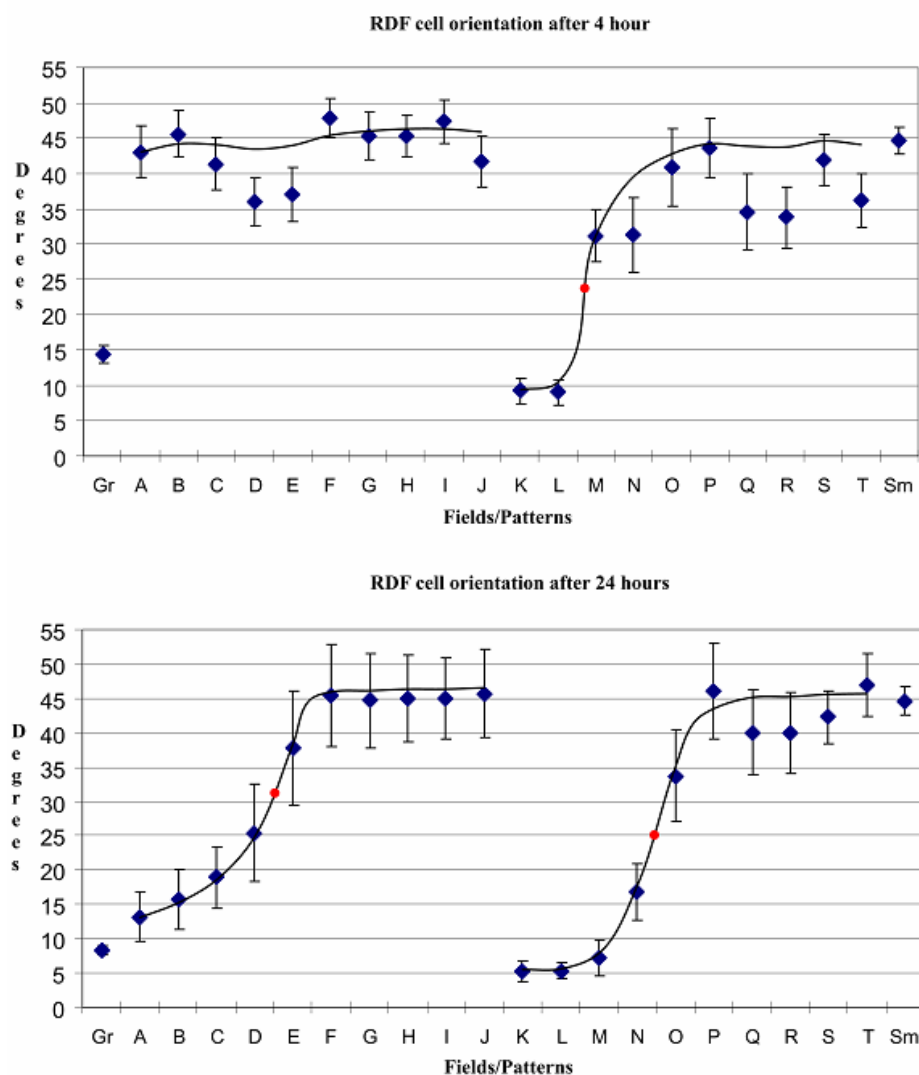


Figure 4. The mean angle and standard error of the mean showing the distribution of cellular orientation divided over time. (A) Cellular orientation after 4 hours culture shows alignment for the groove pattern and fields K and L. All other surfaces, smooth pattern and fields with small groove dimensions do not elicit orientation at this point. (B) After 24 hours cell alignment has appeared or improved on the several patterns and fields. Polynomic trend line in black with the turning point in red. Gr = 1 μ m Groove pattern, Sm = Smooth pattern, nanometric Fields A through T (see also: Table 1).

Figure 4 presents these trend lines and illustrates the turning point between 23 and 31 degrees. Regarding topography; RDFs cultured on smooth substrata displayed a random cell spreading (average orientation angle around 45°), while those cultured on the 1 μ m wide groove pattern showed a clear alignment along the grooves for 82% of the cells. Nanopatterns with depth 80 – 150 nm also resulted in cellular orientation on fields with larger pitch values (Fields K, L, M, and N). Nanopatterns with depths of 35 nm did not result in orientation of the fibroblasts at 4 hours, however when cultured for a prolonged period of time, the fields A and B did elicit cell alignment. Time played a key part in cell response towards the grooves; 24 hours groups showed improved alignment compared to 4 hours samples. As mentioned earlier, analysis of cells cultured on the deeper grooved nanopattern for 24 hours showed an orientation trend, which gradually decreased with decreasing pitch width. After 24 hours of culturing, the deep nanopattern resulted in enhanced alignment with the cut-off at 100 nm (Field O), after which cells appeared not to be aligned anymore.

DISCUSSION

The aim of this study was to understand the morphological cell response of fibroblasts *in vitro*, particularly their orientation along a nanogroove pattern. Fibroblasts were cultured on polystyrene substrata, both smooth and grooved. In the latter case, both width and depth of the

grooves were varied. The patterns were characterized and cell behavior was analyzed using microscopic techniques. From our data it can be concluded that RDFs adjust their shape according to nano topographical features down to a cut-off value of 100 nm width and a depth of 70 nm, which is a novel finding. Given sufficient culturing time, fibroblasts will even align themselves on groove depths as shallow as 35 nm, provided that ample ridge-surface (150 nm wide ridges) is available to the cells. It appears depth is the most essential parameter in cellular alignment on groove patterns with a pitch ratio of 1:1.

In order to obtain nanogroove patterns, electron beam lithography and reactive ion etching have been employed. In the latter technique, the phenomenon of diffusion limitation plays a role, especially in smaller grooves; the chemical reactants will insufficiently reach the bottom of the proposed design of the grooves, resulting in shallower depths or grooves becoming more concave. Simply increasing the etching time in RIE may result in the desired depth locally. However, this would lead to the top edges of the ridges enduring more etching, resulting in a reduced sharpness and somewhat convex and concave profiles of, respectively, the wafer ridges and the ensuing polystyrene duplicates. The characteristics of the actual wafers were not the focus of our study, as our main interest is in the substrata onto which the cells are cultured. In addition, polystyrene casting could be influenced by capillary forces elicited by the nano-grooves which may affect the reproduction accuracy, although literature data concerning imprint lithography techniques suggest that 20 nm details can easily be accomplished when pressing a mould into polymers [17; 18].

Another possible explanation for the concave appearance of the grooves, from fields E and O onwards, is the intrinsic limitation of AFM measurements related to tip convolution. Also, this phenomenon can have an effect on the reliability of the depth measurement. In order to minimize these effects during our AFM measurement, a high aspect ratio tip especially designed for scanning grooves was used.

Scanning electron microscopy, cell staining, and subsequent image analysis all confirmed that fibroblasts were oriented on nanogrooved surfaces. Because the pitch dimensions used on both nanopattern wafers were equal, the difference in rate of cellular orientation was predominantly determined by the groove depth. These results are in accordance with work of Clark *et al.* on micrometric textures [15; 16]. They concluded that groove depth is much more important in alignment of cells than the spacing of the grooves. Even when nano-scale patterns were used, an increase in groove depth led to better orientation [19]. Teixeira *et al.* [2], who cultured epithelial cells on patterned substrata showed an approximate 35% of cells aligned; this value could be the result of shallow ridge width (70 nm, pitch 400 nm) with appropriate depth (600 nm). However, it could also be that cell orientation is the result of both (or more) parameters. Current e-beam lithography permits the fabrication of large areas of features comparable in size to those found in fibrillar ECM. Individual collagen fibrils have diameters that are commonly in the range 20 – 100 nm although they often form larger aggregates [19; 20]. This study shows that fibroblast cells display meagre alignment on fields with ridge/groove widths of 100 nm or less. So, it is possibly a combination of factors that lead to cell guidance by the environment (be it substrata or tissue) rather than simply one parameter.

Similar to Teixeira's results and our own work [9], in this study it was observed that cells extend themselves while probing the substrata, since the grooves patterns are too narrow for the cells to get into contact with the bottom. The cellular extensions, probing the substrate surface, only found the ridges, resulting in extension of the cellular body along these ridges. Early responses of fibroblasts growing on textured substrata have been described before [21]; and cell orientation starts with the cell exploring the surroundings with the appearance of membrane extensions. Connective tissue cells need ECM in order to survive; since none is present, the aforementioned

extensions are produced in all directions. Within hours, fitting anchor points are found and focal adhesion contacts are established with deposited ECM material, and the cell flattens and spreads, followed by the formation of filaments in the longitudinal direction [22; 23]. This study showed it was clear that cell alignment occurred immediately on Fields K, L, and 1 μm grooves during cell spreading and in accordance with the grooves. An alternative view concerning cell guidance on such small features is that not the increasing amount of ECM proteins with time, but the lag time between guidance on a small scale (filopodia, lamellapodia) and the influence on the entire cell might perhaps explain the increase in orientation [24; 25].

As explained earlier, having the ability to control cell behaviour is of great advantage in tissue engineering. And topography is just one method of gaining control. It is now clear that cells as a whole respond strongly to structured nano topography to a cut-off value of 35 nm. However, as Dalby *et al.* [25] pointed out for filopodia and to some extent lamellapodia, this value may be as low as 10 nm when random distributed “nano islands” are applied to induce interaction.

By using a pattern design which surface is large enough to extract quantitative data, future research will, besides visualisation of cell cytoskeleton components and quantification of the cell's responses on a molecular level, look at the interaction of these groove dimensions and a dynamic force, like mechanical strain or fluid flow on cell conduct.

CONCLUSION

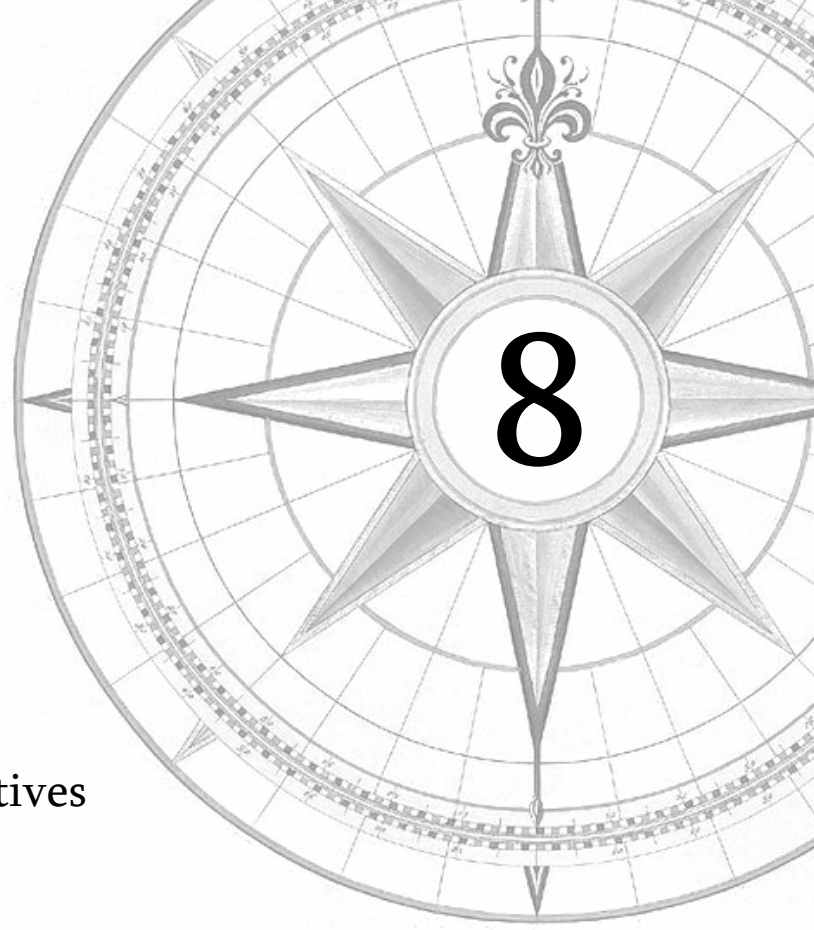
Since e-beam lithography is able to generate diverse patterns, a new approach was made possible to conduct research on cell behaviour on a wide variety of fields. This in turn allowed us to ascertain the cellular divide as presented in this study. The gradual decrease in dimension values allowed us to investigate in more detail the fibroblasts response towards topography. It is proposed that criteria concerning cellular orientation go beyond an arbitrary value, since those values are derived from measurements on specified topographies. By approaching natural dimensions these theoretical standards are no longer valid. Cellular alignment is triggered by a combination of ridge width and groove depth and most likely by other external (dynamic) factors as well, such as mechanical stress or compression. In this static study, design groove depths below 35 nm or ridge widths smaller than 100 nm do not result in fibroblast alignment.

It is concluded that fibroblast cells, cultured upon increasingly smaller nano-scale topography, experience, in accordance with our hypothesis, a decisive point where they no longer demonstrate contact guidance. This threshold seems to be at a 35 nm for whole cell alignment.

REFERENCES

1. Miller, D. C., Thapa, A., Haberstroh, K. M., and Webster, T. J. Endothelial and vascular smooth muscle cell function on poly(lactic-co-glycolic acid) with nano-structured surface features. *Biomaterials* 2004, 53-61, 2004.
2. Teixeira, A. I., Abrams, G. A., Bertics, P. J., Murphy, C. J., and Nealey, P. F. Epithelial contact guidance on well-defined micro- and nanostructured substrates. *J Cell Sci* 2003, 1881-92, 2003.
3. Dalby, M. J., Riehle, M. O., Sutherland, D. S., Agheli, H., and Curtis, A. S. Morphological and microarray analysis of human fibroblasts cultured on nanocolumns produced by colloidal lithography. *Eur Cell Mater* 2005, 1-8; discussion 8, 2005.
4. Dalby, M. J., Riehle, M. O., Johnstone, H. J., Affrossman, S., and Curtis, A. S. Polymer-Demixed Nanotopography: Control of Fibroblast Spreading and Proliferation. *Tissue Eng* 2002, 1099-1108, 2002.
5. Dalby, M. J., Riehle, M. O., Sutherland, D. S., Agheli, H., and Curtis, A. S. Use of nanotopography to study mechanotransduction in fibroblasts--methods and perspectives. *Eur J Cell Biol* 2004, 159-69, 2004.
6. Walboomers, X. F., Croes, H. J., Ginsel, L. A., and Jansen, J. A. Growth behavior of fibroblasts on microgrooved polystyrene. *Biomaterials* 1998, 1861-1868, 1998.

7. den Braber, E. T., de Ruijter, J. E., Smits, H. T., Ginsel, L. A., von Recum, A. F., and Jansen, J. A. Quantitative analysis of cell proliferation and orientation on substrata with uniform parallel surface micro-grooves. *Biomaterials* 1996, 1093-9, 1996.
8. Brunette, D. M. and Chehroudi, B. The effects of the surface topography of micromachined titanium substrata on cell behavior in vitro and in vivo. *J Biomech Eng* 1999, 49-57, 1999.
9. Loesberg, W. A., Walboomers, X. F., van Loon, J. J., and Jansen, J. A. The effect of combined cyclic mechanical stretching and microgrooved surface topography on the behavior of fibroblasts. *J Biomed Mater Res A* 2005, 723-732, 2005.
10. Van Delft, F. C. M. J. M., Wterings, J. P., Van Langen-Suurling, A. K., and Romijn, H. Hydrogen silsesquioxane/novolac bilayer resist for high aspect ratio nanoscale electron-beam lithography. *J. Vac. Sci. Technol. B* 2000, 3419-3423, 2000.
11. Van Delft, F. C. M. J. M., Van Den Heuvel, F. C., Kuiper, A. E. T., Thüne, P. C., and Niemantsverdriet, J. W. Micro-contact printing on oxide surfaces for model catalysts using e-beam written masters in hydrogen silsesquioxane. *Microelectronic Engineering* 2004, 202-208, 2004.
12. Van Delft, F. C. M. J. M. Delay-time and aging effects on contrast and sensitivity of hydrogen silsesquioxane. *J. Vac. Sci. Technol. B* 2002, 2932-2936, 2002.
13. Chesmel, K. D. and Black, J. Cellular responses to chemical and morphologic aspects of biomaterial surfaces. I. A novel in vitro model system. *J Biomed Mater Res* 1995, 1089-1099, 1995.
14. Freshney, R. I. Culture of animal cells: a multimedia guide. 99. Chichester, John Wiley & Sons Ltd.
15. Clark, P., Connolly, P., Curtis, A. S., Dow, J. A., and Wilkinson, C. D. Topographical control of cell behaviour: II. Multiple grooved substrata. *Development* 1990, 635-644, 1990.
16. Clark, P., Connolly, P., Curtis, A. S., Dow, J. A., and Wilkinson, C. D. Topographical control of cell behaviour. I. Simple step cues. *Development* 1987, 439-448, 1987.
17. Haisma, J., Verheijen, M., van dem Heuvel, C. A., and van den Berg, J. Mold assisted nanolithography: a process for reliable pattern replication. *J Vac Sci Technol B* 1996, 4124-4128, 1996.
18. Chou, S. Y., Krauss, P. R., and Renstrom, P. J. Nanoimprint lithography. *J Vac Sci Technol B* 1996, 4129-4133, 1996.
19. Clark, P., Connolly, P., Curtis, A. S., Dow, J. A., and Wilkinson, C. D. Cell guidance by ultrafine topography in vitro. *J Cell Sci* 1991, 73-7, 1991.
20. Dunn, G. A. and Heath, J. P. A new hypothesis of contact guidance in tissue cells. *Exp Cell Res* 1976, 1-14, 1976.
21. Walboomers, X. F., Ginsel, L. A., and Jansen, J. A. Early spreading events of fibroblasts on microgrooved substrates. *J Biomed Mater Res* 2000, 529-534, 2000.
22. Hynes, R. O. and Destree, A. T. Relationships between fibronectin (LETS protein) and actin. *Cell* 1978, 875-86, 1978.
23. Hynes, R. O. Cell adhesion: old and new questions. *Trends Cell Biol* 1999, M33-7, 1999.
24. Dalby, M. J., Gadegaard, N., Riehle, M. O., Wilkinson, C. D., and Curtis, A. S. Investigating filopodia sensing using arrays of defined nano-pits down to 35 nm diameter in size. *Int J Biochem Cell Biol* 2004, 2005-15, 2004.
25. Dalby, M. J., Riehle, M. O., Johnstone, H., Affrossman, S., and Curtis, A. S. Investigating the limits of filopodial sensing: a brief report using SEM to image the interaction between 10 nm high nano-topography and fibroblast filopodia. *Cell Biol Int* 2004, 229-36, 2004.



Summary and future perspectives

SUMMARY

For over a century, millions of hours of research have been spent on solving the fundamental engineering problems of escaping Earth's gravity well and developing systems for in-space propulsion. Even now, the research and development put into the mechanics of space voyaging is substantial, owing to man's wish to revisit our Moon and make landfall on Mars. The issue of how humans will actually survive and work in space for long periods of time requires input from the whole gamut of physical and biological sciences and has become a great challenge to deep space exploration. A fundamental step in meeting this challenge is: understanding the effects of altered gravity circumstances on cellular organisms. These effects are the subject of this thesis.

Biology (cells), material (microgrooves), and force (gravity) are the interacting aspects of this research, which in the larger playfield of tissue engineering, affect the behaviour and longevity of artificial constructs in living tissue. **Chapter 1** describes broadly our current knowledge of cell biology and cellular responses towards both stationary and dynamic forces. It touches on the fabrication of a structured topography and the various physical phenomena encountered in a changing gravity environment.

FIBROBLAST BEHAVIOUR TOWARDS COMBINED STRETCHING AND MICROGROOVES

The initial research was focused on obtaining a general view of cell responses towards microgrooved surface topography and mechanical loading. **Chapter 2** describes the influence of unilateral cyclic stretch and the resulted tendency of cultured fibroblasts to orient perpendicular to the stress direction. Similar cell alignment can be induced by guiding cells along topographical clues, like microgrooves. The aim of this study was to evaluate cell behaviour on micro-grooved substrates, exposed to cyclic stretching. We hypothesized that cellular shape is mainly determined by topographical clues. On basis of earlier studies, a 10 μm wide square-groove and a 40 μm wide V-shaped groove pattern were used. Smooth substrates served as controls. Onto all substrates, fibroblasts were cultured and 1-Hz cyclic stretching was applied (0, 4, or 8%) for 3-24h. Cells were prepared for scanning electron microscopy, immuno-staining of filamentous actin, alignment measurements, and PCR (collagen-I, fibronectin, $\alpha 1$ - and $\beta 1$ -integrins). Results showed that cells aligned on all grooved surfaces, and fluorescence microscopy showed similar orientation of intracellular actin filaments. After 3 hours of stretch, cellular orientation started and after 24 hours the cells had aligned themselves almost entirely. Image analysis showed better orientation with increasing groove depth. Statistical testing proved that the parameters groove type, groove orientation, and time all were significant, but the variation of stretch force was not. Substrates with microgrooves perpendicular to the stretch direction elicit a better cell alignment. The expression of $\beta 1$ -integrin and collagen-I was higher in the stretched samples. In conclusion, we can maintain our hypothesis, as microgrooved topography was most effective in applying strains relative to the long axis of the cell, and only secondary effects of stretch force were present.

FIBROBLAST RESPONSES TO COMBINED HYPERGRAVITY AND MICROGROOVES

Mechanical stress is an important regulator of cell shape and extracellular matrix component production. The notion that changes in cell shape under varying gravity levels contributes to the idea of direct effects of gravity onto cells has led to the study as described in **chapter 3**. This study reports the differences in morphological behaviour between fibroblast cultured on smooth and microgrooved substrata (groove depth: 1 μm , width: 1, 2, 5, 10 μm), which undergo artificial hypergravity by centrifugation (10, 25, and 50 g; or 1g control). The aim of the study was to clarify which of these parameters is more important to determine cell behaviour. Morphological characteristics were investigated using scanning electron microscopy and fluorescence microscopy

in order to obtain qualitative information on cell spreading and alignment. Confocal laser scanning microscopy visualised distribution of actin filaments and vinculin anchoring points through immuno-staining. Finally, expression of collagen type I, fibronectin, and $\alpha 1$ - and $\beta 1$ -integrin were investigated by PCR. Microscopy and image analysis showed that the fibroblasts aligned along the groove direction on all textured surfaces. On the smooth substrata (control) cells spread out in a random fashion. The alignment of cells cultured on grooved surfaces increased with higher g-forces until a peak value at 25g. An ANOVA was performed on the data, for all main parameters: topography, gravity force, and time. In this analysis, all parameters proved significant. In addition, most gene levels were reduced by hypergravity. Still, collagen type 1 and fibronectin are seemingly unaffected by time or force. From our data it is concluded that the fibroblasts primarily adjust their shape according to morphological environmental cues like substratum surface whilst a secondary, but significant, role is played by hypergravity forces.

REACTIONS OF FIBROBLASTS TO COMBINED MICROGRAVITY AND MICROGROOVES

Although mechanical stress is important, cells can also experience mechanical unloading by removing the most constant force in nature, namely gravity. **Chapter 4** is about the first of two studies which focused at the effects of simulated microgravity on cell behaviour by describing *in vitro* the differences in morphological behaviour between fibroblast cultured on smooth and microgrooved substrata (groove depth: 0.5 μm , width: 1, 2, 5, 10 μm), that were subjected to simulated microgravity. The aim of the study was to clarify which of these parameters is more dominant to determine cell behaviour. Morphological characteristics were investigated using scanning electron microscopy and fluorescence microscopy in order to obtain qualitative information on cell alignment and area. Confocal laser scanning microscopy visualised distribution of actin filaments and focal adhesion points. Finally, expression of collagen type I, fibronectin, and $\alpha 1$ - and $\beta 1$ -integrin were investigated by PCR. Microscopy and image analysis showed that the fibroblasts aligned along the groove direction on all textured surfaces. On the smooth substrata, cells had spread out in a random fashion. The alignment of cells cultured on grooved surfaces decreased under simulated microgravity, especially after 24 hours of culturing. Cell surface areas on grooved substrata were significantly smaller than on smooth substrata but simulated microgravity on the grooved groups resulted in an enlargement of cell area. ANOVA was performed on all main parameters: topography, gravity force, and time. In this analysis, all parameters proved significant. In addition, gene levels were reduced by microgravity particularly those of $\beta 1$ -integrin and fibronectin. From our data it is concluded that the fibroblasts primarily adjust their shape according to morphological environmental cues like substratum surface, whilst a secondary but significant role is played by microgravity conditions.

ACTIVATION OF MAPK PATHWAYS IN FIBROBLAST DURING MICROGRAVITY

Chapter 5 expands the knowledge obtained from the previous study by looking into the intracellular molecular mechanics which mediates the extracellular cell response. Mechanotransduction is the key element behind this study which considers *in vitro* the differences in morphological behaviour between fibroblast cultured on smooth and microgrooved substrata (groove depth: 0.5 μm , width: 1 μm), which were subjected to simulated microgravity. The aim of the study was to clarify which of these parameters was more dominant to determine cell behaviour. Morphological characteristics were investigated using scanning electron microscopy and fluorescence microscopy in order to obtain qualitative information on cell alignment. Confocal laser scanning microscopy visualised distribution of actin filaments and focal adhesion points. Expression of collagen type I, and $\alpha 1$ -, $\beta 1$, $\beta 3$ -integrin were investigated by QPCR. Finally, immunoblotting was applied to visualise MAPK signalling pathways. Microscopy

and image analysis showed that the fibroblasts aligned along the groove direction on all textured surfaces. On the smooth substrata, cells had spread out in a random fashion. The alignment of cells cultured on grooved surfaces under simulated microgravity, after 48 hours of culturing appeared similar to those cultured at 1g, although cell shape was different. ANOVA was performed on all main parameters: topography, gravity force, and time. In this analysis, all parameters showed significant differences. In addition, gene levels were reduced by microgravity particularly those of β 3-integrin and collagen, however alpha-1 and beta-1 integrin levels were up-regulated. ERK1/2 was reduced in zero g, however, JNK/SAPK and p38 remained active. The members of the small GTPases family were stimulated under microgravity, particularly RhoA and Cdc42.

The results are in agreement with the hypothesis that the application of microgravity promotes fibroblasts to change their morphological appearance and their expression of cell-substratum proteins through the MAPK intracellular signalling pathways. We conclude that fibroblasts cultured on a grooved pattern adjust their shape accordingly and that this model could be employed as useful model to unravel the effects of gravity perception and cellular response.

MECHANOSENSITIVITY OF FIBROBLASTS TOWARDS INERTIAL SHEAR

To date, inertial shear force, which is inherent in centrifugation set-ups, is described as a theoretical model. From this model it became apparent that inertial shear force results in artefacts which influence the outcome of control samples being centrifuged at 1 x gravity on-board a spacecraft. In **chapter 6** we undertook a study to identify *in vitro* the magnitude of inertial shear forces on fibroblast cells cultured on polystyrene substrata, both smooth and equipped with a surface micro topography (groove depth: 0.25 μ m, width: 1 μ m). The cells were placed in a centrifuge environment. Samples were subjected to 0, 1.5, and 3.0 Pascal for 0.5, 2, and 4 hours. To ascertain the impact of inertial shear force we looked at both a morphological (scanning electron and fluorescence microscopy) and molecular level (mRNA transcription and Western blotting). The underlying aim was to understand to what extent shear forces can alter cell behaviour and which parameter is more important in determining this cell response. Microscopy and image analysis showed that the fibroblasts aligned along the groove direction on all textured surfaces. On the smooth substrata, cells had spread out in a random fashion. After 4 hours of culturing the alignment of cells cultured on grooved surfaces under inertial shear force appeared dissimilar to those cultured at 0.0 Pascal. Actin filament numbers and thickness were decreased, and talin anchor-points were reduced. ANOVA was performed on the three main parameters: topography, shear force, and time. In this analysis, all parameters proved significant. Furthermore, gene levels were reduced by shear force, particularly those of beta-3-integrin and alpha-1. However, collagen and beta-1 integrin levels were up-regulated. ERK1/2 was present and JNK/SAPK and p38 were increased during inertial shear. The members of the small GTPases family were stimulated under shear force, particularly RhoA and Cdc42.

In addition to the gravity acceleration component of a simulated microgravity study in spaceflight facility, inertial shear force is a force to be taken into account, because of its substantial impact on adherent cell colonies. Inertial shear force artefacts should be considered for interpretation of spaceflight and ground-based data.

NANO-TOPOGRAPHY AND THE ORIENTATION LIMITS OF FIBROBLASTS

One of the main parameters in all of the previous chapters is topography. A structured, groove/ridge surface of known dimensions, of which we know what sort of cell response it can elicit. Since these surfaces mimic the natural surroundings these patterns have been extensively studied. However, collagen fibres, which are the natural surroundings of dermal fibroblast, occur in a smaller range (nano scale) than we currently simulated with our substrates (micro scale). Due

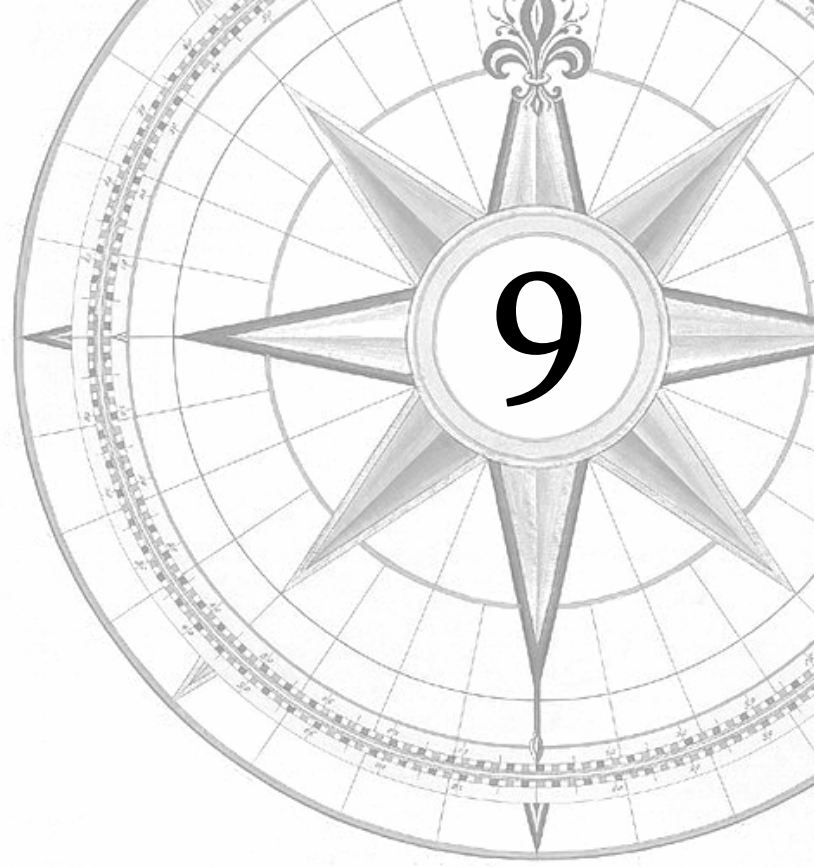
to technical limitations and knowing that collagen fibres usually aggregate into much bigger structures, we resorted to microgrooves up until now. Through cooperation with Philips Research, we have been able to study the differences in morphological behaviour between fibroblasts cultured on smooth and genuine nano-grooved substrata (groove depth: 5 – 350 nm, width: 20 – 1000 nm) *in vitro*. The aim of the study in **chapter 7** was to clarify to what extent cell guidance occurs on increasingly smaller topographies. Pattern templates were made using electron beam lithography, and were subsequently replicated in polystyrene cell culture material using solvent casting. The replicates were investigated with atomic force microscopy (AFM). After seeding with fibroblasts, morphological characteristics were investigated using scanning electron microscopy (SEM) and light microscopy, in order to obtain qualitative and quantitative information on cell alignment. AFM revealed that nanogroove/ridge widths were replicated perfectly, although at deeper levels the grooves became more concave. The smooth substrata had no distinguishable pattern other than a roughness amplitude of 1 nm. Interestingly, microscopy and image analysis showed that after 4 hours fibroblast had adjusted their shape according to nano-topographical features down to cut-off values of 100 nm width and 75 nm depth. After 24 hours culturing time, some fibroblasts even aligned themselves on groove depths as shallow as 35 nm. It appears depth is the most essential parameter in cellular alignment on groove patterns with a pitch ratio of 1:1. On the smooth substrata, cells always spread out in a random fashion. Analysis of variance (ANOVA) demonstrated that both main parameters, topography and culturing time, were significant. We conclude that fibroblast cells cultured on nanotopography experience a threshold feature size of 35 nm; below this value contact guidance does no longer exist.

CLOSING REMARKS AND FUTURE PERSPECTIVES

In this thesis the interaction between static and dynamic factors was investigated from a cell mechanotransduction point of view. By mimicking a fibrillar appearance through application of surface topography onto a biomaterial and subjecting the cells to a stressful environment we were able to obtain insight on the mechano- and gravi-sensing capabilities of primary fibroblast cells.

Ground-based (Earth) gravitational cell biology is a field or research with a bright future: human's curiosity and desire to understand the natural world, from the depths of the oceans to the far reaches of space, joint with the relatively low cost and ease of availability of experimental hardware, will foster further studies. The results described in this thesis and the works of others in this field, have shown that the outcomes of ground-based research are similar to those found in "true" weightlessness conditions.

The micron scale grooved pattern used in the earlier chapters was rather –and perhaps too much– the dominant factor. Therefore future research should expand the knowledge currently obtained by combining cells cultured on a nano-topography and subjecting them to mechanical (un)loading in a variety of ways. This most likely will result in an enhanced interaction between the various parameters. Analysis of cell feedback should be broad: ranging from visualisation of morphological changes of the cell shape by means of microscopy to quantifiable data achieved through molecular analysis methods such as Q-PCR and particularly SDS-PAGE and Western blotting. Monitoring the cell in real-time will not only benefit our understanding of cell behaviour but also will stimulate the development of high-tech experimental hardware. Linking the processes inside the cell to the cells outside appearance, may illuminate the mechanisms by which cells respond to environmental stimuli. This fundamental knowledge could be also beneficial in the construction and application of biomaterials used for repair and regeneration of novel, functional tissues.



Samenvatting en toekomst visie

SAMENVATTING

Voor meer dan een eeuw zijn miljoenen man uren aan onderzoek zijn gespendeerd in het oplossen van de fundamentele werktuigkundige problemen ten aanzien van het ontsnappen aan de Aardse zwaartekracht en de ontwikkeling van aandrijvingsystemen voor ruimtevaartuigen. Zelfs nu is de moeite en tijd geïnvesteerd in onderzoek en ontwikkeling in de technologische kant van de ruimtevaart substantieel, dit alles is te danken aan de wens van de mensheid om onze Maan nogmaals te bezoeken en vandaar een landingsexpeditie naar de planeet Mars op te zetten. Hoe mensen eigenlijk gaan overleven en werken in de ruimte voor zeer lange tijd is een zaak waar het hele scala aan fysiologische en biologische wetenschappen voor nodig zijn en is geworden tot een van de grootste uitdagingen binnen de exploratie van ons zonnestelsel. Een fundamentele stap om deze uitdaging tot een goed einde te brengen is begrijpen wat de effecten van veranderende zwaartekracht omstandigheden zijn op cellichamen. Over die effecten gaat dit proefschrift.

Biologie (cellen), materialen (microgroeven) en kracht (gravitatie) zijn de interactieve aspecten van dit onderzoek, gezamenlijk zijn ze onderdeel van het grote onderzoeksveld van de tissue engineering, en beïnvloeden het gedrag en levensduur van kunstmatige materialen in levend weefsel. **Hoofdstuk 1** beschrijft in brede zin onze huidige kennis van cel biologie en cel respons op zowel statische als dynamische krachten. Er wordt kort ingegaan op de fabricatie van ondergronden met een topografie en de verschillende fysieke fenomenen zoals die voorkomen in een veranderende zwaartekracht omgeving.

FIBROBLAST GEDRAG OP GECOMBINEERDE TREKKRACHTEN EN MICROGROEVEN

De eerste studie was gericht op het verkrijgen van een algemeen beeld van cel respons op een ondergrond voorzien van een microgroef topografie en mechanische stress. **Hoofdstuk 2** beschrijft de invloed van unilaterale cyclische trekkracht en de daaruit volgende tendens van fibroblasten om zich haaks te oriënteren op de stress richting. Overeenkomstige cel oriëntatie kan worden geïnduceerd door cellen te geleiden langs topografische richels en groeven. Het doel van de studie was het evalueren van cel gedrag op microgroef substraten en blootgesteld aan cyclische trekkracht. De hypothese was dat cel vorm hoofdzakelijke wordt bepaald door topografie. Op basis van voorgaande studies, werd er gekozen voor een 10 micron wijde vierkante groef en een 40 micron wijde V-vormige groef patroon. Gladde substraten diende als controle. Op alle drie de type substraten werden fibroblasten gezaaid en een 1 Hz cyclische trekkracht op los gelaten (0, 4, of 8%) voor een periode van 3 tot 24 uur. Cellen werden voorbereid op verder analyse met scanning electron microscoop, immuno-kleuring van actine filamenten, alignement metingen en PCR (collageen type I, fibronectine, α 1- en β 1-integrinen). Resultaten lieten zien dat cellen zich oriënteren op alle gegroefde ondergronden en fluorescentie microscopie toonde eenzelfde oriëntatie van intracellulaire actine filamenten. Na 3 uur van trekken, begint cel oriëntatie en na 24 uur hebben cellen zich vrijwel volledig georiënteerd. Beeld analyse liet een verbeterd alignement zien bij diepere groeven. Statistiek bewees dat de parameters groef type, groef richting en tijd alle significant waren, maar de trekkracht variatie niet. Substraten met groeven haaks ten opzichte van de trekrichting leidde tot een beter cel oriëntatie. De expressie van β 1-integrine en collageen-I was hoger in de experiment groepen. Concluderend kunnen we onze hypothese handhaven, omdat microgroef topografie het meest effectief was in het aanwenden van spanning relatief op de lengte as van de cel en trekkracht alleen leidde tot secundaire effecten op de cel.

FIBROBLAST RESPONS OP EEN COMBINATIE VAN HYPERGRAVITATIE EN MICROGROEVEN

Mechanische stress is een belangrijke regulator van cel vorm en extracellulaire matrix component productie. Het denkbeeld dat veranderingen in cel vorm als gevolg van variabele zwaartekracht bijdraagt aan het idee van directe effecten van zwaartekracht op cellen leidde tot de studie zoals beschreven in **hoofdstuk 3**. Deze studie rapporteert over de verschillen in morfologisch gedrag tussen fibroblasten gekweekt op gladde en gegroefde ondergronden (groef diepte: 1 μm , breedte: 1, 2, 5, 10 μm), welke hyperzwaartekracht ondergaan door middel van centrifugatie (10, 25 en 50 g; 1 g voor de controle). Het doel van de studie was het duidelijk maken welke van deze parameters het belangrijkste is in het bepalen van cel gedrag. Morfologische karakteristieken werden onderzocht met scanning electron microscopie en fluorescentie microscopie voor het verkrijgen van kwalitatieve informatie over cel spreiding en alignment. Confocal laser scanning microscopie liet de verdeling van actine filamenten en vinculine anker punten zien door immuno-kleuring. Ook de expressie van collageen type I, fibronectine en $\alpha 1$ - en $\beta 1$ -integrinen werden onderzocht met PCR. Microscopie en beeld analyse toonde aan dat fibroblasten zich oriënteren langs de groef richting op alle gestructureerde ondergronden. Op het gladde substraat (controle groep) vertoonden cellen een willekeurige cel spreiding. The oriëntatie van cellen gekweekt op gegroefde verbeterde bij hogere g-krachten tot een optimum was bereikt bij 25 g. ANOVA analyse van de data voor alle parameters: topografie, zwaartekracht en tijd bleek uit te wijzen dat alle parameters significant verschil uitmaken. Daarnaast waren de meeste gen expressie niveaus verlaagd onder hypergravitatie. Toch lijkt het erop dat collageen type I en fibronectine niveaus onbewogen blijven door tijd of kracht. Uit onze data concluderen we dat fibroblasten zich voornamelijk aanpassen aan de morfologie van hun omgeving, zoals het substraat oppervlak, terwijl een secundaire, maar significante rol is weggelegd voor hyperzwaartekracht.

REACTIES VAN FIBROBLASTEN OP EEN INTERACTIE VAN MICROGRAVITATIE EN MICROGROEVEN

Hoewel mechanische belasting belangrijk is, kunnen cellen ook mechanische ontlasting ervaren door de meest constante natuurkracht, namelijk zwaartekracht, te verwijderen. **Hoofdstuk 4** handelt over de eerste van twee studies welke de effecten van microgravitatie op cel gedrag bekijken door *in vitro* gebeurtenissen te beschrijven over de verschillen in morfologisch gedrag tussen fibroblasten gekweekt op gladde en microgroef substraten (groef diepte: 0.5 μm , breedte: 1, 2, 5, 10 μm), welke onderworpen worden aan gesimuleerde gewichtloosheid. Het doel van de studie is er achter komen welke parameter determinerend is in het sturen van cel gedrag. Morfologische kenmerken als cel vorm, oriëntatie en cel oppervlak werden onderzocht met scanning electron en fluorescentie microscopie. Confocal laser scanning microscopie visualiseerde de actine filamenten en focale adhesie punten. Ook werd de expressie van collageen type I, fibronectine en $\alpha 1$ - en $\beta 1$ -integrinen bekeken met PCR. Microscopie en beeld analyse lieten zien dat fibroblasten zich voegde naar de groef richting op alle gegroefde patronen. Op gladde ondergronden lieten cellen een willekeurige cel spreidingsvorm zien. De alignment van cellen gekweekt op gegroefde oppervlakte verminderde onder gesimuleerde microgravitatie, in het bijzonder na 24 uur kweken. Cel oppervlak grootte was aanzienlijk kleiner dan op gladde substraten, maar gesimuleerde microzwaartekracht leidde tot een vergroting van cel oppervlak van cellen gekweekt op gegroefde substraten. ANOVA werd toegepast op alle parameters; topografie, zwaartekracht en tijd. Uit deze analyse kwam naar voren dat alle parameters een significant verschil uit maakte. Gen expressie niveaus waren verlaagd als gevolg van microgravitatie, vooral $\beta 1$ -integrine en fibronectine. Uit onze data kan worden geconcludeerd dat

fibroblasten hun vorm aanpassen aan de fysieke omgeving zoals de substraat textuur, microgravitatie heeft een weliswaar significant, maar secundaire rol.

ACTIVATIE VAN MAPK ROUTES IN FIBROBLASTEN TIJDENS MICROGRAVITATIE

Hoofdstuk 5 breidt de kennis opgedaan in de vorige studie uit door te kijken naar het intracellulaire moleculaire mechanisme welke de extracellulaire cel respons bemiddelt. Mechanotransductie is een belangrijke drijfveer achter deze studie waarin de morfologie van fibroblasten werd vergeleken die gekweekt waren op zowel gladde als gegroefde ondergrond (groef diepte: 0.5 μm , breedte: 1 μm) en werden blootgesteld aan microzwaartekracht. Morfologie werd onderzocht met behulp van scanning electron microscopie en fluorescentie microscopie werd gebruikt om kwalitatieve informatie over cel alignement te verkrijgen. Confocal laser scanning microscopie visualiseerde de actine filamenten en focale adhesie punten. Expressie van collageen type I en $\alpha 1$ -, $\beta 1$, $\beta 3$ -integrinen werd geanalyseerd met QPCR. Immunoblotting werd toegepast om de verschillende proteïnes van de MAPK signalering routes zichtbaar te maken. Microscopie en beeld analyse liet zien dat fibroblasten op gegroefde ondergrond zich georiënteerd hadden langs de groeven. Gladde substraten resulteerde in fibroblasten met willekeurig spreidingspatroon. De oriëntatie van cellen op een microgroeven oppervlak tijdens microgravitatie na 48 uur verschilt nauwelijks van de 1 g controle groep, hoewel cel vorm wel verschilde. ANOVA analyse bewees dat alle parameters een significante invloed hebben op cel oriëntatie. Microzwaartekracht reduceerde expressie van voornamelijk $\beta 3$ -integrin en collageen. Alpha-1 en beta-1 integrinen waren echter opgereguleerd. ERK1/2 was verminderd in 0 g hoewel JNK/SAPK en p38 actief bleven. The familieleden van de kleine GTPases waren gestimuleerd tijdens microgravitatie, in het bijzonder RhoA en Cdc42.

De resultaten zijn conform het gegeven dat microgravitatie fibroblasten ertoe aanzet hun morfologie en expressie van cel-substraat proteïnen aan te passen via de MAPK intracellulaire signalering routes. We concluderen dat fibroblasten op een gegroefd patroon hun vorm al zo dus aanpassen en dat dit model kan worden gebruikt om de effecten van zwaartekracht perceptie en cel respons te ontrafelen.

MECHANOSENSITIVITEIT VAN FIBROBLASTEN OP INERTIËLE SCHEERKRACHTEN

Al enige jaren is inertieële scheerkracht, welke inherent is aan centrifugatie, beschreven als theoretisch model. Uit dit model kwam naar voren dat inertieële scheer resulteert in artefacten welke de uitkomst beïnvloedt van controle monsters welke gecentrifugeerd worden bij 1 x g aan boord ruimtevaartuigen. In **hoofdstuk 6** voerde we een studie uit waar *in vitro* geprobeerd werd te achterhalen wat de invloed is van inertieële scheer krachten op fibroblast cellen gekweekt op polystyreen substraten, zowel glad als gegroefd (groef diepte: 0.25 μm , breedte: 1 μm). Deze cellen werden geplaatst in een centrifuge in aangepaste kweek dozen. Monsters werden onderworpen aan 0, 1.5 en 3.0 Pascal (N/m) voor 0.5, 2 en 4 uur. Om de invloed van inertieële scheer vast te stellen analyseerde we zowel de cel morfologie (scanning electron en fluorescentie microscopie) alsook op een moleculair niveau (mRNA transcriptie en Western blotting). Het achterliggende doel was het begrijpen in hoeverre scheer krachten cel gedrag kan beïnvloeden en welke parameter het belangrijkste is in het bepalen van de cel respons. Microscopie en beeld analyse toonde aan dat fibroblasten zich oriënteerde langs de groef richting en een willekeurige spreiding vertoonde op gladde substraten. Alignement van cellen op microgroeven tijdens inertieële scheer kracht is na 4 uur kweken heel anders in vergelijking met de 0.0 Pa controle groep. Actine filament aantallen en dikte waren verminderd en het aantal talin ankerpunten gereduceerd.

ANOVA was toegepast op de belangrijkste parameters: topografie, scheer kracht en tijd. Uit deze analyse bleek dat alle parameters significant waren. Daarnaast, waren geen niveaus gereduceerd als gevolg scheer kracht in het bijzonder die van beta-3 integrin en alpha-1 integrin. Collageen type I en beta-1 integrin waren juist verhoogd. Erk1/2 was aanwezig en JNK/SAPK en p38 waren verhoogd tijdens scheer kracht. The familieleden van de kleine GTPases waren gestimuleerd tijdens scheer kracht, vooral RhoA en Cdc42.

Inertiële scheer kracht is in vergelijking met de zwaartekracht versnellingscomponent tijdens een nagebootste microgravitatie studie een kracht waar rekening mee moet worden gehouden, omdat ze een aanzienlijke impact heeft op gehechte cel kolonies. Inertiële scheer kracht moet in de interpretatie van resultaten van ruimtevlucht en grond data worden meegenomen.

NANOTOPOGRAFIE EN DE ORIËNTATIE LIMIETEN VAN FIBROBLASTEN

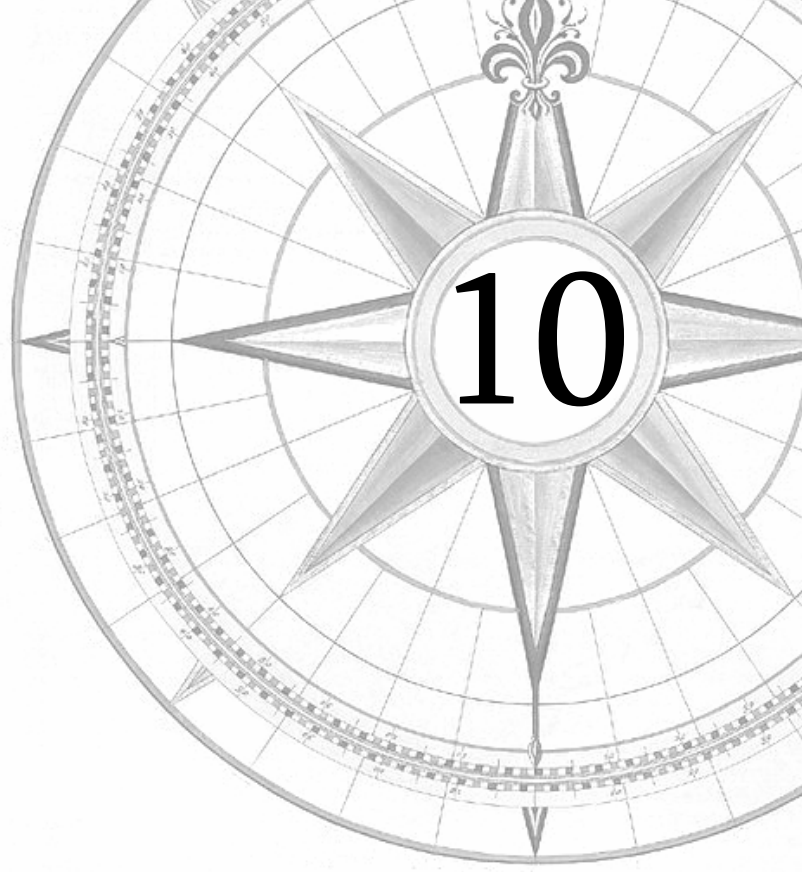
Een van de belangrijkste parameters van de voorgaande hoofdstukken is topografie. Een gestructureerde, groef/richel oppervlak van bekende afmetingen, en waarvan we weten welke cel respons dit patroon kan opwekken. Omdat deze oppervlakken de natuurlijke situatie nabootsen, zijn deze patronen intensief bestudeert. Echter, collageen fibrillen, welke de natuurlijke omgeving vormen van dermale fibroblasten, zijn kleiner van schaal (nano meters) dan de momenteel gebruikte substraten (micro meters). Als gevolg van wat technische haalbaar was en de wetenschap dat collageen fibrillen samenklonteren tot structuren vele malen groter dan een enkele fibril hebben we gebruik gemaakt van deze microgroeven tot nu toe. In samenwerking met Philips Research, hebben we nu de mogelijkheid om de verschillen in morfologie gedrag te bestuderen van fibroblasten op gladde en echte nano-groef substrata (groef diepte: 5 – 350 nm, breedte: 20 – 1000 nm) *in vitro*. Het doel van deze studie in **hoofdstuk 7** was het ophelderen in hoeverre cel geleiding voorkomt bij een steeds kleinere topografie. Matrijzen van patronen werden gemaakt met electron beam lithografie en werden gerepliceerd in polystyreen cel kweek materiaal. De replica's werden gekarakteriseerd met de atomic force microscoop (AFM). Na het zaaien van fibroblasten, werden de morfologische eigenschappen onderzocht met scanning electron microscopie en licht microscopie, zodat kwalitatieve en kwantitatieve informatie kon worden verkregen over cel alignment. AFM liet zien dat nanogroef/richel breedtes perfect werden gerepliceerd, hoewel in diepere delen van de groef meer concaaf waren. De gladde substrata lieten geen kenmerkend patroon zien, behalve een ruwheid van 1 nm. Microscopie en beeldanalyse van fibroblast oriëntatie liet zien dat na 4 uur cellen zich hebben gevormd naar het nano-topografische patroon tot een groote van 100 nm breed en 75 nm diep. Na 24 uur kweken, oriënteren fibroblasten zelfs naar nog kleinere dimensies: 35 nm groef diepte. Blijkbaar is diepte de meest belangrijke parameter in cell alignment op groef patronen met een pitch ratio van 1:1. Op gladde ondergronden groeiden cellen uit tot een willekeurige spreidings patroon. Variantie analyse (ANOVA) bewees dat zowel topografie als kweek tijd een significante invloed heeft op celgedrag. Wij concluderen dat fibroblast cellen gekweekt op nanotopografie een drempelwaarde ervaren ter groote van 35 nm, onder deze waarde vindt er geen contact geleiding meer plaats.

AFSLUITENDE OPMERKINGEN EN TOEKOMST VISIE

In dit proefschrift is de interactie tussen statische en dynamische factoren onderzocht vanuit het perspectief van de cel mechanotransductie. Door het nabootsen van een fibril uiterlijk door middel van oppervlak topografie op een biomateriaal en door cellen bloot te stellen aan een stressvolle omgeving zijn we erin geslaagd meer inzicht te verkrijgen in de mechano- en gravitatie gevoeligheid van primaire fibroblasten.

Gravitationele cel biologie uitgevoerd op Aarde is een onderzoeksveld met een rooskleurige toekomst: menselijke nieuwsgierigheid en wil om de natuurlijke wereld te begrijpen, van de oceaan dieptes tot de verre ruimte, gecombineerd met de lage kosten en hoge beschikbaarheid van apparatuur maakt dat verder onderzoek mogelijk is. De resultaten zoals beschreven in dit proefschrift en in het werk van anderen heeft laten zien dat de uitkomsten van ground-based onderzoek vergelijkbaar is met resultaten zoals gevonden in “echte” gewichtloosheid.

De groefpatronen op micron schaal gebruikt in de eerste hoofdstukken was een zeer –misschien wel te– dominante factor, vandaar dat toekomstig onderzoek zich zou moeten richten op het uitbreiden van de huidige kennis door het combineren van cellen gekweekt op een nanotopografie en onderworpen aan mechanische (on)belasting op verschillende manieren. Dit resulteert waarschijnlijk in een verbeterde interactie tussen de verschillende parameters. Analyse van cel terugkoppeling zou op een brede schaal moeten plaatsvinden: van de visualisatie van morfologische veranderingen van cel vorm door middel van microscopie tot kwantificeerbare data verkregen via moleculaire analyse methodes zoals Q-PCR en in het bijzonder SDS-PAGE en Western blotting. Het volgen van de cel in real-time tijdens experimenten zal niet alleen positief bijdragen aan ons begrip van cel gedrag, maar ook de ontwikkeling stimuleren van hoogwaardig experiment hardware. Verbindingen leggen tussen processen in de cel en het uiterlijk van de cel zullen een licht werpen op welke mechanismen cellen exact gebruiken in hun respons op omgevings stimuli. Deze fundamentele kennis kan ook gunstig zijn in de constructie en toepassing van biomaterialen geschikt voor reparatie en regeneratie van nieuwe en functionele weefsels.



Dankwoord

Dankwoord

De eerlijkheid gebied mij te zeggen dat ik niet helemaal wist waar ik aan begon bij de start van dit onderzoeksproject. Promotie onderzoek was een logische stap op weg naar zelfstandig onderzoek uitvoeren en aldus geschiedde. Op de vraag wat ik nou ging doen daar in Nijmegen en Amsterdam, kwam ik in eerste instantie niet veel verder dan: cel gedrag onderzoeken onder verschillende omstandigheden. Waarop de vraagsteller reageerde met: goh, wat leuk. Nu, 4 jaar later, zou ik enthousiast kunnen vertellen over die cellen en hun gedrag, maar ook over de mensen die dit allemaal mogelijk hebben gemaakt. Niet alleen hun inhoudelijke inzet, maar ook het sociale aspect van werken op een onderzoeksafdeling heeft me diep geraakt en heb ik ervaren als hartverwarmend. Hierbij gaat mijn dank uit naar iedereen, die ook maar enige interesse heeft getoond in wat ik in de afgelopen jaren heb uitgevoerd, geschreven en gepresenteerd. Mijn dank gaat uit in het bijzonder naar degene die hebben meegeholpen in de totstandkoming van dit werk.

Prof. JA Jansen – beste John, ik ben je zeer dankbaar voor wat je voor mij betekent hebt. Zolang er goed werk geleverd werd liet je me vrij in mijn doen en laten en dat heeft me de mogelijkheid gegeven om me te ontwikkelen, maar ook om me voor te bereiden in mijn nieuwe vakgebied. Ik bewonder je om je altijd parate kennis van nieuwe ontwikkelingen op wetenschapsgebied en de manier waarop je invulling geeft aan het hoogleraarschap. Je relaxte manier van communiceren tijdens de meetings gaven me altijd een goed gevoel in het halen van de doelstellingen van het project. En je snelle manier van werken is legendarisch in de AiO-kamers. Het is dit samenspel van gedrevenheid en ervaring waar ik diep respect voor heb.

Dr XF Walboomers – ik had me geen betere begeleider kunnen treffen dan jou Frank. Je hebt me vertrouwen en vrijheid gegeven in de uitvoer van het onderzoek. Je zorgde niet alleen dat het werk correct was, maar ook tijdig werd ingeleverd. Jouw doelgerichtheid hield mij en het project op de juiste koers. Het was keer op keer leerzaam en vermakelijk om getuigen te zijn van je snelle manier van replek dienen, gepaard gaande met een hoop humor, op opmerkingen van reviewers. In de eerste week van mijn aanstelling werd jouw zoon Luc geboren, ik heb grote bewondering voor hoe jij het vaderschap weet te combineren met die van wetenschapper.

Dr JJWA van Loon – Jack, jou “down to earth” aanpak van problemen en de bereidheid om verder te kijken dan het voorgeschreven protocol heb ik het meest gewaardeerd. Deze kleine experimentjes om te kijken “wat gebeurt er als...”, maakte dit onderzoek zo ontzettend leuk en hebben me geholpen om menig vraag te beantwoorden uit het publiek na een presentatie. Je kennis op het gebied van space life-sciences: wat al is uitgevoerd en wat niet, wat de sterke en zwakke punten waren, is ongelofelijk. Ik heb vaak gedacht dat hieruit jou gedrevenheid uit voortkomt om goed onderzoek te doen, met correcte controlegroepen zodat er geen tijd en moeite verloren gaat in dit onderzoeksveld. Ik denk met plezier terug aan de ASGSB conferentie, waar je me bij veel gelijkgestemde hebt geïntroduceerd en het de eerste keer was dat ik in contact kwam met andere ruimtevaart biologen. Een hele geruststelling dat er nog genoeg andere vakidioten rondlopen op deze planeet.

Dr. JGC Wolke – Joop, ik zal je altijd blijven herinneren als: met het hart op de tong en grote kennis van materialen. Ik heb je leren kennen als iemand die recht door zee is, met oog voor detail. Je doorzettingsvermogen en oprechtheid hebben grote indruk op me gemaakt.

Dr. J van den Dolder – Door jou inspanning, Juliet, kan onze afdeling nu bogen op uitstekende moleculaire analyse methoden. Ik deel jou mening dat op (intra)cel niveau er nog veel te leren valt en dat daar de sleutel ligt om de interactie tussen cellen en hun omgeving te begrijpen. De resultaten van jouw voorwerk vinden zijn weg terug in mijn artikelen. Ik ben je hiervoor erg dankbaar.

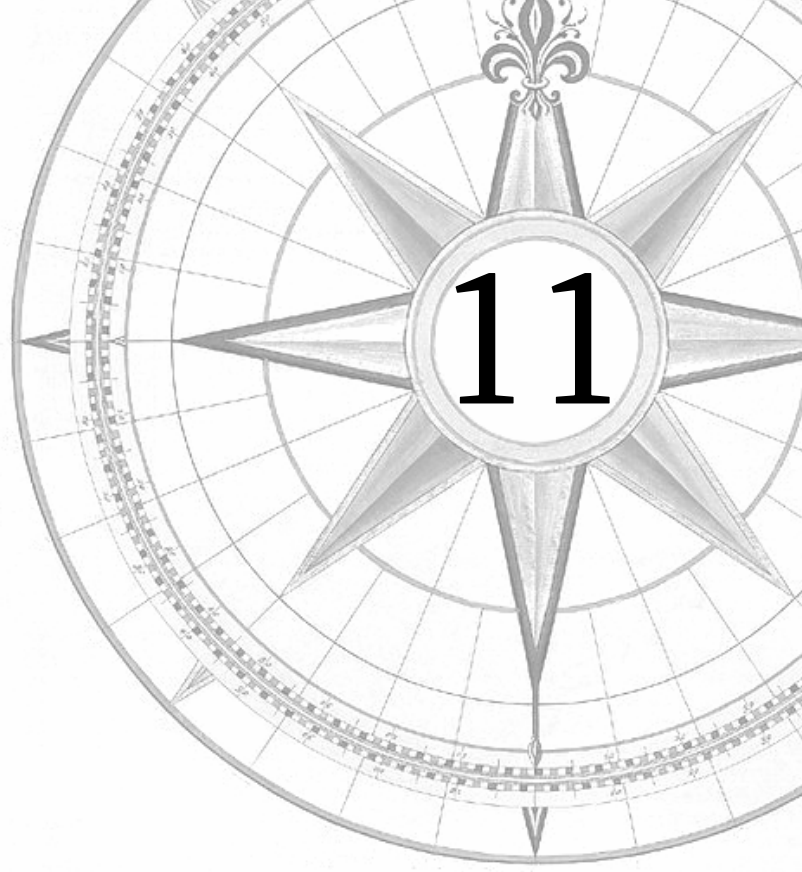
Ik wil alle mensen van de afdeling Biomaterialen bedanken, niet alleen voor hun hulpvaardigheid, maar vooral voor de gezelligheid. Met jullie samen was het altijd een feestje zowel op het lab, als in de kroeg, als op congres. Ik heb veel genoeg gevonden in het delen van levens ervaringen en de levendige discussies, die de onderlinge banden versterkte. Hartelijk dank hiervoor: Corinne, Dennis, Esther, Fang, Jeroen, Lise, Manal, Marijke, Meike, Natasja, Olga, Quinten, Remco, Sander, Weibo, Wouter, Anne, Bas, Daniel, Diederik, Dimitris, Hongbin, Jacky, Jurgen, Juliet Moeljoredjo, Ken, Xuechao en Yonggang.

In het bijzonder wil ik Anja en Vincent bedanken. Ik heb veel steun gehad van jullie beide wat betreft de inhoudelijke kant van het onderzoek. Ook jullie kijk op onderzoek op een grotere schaal dan alleen de afdeling werkte heerlijk bevrijdend: lekker relativerend en zeggen waar het op staat.

De uitvoering van het leeuwendeel van de experimenten vonden plaats aan de afdeling Orale Cel Biologie van de Vrije Universiteit in Amsterdam. Ik ben dan ook veel dank verschuldigd aan volgende mensen: Prof. Vincent Everts, als hoofd van de afdeling waar ik als gast onderzoeker met plezier heb mogen werken; Prof. Jenneke Klein-Nulend, voor haar interesse in en de prikkelende opmerkingen over wat ik nou precies aan het doen was; Cor Semeins, voor het wegwijs maken op het lab en het delen van (zeil)ervaringen op hoge breedtegraden; Jolande de Blicck voor haar aanstekelijke gelach en haar gave om je meteen thuis te laten voelen. Ook wil ik bedanken Mel Bacabac (collega microgravity onderzoeker), Marlene Knippenberg (voor het leren maken van caipirinha cocktails), Manon Joldersma en Dirk-Jan Bervoets.

Tevens wil ik mijn vrienden bedanken die me hebben bijgestaan in de afgelopen jaren; met advies, met grappen en grollen, met diepgaande gesprekken of gewoon er te zijn: Martijn en Esther Landwaart, Ben de Wachter, Laurens Platteel, Remco Rohaan, Wendy Lieuwes, Paul Cavadino, Bas en Marjolein, Gerwin Schaafsma, Lianna Braid, Helena Alexanderson, Lori Schmidt, Donna Prichard, Joyce Riveroll, Jim Zabruski, en Greg MacMillan.

Ten slotte wil ik mijn ouders George en Jeannette, zus Nathalie, schoonbroer Peter en mijn grootouders bedanken voor hun steun en liefde gedurende al die jaren. Zij vormden een goede, vertrouwde basis om uit te vliegen over de wereld en weer terug te keren.



Curriculum Vitae

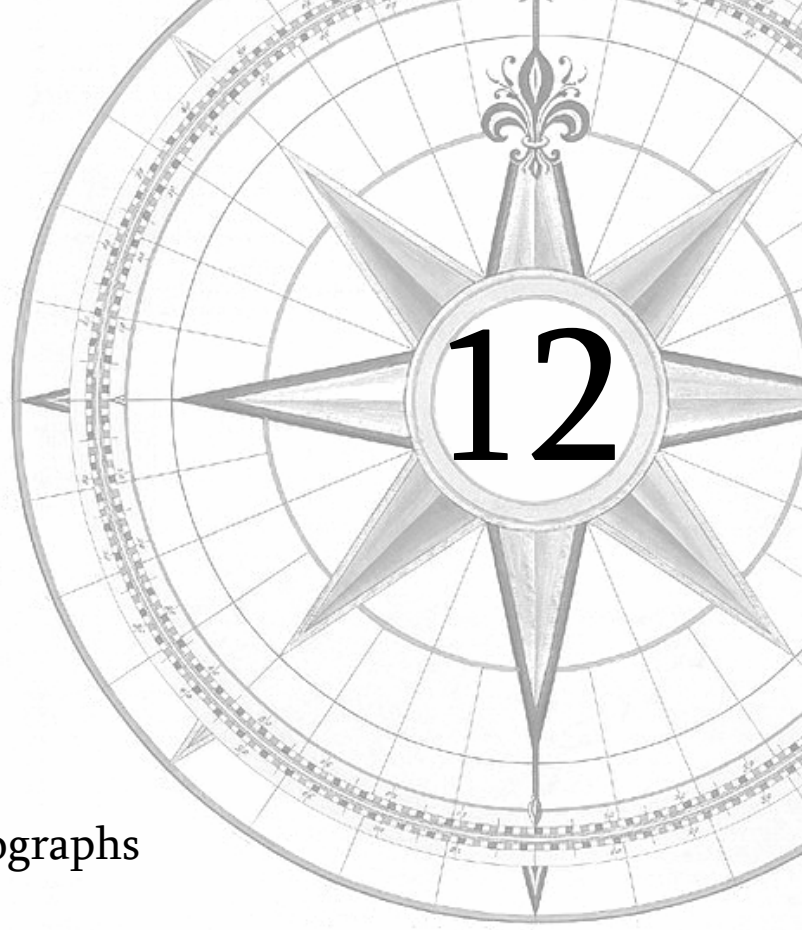
Curriculum vitae

Walter Loesberg – born on March 22nd 1976 – grew up in the rural town of Kortenhoef where he followed elementary school, and attended high school (Atheneum) at the Comenius College in Hilversum.

He obtained his Master of Science degree in Biomedical Sciences from the Radboud University Nijmegen in 2003. Within the area of this education, he was a trainee at the Department of Matrix Biochemistry (dr. Toin van Kuppevelt) of the Nijmegen Center for Molecular Life Sciences (NCMLS) isolating elastin, fabricating collagen-elastin matrices, and studying the effects of these matrices *in vivo* and *in vitro*. Additionally, he was an apprentice at the Department of Rheumatology Research and Advanced Therapeutics (prof. dr. Wim van den Berg) modulating Interleukin-1 mediated signalling transduction through a soluble receptor, as well as, the creation of a stable reporter cell line, which expresses the NF- κ B luciferase gene.

He started working as a PhD-student in 2003 at the Department of Periodontology & Biomaterials (prof. dr. John A. Jansen and dr. X. Frank Walboomers) of Radboud University Nijmegen Medical Centre. The project, in collaboration with the Department of Oral Cell Biology of the Vrije Universiteit (prof. dr. Vincent Everts) in Amsterdam and the Dutch Experiment Support Center (dr. Jack van Loon), investigated the effects of gravity or the lack thereof on the behaviour of fibroblast cells cultured on microgrooved surfaces. This PhD-research came to a successful end in the summer of 2007. The results of the performed experiments are described in this thesis.

To advance his preference for the outdoors and his keen interest in the natural surroundings he participated in several programmes on animal behaviour and ecology in Minnesota, United States of America for which he achieved graduate points from both Hamline University and University of St. Thomas. It was during this period that he came into contact with Hans Jansen of Wageningen University where an education programme was devised. He is currently enrolled in the Master phase of Forest and Nature Conservation study at Wageningen University.



List of publications
Colour images of CLSM micrographs

Publications related to this thesis

1. Loesberg WA, Walboomers XF, van Loon JJWA, Jansen JA. The effect of combined cyclic mechanical stretching and microgrooved surface topography on the behaviour of fibroblasts. *J Biomed Mater Res A* 75 (3), 723-732, 2005
2. Loesberg WA, Walboomers XF, van Loon JJWA, Jansen JA. The effect of combined hypergravity and microgrooved surface topography on the behaviour of fibroblasts. *Cell Motil Cytoskeleton* 63 (7), 384-394, 2006
3. Loesberg WA, Walboomers XF, Bronkhorst EM, van Loon JJWA, Jansen JA. The effect of combined simulated microgravity and microgrooved surface topography on fibroblasts. *Cell Motil Cytoskeleton* 64 (3), 174-185, 2007
4. Loesberg WA, te Riet J, van Delft FCMJM, Schön P, Figdor CG, Speller S, van Loon JJWA, Walboomers XF, Jansen JA. The threshold at which substrate nanogroove dimensions may influence fibroblast alignment and adhesion. *Biomaterials* 28 (27), 3944-3951, 2007
5. Loesberg WA, Walboomers XF, Bronkhorst EM, van Loon JJWA, Jansen JA. Simulated microgravity activates MAPK pathways in fibroblasts cultured on microgrooved surface topography. *Cell Motil Cytoskeleton*, *in press*, 2008
6. Loesberg WA, Walboomers XF, Jansen JA, van Loon JJWA. Mechanosensitivity of fibroblasts towards inertial shear force and microgrooved surface topography. *Annals of Biomechanical Engineering*, submitted, 2008

Other publications

1. Smeets RL, van de Loo FA, Joosten LA, Arntz OJ, Bennink MB, Loesberg WA, Dmitriev IP, Curiel DT, Martin MU, van den Berg WB. Effectiveness of the soluble form of the interleukin-1 receptor accessory protein as an inhibitor of interleukin-1 collagen-induced arthritis. *Arthritis Rheum* 48 (10), 2949-2958, 2003

CLSM colour micrographs

Chapter 3, Combined hypergravity and surface topography, figure 5 162

Chapter 4, Combined microgravity and surface topography, figure 4 163

Chapter 3, figure 5

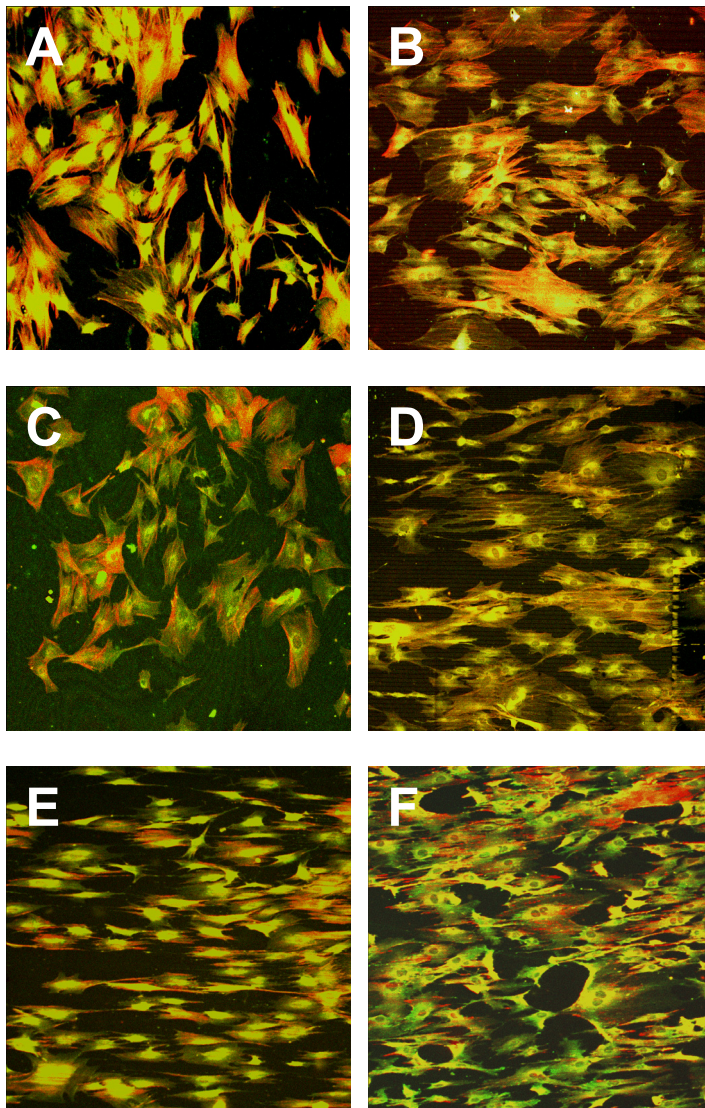


Figure 5. CLSM micrographs of RDFs cultured under several conditions. (A) Smooth substratum showing random orientated cells at normal gravity after 24 hours. (B) Aligned cells on a grooved substratum (10 μm wide) at 1 g. (C) 24 hours at 50 g on a smooth surface results in very little changes to alignment compared to A). Micrograph D is a 24hours/10g sample with 2 μm wide grooves while E is that of a 4hours/25g sample with 1 μm wide grooves, together with B the increased cell alignment with increasing gravitational force is evident, reaching its optimum at 25g. After 24 hours at 50g (F) cells alter their shape and display less alignment and cell surface area is wider (5 μm wide grooves).

Chapter 4, figure 4

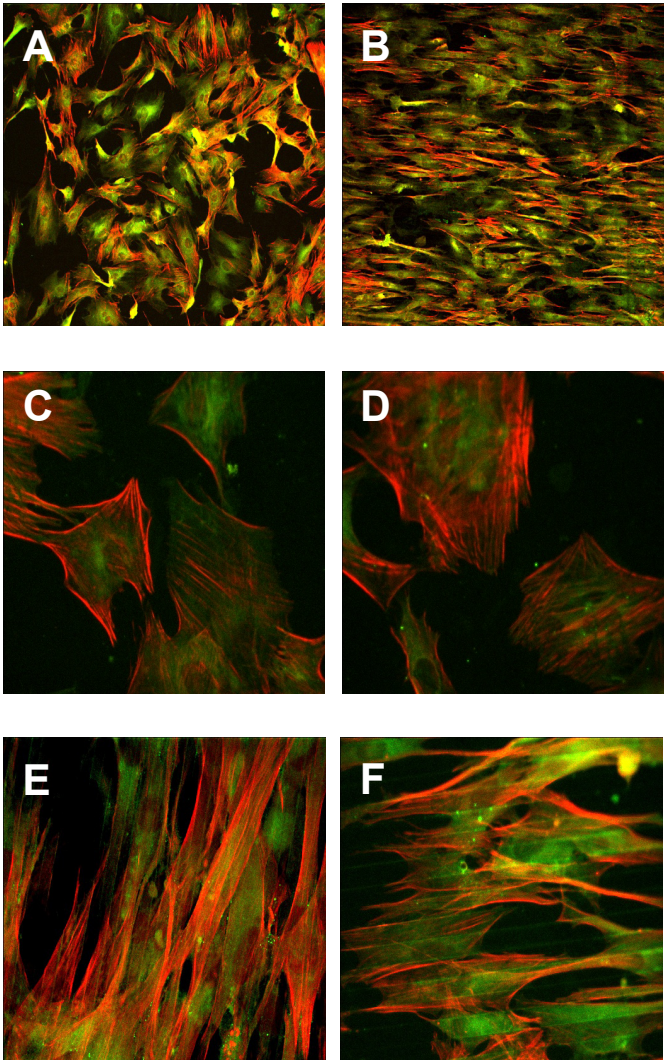


Figure 4. CLSM micrographs of RDFS cultured under several conditions. (A) Smooth substratum showing random orientated cells at normal gravity after 4 hours. (B) Aligned cells on a grooved substratum (5 μm wide) at 1g. (C) Cells cultured on planar substratum after 24 hours in RPM results in little changes in cell shape compared to a 24hours/1g sample (D). In contrast, on topographic substrata cells displayed decreased orientation towards the grooves under near weightlessness conditions; E shows cellular alignment after 4 hours in RPM, while F shows cell orientation after 24 hours.

CLSM colour micrographs

Chapter 5, Microgravity activation of MAPK pathways, figure 4 166

Chapter 6, Combined shear force and surface topography, figure 4 167

Chapter 5, figure 4

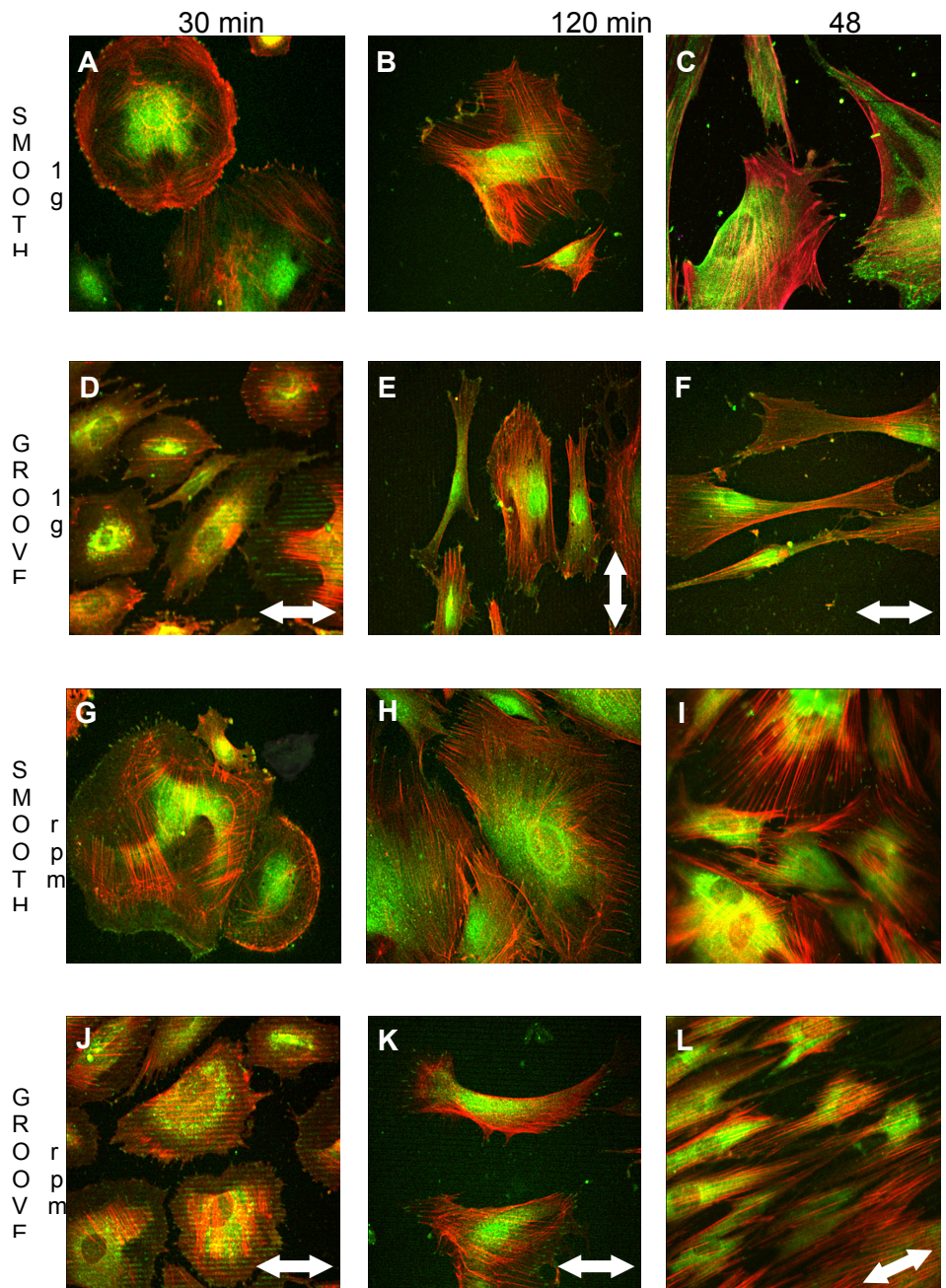


Figure 4. CLSM micrographs of RDFs cultured under several conditions. Normal gravity: (A) Smooth substratum, 30 minutes, (B) Smooth, 120 minutes, (C) Smooth, 48 hours and (D) Grooved surface, 30 minutes, (E) Groove, 120 minutes, (F) Groove, 48 hours. Simulated microgravity: (G) Smooth 30 minutes, (H) Smooth, 120 minutes, (I) Smooth, 48 hours and (J) Groove surface, 30 minutes, (K) Groove, 120 minutes, (L) Groove, 48 hours. Double ended arrow denotes groove direction.

Chapter 6, figure 4

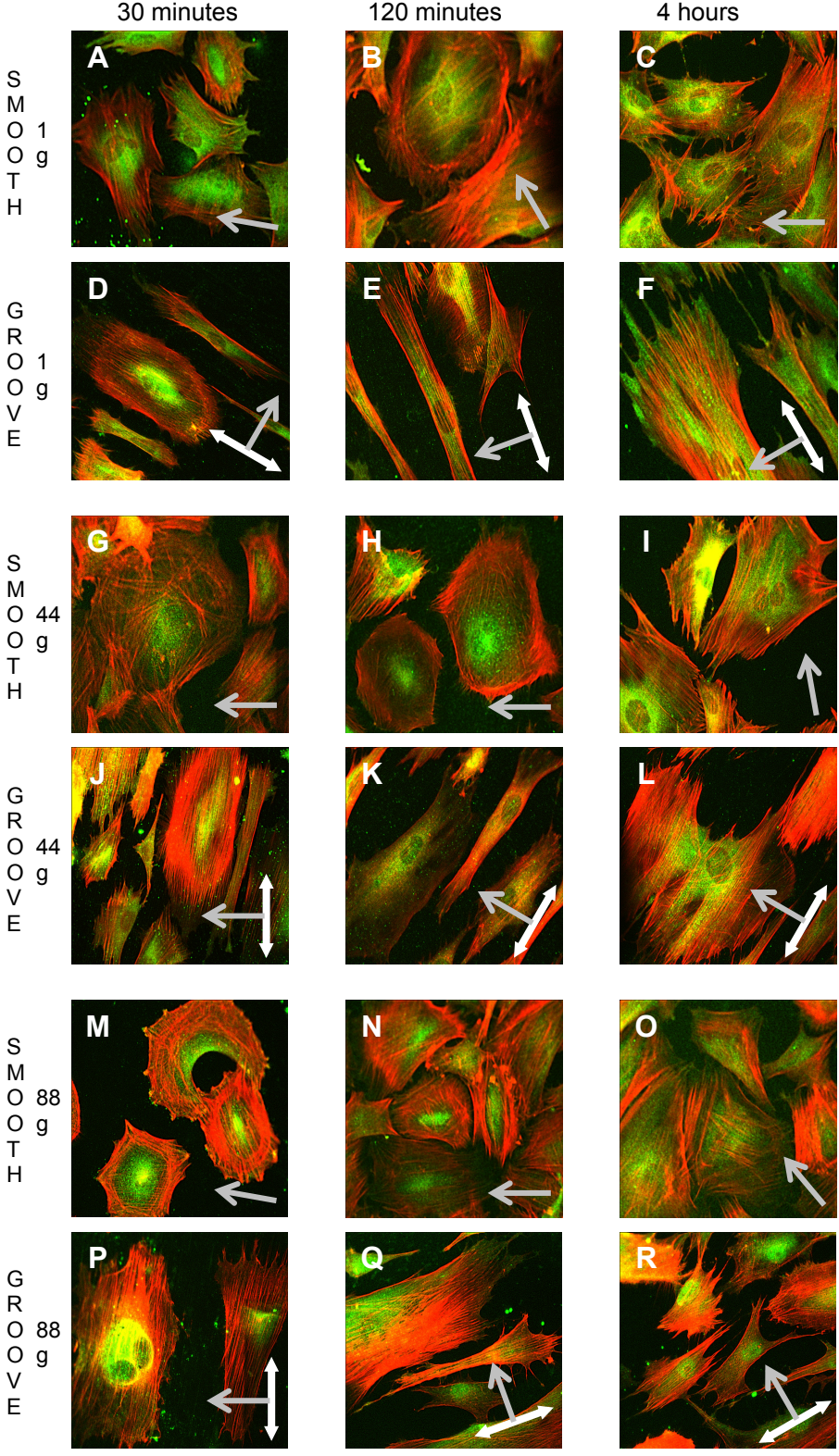


Figure 4. CLSM micrographs of RDFs cultured under several conditions. Columns represent time; from left to right: 30, 120 minutes and 4 hours. Rows represent a combination of topography and amount of shear force applied. First two rows 1 g, Smooth and Grooved. Next two rows: 44 g, last two rows: 88 g. Double ended white arrow denotes groove direction, single grey arrow denotes shear direction.